Investigating the control of homologous chromosome pairing and crossover formation in meiosis of *Arabidopsis thaliana*

by

NICOLA YVETTE ROBERTS

A thesis submitted to
The University of Birmingham
for the degree of
DOCTOR OF PHILOSOPHY

School of Biosciences
University of Birmingham
September 2009

Abstract

During meiosis, homologous chromosomes pair and become connected by formation of the synaptonemal complex. Recombination is initiated by DNA double strand breaks (DSBs), formed by the protein SPO11-1. In *Arabidopsis,* ~10% of DSBs are repaired as crossovers, which are reciprocal exchanges of DNA between homologues. These physical connections ensure the correct segregation of chromosomes and generate genetic diversity. The remainder are processed as non-crossovers, important for pairing and synapsis. How these processes are integrated and controlled remains poorly understood.

Telomeres are thought to play a role in pairing of homologues. The role of telomeres was investigated in *Arabidopsis* by treatment with colchicine, a microtubule-depolymerising drug, known to disrupt telomere clustering and pairing in rye. A mutant deficient for the telomerase reverse transcriptase TERT was studied, in which telomeres were severely shortened and showed reduced fertility. To track the movement of telomeres during meiosis the telomere binding proteins POT1a and POT1b were chosen for antibody production. Telomeres were found to be dispensable for pairing and synapsis.

SPO11-1 RNA interference lines with varying reductions in DSBs were analysed, to investigate how reducing DSBs affects pairing, synapsis, and the crossover/non-crossover decision. Chromosomes showed autonomous crossover control. The synaptonemal-complex was shown to be important in preventing non-homologous interactions.

Acknowledgements

I would like to thank my supervisor Sue Armstrong for providing me with the opportunity to do the project and for her support and advice throughout my PhD. I would also like to thank Chris Franklin for his guidance and support.

I would especially like to thank James Higgins for general advice and helpful discussions over the years, and for providing me with the *SPO11-1* RNAi lines. I am grateful to Dorothy Shippen for providing the *tert* mutant line, the *pot1b1* and double mutant together with the POT1A peptide antibody. I am also thankful to all members of the Franklin and Franklin-Tong labs past and present for their help and guidance, and to Dan for showing me the ropes of real-time PCR. I am grateful to Steve price for technical assistance and to Karen Staples and the other horticultural staff. Funding for the project was provided by the Biotechnological and Biological Sciences Research Council (BBSRC).

I would like to thank my family and my partner Andrew for their love and support over the past few years, which helped me through the difficult times of my PhD, and to my friends for the fun times along the way.

List of Contents

CHAPTER 2

List of Figures

List of Tables

List of Abbreviations

At	*Arabidopsis thaliana*
BAC	Bacterial artificial chromosome
BIO	Biotin
BrdU	Bromodeoxyuridine
BSA	Bovine serum albumin
COL-0	Columbia ecotype
CYTD	Cytochalasin D
DAPI	4, 6-diaminido-2-phenlyinidole
DEPC	diethyl procarbonate
DIG	Digoxygenin
DSB	Double strand break
ECL	Enhanced chemiluminescence
FISH	Fluorescence in situ hybridisation
GFP	Green fluorescent protein
GAPD	Glyceraldehyde-3-phosphate dehydrogenase
HIS	Histidine
HRP	Horseradish peroxidase
IPTG	Isopropylthio-β-D-galactosidase
LATB	Latrunculin B
MT	Microtubule
MTOC	Microtubule organising centre
NE	Nuclear envelope
NOR	Nucleolar organising region
O/N	Overnight
PBS	Phosphate buffered saline
T-DNA	Transfer-DNA
PCD	Programmed cell death
PCR	Polymerase chain reaction
PMC	Pollen mother cell
IPCR	Inverse polymerase chain reaction
TAIL PCR	Thermal asymmetric interlaced polymerase chain reaction
RT-PCR	Reverse-transcription polymerase chain reaction
RT	Room temperature
RNAi	RNA interference
SC	Synaptonemal complex
SDW	Sterile distilled water
SPB	Spindle pole body
SDS-PAGE	Sodium-dodecyl-sulfate polyacrylamide gel electrophoresis
SSC	Saline sodium citrate
WT	Wild-type

AHP2	Arabidopsis homologue pairing 2
ASY1	Asynaptic 1
BRCA2	Breast Cancer 2
Bqt1	Bouquet formation protein 1
Bqt2	Bouquet formation protein 2
CSM4	Chromosome segregation in meiosis 4
DMC1	Disruption of meiotic control 1
MRE11	Meiotic recombination 11
MLH1	MutL homolog 1
MLH3	MutL homolog 3
MND1	Meiotic nuclear division 1
MSH4	MutS homolog 4
MSH5	MutS homolog 5
MUS81	MMS and UV sensitive 81
NBS1	Nijmegen breakage syndrome 1
NDJ1	Non-disjunction protein 1
PRD1	Putative recombination defect 1
PAM1	Plural abnormalities of meiosis 1
POT1	Protection of telomeres 1
RAP1	Repressor/activator protein 1
REC8	Abnormal recombination 8
SAD1	S-phase arrest-defective
SCP3	Synaptonemal complex protein 3
SMC3	Structural maintenance of chromosomes 3
SPO11	Sporulation specific protein 11
STAG3	Stromal antigen 3
STN1	Suppressor of cdc thirteen 1
SUN1	Sad 1 unc-84 domain protein 1
TAZ1	Telomere associated in *Schizosaccharomyces pombe*
TBP	Telomere binding protein
TIN2	TRF interacting factor 2
TRF	Telomere repeat binding factor
TRFL	Telomere repeat binding factor like
TRP	Telomere repeat binding protein

Chapter 1
Introduction

1.1 Overview of meiosis

Meiosis is central to the life cycle of all sexually reproducing organisms and is a highly conserved process. It results in the production of haploid gametes by undergoing a special type of cell division. Homologous recombination generates genetic variation through the production of genetically distinct gametes. An important aspect of meiosis is formation of reciprocal crossovers. These form connections (chiasmata) between non-sister chromatids, which together with attachment of the spindle apparatus ensures the correct segregation of homologues during the first division. If this does not take place, it can result in aneuploidy, which is a major cause of reduced fertility (Gerton and Hawley, 2005). Meiosis also prevents changes in the chromosome number (ploidy) from one generation to the next by reducing the chromosome number by half, thus compensating for fertilisation (Hamant et al, 2006). Meiosis research is important for understanding fertility, improving crop breeding, and genetic studies.

During the meiotic pathway, a single round of DNA replication is followed by two rounds of chromosome segregation, which results in a halving of the chromosome number (Roeder, 1997). The diploid state is then restored during sexual reproduction by fusion of the male and female gametes. The first meiotic division is a reductional division, whereby homologous chromosomes separate to result in halving of the chromosome number. It consists of four stages, prophase I, metaphase I, anaphase I, and telophase I (Zickler and Kleckner, 1998). A unique set of programmed events are initiated at prophase I, which makes up the longest stage of meiosis and consists of five cytologically recognisable stages (**Figure 1.1**). Firstly, homologous chromosomes pair and become synapsed by a proteinaceous structure called the synaptonemal complex. Homologous recombination is initiated by the formation of double strand breaks (DSBs), which is mediated by the protein Spo11 (Keeney et al, 1997). These DSBs may then be repaired to form a reciprocal crossover, which involves the exchange of genetic material between the maternal and paternal homologues (Jones, 1987). Alternatively, this can result in gene conversion without a crossover; termed a non-crossover (Pacques and Harber, 1999). Crossovers are essential for physically connecting homologues at metaphase I, ensuring their faithful segregation. The second division resembles haploid mitosis, with sister chromatids separating to either pole.

1.2 Cytogenetic landmarks of *Arabidopsis* meiosis

Cytogenetic studies in plants have traditionally been used to elucidate the mechanisms underlying the meiotic process. *Arabidopsis* has emerged as an important model for cytogenetic analysis, with recent advances in techniques. The cytology of *Arabidopsis* meiosis has been well characterised by 4',6-diamidino-2-phenlyindole (DAPI) staining (of chromatin) of pollen mother cell chromosome spreads. **Figure 1.1** illustrates these cytogenetic landmarks of wild type ecotype Columbia (Col-0). Images (a-f) make up prophase I of meiosis, which is characterised by increasing chromatin condensation. It can be observed that homologous chromosomes become progressively paired between leptotene (b), and pachytene (d), where homologues are completely synapsed (Zickler and Kleckner, 1999). Recombination is initiated during leptotene (b), with the products of this seen at diakinesis (f) as chiasmata (physical manifestation of crossover). At this point homologues are held together only by these chiasmata. The segregation of homologues at anaphase I, and sister chromatids at anaphase II is permitted by progressive loss of meiotic cohesin proteins (Ishiguro and Watanabe, 2007). The duration of meiosis in *Arabidopsis* has been shown to be 33h, from time course experiments using pulsed labelling of nuclear DNA with bromodeoxyuridine (BrdU) (Armstrong et al, 2003).

1.3 Meiotic recombination

1.3.1 Early recombination events; double strand breaks and SPO11

Meiotic homologous recombination is initiated by the formation of DNA double strand breaks (DSBs) during leptotene. These DSBs are generated by a topoisomerase type-II like protein called SPO11, which is widely conserved between all organisms studied to date (Keeney, 2001). Recently *Arabidopsis* has been shown to encode three homologues of the SPO11 gene (*AtSPO11-1*, *AtSPO11-2*, and *AtSPO11-3* respectively). *SPO11-1* and *SPO11-2* have been shown to be required for accurate meiotic recombination (Grelon et al, 2001, Stacey et al, 2006).

The *Arabidopsis* homologues of SPO11 were first discovered based on sequence similarity with the SPO11 protein sequence of *C. elegans* (Hartung and Puchta, 2000). The *Arabidopsis* proteins were shown to be 28% identical, suggesting that they did not arise from a duplication event, as has been observed for so many *Arabidopsis* genes. The first *AtSPO11-1* mutants to be described were identified by screening of the Versailles collection of T-DNA transformed, and ethyl-methane mutagenised lines (Grelon et al, 2001). Two mutant alleles were studied of the ecotype WS (Wassilewskija), named *spo11-1-1* and *spo11-1-2* respectively. The growth and development of these lines was shown to be normal, with vegetative morphology resembling that of WT. However, both alleles exhibited a phenotype of reduced fertility, with an average of two seeds per silique, suggestive of a role in meiosis. Both male and female meiosis were shown to be perturbed by the mutation, and male meiosis investigated in more detail. DAPI staining of pollen mother cell (PMC) nuclei revealed that bivalent formation at metaphase I was reduced, with a chiasma frequency of only ~7% of wild-type, and univalents primarily observed. The recombination frequency was also shown to be reduced. The *spo11-1-1* insertion was found to occur in the first exon of the *AtSPO11-1* gene, which was thought, would lead to a null mutation. It was proposed that one of the other *AtSPO11* homologues, or DNA damage from environmental stimuli could account for these residual chiasmata (Grelon et al, 2001). As studies in other organisms, such as budding yeast and *C. elegans* observed no recombination in SPO11 mutants. (Keeney et al, 1997; Derburg et al, 1998). More recent evidence has suggested this not to be a null mutation, with the analysis of a third mutant allele, *spo11-1-3*. Sanchez-Moran et al, (2007) further analysed the chiasma frequency of this line to show no bivalent formation in more than 300 meiocytes at metaphase I; indicating this

line as completely defective for recombination. The line was also shown to be completely asynaptic by immunolocalisation of the *AtZYP1* SC protein. Together this data shows *spo11-1-3* to be a null mutation, and suggests the *spo11-1-1* allele is able to produce a truncated semi-functional version of the protein (Sanchez-Moran et al, 2007).

Stacey et al, (2006) analysed the function of *AtSPO11-2*. Two mutant alleles were screened from the RIKEN collection, and Syngenta insertion library collection, named *spo11-2-1* and *spo11-2-2* respectively. Homozygous mutants showed a severe sterility phenotype similar to that described for *spo11-1-3*. An average of 0.13 seeds was recovered from each silique. *AtSPO11-2* was also shown to be necessary for completion of synapsis and recombination. No bivalents were observed at metaphase I, showing crossover formation is lost in this mutant. The two *Arabidopsis* genes were shown to interact genetically, with plants heterozygous for both *spo11-1* and *spo11-2* exhibiting a sterile phenotype, which has been termed non-allelic non-complementation (Stacey et al, 2006).

These results suggest that the functions of the two proteins overlap, but that they are non-redundant. In the *spo11-1-3* mutant no DSBs are formed, showing *AtSPO11-2* cannot function in the absence of *AtSPO11-1* (Sanchez-Moran et al, 2007). This combined data has led to the suggestion that the two proteins may function as a heterodimer (Hartung et al, 2007), although this has yet to be proved. It is also possible that the AtSPO11 proteins form part of a complex with others. In budding yeast, DSB formation has been shown to require the collective activity of nine other meiotic proteins (Keeney et al, 2001). Evidence for such a complex in *Arabidopsis* comes from the identification of *AtPRD1*, which has been shown to be necessary for DSB formation, and to interact with *AtSPO11-1* in a yeast two-hybrid screen (De Muyt et al, 2007).

To monitor the numbers of DSBs formed in these meiotic mutants labelling of γH2AX has been widely utilized (Mahadeviah et al, 2001; Chicheportiche et al, 2007). H2AX is rapidly phosphorylated at the C-terminal serine on the onset of DSB formation. This phosphorylation extends over 50Kb each side of the break; providing a useful cytological marker of DSBs by immunolocalisation with a specific antibody. Formation of these γH2AX foci has been shown to be SPO11 dependent in *Arabidopsis*, with no foci observed in the *spo11-1-3* mutant

(Sanchez-Moran et al, 2007). From immunolocalisation analysis combined with a BrdU time course, *AtSPO11-1* expression was shown to be transient with the number of foci at 3h post S-phase an average of 88.4. Up to 100 foci were observed at leptotene (Sanchez-Moran et al, 2007). γH2AX labelling was shown to be delayed following this, suggesting a delay between association of SPO11 with the DNA and actual DSB formation. A recent study in mouse has revealed that not all γH2AX foci were SPO11 dependent. Two distinct types of foci were observed in this organism. Small γH2AX foci were observed to mark DSB events; as they were absent in null *spo11* mice. Large foci were also observed, which they suggested might correspond to an uncharacterised chromosome alteration, as they were also observed in *spo11-/-* cells. (Chicheportiche et al, 2007).

1.3.2 Early stages of DSB repair

Subsequent to the formation of DSBs, they are processed by the MRX complex. In *Arabidopsis*, as in yeast, this complex is made up of the proteins RAD50 (Bleuyard et al, 2004), MRE11 (Puizina et al, 2004), and NBS1 (Waterworth et al, 2007). Plants deficient for RAD50 or MRE11 show SPO11 dependent chromosome fragmentation and fail to pair and synapse. Nucleolytic processing by these enzymes results in the removal of SPO11, and resection of the 5' ends of the DSB. This leaves a 3' single stranded overhang, which provides a substrate for the strand exchange proteins, RAD51 and DMC1. These proteins are homologues of the bacterial RecA protein, and have been shown to work together to catalyse strand invasion of the homologous non-sister chromatid by the 3' overhang. In *Arabidopsis*, plants deficient for RAD51 exhibit SPO11 dependent fragmentation, and chromosomes fail to synapse and recombine (Li et al, 2004). In the *dmc1* mutant DSBs are repaired but synapsis and crossover formation fail (Couteau et al, 1999). It is likely that the sister chromatid is used for repair in this case (Siaud et al, 2004). A number of proteins are associated with RAD51/DMC1, to promote strand invasion. Including the MND1/AHP2 complex (Vignard et al, 2007), and BRCA2 (Siaud et al, 2004).

1.3.3 Two crossover pathways in Arabidopsis

Meiotic recombination is initiated by the formation of programmed DSBs. It is thought that DSBs are subject to a sequential selection process whereby a subset of DSBs are directed to

form a crossover, whilst others form non-crossovers with gene conversion via the synthesis dependent strand annealing pathway. Borner et al, (2004) proposed that this decision is made early, prior to the formation of stable strand exchanges at the point of single strand invasion (for model see **Figure 1.2**). Studies in yeast have shown evidence for the existence of at least 2 separate pathways which give rise to crossovers (de los Santos et al, 2003; Argueso et al, 2004). Class I crossovers are associated with the bacterial MutS homologues MSH4, and MSH5, which are thought to stabilise Holliday junction formation (Snowden et al, 2004). The MutL homologues MLH1 and MLH3 have also been shown to be associated with crossovers (Jackson et al, 2006). These crossovers exhibit interference, which means they are not randomly distributed. Class II crossovers do not exhibit interference and are thought to be associated with the proteins MUS81/MMS4 in budding yeast (de los Santos et al, 2003).

The ratio of class I to class II crossovers varies between organisms (Baudat and Massey, 2007). In budding yeast class I crossovers account for most recombination events. Current studies suggest that crossover control in *Arabidopsis* is similar to that described for budding yeast. The first evidence for the existence of 2 crossover pathways in *Arabidopsis*, came from statistical analysis of crossover distribution in tetrads. From this analysis, it was predicted that the proportion of crossovers without interference was close to 20% (Copenhaver et al, 2002). Plants deficient for the MutS homologue MSH4, have been shown to exhibit a reduced crossover frequency of 15% of wild-type. These residual chiasmata were shown to follow a poisson (random) distribution, indicating that they are not subject to interference (Higgins et al, 2004), which supports those previous predictions. Further evidence for the existence of at least two pathways, comes from analysis of other mutants for MutS homologues. Plants deficient for MER3 showed similar levels of chiasma formation as the *msh4* mutant. The residual chiasmata were shown not to exhibit interference, by genetic analysis of a set of adjacent intervals (Mercier et al, 2005). MSH4 is thought to act together with MSH5 as part of a heterodimer; analysis of the *msh5* mutant showed a similar phenotype to the *msh4* mutant (Higgins et al, 2008a).

Higgins et al, (2008b) demonstrated that the *Arabidopsis* MUS81 homologue accounts for the formation of some of the class II crossovers, as the *msh4/mus81* double mutant showed a

more severe decrease in the number of chiasmata than in *msh4*. Together these data support the notion of two crossover pathways in *Arabidopsis*.

1.4 Mechanisms of crossover control

It is known that the distribution and the number of crossovers are tightly regulated, although how this is brought about is less well understood. At least one crossover must be formed per chromosome pair to ensure their correct disjunction at metaphase I; termed the obligate crossover (Jones, 1984). Once a crossover is formed, the likelihood of a second crossover forming in an adjacent region is greatly reduced. This mechanism of control is known as interference and acts on approximately 85% of crossovers in budding yeast and *Arabidopsis* (Higgins et al, 2004). Crossover interference reduces with increasing distance from the crossover site, to produce a non-random distribution of crossovers (Bishop and Zickler, 2004). How interference is established is not well understood. It was originally thought that the synaptonemal complex (SC) may convey interference, although it is now known that interference is established prior to the formation of the SC (Fung et al, 2004).

Two further models have been postulated to explain the mechanism of interference. The first is the counting model, which proposed that adjacent crossovers are separated by a fixed number of non-crossovers (Stahl et al, 2004). The second is the mechanical stress relief model (Borner et al, 2004; Kleckner et al, 2004). It was proposed that the signal of stress leads to crossover designation, and that relief of stress adjacent to the crossover prevents formation of further crossovers. In support of this, Storlazzi et al, (2008) showed that late recombination nodules (crossover sites) caused a localised destabilisation of the chromosome axis in wild-type *Sordaria*. In yeast, it has been discovered that chromosome axes are modified at future crossover sites, which is controlled by the protein Pch2 (Joshi et al, 2009).

In addition to these fundamental principles for crossover control, there are increasingly more complex controls being uncovered. The distribution of DSBs along chromosomes is not random, but exhibit hot and cold spots (Gerton et al, 2000). This therefore provides a primary control of crossover distribution. The localisation of DSBs is controlled locally by the structure of chromatin. It has been proposed that histone modifications that lead to a more open conformation of chromatin may be involved. Borde et al, (2009) showed that in budding yeast, histone H3 lysine 4 trimethylation was increased close to sites of DSBs, independent of

local gene transcript level, and that this mark preceded the onset of meiosis. In yeast, the meiotic cohesin Rec8 has been implicated in the distribution of DSBs. In the *rec8Δ* mutant, DSB formation and binding of Spo11 to DSB sites was impaired (Kugou et al, 2009). DSBs are also controlled on a chromosome wide basis. Blitzblau et al, (2007) mapped DSBs in budding yeast and found DSB hotspots in sub-telomeric regions. This resulted in an increased density of DSBs on short chromosomes. It was proposed that a telomere-directed mechanism could provide sufficient DSBs on each chromosome to ensure that homologues receive at least one crossover.

Crossover distribution is also thought to be influenced by higher order chromosome structure. A microarray based method has recently been described, which allows a genome wide measurement of crossover and non-crossover levels in budding yeast. Chen et al, (2008) showed that the frequency of crossovers is reduced at both centromeres and telomeres. This supports previous findings that crossovers close to the centromeres cause aberrant segregation of homologues, and crossovers telomeric sequences could cause non-homologous recombination (Martinez-Perez and Colaiacovo, 2009).

1.5 Crossover homeostasis

Meiotic recombination is initiated by the formation of DSBs by the protein SPO11. The number of these crossover initiating events exceeds the number of eventual crossovers formed, however it remains unknown why this is important. It is currently thought they may play a role in promoting homologous chromosome pairing and synapsis (Baudat and Massy, 2007). In *Arabidopsis*, up to 100 foci are observed by immunolocalisation of SPO11, although the number of RAD51 and DMC1 foci, which localise to sites of DSBs has been observed to vary up to 120 and 140 respectively. This suggests there may be more DSBs than observed by SPO11 immunolocalisation (Sanchez-Moran et al, 2007). Of these only 9-10 are directed to form a crossover (Franklin, et al, 2006). This suggests there is a progressive selection of crossover initiating events towards a crossover (Jones and Franklin, 2006). It is unknown how this crossover/non-crossover decision is made, but recent evidence suggests that this occurs early, prior to or during the formation of stable strand exchanges (Borner et al, 2004). A model of the early crossover decision is shown in **Figure 1.2**.

The ratio of DSBs to crossovers differs between organisms. In mouse, approximately 10% of DSBs are directed to form crossovers (Moens et al, 2002), whereas genetic studies in budding yeast, suggest that approximately 3 times more DSBs than crossovers are formed (Fogel et al, 1981; cited by Kauppi et al, 2004). One study has investigated the effect of altering this ratio in order to study the crossover/noncrossover decision. Martini et al, (2006) analysed a series of allelic *spo11* mutants, where the number of DSBs were reduced to varying degrees (80%, 30%, and 20% of wild-type) in budding yeast. They measured the crossover frequency in eight different genetic intervals across three chromosomes. It was found that reducing the number of DSBs did not cause a subsequent reduction in crossovers, but that the number of crossovers tended to be maintained (**Figure 1.3**). Analysis of the *ARG4* locus hotspot showed that reducing the numbers of DSBs resulted in an increase of crossovers at the expense of non-crossovers. This showed that the ratio of crossovers/non-crossovers could be altered. This effect was termed crossover homeostasis. They suggested that this process might be important for promoting formation of the obligate crossover. However, crossover homeostasis was found not to be 100% efficient. Different genomic loci differed in their strength of crossover homeostasis, with some less capable than others. In mutants with 20-30% of DSBs, the number of 4-spore viable tetrads was reduced, which is an indication of chromosome non-disjunction. Furthermore, it was found that interference was maintained in these lines, showing that interference is independent of the numbers of DSBs in that interval (Martini et al, 2006). These results were shown to be consistent with the mechanical stress relief model of interference (Kleckner et al, 2004), and give evidence against the counting model (Stahl et al, 2004). A more recent study has developed a microarray-based approach for measuring crossovers and non-crossovers on a genome wide basis in budding yeast (Chen et al, 2008). Crossover homeostasis was found to occur in wild-type. Mutants deficient for the proteins *zip2* and *zip4,* which affect synapsis, were found to show reduced crossover interference. Crossover homeostasis was also reduced in these mutants, which illustrated a link between these forms of crossover control (Chen et al, 2008).

1.6 Linking pairing and synapsis to recombination

A number of organisms exhibit a complex interplay between the processes of pairing, synapsis, and recombination, where one process is dependent upon the other. For recombination to be completed, homologous chromosomes must firstly become tightly juxtaposed to a distance of 400nm (Tesse et al, 2003), and subsequently become connected by formation of the synaptonemal complex (SC). In most organisms studied, pairing and synapsis of homologues has been shown to require formation of DSBs. However, there are notable exceptions. In *C. elegans* a mutant for SPO11 showed normal pairing and SC formation (Derburg et al, 1998). A similar situation has been observed for *Drosophila* females, whereby mutants that failed to form crossovers were able to synapse (McKim et al, 1998). Pairing of homologues in these organisms appears to be regulated by an alternative mechanism. Specific pairing centres on chromosomes are thought to be important for the homology search and pairing in these cases. (Phillips and Dernburg, 2006).

In organisms that do require DSBs, it has been proposed that pairing proceeds by 3 sequential steps (Tesse et al, 2003). This includes homologue recognition independent of recombination; subsequently homologues become closely juxtaposed, which requires DSBs. Finally chromosomes become connected by formation of the SC. DSB formation by the protein SPO11 has been shown to be necessary for pairing of homologous chromosomes in budding yeast (Peoples et al, 2002; Henderson and Keeney, 2004), *Sordaria* (Tesse et al, 2003; Storlazzi et al, 2003), and 2*Arabidopsis* (Grelon et al, 2001). Tesse et al, (2003) showed that the extent of pairing correlated with the number of DSBs and numbers of RAD51 foci in the *ski8* mutant with varying numbers of irradiation induced DSBs. This leads to the question of how DSBs mediate the close juxtaposition of homologues. Pairing has been shown to require progression through the early stages of the DSB repair pathway (Peoples et al, 2002). In a variety of organisms, it has been noted that the number of early recombination nodules far exceeds the eventual numbers of crossovers formed, which led to the proposal for their role in the homology search (Franklin et al, 1999). In a *Sordaria* mutant with reduced DSBs, the few regions of homologue co-alignment were often associated with the presence of RAD51 foci (Tesse et al, 2003). Similar observations have been made in a number of organisms. In maize, RAD51 foci have been shown to localise between aligned chromosomes (Franklin et al, 1999). The numbers of RAD51 foci have also been shown to correlate with the extent of

pairing in several mutants (Pawlowski et al, 2003). Immunoelectron microscopy studies in mouse have shown that RAD51 and DMC1 localise to bridges that link homologous axes (Moens et al, 2002). Tesse et al, (2003) proposed a model of presynaptic pairing, whereby a DSB may interact with its homologous sequence on a partner chromatin loop, and bring the axes into a close alignment by moving along the chromatin loop to permit formation of bridge associated with meiotic DNA repair proteins.

DSBs are also important for formation of the SC. The SC is a proteinaceous structure that connects homologous chromosomes along their lengths (**Figure 1.4**). The SC consists of 2 lateral elements derived from the axial elements. These are held together in parallel by a central element, and transverse filament protein, identified as ZYP1 in *Arabidopsis* (Higgins et al, 2005). Mutants where DSBs are abolished show no SC formation (Higgins et al, 2005). In *Sordaria ski8* and *spo11* mutants with low levels of irradiation induced DSBs, limited regions of pairing, but no SC formation has been observed. Much higher levels of DSBs were shown to be required for partial SC formation (Tesse et al, 2003). Similar observations have been made in budding yeast, where *spo11* mutants with partial reductions in DSBs showed only partial SC formation (Henderson and Keeney, 2004). It is thought that the SC is initiated at a small subset of DSB sites, which would explain why lower numbers of DSBs are sufficient for pairing but not SC initiation (Henderson and Keeney, 2004). In budding yeast, it has been proposed that synapsis initiation sites correspond to sites that will eventually give rise to crossovers (Henderson and Keeney, 2004). *spo11* mutants with reduced DSBs also showed a reduction in the number of zip3 complexes, which correspond to SC initiation sites. Previous studies have demonstrated that there is a one-to-one correlation between the number of initiation sites and late recombination nodules; for example in 2 *Sordaria* mutants (Zickler et al, 1992). These synapsis initiation sites are not randomly distributed on chromosomes, but are thought to exhibit interference, which supports the idea that these sites correspond to those of crossovers (Fung et al, 2004). Earlier studies suggested that the SC might mediate the interference signal, by preventing further crossovers in synapsed regions (Egel, 1978; cited by Fung et al, 2004). Fung et al, (2004) showed that interference preceded SC formation, which suggests that the SC does not mediate interference. In many plants studied, the number of synapsis initiation sites far exceeds the numbers of crossovers formed. It has been proposed that this could be due to the longer chromosomes found in plants, as the modal distances

between SC initiation sites did not vary by more than 4-fold in species studied (Zickler and Kleckner, 1999).

Conversely, the SC is thought to be important in maintaining the fidelity of recombination. Mutants for the central proteins have been described for a number of organisms. The extent to which recombination is affected appears to vary between organisms. In *Arabidopsis*, plants deficient for the transverse filament protein ZYP1 formed 80% of the wild-type levels of crossovers, but showed extensive non-homologous connections and multivalent formation (Higgins et al, 2005). This suggests that the SC may play a role in removing non-homologous connections, or in resolving interlocks. *Arabidopsis* contains a high percentage of duplicated sequences (The *Arabidopsis* Genome Initiative, 2000), making accurate pairing more complicated.

1.7 Telomeres and their role in meiosis

Meiosis is a dynamic process, which requires large-scale chromosome movement in many organisms. Telomeres are thought to be important for the movement of homologous chromosomes during prophase I of meiosis, and maintaining the fidelity of recombination. Mutations in which telomeres are disrupted show defects in synapsis and recombination. For example, the *ndj1Δ* mutant of budding yeast (Trelles-Sticken et al, 2000). Most cytological studies of meiosis have analysed fixed meiocytes. Live imaging of meiocytes is becoming an increasingly important technique for elucidating the mechanisms of control during meiosis, for example, in pairing of homologous chromosomes. Telomere binding proteins have been shown to be an appropriate site for tagging. A Rap1-GFP (Green fluorescent protein) fusion protein was used to investigate chromosome movements in budding yeast meiosis (Trelles-Sticken et al, 2005). This could be an effective approach in elucidating the role of telomeres and chromosome movements in plant species like *Arabidopsis*.

Telomeres are protein-DNA complexes that cap the ends of linear chromosomes to protect them from being recognised as double stranded breaks (DSB). They are composed of tandem repeat sequences. *Arabidopsis* has the sequence $^{5'}$-TTTAGGG-$^{3'}$, which is highly conserved throughout the plant kingdom. Telomere length varies enormously between species. *Arabidopsis* has short telomeres of approximately 2-5kb (Riha and Shippen, 2003). Telomeres are thought to exist in two conformations. An open conformation, which is thought to be necessary for telomerase to access the DNA, and a closed conformation (T-loop), thought to be a protected state. The T-loop conformation has been observed in pea (Rhia and Shippen, 2003). Telomeres cannot be completely copied by the normal DNA polymerases of the cell, as these require short RNA primers for initiation. Since chromosomes are linear, the last RNA that primes lagging strand synthesis leaves a gap. This creates a single stranded 3' overhang, which is usually rich in guanine bases. Due to this end replication problem, telomeric DNA can be progressively lost during successive rounds of DNA replication (Riha and Shippen, 2003).

Maintenance of the telomere structure is essential for function. Chromosomes where telomeres have been degraded are processed as DSBs. This leads to degradation and end joining of non-homologous chromosomes, resulting in chromosome fusions, and genomic

instability (Heacock et al, 2004). To prevent this, telomeres can be maintained by an enzyme called telomerase (Greider and Blackburn, 1985). Telomerase is a ribonucleoprotein composed of a highly conserved reverse transcriptase (TERT), and an associated RNA template. This template is used to synthesise the telomeric repeat sequence *de novo*, preventing shortening of the telomeres (McKnight and Shippen, 2004). Telomerase activity is usually confined to germ lines cells and adult somatic cells continually undergoing regeneration. Telomerase is often reactivated in tumours, giving these cells unlimited proliferative potential (Stewart and Weinberg, 2000).

1.8 Telomere Binding Proteins

1.8.1 Human Telomeres

A number of proteins are also associated with telomeres. They are thought to function as regulators of telomere length and prevent them being processed as DSBs (de Lang, 2005). They include proteins that bind to double stranded DNA in humans, such as TRF1, and TRF2. TRF1 has been observed to be a negative regulator of telomere length, with over expression causing shortening of telomeres. TRF2 has been shown to be involved in formation and protection of T-loops, as TRF2 deficient human telomeres are recognised as DSBs (de Lang, 2005). These proteins bind to DNA via a Myb domain, known as a telobox (Kuchar, 2006). Some proteins, for example POT1, bind to the single stranded DNA of the 3' overhang. Single stranded telomere binding proteins have been shown to contain a structurally conserved domain called an oligonucleotide binding fold (OB fold), by which they bind to the ssDNA. POT1 has a negative regulatory function, by preventing telomerase from lengthening the chromosome (Shakirov et al, 2005). These proteins make up part a complex known as shelterin, which is thought to be a dynamic structure. It includes the proteins TIN2, TPP1, and Rap1 that associate via protein interactions (de Lang, 2005). DNA repair proteins are also associated with the telomeres, for example, RAD50/MRE11 and Ku70/Ku80 (Riha and Shippen, 2003). Ku proteins have two roles in protecting the genome. Ku70/80 forms a heterodimer, which binds DSBs and facilitates non-homologous end joining, and is important for protection of the telomeres (Rhia and Shippen, 2005). A number of these proteins are shown in **Figure 1.5**, which illustrates the proteins associated with human telomeres.

1.8.2 Double stranded TBPs in Arabidopsis

A number of homologues of these proteins have been found in *Arabidopsis*. However, these have not been demonstrated to interact with telomeres *in vivo* at the plant level. Proteins that bind double-stranded DNA can be separated by those containing a Myb domain in the C-terminal, or N-terminal (Kuchar, 2006). The *Arabidopsis* proteins containing a C-terminal domain include, AtTRP1 (telomere repeat binding protein 1), and AtTBP1 (telomere binding protein 1). Homologues of the TRF proteins of humans have also been found, including, TRFL1, TRFL2, TRFL4, and TRFL9 (Karamysheva et al, 2004). Proteins containing the N-terminal Myb domain include AtTRB2, and AtTRB3 (telomere repeat binding factor), which have been shown to associate with telomeric DNA *in vitro* (Kuchar, 2006).

AtTBP1 was discovered by Hwang et al, (2001) who found it to be a single copy gene, which is ubiquitously expressed. They discovered that the protein could bind telomeric DNA *in vitro*. Another protein called AtTRP1, homologous to AtTBP1 was discovered by Chen et al, (2001).This gene was also shown to be present as a single copy, with the c-terminal containing the Myb domain being sufficient to bind plant telomeric DNA. Hwang et al, (2005) observed two homologues of AtTBP1, named AtTBP2, and AtTRP2. These were found based on amino acid sequence homology to AtTBP1, by searching the *Arabidopsis* genome. Both proteins were observed to be ubiquitously expressed like other telomere binding proteins. Multiple sequence alignment has shown that they each contain a characteristic single Myb domain at the c-terminus, together with a putative nuclear localisation signal, and were also shown to specifically bind plant telomeric DNA. This study also found that binding of either of these proteins induced bending of telomeric DNA. The degree of bending for AtTBP2 was similar to hTRF1 (Hwang et al, 2005). Taken together these results give a good indication that these represent genuine TBPs.

Further homologues of human TRF proteins have been discovered in *Arabidopsis*. Karamysheva et al, (2004) carried out a BLAST of the *Arabidopsis* genome using the human TRF, and AtTRP1 myb domain sequences. In total 12 TRF-like (TRF-L) genes were found, including AtTRP1, and AtTBP1, which were separated into 2 families. Family 1 consisting of TBP1, TRP1, TRFL1, TRFL2, TRFL4, and TRFL9, and the second family comprising of TRFL3, TRFL5-8, and TRFL10 (Karamysheva et al, 2004). They found that 4 of these genes

were located in regions of duplication, including TRP1, TRFL1, TRFL6, and TRFL3. It was noted that a number of the proteins were functionally redundant, as T-DNA knockout lines did not affect telomere length, growth, or development. Evidence that these proteins act as telomere binding proteins came from experiments into the binding of telomeric DNA *in vitro*. It was discovered that only family 1 proteins showed sequence specific binding to plant telomeric DNA. Family 1 proteins were found to contain a unique Myb-extension domain, and a central domain, not present in the family 2 proteins. It was discovered that this Myb-ext domain was required for binding of telomeric DNA, as when this domain was transferred to a family 2 protein, DNA binding was observed (Karamysheva et al, 2004). However, it could not be ruled out that the family 2 proteins may interact with the telomeres *in vivo* via protein interactions, as for TIN2 and Rap1 of humans. The proteins were demonstrated to form homo- or hetero-dimers, as has been observed for TRFs in humans *in vivo*. The family 1 proteins, TRP1, TRFL1, -2, -4, and -9, were found to form homodimers, whilst TRP1, with TRFL1, and TRP1 with TRP9 formed heterodimers.

Although these studies show that the proteins interact with telomeric DNA *in vitro*, the function of these proteins at the telomeres has yet to be elucidated. A study by Kuchar and Fajkus, (2004) set out to ascertain how known or candidate telomere binding proteins interact in *Arabidopsis*. cDNA coding for the proteins AtTRP1, AtTBP1, AtTRB1, AtKu70, and AtPOT1 was isolated from RNA extracts for yeast two-hybrid analysis. AtTRB1 was shown to interact with two similar proteins, AtTBP2, and AtTBP3, which have previously been observed to interact (Schrumpfova et al, 2004; cited by Kuchar and Fajkus, 2004). AtTRB1 was also found to interact with AtPOT, which is similar to the interaction of human TRF1 with POT1. This study also observed an interaction between AtKu70 and AtTRP1. As it is known that in humans TRF2 interacts with Ku70, this may imply that the interaction is of functional importance (Kuchar and Fajkus, 2004). It was also postulated that AtTRP1 might be an ortholog of human TRF2 due to this interaction, and the fact that each contains a Myb domain in the c-terminal region. To establish whether these proteins are genuine TBPs, it will be important to demonstrate their interaction with plant telomeres *in vivo*.

1.8.3 AtPOT1

In *Arabidopsis* the most well characterised telomere binding proteins are the POT1 (protection of telomeres) proteins. Shakirov et al, (2005) found two homologues of the yeast and human POT1 proteins in *Arabidopsis*, named POT1a, and POT1b. A possible third gene, POT1c has now been found which encodes a protein that may have formed by a partial duplication of POT1a (Rossignol, et al 2007). AtPOT1a and AtPOT1b have been shown to contain the structurally conserved OB fold seen in other organisms. The proteins were found based on sequence similarity, by using the *S. pombe* POT1 protein sequence in a BLAST of the *Arabidopsis* genome. It was observed that both genes were ubiquitously expressed using reverse transcription-PCR analysis, and found that the proteins had a weak, but specific affinity for ssDNA of plants (Shakirov et al, 2005). Another study by Tani and Murata, (2005) observed three variants of AtPOT1a, and two of AtPOT1b, suggesting that they are subject to alternative splicing. Antibodies against the N-terminus of AtPOT1a were shown to bind to three polypeptides, giving evidence that each of the splice variants is translated. To assess the functions of these proteins Shakirov et al, (2005) studied the effect of overexpressing truncations of the AtPOT1a, and AtPOT1b genes. It was determined that AtPOT1a functions in telomere length regulation. Overexpression of the C-terminus of AtPOT1a caused telomeres to shorten. The average length of the telomeres after overexpression was 1- 1.5 kb shorter than wild type, which suggested that AtPOT1a functioned as a positive regulator of telomere length. AtPOT1b was shown to be functionally divergent from AtPOT1a, with a role in telomere protection. Overexpression of the N-terminus of AtPOT1b was shown to cause genome instability, sterility, and growth defects; resembling late generation telomerase deficient mutants (Shakirov et al, 2005). It was proposed that the known functions of single stranded telomere binding proteins have diverged to form two different proteins in *Arabidopsis*, as they were found to be functionally non-redundant.

A more recent study has further elucidated the role of AtPOT1a. Rossignol et al, (2007) showed that AtPOT1a interacts with the N-terminus of the telomerase TERT by yeast two-hybrid analysis, and showed that these proteins both have a nuclear organisation using GFP tags. A role for POT1a in regulation of telomerase activity through direct interaction with the N-terminal region of TERT was proposed. In addition to this, AtPOT1a was shown to interact with a protein kinase CIPK21, which they suggested could be involved in DNA damage

signalling. These interactors were shown to be specific to POT1a, supporting the findings of Shakirov, et al (2005) for divergent roles of the two proteins. A recent study illustrated that plants null for AtPOT1a appear morphologically the same as wild type, and did not exhibit reduced fertility or growth defects for the first 6 generations (Surovtseva et al, 2007). This supports previous findings, that AtPOT1a is not required for chromosome end protection. Instead, it has been suggested to be required for the maintenance of telomere length. Terminal restriction fragment analysis was used to measure the length of telomeres, which were found to be significantly reduced in null POT1a mutants and shorten at the same rate as TERT mutants (Surovtseva et al, 2007). AtPOT1a and TERT were shown by genetic analysis to act in the same pathway, as the *in vitro* levels of telomerase activity were significantly reduced in AtPOT1a null plants (Surovtseva et al, 2007). The level of AtPOT1a associating with the telomeres was found to be cell cycle dependent. Binding of AtPOT1a to telomeres *in vivo* was shown to be enhanced during S-phase by chromatin immunoprecipitation, when telomerase acts at the telomeres. Shakirov et al, (2009) went further by analysing POT1 proteins of two additional *Brassicaceae* species, *Arabidopsis lyrata*, and *Brassica oleracea*. Recombinant POT1 proteins failed to bind single-stranded telomeric DNA *in vitro* or *in vivo* in all the species studied. Several single-stranded telomeric DNA binding activities were found, however these proteins had a much lower molecular weight than that predicted for the POT1 proteins in *B. oleracea*. It was proposed that POT1 proteins had functionally diverged from other eukaryotes, and that they did not represent the major single-stranded telomeric DNA binding proteins in *A. thaliana*.

Arabidopsis is not the only organism to have evolved multiple copies of POT1. Mouse telomeres have been found to associate with two POT1 paralogs, named mPOT1a and mPOT1b. The mouse proteins share a higher similarity to one another than the *Arabidopsis* proteins, 72% and 49% respectively. The mouse proteins also show diverged function. Conditional deletions have shown that mPOT1a is important for preventing recognition of the telomere as DNA damage, and mPOT1b controls the length of telomeric DNA. However, some redundant function has been found, as both appear to be important for telomere protection (Hockemeyer et al, 2006). Antibodies raised against mPOT1a and mPOT1b have been shown to co-localise to TRF1, demonstrating that they are located at telomeres.

A second potential single stranded telomere binding protein has been described for *Arabidopsis*, named STN1. This is a homolog of the budding yeast STN1, which forms part of a complex of proteins known as CST (Grandin et al, 2001). It was shown to be a single copy gene, with a conserved OB fold. Song et al, (2008) demonstrated that plants deficient for STN1 showed developmental defects and a reduction in fertility in the first generation. Plants showed extensive telomere erosion together with chromosome end fusions, at a much faster rate than plants deficient for TERT. It was proposed that STN1 was indispensable for chromosome end protection. YFP tagged STN1 was shown to co-localise to the telomere repeat probe in somatic cells (*in vivo*).

1.8.4 Other telomere-associated proteins of Arabidopsis

1.8.4.1 TERT

A homologue of the telomerase reverse transcriptase (TERT) has been identified in *Arabidopsis*. Plants that are homozygous for a T-DNA insertion in the gene have been shown to lack telomerase activity, leading to a progressive shortening of the telomeres from 1 generation to the next of approximately 500bp (Fitzgerald et al, 1999). Plants deficient for telomerase may survive for up to 10 generations. The growth and development of *tert* plants has been shown to be indistinguishable from wild-type for the first 5 generations. Subsequent to this, progressively more severe abnormalities in growth and development become apparent. Firstly, defects in leaf or shoot meristem morphology become apparent. In late generation mutants, plants exhibit severe defects in reproductive organs including anthers, and at the terminal phenotype plants arrest in vegetative development (Rhia et al, 2001). A critical size threshold for *Arabidopsis* telomeres has been identified, under which telomeres readily undergo fusion events. Heacock et al, (2007) found that the appearance of telomere fusions corresponded to the presence of at least 1 telomere of 1kb or shorter. Numerous anaphase bridges have been observed in late generation *tert* mutants, which correlate with the onset of the developmental defects described (Heacock et al, 2004). Breakage of anaphase bridges has been shown to cause genome rearrangements and aneuploidy (Siroky et al, 2003).

In mammals, lack of telomerase has been associated with chromosome instability and apoptosis in both somatic and male germ line cells (Liu et al, 2004). Analysis of late

generation telomerase deficient oocytes in mice has revealed defects in meiotic synapsis and recombination. It was found that the number of oocytes that formed an SC per ovarian section was severely reduced. In addition to this, the number of MLH1 foci (indicative of crossover sites) was significantly reduced in late generation telomerase deficient mice. These results suggest that in mammals at least, functional telomeres are important for progression of meiosis. Whether the reduced fertility observed for the *Arabidopsis tert* mutant is due to a defect in meiotic progression as in mice remains to be elucidated.

1.8.4.2 DNA repair proteins

Homologues of DNA repair proteins have also been discovered in *Arabidopsis*. AtKu70 and AtKu80 were discovered from their amino acid sequence homology to human proteins, which Tamura et al, (2002) showed to share 28.6% and 22.5% similarity respectively. Both genes were found to be expressed by reverse transcription-PCR in all tissues studied, although the levels of expression were low. Yeast-two-hybrid analysis showed that these proteins form a heterodimer as in human cells. Expression of both genes was shown to be induced by treatment with DNA damaging agents (bleomycin and methylmethane sulfonate) which induced DSBs (Tamura et al, 2002). Mutants of either of these proteins show an increased sensitivity to DNA damage, and have elongated telomeres (Riha and Shippen, 2003). These studies give evidence that these genes are homologous to those in humans, and exhibit an evolutionary conserved function.

AtRAD50 and AtMRE11 have also been characterised in *Arabidopsis* (Riha and Shippen, 2003). Gallego and White, (2001) found that mutants of Rad50 showed shortening of their telomeres and were sterile. This study also observed an increase in cell death in cultures of homozygous mutants, and that cells which did survive possessed longer telomeres, which they suggested might be indicative of a Rad50 independent mechanism for maintaining the telomeres. Mutants have been previously found to be sensitive to DNA damaging agents showing that the protein is involved in DNA repair at the telomeres (Gallego and White, 2001). AtMRE11 has been shown to be involved in telomere maintenance. T-DNA knockout mutants of this gene were observed to be sensitive to DNA damaging agents, and telomeres were found to be elongated (Bundock and Hooykaas, 2002).

1.9 Telomeres and pairing of homologous chromosomes during meiosis

1.9.1 The bouquet

As well as their central role in protecting the ends of chromosomes, telomeres are also thought to play an important role in meiosis. In many species, it is known that telomeres pair during early prophase, where they form a characteristic bouquet arrangement (Bass et al, 2000). The bouquet is formed in early prophase and is widely conserved amongst eukaryotes that sexually reproduce (Bass et al, 2000). It was named from its resemblance to a bouquet of cut flowers, and was first observed in the late 19th century (Scherthan, 2001). The bouquet consists of a cluster of telomeres in a polarised organisation, attached to the inner nuclear envelope (NE), as shown in **Figure 1.6**. The bouquet is formed during the leptotene-zygotene transition of prophase I, and persists until pachytene (Bass, 2003). Preceding this arrangement, chromosomes of a number of organisms exist in a so-called Rabl orientation. This consists of a clustering of centromeres close to the spindle poles, while the telomeres are distributed across the other side of the nucleus (Zickler and Kleckner, 1998). This is in contrast to the bouquet arrangement, where telomeres are clustered towards the microtubule organising centre (MTOC), whilst the centromeres are distributed across the nucleus (Harper et al, 2004). The bouquet arrangement is not dependent on the interaction with the spindle pole. In mammals, the telomeres cluster towards the centrosome, and in yeast, they face the spindle pole body (SPB). Plants lack a MTOC and instead telomeres cluster in the microtubule poor region (Cowan et al, 2002). The bouquet is a de novo formation, which requires chromosomes to switch their orientation (Harper et al, 2004). The bouquet is known to form in two stages; telomeres become attached to the nuclear envelope, and subsequently move along the nuclear envelope to form a cluster (Golubovskaya et al, 2002). Formation of the bouquet has been shown to require the telomeric repeat sequence. Mice deficient for telomerase in which telomere lengths are severely reduced show defects in pairing and synapsis (Liu et al, 2004). In addition to this, ring chromosomes without telomeric repeats have been shown not to attach to the nuclear envelope (Voet et al, 3003). However, maize ring chromosomes containing telomeric repeats have been shown to participate in bouquet formation (Carlton and Cande, 2002). Bouquet formation in yeast has been shown to require a number of telomere associated proteins; see section 1.11.

The role of the bouquet is thought to promote pairing and synapsis of homologous chromosomes, because telomere clustering occurs before these events (Bass et al, 2000). It is thought that telomere clustering aids pairing of homologous chromosomes by bringing them into close association during bouquet formation (Cowan et al, 2001). It has been suggested from observations in *Saccharomyces pombe*, that telomere mediated chromosome movements promote pairing of the chromosomes (Chikashige et al, 1994). Homologue pairing has been found to be delayed in mutant budding and fission yeast where clustering is not present (Trelles-Sticken et al, 2005). It is also thought to aid the homology search, by aligning the homologous regions of chromosomes (Cowan et al, 2001). Bass et al, (2000) observed that homologous chromosomes paired and synapsed during the bouquet stage, suggesting that bouquet formation is necessary for homologue pairing in maize. However, there is also evidence that contradicts this hypothesis. For example, Storlazzi et al, (2003) studied meiosis in *Sordaria macrospore*, and showed that homologue pairing took place prior to formation of the bouquet, suggesting that it is not necessary for the homology search process. For further discussion in yeast, see section 1.11. A number of other roles for the bouquet have been suggested, which include regulation of recombination, and interlock resolution (Zickler and Kleckner, 1998). For example it may bring chromosomes close enough together for strand invasion to occur (Harper et al, 2004). Studies of mutants defective for bouquet formation will be valuable in determining the precise functions of the bouquet (Harper et al, 2004).

A number of mutants have been identified that show defects in bouquet formation. However, the causes of these remain unknown. In maize, a genuine bouquet mutant has been described, named *pam1*. In the *pam1* mutant telomeres associate with the nuclear envelope, but fail to cluster into the bouquet (Golubovskaya et al, 2002). This defect subsequently resulted in impaired pairing and synapsis of homologues, which was shown to cause a concomitant delay in meiotic progression. However, some meiocytes were observed to complete meiosis, suggesting that bouquet formation is not required for meiosis (Golubovskaya et al, 2002). Evidence so far suggests that the bouquet is not required for pairing of homologous chromosomes, but may facilitate this process in some organisms. In many of these organisms, pairing has been shown to require formation and repair of DSBs, which is likely to involve the homology recognition process.

1.9.2 Telomeres and Arabidopsis meiosis

Arabidopsis telomeres are associated with the nucleolus throughout meiotic interphase, and a bouquet has not been observed, unlike other species (Armstrong et al, 2001). Armstrong et al, (2001) observed a reduction in the number of telomere probe foci during FISH; showing telomeres begin to pair at the G_2 to leptotene transition prior to synapsis (see **Figure 1.6** for representation). FISH studies with sub-telomeric probes have demonstrated that during early leptotene pairing of telomeres involves homologous chromosomes, although it is still unknown how homologous chromosomes recognise one another (Armstrong et al, 2001). It is thought that as the telomeres are composed of the same consensus sequence, that the unique sub-telomeric sequences may be involved in homologue recognition. As leptotene progresses, telomeres dissociate from the nucleolus and become widely dispersed. During zygotene, telomeres form a loose cluster within one hemisphere, which may represent a relic bouquet (Armstrong et al, 2001). Because pairing takes place whilst telomeres are associated with the nucleolous and the characteristic bouquet arrangement is not formed in *Arabidopsis*, Armstrong et al, (2001) proposed that it might be that the nucleolus associated clustering is equivalent to the bouquet of other species.

1.10 Movement of telomeres

The mechanism of bouquet formation is not well understood. Recent studies have focused on the mechanism by which telomeres and chromosomes move. It has been speculated that because in mammals and yeast, telomeres either are associated with the centrosome, or spindle pole body respectively, that cytoplasmic microtubules may be involved in telomere clustering. So far there has been no evidence to prove this, and is now thought not to be the case (Harper et al, 2004). Many investigations using drugs to disrupt progression of meiosis have been used to study the mechanisms that are involved in movement of the telomeres around the cell during meiosis, and importantly during bouquet formation. The most widely studied of these is colchicine.

1.10.1 Investigating a role for microtubules

Colchicine is a microtubule depolymerising drug, which is known to disrupt spindle formation. It has been known for many years to disrupt progression of meiosis. It has been shown to block the later stages of meiosis because the spindle is not correctly formed, and therefore chromosomes are not correctly segregated at anaphase. This has been observed in a number of species, including *Allium* (Levan, 1939 cited by Bennett and Smith, 1979) and *Lilium* (Bennett et al, 1979). Addition of colchicine has also been shown to reduce the frequency of chiasmata, as noted in *Lilium* (Bennett et al, 1979), *Triticum* (Driscoll et al, 1967), and *Triticale* (Thomas and Kaltsikes, 1977); for review see Zickler and Kleckner, (1998). Colchicine has been shown to disrupt formation of the SC in many organisms, for example in *Allium* (Loidl, 1988) and mouse (Tepperberg et al, 1997), for discussion see Zickler and Kleckner, (1998).

Evidence for colchicine having an effect on bouquet formation first came from experiments into the timing of the colchicine sensitive stage; the point of the cycle where meiosis is disrupted, which has been shown to differ between species. A number of studies have found the leptotene-zygotene transition to be the sensitive point. Bennett et al, (1979) found that in *Lilium* sensitivity to colchicine started at pre-meiotic interphase, and lasted until mid-zygotene, with treatments after this stage having no consequence for meiosis. This is also the case in mice. Tepperberg et al, (1997) observed that the number of ^{3}H-thymidine labelled

spermatocytes with damage to the SC was highest after injection of colchicine at the leptotene-zygotene transition. A study of the hybrid hexaploid triticale x tetraploid wheat also found the colchicine sensitive stage was the bouquet at leptotene-zygotene (Thomas and Kaltsikes, 1976). Driscoll et al, (1967) observed that addition of colchicine prior to meiosis prevented the association of premeiotic homologues in hexaploid wheat. It was also found that after pairing of homologues had been achieved, colchicine no longer had an effect.

Evidence that the colchicine sensitive stage was actually formation of the bouquet came from a later study, in which an isochromosome was treated with colchicine, and shown to pair and form chiasma at the same frequency as the untreated control (Driscoll and Darvey, 1970). An isochromosome consists of two homologous arms joined by a centromere. It was proposed that the movement of homologous chromosomes (bouquet formation) was sensitive to colchicine. As homologues of the isochromosome are attached, movement of chromosomes is not required for them to come into close association. This is in contrast to normal chromosomes, where they only come into a close association during the bouquet. As the homologues of the isochromosome are closely associated prior to bouquet formation, colchicine had no effect (Driscoll and Darvey, 1970).

Cowan and Cande, (2002) proposed that due to this and other previous studies that bouquet formation may be sensitive to colchicine. They used cultured rye anthers to investigate the mechanism of bouquet formation. This study used a number of microtubule depolymerising drugs to determine whether microtubules were necessary for telomere movement and bouquet formation. It was observed that depolymerisation of cytoplasmic microtubules did not affect clustering of the telomeres. Anthers in early meiotic prophase were treated with the MT depolymerising drug amiprophos-methyl at 25μM, with treated cells showing no visible MTs. It was observed that telomeres were clustered in both treated and untreated cells, giving evidence that in plants cytoplasmic microtubules are not required for telomere clustering. The study showed that colchicine and a related drug podophyllotoxin did prevent clustering of telomeres during meiosis. Colchicine at 100μM was used for culturing anthers at pre-meiotic interphase-early leptotene for 10-16 hours. FISH analysis was carried with a probe specific for the telomere repeat sequence to investigate the distribution of telomeres. Colchicine prevented bouquet formation at this concentration, which did not affect cytoplasmic

microtubules. These results lead to the proposal that in rye, the target of colchicine may be involved in the movement of telomeres during bouquet formation. This study suggested that the target of colchicine may be a specialised non-microtubule tubulin or related protein. This is because colchicine and podophyllotoxin bind the same site of β-tubulin. Because colchicine has been shown to block pairing and synapsis of homologous chromosomes, this could point to a role for bouquet formation in homologous chromosome pairing (Cowan and Cande, 2002).

The finding that microtubules are not involved in the movement of telomeres during meiosis has been supported by studies in yeast. Trelles-Sticken et al, (2005) observed that microtubule-disrupting drugs had no effect on telomere clustering in *S. cerevisiae.* In this study, they investigated whether microtubules have a role in movement of telomeres into the bouquet by using microtubule depolymerising drugs. To visualise the telomeres, a Rap1-GFP (Rap1 a telomere binding protein) construct was developed, and live cell imaging or fluorescence *in situ* hybridisation carried out. To examine the role of microtubules in telomere movement, the drugs nocodazole and benomyl were simultaneously used in the culture medium. It was observed that astral and radial microtubules were broken down, and that addition of these drugs at a number of different time points throughout meiosis did not block telomere clustering. They also treated meiocytes deficient for the *rec8Δ* cohesin, which show a persistent bouquet arrangement. In this mutant, telomere clustering did not reach the level shown in untreated cells. It was also found that disruption of astral microtubules led to a small reduction in telomere clustering in wild-type and *rec8Δ* cells, and proposed that microtubules could provide a scaffold support for telomeres to undertake ordered movements.

1.10.2 The role of actin in telomere movement

Recent work has focused on the role of actin in the movement of telomeres. To examine this, meiocytes were treated with a drug called Latrunculin B (LatB), which blocks the polymerisation of G-actin. Trelles-Sticken et al, (2005) observed that addition of LatB to the wild-type meiotic culture prevented clustering of telomeres, using live imaging of Rap1-GFP. They also found that after incubation of *rec8Δ* meiocytes with LatB the persistent clustering of telomeres usually observed was dispersed, which gives evidence for a role of actin in the movement of telomeres. Disruption of telomere clustering resulted in a delay in pairing of

homologous chromosomes, as has been previously observed for colchicine. It was proposed that actin was only important for the clustering of telomeres, as vegetative movements of the telomeres were not affected. Telomere movement on the nuclear envelope was prevented, but disruption of actin did not affect telomere attachment in the membrane. This demonstrates that actin is not required for attachment. Whether cytoplasmic or nuclear actin was involved was not ascertained in this study (Trelles-Sticken et al, 2005).

Further work in budding yeast has unveiled the nature of actin mediated chromosome movements. Analysis of Zip1-GFP lines revealed that the chromosome at the leading edge of the motion moves dramatically. The other chromosomes then move in the direction of this lead chromosome. Rap1-GFP labelling demonstrated that telomeres were present at the leading end (Koszul et al, 2008). These dramatic movements also cause protrusions in the nuclear envelope. Dramatic chromosome movements were shown to be associated with the onset of zygotene and continued throughout pachytene, and were prevented in the presence of LatB (Scherthan et al, 2007; Koszul et al, 2008). Cytoskeletal rather than nuclear actin cables were found to be involved, with a few being intimately associated with the NE. These associated actin cables were mostly observed close to the nucleus/cell periphery and the SPB. It was proposed that this might explain the localisation of the bouquet (Koszul et al, 2008).

The precise role of these mid-prophase I chromosome movements remains to be elucidated. It has been proposed that these movements may create stirring motions, which could bring homologous sequences into close proximity (Scherthan et al, 2007: Koszul et al, 2008). However, Koszul et al, (2008) thought that this was unlikely and postulated that these movements may prevent chromosome entanglements. The movements observed were directed along actin cables, which does not suggest a stirring motion, and it is known that homology recognition begins prior to the onset of these chromosome movements. This may also serve to remove non-specific connections between non-homologous connections. The introduction of LatB around the point of DSB formation resulted in reduced crossover and non-crossover formation, which was thought to be due to prevention of some DSBs finding the opposing chromosome axis (Koszul et al, 2008).

Chromosome movements in budding yeast have been shown to require a number of proteins. In the *ndj1Δ* mutant, pachytene chromosome movement was greatly reduced, but NE deformations were still evident. These were shown to be LatB sensitive, demonstrating that actin mediated movements do not require telomere attachment. In the *csm4Δ* mutant, chromosome movements and NE deformations were eliminated, suggesting that this protein is involved in coupling the telomere/NE complexes to the force generating mechanism (Koszul et al, 2008). In agreement with this, Conrad et al, (2008) showed that the *ndj1Δ* and *mps3Δ* mutants were defective for telomere attachment to the NE, whilst the mutant for *csm4Δ* showed nuclei with peripherally located chromosomes.

1.11 Proteins involved in bouquet formation

1.11.1 Yeast Proteins

The first protein discovered to be necessary for bouquet formation was Ndj1, by studying mutants defective in bouquet formation in *S. cerevisiae* (Trelles-Sticken et al, 2000). To study the distribution of telomeres in the meiotic nucleus, fluorescence *in situ* hybridisation (FISH) using Rap1 staining was carried out, and the distance between the nuclear periphery and telomere signals calculated. It was observed that in *ndj1Δ* meiocytes telomeres did not cluster into a bouquet but instead remained dispersed throughout the nucleus, which was suggested meant that *ndj1Δ* could function in securing meiotic telomeres to the nuclear periphery. It was also noted that Ndj1 was required for bouquet formation. FISH showing a single probe signal was noted to indicate a bouquet. It was observed that the number of single FISH signals never surpassed that observed in pre-meiotic cells in *ndj1Δ* meiocytes. Immunolocalisation of the spindle pole body and telomeres simultaneously showed no interaction between the two in the mutant meiocytes, which is in contrast to wild type cells where during the bouquet telomeres are found to be associated with the SPB (Trelles-Sticken et al, 2000). It was also found that pairing of homologous chromosomes was affected in the *ndj1Δ* meiocytes, with pairing being delayed by 2-3h. Although pairing of larger chromosomes was delayed less than smaller chromosomes, which may be because these have a higher chance of finding their homologue randomly. From these findings Trelles-Sticken et al, (2000) proposed that the bouquet may not be required for the homology search, but facilitates homologue pairing by bringing telomeres into close association, as previous studies have found. A more recent paper

by Wu and Burgess, (2006) does not concur with this view, and suggests that the bouquet does not promote the pairing of homologues in *S. cerevisiae*. The effect of the mutation *ndj1Δ* on meiotic recombination was studied. It was observed that single end strand invasion levels were similar to those of wild type meiocytes. It was therefore proposed that recognition of homology does not require bouquet formation. However, formation of double Holliday junction intermediates was delayed, pointing to a role in recombination. It was proposed that an Ndj1-dependent function could be important in stabilising strand invasion intermediates; although whether the protein plays a direct role has yet to be elucidated (Wu and Burgess, 2006).

Another protein in budding yeast associated with the telomeres during meiosis that has been implicated in recombination is Csm4. As previously mentioned this protein is involved in connecting telomeres to the force generating mechanism. Kosaka et al, (2008) demonstrated that crossover formation was severely delayed. In addition to this, the frequency of crossovers was increased, and interference decreased (Wanat et al, 2008). It is possible that the protein has a direct role in recombination; however, it has been proposed that the defects in recombination observed are likely to be due to its affect on telomere/chromosome movement for example, by regulating the spatial relationships of chromosomes (Wanat et al, 2008). It was proposed that chromosome movement may facilitate recombination by removing non-specific connections.

In *S. pombe* telomere maintenance protein Taz1, and proteins involved in maintenance of the spindle pole body have been shown to be required for telomere clustering (Cooper et al, 1998). Cooper et al, (1998) showed that in the absence of Taz1, the clustering of telomeres at the SPB was disturbed and meiotic recombination levels were subsequently reduced. Rap1, which binds to the telomeres, has been observed to interact with this protein. These are both required for the clustering of telomeres at the SPB during meiosis (Scherthan, 2006).

1.11.2 SUN domain proteins

A class of proteins have been recently discovered in fission yeast, which are important for anchoring telomeres to the nuclear membrane during meiosis. Chikashige et al, (2006) carried out a microarray to study meiosis specific genes. Genes that bound to RNA from cells

reacting to the mating pheromone, known to induce meiosis in yeast, were selected. Knockouts of the genes selected were then produced, and one gene named Bqt1 was found to prevent meiotic telomere clustering. A yeast two-hybid screen then led to the discovery of an interacting protein called Bqt2. Both these proteins were observed to localise to the SPB, and yeast two-hybrid screens were used to find interacting proteins. Chikashige et al, (2006) found that Bqt1 bound to a component of the SPB called Sad1, and that Bqt1 and Bqt2 together bind Rap1 of telomeres. It was proposed that these proteins may interact to form a link between the nuclear membrane and telomeres. Sad1 binds to the nuclear membrane and Bqt1, which subsequently recruits Bqt2, this complex then binds Rap1, which is known to localise to the telomeres. Bqt1 was shown to bind to a SUN domain of Sad1, it was noted that proteins that tether other proteins to the nuclear membrane contain this SUN domain (Tomita and Cooper, 2006).

SUN domain proteins that link telomeres with the nuclear envelope have been discovered in a number of other organisms. Schmitt et al, (2007) discovered a mammalian SUN domain protein, named SUN2, localised to the attachment sites of meiotic telomeres at the nuclear envelope. Electron microscopy showed that SUN2 is part of a membrane-spanning complex that connects attached telomeres to cytoplasmic structures, proposed to be the actin cytoskeleton. This study demonstrated that the mechanism for telomere attachment to the nuclear envelope is conserved between eukaryotes. Mice deficient for the nuclear envelope protein SUN1 show no telomere attachment to the membrane and subsequent clustering. Ding et al, (2007) showed that pairing of homologous chromosomes, together with synapsis and recombination was impaired in this mutant. This supports the notion that attachment of telomeres to the nuclear envelope is important for meiotic progression. In *C. elegans* SUN-1 protein has also been implicated in facilitating homologue pairing (Penkner et al, 2007).

1.12 *Arabidopsis* the model plant

Arabidopsis is a useful model organism for the study of meiosis. For example, a very important advantage of this plant is the availability of meiotic cells all year round, as plants can be grown in any season (Jones et al, 2003). As with all model organisms, *Arabidopsis* has a short generation time. This is typically 6-8 weeks under laboratory conditions. It also requires little space, so hundreds of plants may be grown in the same area (Jones et al, 2003).

Another important characteristic that this plant has is a small genome size; currently estimated to be 125Mb (Armstrong and Jones, 2003). Importantly the *Arabidopsis* genome has now been sequenced, which allows comparisons to be made with other higher eukaryotes, and allows homology searches to identify similar genes (The *Arabidopsis* Genome Initiative, 2000). For example, homology searches can be used to characterise meiotic genes using reverse genetics, where homologues of known meiotic genes are identified, and further investigated (Jones et al, 2003). A number of mutant lines where progression of meiosis, or the maintenance of telomeres are affected, are now available. These can also be used to characterise meiotic genes (Jones et al, 2003). It has only five pairs of chromosomes, which makes cytological analysis less complicated. Improvements in cytology and molecular cytogenetics, for example an improved spreading method to increase the clarity of chromosome morphology (Armstrong and Jones, 2003) have made *Arabidopsis* a useful model for studying chromatin organisation during meiosis (Armstrong and Jones, 2003).

Another significant advantage of this model plant in this investigation is that it has now emerged as a useful model of telomere biology (Riha and Shippen, 2003). One advantage is the presence of unique sub-telomeric sequences on each chromosome. This permits the study of individual chromosomes, with probes specific to each chromosome arm (Riha and Shippen, 2003).

1.13 Aims and objectives of PhD project

1.13.1 Crossover control

One of the main areas of focus for current research is how the crossover/non-crossover decision is made. Recent evidence has shown that crossover frequency is maintained when the numbers of double strand breaks are reduced, termed crossover homeostasis. An RNA interference (RNAi) construct was developed in our laboratory, which will be used to investigate how reducing the number of DSBs affects this decision in *Arabidopsis*. The objectives are to:

1. Establish whether the phenomenon of crossover homeostasis is present in *Arabidopsis*.

2. Investigate how reducing DSBs affects crossover control, for example, formation of the obligate crossover and interference.

1.13.2 Pairing of homologous chromosomes

How homologous chromosomes recognise one another, pair, and synapse remains poorly understood. *Arabidopsis* provides a unique model for studying these mechanisms, due to the difference in telomere localisation. The aim is to elucidate the mechanisms that control pairing of homologous chromosomes in *Arabidopsis*. Two approaches will be taken. This includes investigation into the role of telomeres and DSBs in pairing and synapsis. The objectives are to:

1. Investigate the role of telomeres by introduction of the microtubule-depolymerising drug colchicine. This has previously been shown to disrupt telomere clustering into the bouquet.

2. Analyse progression of meiosis in a mutant deficient for TERT (subunit of telomerase). This mutant shows progressive shortening of telomeres from 1 generation to the next, resulting in developmental defects and reduced fertility.

3. Investigation of how telomere/chromosome movements are important for pairing. Potential telomere binding proteins that could be used as a label for the telomeres will be analysed. This will enable production of GFP tagged proteins ready to use for live imaging analysis.

4. Analyse how pairing and synapsis are affected by decreasing numbers of DSBs, by analysis of the *SPO11-1* RNAi lines.

Chapter 2
Materials and Methods

For general buffers and solutions, see **Appendix 8.1**. Substances specified were supplied from SIGMA or FISHER, unless otherwise stated. For centrifugation at 13,000 rpm an Eppendorf 5414D desk-top centrifuge was used in all cases.

2.1 Plant material

Seeds of *Arabidopsis thaliana* were sown on soil based compost and grown in a glasshouse at 18-23 ^{o}C with a 16 hour light cycle. The ecotype Columbia 0 (Col-0) was used as a wild-type control in all experiments. The T-DNA insertion lines specified were obtained via NASC, excluding the *pot-b-1* and *pot1a-1/pot1b-1* double, which were provided by D.E. Shippen (Personal communication). The *SPO11-1* RNA interference lines were provided by J.D. Higgins (Personal communication).

2.2 Meiotic chromosome spreading for fluorescence microscopy

Inflorescences were fixed in acetic alcohol (3 parts absolute ethanol (ETOH) to 1 part acetic acid) at room temperature overnight, and the fix replenished. Buds must be fixed for at least 24h prior to digestion. Buds in the range of 0.2-0.9mm were selected under a dissecting microscope and transferred to a watch glass containing the fixative. Buds were subsequently washed in 10mM citrate buffer at pH 4.5 for 3x 2 minutes. The buds were then incubated in an enzyme mixture containing 0.3 % w/v, cellulase (C1794 Sigma) and 0.3% pectolysase (P5936) in 0.01M citrate buffer, for 75 minutes at 37 ^{o}C in a moist box, in order to digest the cell wall. The reaction was stopped by replacing the enzyme mixture with ice cold sterile distilled water (SDW). Buds (1-2) were transferred to clean slides with a minimal amount of water using a Pasteur pipette, and tapped out using a fine needle. To this 7 µl of 60 % acetic acid was added, and the slides placed on a hot block at 45 ^{o}C for a few seconds. This causes cells to dissociate to form a monolayer. The slides were subsequently re-fixed with 100 µl of cold fixative, and the slides dried with a hairdryer. For basic cytology slides are mounted in 10µl of a solution containing 4, 6-diaminido-2-phenlyinidole (DAPI) at 1 µg/ml in Vectashield mounting medium (Vector laboratories).

2.3 Meiotic Time Course

The thymidine analog bromodeoxyuridine (BrdU) was used to label meiotic cells by incorporation into nuclear DNA during meiotic S-phase. Stems were cut under water to a length of approximately 3-4 cm and transferred to 10 mM BrdU from a labelling kit (Roche). Stems were immersed in BrdU for 2 h to allow uptake via the transpiration stream. Stems were subsequently transferred to water. For analysis of BrdU incorporation, inflorescences were fixed in 3:1 ethanol: acetic acid at intervals subsequent to the pulse. Slides were prepared using the method for meiotic chromosome spreading (section 2.2). To detect the BrdU, immunolocalisation was carried out with an anti-BrdU (mouse monoclonal antibody) kit (Roche) according to the manufacturer's instructions. Slides were counterstained with DAPI/ Vectorshield. For analysis, cells at each meiotic stage were classified as BrdU labelled or unlabelled (Armstrong et al, 2003).

2.4 Colchicine time courses

A meiotic time course was used, as described previously, with some modifications. In this case it was used to determine which meiotic cells had been exposed to colchicine. Subsequent to the BrdU pulse, stems were either immersed in 100 μM or 10 mM of colchicine, or water as a control. A concentration of 100μM was chosen due to the fact that Cowan and Cande (2002) found this concentration to disrupt telomere clustering in rye. Influorescences were then fixed at regular intervals. To study the effect of colchicine at G1 of the cell cycle stems were immersed in the treatment for 6 h prior to the BrdU pulse and transferred to water afterwards.

2.5 Preparation of Probes for Fluorescence *in situ* Hybridisation

2.5.1 Telomere FISH probe by PCR from oligos

A working solution of 5 μM of the oligos T1 ($TTTAGGG_5$) and T2 ($CCCTAAA_5$) stored at -20 ^{0}C were prepared in SDW. The reaction mix (50 μl) was made up as shown in **Table 2.1**, which shows the volume of each component and its final concentration. PCR amplification was subsequently carried out using the temperature cycle shown in **Table 2.2**.

Following to the PCR reaction, 38 µl of chloroform was added to each PCR tube vortexed for 20 seconds, and centrifuged for 2 min. The upper aqueous layer was removed using a pipette and transferred to a new microfuge tube. To ensure that the PCR had worked, 5 µl of the PCR product was run on a 1 % agarose gel. A secondary PCR was carried out to incorporate the DIG label into the probe. To do this 3 µl of the primary PCR product was transferred to a new tube together with 23 µl SDW. The solution was incubated at 95 ^{0}C for 5min, and the PCR reaction mix made up as shown in **Table 2.1**, replacing dTTP with the 1 µl of the label 1 mM DIG-16-dUTP. The reaction mixture was transfered to the primary PCR product, and the secondary PCR performed using the conditions specified in **Table 2.3**. Subsequent to this, each sample was treated as for the primary PCR, and stored at -20 ^{0}C prior to use in fluorescence *in situ* hybridisation.

Solution	Volume (µl)	Final Concentration
10x Buffer	**5**	**50 mM**
50mM $Mgcl_2$	**1**	**2 mM**
10mM dGTP	**1**	**0.2 mM**
10mM dATP	**1**	**0.2 mM**
10mM dTTP	**1**	**0.2 mM**
10mM dCTP	**1**	**0.2 mM**
5µM T1	**3**	**0.3 µM**
5µM T2	**3**	**0.3 µM**
5units/µl Biotaq polymerase	**0.5**	**2.5 units**

Table 2.1: Solutions of the first PCR reaction

Temperature (^{0}C)	Time (min)	Number of Cycles
94	**1**	**8**
55	**0.5**	
94	**1**	**24**
60	**0.5**	
72	**1.5**	
72	**5**	**1**

Table: 2.2 Primary PCR temperature cycle.

Temperature (^{0}C)	Time (min)	Number of Cycles
95	**1**	**25**
60	**0.5**	
72	**1**	
72	**2**	**1**

Table 2.3: Temperature cycle for secondary PCR.

2.5.2 BAC extraction

Glycerol stocks of the BAC (Bacterial Artificial Chromosome) clones were plated out on LB agar together with a suitable antibiotic, and incubated at 37 ^{0}C overnight to allow growth. A single colony was then inoculated in 5ml of LB broth with 12.5 ug/ml of choramphenicol, and incubated on a shaker at 37 ^{0}C overnight. The overnight culture was subsequently centrifuged at 13,000 rpm for 10 min. The supernant was removed, and the pellet re-suspended in the remaining culture by vortexing. This suspension was transferred to a 1.5 ml microfuge tube using a tip with the end 2 mm cut off (before autoclaving). Following this 200 µl of a solution consisting of 50 mM glucose, 10 mM EDTA, and 25 mM Tris buffer (pH 8) was added, and

incubated on ice for 5min. To this, 400 µl of 0.2 N NaOH, 1% SDS was added, and solutions mixed by inversion and incubated for a further 5 min on ice. While on ice, 300 µl of 3 M potassium acetate stock (pH 5.3-5.5) was added, and mixed by inversion. This solution was then frozen at -80 ^{0}C for 15 min. The solution was thawed at room temperature, mixed by inversion, and centrifuged at 13000 rpm for 15 min, and the pellet discarded. The supernant was transferred to a new microfuge tube, together with a 0.6 x volume of isopropanol (600µl in 1 ml). This solution was then inverted once and left to precipitate for 10min. This was centrifuged at 13000 rpm for 15 min to pellet the DNA. The supernatant was removed, the pellet washed in 70 % ethanol, and centrifuged for 2 min. The ethanol was removed, and the DNA pellet air dried by inverting the tube, allowing the ethanol to drain off. Care was taken not to let the pellet dry completely. Following this, 40 µl of SDW was added to re-suspend the DNA, and kept at -20 ^{o}C overnight. Subsequent to this 1 µl RNAse (10 µg/ml) was added and incubated at 37 ^{0}C for an hour. Extracted DNA was stored at -20 ^{0}C prior to use.

2.5.3 Preparation of probes using nick translation

To produce the probes, 3 µl of template DNA from the BAC extraction was added together with SDW to a final volume of 16 µl in an microfuge tube. To this, 4 µl of BIO (Biotin) or DIG (Digoxygenin) nick translation mix (Roche) was added, and tubes centrifuged briefly. The preparations were then incubated at 15 ^{0}C for 90 min. The reaction was stopped using 1 µl of 0.5M EDTA (pH 8.0), and heated for 10 min in a water bath at 65 ^{0}C. For the 45s and 5s probes the following vector constructs were used:

45s: Clone pTa71 (Gerlach and Bedbrook 1979) containing a9-kb *Eco*RI fragment of *Triticum aestivum* consisting of the 18S-5.8S-25S rRNA genes and the spacer regions.

5s: Plasmid pCT4.2 containing the 5S rDNA gene from *A. thaliana* as a 500-bp insert cloned in pBlu.

These probes were labelled with the BIO or DIG nick translation mix as stated for the BACs. The probes were kept on ice prior to the *in situ* hybridisation. For the localisation of the probes used, see **Figure 2.1**.

2.6 Fluorescence *in situ* hybridisation

Slides were made as described in section 2.2. Slides were pre-treated for in-situ hybridisation by washing in 2x SSC for 10 min at room temperature. Slides were then placed in a solution of 0.01 % pepsin in 0.01 M hydrochloric acid, for a period of 50 seconds, and rinsed in 2x SSC. The slides were subsequently fixed in 4% paraformaldehyde for 10 min. The slides were rinsed in distilled water and then dehydrated, using treatments of increasing concentrations of ethanol. Slides were washed with each concentration for a period of 2 min, 70 %, 85 %, and 100 % ethanol was used. This was followed by an *in situ* hybridisation. To each slide, a solution of 14 µl of hybridisation mix, 3 µl of water and 3 µl of the required probe were applied. A cover slip was then added and sealed with rubber solution. The slides were placed on a hot block at 75 ^{0}C for 4 min (70 ^{0}C for 3 min for *tert* mutant) before incubation over night at 37 ^{0}C in a moist chamber. Post hybridisation washes were subsequently performed. The slides were washed with 50 % formamide in 2x SSC 3 times each for 5 min, and 5 min washes in 2x SSC, 4x SSC, and 0.05 % tween 20, each at 45 ^{0}C, and 1 of 4x SSC, and 0.05% tween 20 at room temperature. For detection of the probe, a 50 µl solution containing fluorescent secondary antibodies; either BIO labelled (1:200 EM block), or DIG labelled (1:40 EM block) was added to each slide, covered with parafilm, and incubated at 37 ^{0}C for 30 min in a moist box. Slides were again washed for 3 x 5min in 4x SSC, and 0.05% tween 20, de-hydrated using a series of ethanol washes and mounted in 10 µl DAPI/Vectorshield.

2.7 Immunolocalisation by spreading

Buds were dissected out on damp filter paper, and those of approximately 0.2-0.6 mm were used for the immunolocalisation. To each slide, dissected anthers from approximately 10 buds were added together with 5 µl EM digestion medium containing, 0.4 % cytohelicase (C8274), 1.5% sucrose , and 1% polyvinylpyrollidone. The anthers were gently tapped out using a brass rod, and as the slide started to dry a further 5 µl of enzyme mix was added. Each slide was placed in a moist box on a hot block set at 37 ^{0}C for 5 min. This was followed by a 2 min treatment with lipsol. To each slide, 10 µl of 1 % lipsol was applied, and spread with a needle. Spreads were fixed in 2% paraformaldehyde. In this case 20 µl (4% paraformaldehyde) was applied, after which slides were transferred to the fume cupboard to dry. To each slide, a 50 µl solution containing the primary antibodies in EM block (1% Bovine Serum Albumen in 1% PBS, 0.1%Triton) was applied, and slides incubated overnight at 4 ^{0}C in a moist box. Slides can be incubated in block for 20 min prior to this, but was not usually required. Slides were washed 2 x 5min in PBS with 0.1% Triton, and the secondary antibody applied and incubated in a moist box at room temperature for 30 min. For antibodies used and their dilutions in EM block, see **Table 2.4**. Slides were washed as previously and mounted in DAPI/Vectashield.

Antibody	Type	Dilution
Rabbit Zyp1	**Primary**	**1:200**
Rat ASY1	**Primary**	**1:200**
Rabbit γH2AX	**Primary**	**1:200**
Rabbit Rad51	**Primary**	**1:200**
Rabbit DMC1	**Primary**	**1:200**
Rabbit Texas Red	**Secondary**	**1:200**
RAT FITC	**Secondary**	**1:50**

Table 2.4: Antibodies and respective working dilutions in EM block used for immunolocalisation

2.8 Combined Immunolocalisation with FISH

Immunolocalisation of slides using the spreading technique described were made and incubated with the primary antibody overnight. Anti-biotin (1:50 EM block) was added to protect the primary antibody through subsequent treatments. Slides were incubated for 30 min at 37 ^{o}C in a moist box. Slides were subsequently taken through the FISH protocol and the primary antibody detected using anti-biotin FITC or Cy3 (1:50, or 1:200 EM block respectively), incubated as before, washed and mounted in DAPI/Vectorshield.

2.9 Combined Immunolocalisation with BrdU labelling

The BrdU pulse is applied as described in the meiotic time-course protocol. Instead of fixing buds, buds are used for preparation of immunolocalisation slides. The primary antibody to the protein was incubated at 4 ^{o}C overnight in a moist box. The BrdU was subsequently detected as described in the manufacturer's instructions (Roche), with the addition of the secondary antibody to the protein in the second incubation.

2.10 Combined FISH with BrdU labelling

Slides are taken through the FISH protocol, and BrdU labelling carried out subsequent to this.

2.11 Alexander's staining of pollen viability

Anthers were dissected from buds of 1-2mm and fixed overnight in 10% ethanol. Anthers are placed on a slide in a drop of water and teased with a needle to release the pollen. To this, 2-3 drops of Alexander stain were added together with a coverslip. Light pressure was exerted before sealing with rubber solution. Slides were subsequently placed on a hot block at 50 ^{o}C for 1 hour, and observed under a light microscope. The pollen wall appears green and the cytoplasm of viable pollen grains appears dark red.

2.12 Microscopy and image analysis

Slides were examined by fluorescence microscopy using a Nikon E600, or Olympus BX61 microscope. Capture and analysis of the images was carried out using Smart Capture 3.

2.13 DNA and RNA Manipulations

2.13.1 Nucleon Phytopure plant DNA extraction (Amersham Biosciences)

This kit was used when clean DNA was required. To extract genomic DNA, leaf material was gathered by placing an microfuge tube over the end of a young leaf, and closed to cut off the end of the leaf. This ensures there is no cross contamination as the tubes are sterile. Approximately 5 small leaves were collected for a 0.1g DNA extraction. Samples were snap frozen in liquid nitrogen, and stored at -80 ^{o}C until required. The extraction was carried out as per the manufacturer's instructions. After pelleting the DNA was re-suspended in 100 µl RNaseA 40 µg/ml.

2.13.2 Phenol-Chloroform Extraction

This was performed to remove contamination from DNA extractions, resulting in cleaner DNA. To each sample, 100 µl of phenol was added and centrifuged at high speed for approximately 30 seconds. The upper aqueous phase was transferred to a new microfuge tube and 100 µl of chloroform (stored at -20 ^{o}C prior to use) added. This removes polysaccharide contamination. Samples were again centrifuged as before and the upper phase transferred to a fresh tube. To precipitate the DNA 10 µl of 3M sodium acetate was added together with 250 µl of absolute ethanol. Samples were then centrifuged at 13,000 rpm for 10 min at 4 ^{o}C. If DNA did not pellet at first, samples were incubated at -20 ^{o}C for approximately 30 min, before repeating the final spin. The supernatant was removed and pellets air-dried for 10 min prior to re-suspension in 100 µl RNaseA 40µg/ml.

2.13.3 Extract-N-Amp™ Plant PCR (Sigma)

DNA from leaves was extracted for genotyping plants with a possible T-DNA insertion. The tip of a young leaf was collected using a 0.5 ml microfuge tube. Samples could then be frozen at -20 ^{o}C until required. To each sample 40 µl of extraction buffer was added and leaf material broken up using the pipette tip. This was followed by a 10 min incubation at 95 ^{0}C using a PCR machine. To each sample 40 µl of dilution buffer was added, mixed and briefly centrifuged. For genotyping, 1µl of the supernatant containing the DNA was used in a 20 µl PCR. DNA stored at -20 ^{0}C.

2.13.4 Removal of RNase contamination from equipment

All microfuge tubes and pestles were treated with diethyl pyrocarbonate (DEPC). Equipment was immersed in DEPC (1:1000 with dH_2O) o/n and subsequently autoclaved to remove the DEPC.

2.13.5 Trizol® RNA isolation (Invitrogen)

Isolations were performed as stated in the manufacturer's protocol with some modifications. In most cases RNA was extracted from the inflorescences. 1.5ml microfuge tubes were filled half with inflorescence material, and either used directly or snap frozen in liquid nitrogen and stored at -80 ^{o}C for future use. Liquid nitrogen was used to keep the samples frozen while homogenising with a pestle. 1 ml of Trizol reagent was added to this material, incubated at room temperature (RT) for 5 min, and centrifuged at 13,000 rpm for 10 min. The cleared homogenate was subsequently transferred to a fresh tube together with 200 µl of chloroform. This was mixed by vigorous shaking and contamination removed by centrifugation at 13,000 rpm for 15 min. The upper aqueous layer of the supernatant was transferred to new tube together with 500 µl of cold isopropanol for RNA precipitation. Samples were centrifuged at 13,000 rpm for 10 min at 4 ^{o}C. The pellet was washed in 75 % ethanol, pelleted again, and re-dissolved in 100 µl RNase free water after air drying for 6 min.

2.13.6 RNA extraction using RNeasy mini kit (Qiagen)

RNA was extracted from buds using the purification method specified for plant material, as described in the manufacturer's handbook, using buffer RLT.

2.13.7 DNase I Treatment (Invitrogen)

RNA (<500 ng) was treated by addition of 1 µl 10X buffer, 1 µl RNasein (Promega), 1 µl DNase 1 (Invitrogen), and made up to 10 µl with DEPC treated water. This was incubated at RT for 15 min. EDTA (to a concentration of 2 mM) was added and the solution incubated at 65 ºC for 10 min to denature the DNase. A phenol-chloroform extraction was then performed to remove any remaining DNase.

2.13.8 DNase I treatment of RNA using RNase free DNase set (Qiagen)

DNase I treatment was carried out as described in the manufacturer's handbook. Subsequent to the RNA extraction, RNA was cleaned using the RNA cleanup protocol, also described in the manufacturer's handbook.

2.13.9 cDNA synthesis (Superscript® II Invitrogen)

cDNA was synthesised by reverse transcription, using the 1st strand cDNA synthesis Superscript® II reverse transcriptase kit according the manufacturer's protocol. 1.5 µl of Oligo (dt) 24 was added together with 1 µg of RNA and 1 µl of dNTP mix, and made up to 12 µl with RNase free water. The RNase inhibitor used was RNasein (Promega). cDNA stored at -20 ^{o}C.

2.13.10 Measuring the concentration of DNA and RNA

DNA was diluted 1:100, and RNA diluted 1:200 with DEPC treated water. The absorbance of the samples was measured with a spectrophotometer (Jenway 6305) at a wavelength of 260 nm in a quartz cuvette. The concentrations were then calculated given that an RNA solution of concentration 40 µgml^{-1}, and DNA of 50µg ml^{-1}, has an absorbance (OD_{260}) of 1.0.

2.13.11 DNA agarose gel electrophoresis

Agarose gels were made in 0.5x TBE by dissolving in a microwave. In all cases 1 % agarose gels were used unless otherwise specified. The molten gel was then cooled and 0.5 µgml^{-1} ethidium bromide added for subsequent visualisation before setting. For estimation of molecular weights, all DNA was run next to a 1kb DNA marker (Invitrogen) with bromophenol blue loading buffer. To visualise DNA during the electrophoresis, samples were run with loading buffer (Bromophenol blue runs ~300 bp or Xylene cyanol, runs at ~4000 bp). Biorad or Hybaid electrophoresis kits were used. Images of gels were captured using a FluorS Multi-imager and analysed using Quantity One software.

2.13.12 RNA agarose gel electrophoresis

RNA gels were prepared, run and visualised as for DNA gels. RNA samples were run with RNA loading dye (Invitrogen) at a ratio of 1:1. Samples were mixed and incubated at 65 ^{o}C prior to loading on the gel to remove secondary structures of RNA.

2.13.13 Cloning

2.13.13.1 Polymerase Chain Reaction (PCR)

PCRs were carried out as described in 2.13.23. For cloning of fragments into vectors, primers were designed with specific restriction digest sequences at the end.

2.13.13.2 Extraction of digested or amplified DNA from agarose gels

Gels were visualised under minimal UV light to cut out desired gel fragments. DNA was then extracted as using a gel extraction kit as stated in the manufacturer's protocol (Qiagen).

2.13.13.3 Ligation of DNA fragments into vectors

pDRIVE (Qiagen)

A 3.85kb vector used for general cloning. For ligation, 2-4 µl of purified DNA insert was mixed with 1µl of pDRIVE vector and 5 µl of 2x ligation buffer. Samples were incubated overnight (o/n) at 15 ^{o}C. This vector permits ampicillin and kanamycin selection in addition to blue/white screening of colonies containing the fragment of interest (X-gal).

pET21-b (Novagen)

A 5.4kb expression vector containing a T7 promoter, under the regulation of the Lac operator (*lac*I), which allows expression to be induced in the presence of isopropylthio-β-D-galactosidase (IPTG). Downstream of the insert are six repeats of the CAC codon encoding a hexahistidine tag to a protein translated from the expressed insert. This allows for easier purification and identification of the protein. Also includes ampicillin resistance. For these experiments inserts were designed with *NdeI* and *XhoI* restriction sites for insertion. For

ligation, 7 µl of purified insert was added to 1 µl of vector, 2 µl ligation buffer, and 0.2 µl of T4 DNA ligase (Invitrogen). This was incubated o/n at 15 ^{o}C.

2.13.14 Preparation of competent cells

Excluding BL21 (DE3) cells ordered as ready-competent (Novagen), all other *E.coli* strains were made competent by the following method. Strains were stored as glycerol stocks, which were streaked on a plate and grown o/n at 37 ^{o}C. LB medium (10ml) was inoculated with a single colony and grown o/n at 37 ^{o}C. Subsequent to this 100 ml of LB was inoculated with 200 µl of the o/n culture into a 250 ml conical flask, and grown for a further ~3h at 37 ^{o}C. The optical density of the culture was measured at $OD_{550,}$ and cultures of 0.3-0.4 chilled on ice for 10 min before transferring to cold 250 ml centrifuge flasks. Samples were centrifuged (SORVALL® RC26) at 3000 rpm for 5 min at 4 ^{o}C to pellet the bacterial cells. The supernatant was immediately discarded and the cells were resuspended in 20 ml TFBI buffer by gentle swirling. Cells were then incubated on ice for 2 h and centrifuged at 3000 rpm for 5 min at 4 °C. Following this, the cells were re-suspended in 4 ml TFBII buffer and left on ice for 1h. The cells were then aliquoted by pipetting into microfuge tubes using cut tips, so as not to disturb the cells. Aliquots were subsequently snap frozen in liquid nitrogen and stored at -70 °C prior to use.

2.13.15 Transformation of E.coli bacterial cells by heat shock

To a 50µl aliquot of competent cells incubated on ice for 10 min, 2x 2 µl of the ligation reaction from pDRIVE, or 1 µl of ligation mixture from pET21b was added, and gently mixed by stirring. Cells were left on ice for 30min to recover before heat shocking at 42 °C for 45 seconds. After a 2 min recovery on ice, 200 µl of LB medium was added to the heat shocked culture and subsequently transferred to a 15ml falcon tube containing 400 µl of LB. Tubes were incubated at 37 °C for approximately 40 min, shaking at 200 rpm. Cells were then plated on LB agar plates with appropriate selective media, and grown inverted o/n at 37 °C.

2.13.16 Selective media

Bacterial cells were plated on LB agar with appropriate selective media. Ampicillin, and/or Kanamycin, was added to the agar prior to setting to a final concentration of 100 μg/ml^{-1} and 50 μg/ml^{-1} respectively. For blue/white selection, 40 μl of 40 μg/ml^{-1} 5-bromo-4-chloro-3-indolyl-β-D-galactosidase (X-gal) was spread onto plates, and allowed to dry before plating cells.

2.13.17 Boil preparations

This was used to extract crude DNA to check for the presence of a fragment of interest in transformed cells. Cultures of 10ml LB broth were inoculated with a colony from a transformation plate and grown o/n at 37 °C shaking at 200 rpm. To pellet the cells, 1 ml of culture was then centrifuged at 13,000 rpm for 1 min. The supernatant was removed and cells resuspended in 120 ml of STET buffer (8 % Sucrose, 5 % Triton x100, 50 mM EDTA, 50 mM Tris pH 8) and 10 μl of lysozyme (10 mg/ml) was added with this and samples incubated in a 100 °C water bath for 1 min to lyse the cells. Tubes were centrifuged for 10 min at 13,000 rpm to remove cells. The pellet was removed and 250 ml of 100 % ETOH together with10 μl 3 M sodium acetate added to precipitate DNA. Samples were centrifuged at 13,000 rpm for 10 min at 4 °C. The supernatant was removed and pellets allowed to air dry for ~10 min before re-suspending in 100 μl RNaseA 40 μg/ml.

2.13.18 Restriction digests

Restriction enzymes were obtained from either New England Biolabs, or Fermentas. Digests were carried out in appropriate buffers supplied with the enzymes. The plasmid DNA was digested at 37 ˚C for approximately 30 min-2 h for DNA from boil preparations, or o/n for other uses. Restriction enzymes were not removed by heat denaturation or phenol/chloroform extraction, unless otherwise stated.

2.13.19 Colony PCR

Allows for the amplification of a fragment of interest directly from a colony, and was used to detect the presence of an insert from transformed cells. A colony was suspended in 50 μl of

water and boiled for 1 min to lyse cells. This could then be used in a PCR, with primers and PCR programme specific to the fragment to be amplified.

2.13.20 Preparation of plasmid DNA for sequencing

To obtain clean DNA for sequencing, a DNA extraction using a Wizard Plus SV kit (Promega), which uses a silica column method, was carried out according to the manufacturer's instructions. Cultures were grown as for the boil preparations and 8ml of culture centrifuged at 3,500 rpm for 10 min for extraction of DNA.

2.13.21 Sequencing of DNA

Sequencing reactions were carried out using plasmid to profile by the Functional Genomics Laboratory in The University of Birmingham. The DNA template and primer mix were made up to 10µl and loaded onto a sequencing plate:

200-600ng Plasmid DNA template
1µl Primer* (3.2 pmol μl^{-1})
xµl SDW (to 10µl total)
(*M13 forward, M13 reverse, T7 promoter).

2.13.22 Sequence analysis

Sequences supplied from the genomics laboratory were analysed using the programme Chromas. Further programmes were used for sequence manipulations (stated in appendix 1). To perform homology searches the programme BLAST, available from the National Centre for Biotechnology Information at www.ncbi.nlm.nih.gov, was employed.

2.13.23 PCR Techniques

PCRs were used to amplify gDNA, cDNA, and plasmid DNA. To amplify the DNA, Reddymix Taq polymerise (Invitrogen) was used for fragments with an overhang, and JumpStart Taq Reddymix (SIGMA) used when highly accurate results were needed (i.e.

removal of non-specific bands); for example for Inverse PCR. Most reaction mixtures were made up to a 20 µl volume as follows:

10 µl Taq polymerase
9 µl Primer mix (final concentration 2 pmol/µl)
1 µl DNA

The PCR techniques which used this reaction mix were:

- PCR amplification for cloning
- Genotyping T-DNA knockout lines
- Reverse Transcription PCR

The cycling conditions used to run the PCR varied according to the fragment being amplified. A general profile of a PCR reaction is shown in **Table 2.5**.

Temperature (^{0}C)	Time (min)	Number of Cycles
93	2	1
93	0.5	35
*	1	
72	1	
72	10	1

Table 2.5: PCR cycling conditions. Shows the times of each temperature and number of cycles performed. Annealing temperature varied depending on the specific fragment to be amplified (*).

The annealing temperature for the primers varied according to the melting temperature (T_m) of the primers. This was set 4 °C below the melting temperature of the primers in genotyping PCRs. For all other PCRs, the annealing temperature was set to the same temperature as the lowest T_m primer. The time of elongation (72 °C) varied according to the length of fragment to be amplified. 1 min was routinely used, but times of up to 3.5 min were performed in cases where longer length fragments were amplified; e.g inverse PCR.

2.13.24 PCR Primers

For all PCRs primers were designed and supplied by MWG. See **Appendix 8.2** for a table of primers used together with sequences.

2.13.25 Inverse PCR

A technique used to specify an unknown sequence adjacent to a known sequence e.g. determine the sequence next to a T-DNA insertion site and therefore the location of the T-DNA insertion. DNA extracted using the Phytopure method is used. DNA is digested with a particular restriction enzyme found in the known sequence; in this case, either *SacI, PstI, or XmaIII* was used. The reaction mixture was made up to 100 µl (40 µl DNA, 10 µl 10x digestion buffer (specific to each enzyme), 1 µl enzyme, 5 µl spermidine 40mM, and 44 µl of water) and incubated overnight at 37 ^{o}C. Following this, the digestion reaction is heated at 70 °C for 20 min to denature the enzymes, and a phenol-chloroform extraction carried out to remove the enzymes. The DNA is then permitted to self ligate, by setting up a dilute ligation reaction (100 µl DNA, 40 µl 5x T4 ligase buffer, 3 µl T4 ligase, 57 µl water), which is incubated at 16 °C o/n. A PCR was performed on this ligated DNA, with a second round using nested primers. For the first reaction 5 µl of DNA was added to 5 µl primer mix, and 10 µl of Taq polymerase; for the second reaction 5 µl of DNA from the first reaction was added to 10 µl Taq, and 10 µl of primer mix. The PCR cycle used for each reaction was (93 °C x 2 min, 1 cycle; 93 °C x 30sec, 56 °C x 1 min, 72 °C x 3.5 min; 72 °C x 10min, 1 cycle). The primers pARTF2 and pARTR2 were used for the first reaction, and pARTF1 and pARTR1 for the second reaction.(for sequences see **Appendix 8.2**).

2.13.26 Thermal asymmetric interlaced PCR

This technique was also used to determine an unknown sequence adjacent to an insert site. DNA extracted using the phytopure method was used. PCR were carried out as described in Liu and Chen, (2007). For primer design, see **Appendix 8.2**. This method uses annealing of random adapter primers to the unknown region in an asymmetric PCR. Products from the first reaction were amplified using nested primers in a further 2 reactions. The specific primers used in these reactions were, pARTRBR3, pARTRBR2, and pARTRBR1 respectively. These

were used in conjunction with one of the degenerate adapter primers AD1, or AD2. The primers AD3i, AD4i contained inosine, which binds to any base, whilst the other primers contained a mixture of different sequences. (Sequences, **Appendix 8.2**).

2.13.27 Real-time PCR (Sensimix Dt kit Quantace)

This technique was utilized to quantify changes in gene expression. This technique employs a fluorescent dye reporter. In this case the fluorophor SYBR® green was used, which upon binding of double-stranded DNA emits a fluorescent signal. Each round of amplification results in a doubling of DNA and fluorescence.

2.13.27.1 Primer design and validation using the standard curve method

Primers were designed using the Primer Express design programme (ABI Applied Biosystems) using default parameters to search the area of the gene, and primers most suitable. Amplicon sizes ranged from 100-130bp in length, which is within the recommended region for real-time PCR analysis. The annealing temperatures of primers were also kept within 2^{o}C of one another. In all cases, at least one of the primer pairs was designed to span an exon-exon junction to prevent amplification of genomic DNA. For this study primers were designed for the genes *Actin-2*, which was used as an endogenous control, and *SPO11-1*, and *SPO11-2* as target genes. See **Appendix 8.2** for primer design.

Due to the fact that SYBR® green binds any double-stranded DNA, it is important to ensure that primers do not amplify non-specific products, which would affect levels of fluorescence. It is also important to ensure that primer efficiency does not alter over a range of target concentrations. To validate each set of primers, real-time PCRs using the standard curve method were employed. A series of 10-fold dilutions of wild-type cDNA were used in reactions, from 100ng to 0.1ng of DNA in triplicate. Reaction mixes were made up as per the manufacturer's instructions, with primers at a final concentration of 300nM each. Samples were loaded on a 96-well plate and run using the default thermocycling conditions (95 ^{0}C x 10min: 1 cycle, 95 ^{0}C x 15sec, 60 ^{0}C x 1min: 40cycles) using an ABI PRISM 7000 (Applied Biosystems). Subsequent to the run, dissociation curves were performed on each well. This

involves melting of PCR products; with different products having different melting temperatures. If more than 1 product is detected, this indicates the primers amplify a non-specific product. A standard curve is generated for each set of primers. To ensure that primers amplify with the same efficiency over different target concentrations, the standard curve must be linear. R^2 should be equal to or greater than R^2 0.985. The efficiencies of each set of primers should be similar. Ideally, the slope of the curve should fall between -3.1 and -3.6 for 90-110% efficiency. See **Appendix 8.3** for standard curves and dissociation curve analysis for each set of primers.

2.13.27.2 Relative quantification and data analysis using the comparative Ct method

For measuring the relative levels of gene expression between different samples, the relative quantification method was employed. In this case, each sample was amplified using each set of primers in triplicate. Reaction mixes were set up as per the manufacturer's instructions, with 20ng of cDNA used as a target in each well, together with a final concentration of each primer at 300nM. For this, an endogenous control was specified as *Actin-2*, and *SPO11-1*, and *SPO11-2* genes specified as target genes for relative quantification. Thermocycling conditions used were the same as for the standard curve method.

To analyse the results the comparative Ct method was used. This utilizes an arithmetic formula to calculate the relative quantity of the target gene's expression in comparison to a calibrator sample; in this case wild-type. The calibrator is assigned an arbitrary quantity of '1'; with other samples expression expressed as a fold difference from the calibrator (corresponds to a real difference). The amount of the target gene is also normalised to an endogenous control (*Actin-2*), which should not vary between samples. The relative quantity is calculated using the formula = $2^{-(\Delta\Delta Ct)}$. Where the Ct value denotes the threshold cycle at which the fluorescence passes the threshold level. This level is set at the region on the amplification curve, where increase in fluorescence is exponential (See **Figure 2.2**). The average Ct values are calculated for each gene, and the average Ct for the endogenous control is subtracted from the average Ct for the target gene to give the ΔCt. The ΔΔCt value is subsequently calculated by subtracting the ΔCt for the calibrator from the ΔCt of the target sample.

2.14 Protein manipulations

2.14.1 Production of recombinant proteins

Regions of the POT proteins to be expressed were amplified by PCR and cloned into pDRIVE to check the sequence was correct and in frame. The insert was then sub-cloned into the pET21b expression vector, which when translated, adds an N-terminal hexa-histidine (HIS) tag. This was transformed into the BL21 expression cells.

2.14.2 Testing expression and cellular localisation

Small-scale protein extractions were performed on transformed *E.coli* to determine the cellular localisation of the recombinant protein (soluble or insoluble) and to determine the optimum growth conditions for expression. Cultures were grown in 250 ml flasks containing 50 ml of LB medium (Ampicillin 100 μg/ml) inoculated with 1 colony, and allowed to grow at 37 °C o/n shaking at 200rpm. Flasks containing 50 ml of fresh LB medium were then inoculated with 200 μl of overnight culture and grown at 37 °C to $O.D._{600}$ ~0.6 before inducing with IPTG to a final concentration of 1mM and growth continued at 37 °C. These conditions were used unless otherwise stated. For test induction, 1 ml of culture was centrifuged at 13,000 rpm for 1 min to pellet cells. Samples were collected at a number of intervals post induction to determine the ideal time for induction. If expression was low, the growth conditions before induction were altered and tested. Pelleted cells were re-suspended in 75 μl of BugBuster containing benzonase at 1 μl ml^{-1} (Novagen), and incubated at RT for 30 min prior to centrigugation at 13,000rpm for 10 min. The supernatant (soluble fraction) was transferred to a new microfuge tube and placed on ice. To the pellet (insoluble fraction) 75 μl of water was added and resuspended. Protein loading buffer (5x) was mixed with both samples and boiled for 5 min before analysing on an SDS-PAGE gel.

2.14.3 Large scale protein purification

2.14.3.1 Purification of recombinant protein from inclusion bodies

Large-scale expression and purification was performed to obtain enough protein for antibody production. A 50ml culture was grown o/n as for the small-scale test. 2 flasks of 2 L each

containing 1 L of LB medium (Ampicillin 100 μg/ml) were inoculated with 1ml of o/n culture and induced with IPTG 1mM when cultures reached $O.D._{600}$ ~0.6. Recombinant protein expression was allowed to occur for 4 h and then centrifuged in large 250 ml centrifuge flasks in a (SORVALL® RC26) for 10 min at 5000 rpm at 4 °C. For each 1 L of culture pellets were re-suspended in 200 ml of cold lysis buffer by gentle swirling. Samples were then centrifuged as before and pellets re-suspended in 20 ml lysis buffer per 1 L of culture. To this, 400 μl of 10 mg/ml lysozyme and 50 μl of 100 mM PMSF were added. These were subsequently incubated at 4 °C for 1.5 h. Sodium deoxcholate (26 mg) was added together with 25 μl of 100 mM PMSF. Following this, cells were sonicated (7x 30 sec) with 30 seconds on ice between pulses to prevent warming. Samples were subsequently centrifuged at 14,000 rpm (SORVALL® RC26) for 30 min at 4 °C, and the supernatant discarded. These crude inclusion body isolations can then be stored at -20 °C until the next step. The inclusion bodies were washed by re-suspension in 20 ml of lysis buffer with sonication and centrifugation approximately 5-7 times until pellet appears white with black spots. To isolate the recombinant protein from the clean inclusion bodies they are re-suspended in 5 ml of 6 M guanidine HCL and 500 mM cysteamine (2-mercaptoethylamine) by gentle shaking for 2 h at RT. Samples are centrifuged at 500 rpm for 15 min at 20 °C and supernatant kept. The protein concentration can then be estimated.

2.14.3.2 Refolding of the recombinant protein

With constant gentle stirring 200 μl aliquots of protein are added to cool (10-15 °C) refolding buffer with the pipette tip immersed. The protein is diluted 1:100 with refolding buffer. The buffer was incubated at 15 °C, and half the protein added. This was left for at least 1h before the second half was added. The refolding protein was incubated at 15 °C o/n. The refolded protein was subsequently dialysed in 12-14 kDa tubing against 3 changes of dialysis buffer with stirring (50 mM Tris, 100 mM NaCl, 2 mM EDTA pH 8).

2.14.3.3 Concentrating the recombinant protein

Dialysis tubing was immersed in ~100 ml of dialysis buffer, and solid PEG6000 sprinkled over the surface. This was left shaking at RT and checked every hour until the protein reached

a suitable volume. The concentration of the protein was measured, and when the necessary concentration reached, the protein was divided into 1ml aliquots, snap frozen in liquid nitrogen, and stored at ⁻80 °C.

2.14.3.4 Purification of protein using cobalt IMAC resin (TALON beads)

To optimise the protocol to give the most efficient purification, test batch purifications were performed according to the manufacturer's instructions. Imidazole was used for the final elutions, as this was found to be more effective than pH elution. For the final large scale extraction of the POT1b-HIS recombinant protein, 2x 1 L of LB was inoculated with 10 ml of o/n culture, grown to an $O.D_{600}$ of 0.6, and protein expression induced with 1mM IPTG for 4 h. The culture was then centrifuged at 5,000rpm (SORVALL® RC26) for 10 min at 4°C to pellet the cells. The pellets were re-suspended in 20 ml of denaturing buffer per 250 ml of culture. These were then incubated at RT for 20min with gentle shaking. Denatured samples were sonicated 7x 10sec, with 30sec on ice between to prevent heating the samples. When a less viscous/translucent solution was obtained, samples were centrifuged at 18,000 rpm for 30 min to pellet unwanted material. A sample before centrifugation (lysate) and after (cleared lysate) was taken for subsequent analysis. The cleared lysate was then incubated with the TALON HIS tagged beads. The beads were first washed in wash buffer, and the buffer removed to leave a 50:50 mixture, which was re-suspended using a pasture pipette. The cleared lysate was then transferred to this. For each 1 L of culture 4 ml or resin was used. For binding of the protein to the resin, samples were incubated for 60 min at RT with gentle shaking to prevent the beads pelleting. Following this, the beads were washed 4 times in denaturing buffer (~10x the amount of beads). To elute the protein from the beads 4 elutions were carried out with 150 mM Imidazol, and a further 2 with 250 mM Imidazol in elution buffer The eluate was then pooled for dialysis (see previous method). After each step of the protocol, a sample was taken for analysis by SDS-PAGE electrophoresis.

2.14.4 Measuring protein concentration

A Biorad assay was performed according the manufacturer's instructions. Bradford reagent was added to protein samples at a specified amount and concentration estimated by spectrophotometer readings at 595 nm, using BSA 10 mg/ml as a standard.

2.14.5 Extraction of protein from buds using PEB

A 1.5 ml microfuge tube was half filled with buds and 200 µl of protein extraction buffer (PEB) added. A pestle was used to homogenise the buds. Subsequent to this, the homogenate was centrifuged at 13,000 rpm for 1 min the pellet the debris. To this, 5x protein loading buffer was added and boiled for 5 min. The protein was resolved by SDS-PAGE electrophoresis.

2.14.6 Extraction of protein from buds using TCA

To extract protein from buds, a 1.5ml microfuge tube was filled with small buds (0.2-0.3mm), in the aim of extracting meiotic proteins. The buds were ground down using a pestle in liquid nitrogen. To this, 200µl of acetone, 10% trichloroacetic acid (TCA), 20mM DTT was added and incubated at $^{-}20\ ^{o}C$ o/n. This was subsequently centrifuged at 13,000 rpm for 15min. The supernatant was removed and the pellet rinsed with acetone, 20mM DTT. This was incubated at $^{-}20\ ^{o}C$ for a further 2h and centrifuged as previously. The supernatant was removed, and the pellet air dried. The pellet was then re-suspended in 5x protein loading buffer. Protein extracts were resolved by SDS-PAGE electrophoresis.

2.14.7 SDS-Polyacrylamide gel electrophoresis

Proteins were analysed using the sodium-dodecyl-sulfate polyacrylamide (SDS-PAGE) gel Biorad 3rd generation self-assembly kits. To cast the gels the resolving gel is made first (Table 2.6) and 7 ml poured into the glass plates. A layer of absolute butanol is then added before the gel is left to set. The butanol is rinsed off prior to adding the stacking gel (2.5 ml), and a comb containing wells of the appropriate size inserted before the gel is allowed to set. For both gels the TEMED is added immediately prior to pouring as this causes the gel to polymerise quickly. The gel tank was assembled as described in the manufacturer's instructions. Proteins to be loaded were mixed with 5x protein loading buffer, and boiled for 5 min prior to loading. Gels were run with a protein weight marker (Sea Blue, Invitrogen) in 1 x reservoir buffer at 80 V to allow proteins to enter the gel, and 150 V subsequent to this.

To visualise the proteins, the gels were labelled with coomassie blue stain for 10min subsequent to warming, and destained for in destain solution. Gels were immersed in gel drying buffer and preserved between cellophane sheets.

	Resolving gel		Stacking gel
	10%	**15%**	
SDW	6.1ml	3.6ml	3.0ml
Resolving buffer (1.5M Tris, pH8.8)	3.75ml	3.75ml	
Stacking buffer (1.0M Tris, pH6.6)			1.25ml
Acrylamide (Protogel)	5.0ml	7.5ml	625 µl
10% (w/v) Sodium dodecyl sulphate (SDS)	150µl	150 µl	50 µl
15% (w/v) APS	75 µl	75 µl	25 µl
TEMED (Sigma)	15 µl	15 µl	5 µl
Final volume	15ml	15ml	5ml

Table 2.6: Components of resolving and stacking gels and their amounts. Different percentage resolving gels are used for analysis of different weight proteins. 10 % used for small proteins of ~15 KDa.

2.14.8 Western blotting

2.14.8.1 Protein transfer

Following resolution of the proteins by SDS-PAGE the stacking gel was removed. The western apparatus was then assembled with the gel according to the manufacturer's instructions (Biorad). Proteins were transferred to a nitrocellulose membrane (Hybond-C extra, Amersham) in most cases. For antibody affinity purification proteins, were transferred to PVDF membrane (Hybond-P Amersham), which has to be soaked in methanol prior to use. The western was transferred in protein transfer buffer. An ice block was also placed in the tank to prevent the solution getting too hot. Biorad power packs were used to blot the gel at 400 mA for 1 h. Subsequent to transfer, the nitrocellulose membrane was removed and placed in milk blocking solution at 4 ˚C o/n.

2.14.8.2 Antibody labelling

Following blocking the primary antiserum was added directly to the block and incubated at RT on a desk top shaker for ~1h. The membrane was then washed 2x in 1x PBS. A secondary antibody conjugated to either alkaline phosphatase or horse radish peroxidase (HRP) was then added at the appropriate concentration, and incubated as before for 1 h in block. The membrane was washed again as previously described prior to antibody detection.

2.14.8.3 Enhanced chemiluminescence (ECL) detection

The membrane was treated with ECL reagents according to the manufacturer's instructions (GE Healthcare). Blots were analysed using the FluorS Multi-imager and Quantity One software (Biorad) or exposed to photographic film for 45min. Photographic films were exposed using an AGFA CURIX 60 Xograph.

2.14.8.4 Alkaline phosphatase detection

The membrane was immersed in a solution of [NBT (66 µl) (NBT, 70 % (v/v) DMF) and 33 µl BCIP (BCIP, 100 % (v/v) DMF) was added to 9.9 ml alkaline phosphatase detection buffer

(100 mM NaCl, 5 mM $MgCl_2$, 100 mM Tris, pH 9.5)], and visualised for appearance of bands.

2.14.9 Affinity purification of POT antibodies

Approximately 0.4 mg of POT1b protein was loaded into a 15 % SDS-PAGE gel with 1 large well and run as previously stated. The protein was transferred to PVDF membrane by western blot, and stained with coomassie to label to protein. The band of interest was cut out and sliced into small strips, which were incubated in block (1x PBS, 0.1 % teen 20, 2%BSA) in a 15 ml falcon tube on a rotor (gently) for 30 min at RT. The strips were subsequently washed 2 times in 1x PBS, 0.1% TWEEN 20, each for 10 min. This was followed by incubated of the strips with the anti-serum (1:4 with 1 x PBS) for 2h at RT shaking gently. The serum was then removed and the strips washed 4x 5min (1 x PBS, 0.1% TWEEN 20), 3 x 5 min (1M KCL, 20 mM Tris pH 8), and 3x 5min (1x PBS only). To elute the bound antiserum from the strips, they were mixed with 1ml of 100 mM glycine pH 2.5 on a rotor for 15 min (removes antibodies bound by acid sensitive interaction). The strips were transferred to a fresh tube containing block, and 100µl of 1M Tris pH 8.8 added to the eluate to neutralise it. To this, BSA was added to a concentration of 1 % and dialysed o/n in 50 mM Tris pH 8 and 150 mM NaCl. The purified antiserum then only contains antibodies to the protein of interest, removing all background proteins. This was then aliquoted and stored at -20 °C.

2.15 Statistical procedures

All statistical procedures described were carried out using MINITAB 15 software.

Chapter 3

Investigating crossover control and pairing using SPO11-1 RNA interference

3.1 Introduction

Meiotic recombination is initiated by the formation of DSBs by the protein SPO11. The number of these crossover initiating events exceeds the number of eventual crossovers formed. How a subset of these initiating events is directed towards a crossover fate is a focus of current research. A small number of DSBs are directed to form a reciprocal crossover, with the remainder repaired as non-crossovers. This decision has been proposed to occur prior to formation of stable strand exchanges (See Bishop and Zickler, 2004 for review).

It is thought that the selection of recombination intermediates towards a crossover fate may involve progressive selection by certain proteins, for example the AtMSH4/MSH5 heterodimer, which may stabilise recombination intermediates (Higgins, 2004). It is also thought that the number of DSBs may affect the frequency of crossovers. Martini et al, (2006) found that in budding yeast, reducing the number of DSBs using a series of *spo11* allelic mutants did not result in an subsequent reduction in crossover frequency. It was observed that the ratio of crossover/non-crossover was altered to maintain the frequency of crossovers, which was termed crossover homeostasis (**Figure 1.3**). This suggests that the number of DSBs may not be important in the control of crossover frequency. The ratio of DSBs to crossovers varies between species; it will therefore be interesting to study whether crossover homeostasis is a conserved mechanism between other eukaryotes. It has been observed in a number of organisms including *Arabidopsis*, that pairing and synapsis of homologous chromosomes is dependent on DSBs (Grelon et al, 2001).

This chapter describes the study of the crossover/non-crossover decision in *Arabidopsis*. The effect of reducing double strand breaks on this decision was studied by reducing the expression of *SPO11-1*. An RNA interference (RNAi) construct was developed in our laboratory, to the *SPO11-1* gene. The aims were to establish whether crossover homeostasis is observed in this organism, and to determine how reducing DSBs affects crossover control; for example formation of the obligate crossover and interference. In addition to this, the dynamics of chromosome alignment and synapsis were investigated. Including analysis of how many DSBs are required for pairing and synapsis, and if this is not achieved, how does this affect meiotic progression.

3.2 RNA interference

RNA interference (RNAi) is used to disrupt expression of a target gene. It involves the introduction of double stranded RNA based on the target sequence. A pathway is then activated, which results in the degradation of the corresponding mRNA. This can result in a null or hypomorphic phenotype. An RNAi construct specific to the *SPO11-1* gene had been previously made in our laboratory in the vector pHANNIBAL, which was ligated into the binary vector pART27 conferring kanamycin resistance, as shown in **Figure 3.1 A** (J.D. Higgins, personal communication). The construct was transferred to *Agrobacterium tumefaciens LBA4404* by electroporation prior to transformation of wild type *Arabidopsis* Col-0 by floral dip. Plants that had taken up the construct were selected by growth on kanamycin plates, and those with reduced fertility selected for subsequent investigation (J.D. Higgins, personal communication).

3.3 Isolation and characterisation of T-DNA insertion line *spo11-1-4*

A number of SPO11-1 mutants have been characterised in *Arabidopsis* to date. Of these, *spo11-1-3* has recently been shown to be null (Sanchez-Moran, et al 2007). For a comparison to the *SPO11-1* RNAi lines a null mutant was needed as a control. However, the lines previously characterised as null are no longer available, which led to the search for another mutant. The NASC database was screened for T-DNA insertions in the *AtSPO11-1* gene (At3g13170), and a Wisconsin line (WiscDsLox461-464J19) was found to be located in Exon 14 of the gene (shown in **Figure 3.1B**). The seeds were grown against a wild type control of Col-0 and primers designed either side of the T-DNA to genotype plants for the insertion site. DNA was extracted from each plant using the plant Extract-N-Amp kit (SIGMA), and two sets of reactions were performed. A reaction with wild type primers (SPO11F4 and SPO11EXPR1) spanning the insertion site and a reaction with the T-DNA left border primer (SPO11EXPR1 and WISC-LB), were carried out to check for the presence of an insert. The products of this reaction are shown in **Figure 3.1C**. This then gave a heterozygous and homozygous line for analysis.

3.4 Preliminary analysis of transformed lines

To confirm the presence of the construct in the selected lines, PCR was carried out with a primer set designed to amplify the intron of the pHANNIBAL construct, as this sequence is unique to the construct. The products of this PCR were analysed by agarose gel electrophoresis, and subsequently cloned and sequenced to ensure the primers amplified the correct region. Plants from the T_2 generation were used for this preliminary analysis. Only those plants that contained the construct were utilized for further analysis. To verify the number of insertion sites of the construct, fluorescence *in situ* hybridisation was carried out on a select number of plants from each line, using a probe of the construct conjugated to a DIG label. **Figure 3.2** below shows an example of this. It illustrates that in line 16C plants contain one heterozygous insert, as indicated by a single focus. It was found that line 7A contained 1 homozygous insert, and that all the other lines analysed contained one homozygous insert, and one heterozygous insert, which would be able to segregate in a Mendelian fashion in the next generation. The plants were numbered from the first (T_1) generation, with the number indicating the original line, and the letter the individual plant from which the seeds were collected.

The levels of *SPO11-1* expression, together with the chiasmata frequency and fertility of the lines, were initially assessed in order to select a range in phenotype for final detailed analysis.

3.4.1 SPO11-1 RNAi plants develop normally but exhibit reduced fertility

The *SPO11-1* RNAi lines were first screened for reduced fertility. This is indicative of a meiotic phenotype, as observed in a number of meiotic mutants (Caryl et al, 2003). As illustrated in **Figure 3.3** (a), vegetative growth appears morphologically normal until seed set, where silique length is observed to be reduced compared to wild-type. A closer view of this phenotype is shown in **Figure 3.3** (b-c), which shows that in the null *spo11-1-4* knockout, silique length is greatly reduced. The images illustrate that the *SPO11-1* RNAi lines exhibit a range in silique length, showing that the construct affects the fertility to varying degrees between lines. To quantify these differences seed counts were taken from each line; with ten siliques counted from each plant. A varying number of plants was analysed for each line. The mean seed number was calculated and is shown in **Figure 3.4 A**. A range in the number of seeds per silique was observed from wild type levels to approximately 30 % of wild type. This data corroborates the observations from the images shown in **Figure 3.3**.

3.4.2 Lines show a reduction in chiasma formation

The chiasma frequency was analysed to establish whether the reduced fertility was due to a reduction in the number of crossovers. If the construct reduces the activity of *SPO11-1*, a range in the number of chiasmata should be observed. A random sample of plants was selected for the counts, based on a range in silique length. Spread meiotic nuclei slides were made from these plants and the chromatin labelled with DAPI. Images of metaphase I chromosomes were subsequently captured for chiasma counts. The results are shown in **Figure 3.4 B**, which illustrates the mean number of chiasmata at metaphase I, for individual plants. The RNAi lines show a range in the number of chiasmata, as was seen for the fertility levels. This suggests that the reduction in chiasma frequency affects fertility. A number of physical connections were observed between bivalents on the metaphase I nuclei. These connections may indicate that the reduction of DSBs causes pairing defects, which may contribute to the reduction in fertility observed. For further analysis, a number of these plants were selected based on a range in the number of crossovers. Seed was collected from plants 12R, 13C, 8A, 10F, 16C, and 7A.

3.4.3 SPO11-1 expression is reduced compared to wild-type

The expression levels of the *SPO11-1* gene were analysed to determine whether the construct was having an effect. For this T_3 plants were analysed. Reverse transcription PCR in a two step reaction was employed. RNA was extracted from influorescences from each line and a wild-type Col-0 control using Trizol RNA extraction solution (Invitrogen). For each sample approximately five inflorescences were taken, with only one plant from each line analysed. Plants with the shortest siliques were analysed, to look for a significant difference in expression levels between plants. The concentration of RNA in each sample obtained from the extraction was estimated by combining data from spectrophotometer readings $O.D._{260}$ and the peak band intensity of RNA resolved by agarose gel electrophoresis. The RNA was DNaseI treated (Invitrogen) to remove any gDNA, which if present would be amplified during the PCR. Following this the RNA was reverse transcribed to cDNA using the superscript II reverse transcriptase (Invitrogen), with an oligo dt-24 primer. This was subsequently used for the PCR with gene specific primers, SPO11-1EXPF1 and SPO11-1EXPR1. A control of a different meiotic gene (*SPO11-2*) was also amplified with gene specific primers, SPO11-2EXPF1 and SPO11-2EXPR1. SPO11-2 is thought to act together with SPO11-1 but does not have functional redundancy (Stacey et al, 2006), and is therefore expected to be expressed at a similar time during meiosis. It was therefore assumed to have equal levels of expression in all samples taken.

The primers were designed to amplify a 600 bp region of the *AtSPO11-1* gene spanning the site of the *spo11-1-4* T-DNA insert, so that the expression level of this sample could be used as a negative control. The products from this PCR were analysed by agarose gel electrophoresis (**Figure 3.5 A**), and the peak band intensity measured for each sample, in order to quantify the levels of expression in comparison to the wild-type control. From this it was observed that *SPO11-1* expression was variable with the same level of *SPO11-2* in each sample. **Figure 3.5 A (c-d)** shows that for the *spo11-1-4* mutant, no expression of *SPO11-1* is observed, in contrast to the control of *SPO11-2*. This not only shows that the *spo11-1-4* insert is a null mutant, but that the primer sets are specific to their gene of interest. The primers were subsequently shown to amplify specific gene products by cloning and sequencing of PCR products.

The gels in **Figure 3.5 A** also illustrate a second band amplified by the *SPO11-1* primers, which is larger than that predicted. By cloning and sequencing of this band, it was found to contain an intron between exons 12-13. Due to there being 7 introns in the sequence amplified, it was concluded that this was likely a splice variant. This had been previously described by Hartung and Puchta, (2000) who observed a number of splice variants of *SPO11-1* to be present in various different tissues. Therefore the 600 bp band was used to measure the peak band intensity (using the programme Quantity1), which was normalised by the band intensities of the relative *SPO11-2* sample. The expression level of each RNAi line was then calculated as a percentage of the WT expression, which is summarised in **Figure 3.5 B**. The level of *SPO11-1* expression in the RNAi lines shows a range between 50% and 80% of wild-type. These results confirm that expression of the construct results in a reduction in *SPO11-1*. The pattern of expression also correlates with the pattern of reduced fertility and crossover frequency, indicating that the phenotype observed is likely to be a result of a reduction in *SPO11-1* expression. It also shows that the construct causes a hypomorphic phenotype. This provided a range in the level of SPO11-1 activity to study the effects of different numbers of DSBs on the crossover/non-crossover decision.

3.5 Quantifying DSBs

In order to measure the different levels of DSBs between the RNAi lines and be able to calculate the ratio of crossovers/non-crossovers, different methods of quantifying DSBs were compared. These included immunolocalisation using a number of recombination proteins, and western blotting using an antibody to phosphorylated H2AX, which becomes phosphorylated either side of a DSB. A comparison of these techniques is discussed.

3.5.1 Immunolocalisation shows the number of DSBs is reduced in RNAi lines

To confirm that the phenotype observed was due to a reduction in *SPO11-1* activity, and consequently a reduction in the number of DSBs produced, immunolocalisation on spread meiotic nuclei from the RNAi lines, and controls of wild-type Col-0 and the *spo11-1-4* null was performed. Different recombination protein antibodies and an antibody to the phosphorylated form of the histone protein H2AX were compared, to determine which to use for final analysis of the lines. Following formation of a DSB, H2AX is phosphorylated either side of the break over a region of approximately 50kb (Sanchez-Moran et al, 2008). Immunolocalisation of these proteins on meiotic chromosome spreads of zygotene nuclei is shown in **Figure 3.6**. Images (a-c) show immunolocalisation of γH2AX on (a) wild-type, (b) 8A, and (c) *spo11-1-4*. A significant reduction in the number of γH2AX foci can be observed between the wild-type and *SPO11-1* RNAi line 8A. Greater than 100 foci can be observed on the wild-type nucleus, whereas only approximately 40 foci are present in 8A. A control of the *spo11-1-4* null (c) shows no labelling of γH2AX, indicating that the labelling is specific and does not occur in the absence of DSBs. However on some nuclei a few large foci can be observed; for example as that shown in image (c). This may be due to not removing all the cytoplasm during slide preparation. The nuclei are also labelled with an antibody to the ASY1 (shown blue), which allows staging of the meiocytes. ASY1 is an axial element protein (Armstrong et al, 2002).

Images (d-f) show immunolocalisation of the DNA repair protein RAD51 that localises to sites of DSBs. Again, a clear reduction in the numbers of foci can be observed between wild-type (d) and the RNAi line 12R (e). A control of *spo11-1-4* (f) shows that the localisation is specific to sites of DSBs. Immunolocalisation of another DNA repair protein DMC1, which

also localises to sites of DSBs, is shown in images (g-i). No clear difference in labelling can be seen between wild-type (g), RNAi line 8A (h), and the *spo11-1-4* null control (i). This suggests that the localisation is not specific to DSBs and the protein may be present but not localised to the chromatin. This demonstrates that the DMC1 antibody is not sufficient for quantification of DSBs.

3.5.2 Quantifying DSBs by western blotting of bud protein extracts

An alternative approach for measuring the levels of DSBs in each line is to infer this by measuring the relative amounts of the SPO11-1 protein. The levels of *SPO11-1* gene expression suggest that the amount of protein produced would be reduced in the *SPO11-1* RNAi lines; however the levels of expression and amount of protein produced can vary, so it is desirable to be able to quantify the amount of protein produced. To examine whether this is a feasible method, western blots were performed on protein extracts from whole buds from wild-type plants and *spo11-1-4* as a control. Approximately half a 1.5ml microfuge tube of buds of 0.2-0.4cm was collected for the extraction and frozen. Protein was extracted using the TCA method, and the protein re-suspended in protein extraction buffer before adding 5x protein loading buffer. To a 15% SDS-PAGE gel 20µl of each protein sample was loaded with a space of 1 well between samples, to prevent cross contamination of lanes. The gel was subsequently blotted to a nitrocellulose membrane for analysis. Antibodies to γH2AX and SPO11-1 were tested. The γH2AX antibody would allow quantification of the relative levels of DSBs between lines, as H2AX is phosphorylated either side of the DSB, whereas the SPO11-1 antibody would allow quantification of the protein. **Figure 3.7 A** shows a blot using γH2AX (rabbit). A secondary antibody of anti-rabbit HRP was applied, and the blot exposed to photographic film for 45 min. The expected size of H2AX in *Arabidopsis* is 15KDa. From the blot a band can be observed to run at 15KDa in the wild-type sample. However, this is also seen in the *spo11-1-4* lane. This is a null mutant, and therefore does not produce any DSBs. This suggests that this is a non-specific band. A more prominent band can be observed to run at approximately 50KDa. This could potentially suggest that the protein has run in a complex, however this can be ruled out, as proteins have been resolved on a denaturing gel. This band is also seen in the null control sample, which suggests this also to be non-specific background labelling.

This blot was then stripped and re-probed with an antibody specific for SPO11-1 (rabbit). This blot is shown in **Figure 3.7 B**. A number of the bands in this blot correspond to those of the previous blot. This demonstrates that the stripping procedure is inefficient, and that some of the primary antibody remains bound, which means it is detected again as the same secondary antibody was used. There is an additional band, which runs at approximately the expected size of the SPO11-1 protein in the wild-type sample (50KDa). However, this is also

present in the *spo11-1-4* control, showing that this is likely to be non-specific background. The reason that neither antibody was able to detect its respective protein may be due to a low concentration of protein in the sample. Within the sample of extracted proteins, only a small proportion of buds would be at the correct meiotic stage for proteins to be present. The SPO11-1 protein has been shown to interact with the chromatin for only a couple of hours, whereas the level γH2AX has been shown to remain constant for 13 hours by immunolocalisation (Sanchez-Moran, et al 2007). Due to the transient nature of SPO11-1 interaction, this points to γH2AX as a superior method of detection. It may be necessary to extract protein from anthers, and use more material than in this case.

To investigate whether it is possible to use the γH2AX antibody to quantify the relative levels of DSBs between lines, cisplatin was introduced to plants to induce extra artificial DSBs to test the antibody without having to collect vast numbers of anthers, which is time consuming. It was hoped that this would yield enough γH2AX protein to be detected by western analysis, therefore testing whether this could be a potentially useful method for DSB quantification if a method could be found to yield a larger amount of protein from the extractions in future. Cisplatin is a cross-linking agent; the excision of these cross-links creates DSBs (Sanchez-Moran et al, 2007). Stems from wild-type plants were cut under water and given a 2h pulse of 2.5mg/ml cisplatin. All buds from the treated inflorescences were collected immediately after the pulse, and protein extracted using the TCA method. Approximately half a 1.5ml microfuge tube of buds was collected for the extraction. The protein was re-suspended in 5x PLB only, so as not to dilute the sample, and allow the total sample be loaded into 1 well. The protein was resolved by SDS-PAGE gel electrophoresis on a 15% gel, and subsequently blotted to nitrocellulose. **Figure 3.7 C** shows the results of this blot. A control of non-treated bud extracts was not run in parallel due to not having enough plant material. However in comparison to **Figure 3.7 A**, the same bands can be observed. This shows that inducing further DSBs did not produce enough protein to be detected by western blotting. It is likely that the amount of protein that can be extracted using the TCA method on *Arabidopsis* buds is not sufficient for detection. This method was therefore thought not to be suitable for quantification of DSBs. Immunolocalisation of the γH2AX antibody was chosen for further analysis, due to its more specific localisation, and distinct foci.

3.6 Locating insertion sites of the RNAi construct

As previously mentioned, a number of the lines chosen for further analysis have been shown to contain two insert sites; one homozygous and one heterozygous. Line 16C was heterozygous for one insert site. These heterozygous inserts would segregate in a Mendelian fashion in the next generation, resulting in a variation in phenotype between plants in the same line. To obtain homozygous lines for more detailed and accurate analysis, it was decided to determine the locations of these insertion sites, so that the plants could be genotyped. This would allow selection of lines without a segregating insert, and for lines to be crossed. Importantly it would also show that the construct did not insert by chance into a meiotic gene, which could present the same phenotype. To do this two methods were employed; inverse PCR and thermal asymmetric interlaced PCR, as described below (**Figure 3.8**).

3.6.1 Inverse PCR

Inverse PCR (iPCR) is a technique used to amplify an unknown sequence adjacent to a known sequence. It is limited because it requires restriction sites to be present in close proximity to the region to be studied. The right border (RB) of the vector was chosen as the start point for amplification. From sequence analysis the region between the right border and the start of the *SPO11-1* construct was shown to contain three different restriction sites; *SacI, PstI,* and *XmaIII*. For each sample one young leaf was collected from five plants for each line and DNA extracted using the Nucleon-phytopure method. Following this, the DNA was digested with the relevant restriction enzyme overnight. The DNA was then purified using a phenol-chloroform cleanup. The fragments obtained from the digestion were then permitted to self ligate, before amplification of the fragment by PCR. Three PCR primer sets were used to amplify the circularised DNA fragments. One reaction was performed with internal primers and 2 subsequent reactions with nested primer sets carried out. These were pARTR3 and pARTF2, followed by pARTR2 and pARTF2, and finally pARTR1 and pARTF1 (**Appendix 2.2**). The nested primer reactions give more specific amplification. The products from this third reaction were subsequently analysed by agarose gel electrophoresis, as observed in **Figure 3.9 A**. This shows the products from an iPCR using *SacI* digested DNA. Bands which looked unique to a particular sample were then selected for cloning and sequencing. The arrow in **Figure 3.9 A** illustrates an example of this. This band was isolated by gel extraction

and cloned into pDRIVE for sequencing. A gene sequence was found adjacent to the RB of the pART27 vector of the gene At2g28050, which is a gene of unknown function (**Appendix 8.5**). Other bands selected had vector sequence only, hence non-specific amplification.

To confirm this as an insertion site for the line 16C, primers were designed either side of the potential insert site. DNA was extracted from 5 plants using the plant Extract-N-Amp kit (SIGMA). A PCR was carried out to genotype the plants, with one reaction using the WT primer set (WT: SPO1116CF2 and SPO1116CR2), and one reaction with the RB primer of the vector (Insert: SPO1116CR2 and pARTR1). See **Appendix 8.2** for primer sequences. The products of these reactions are shown in **Figure 3.9 B**. The wild-type control sample shows a band amplified by the wild-type primers but not with the primer from the right border, confirming that the primer sets amplify the correct fragments. For the 16C plants, products are shown to be amplified in a number of the plants for insert reaction, which confirms this to be a genuine insertion site of the construct. It can also be seen that plant 3 is heterozygous for the insert, and plants 1 and 4 are homozygous for the insert, showing that this is the segregating insertion site for this line. iPCR has been carried out with the other restriction sites, and has been repeated; however no other insertion sites have been found by this method. This may be due to the limited number of restriction sites available close to the right border. Therefore a second technique was employed, which does not rely on the presence of the restriction sites.

3.6.2 Thermal Asymmetric Interlaced PCR (TAIL PCR)

This technique is also used to determine an unknown sequence adjacent to a known sequence. Nested primers are used in successive reactions as for iPCR. Although it uses degenerate primers to hybridise to the unknown region, unlike iPCR, in which the primers are designed to the known sequence (**Figure 3.8**). The method used was as described in (Liu and Chen, 2007). The first reaction involves a set of low stringency cycles at 25 ^{o}C to permit annealing of the degenerate adapter primer to non-specific sequences. A number of cycles are then performed at the annealing temperature of the primer to the known sequence, to permit amplification of a specific sequence. Two subsequent reactions with nested primers are then carried out to select for the specific sequences between the known sequence primer and the adapter primer.

Figure 3.10 A shows the products from the TAIL PCRs with adapter primer 1 and 2. Products of over 300 bp which appear unique to a sample are chosen for cloning and sequencing, as this is the minimum length required to sequence out of the right border. If bands appear in all lanes, it suggests they correspond to non-specific amplification, for example between right borders of two insert sites. **Figure 3.10 A** shows the 9H band from the adapter primer 1 reaction, and the 16C band from the adapter primer 2 reaction that were cloned and sequenced (bands indicated by the arrows). The 16C band was found to be the insert site found previously by the iPCR method. This confirms the TAIL PCR technique works, and also verifies this to be a genuine insert site. Sequencing of the 9H band revealed a gene sequence of a BAC, which was found to be located between two genes (At3g59845 and At3g59850). Primers were designed spanning the potential insert site as previously described, and PCR carried out to genotype the plants. For the reaction (WT) wild type primers spanning the insert were used (SPO119HF1 and SPO119HR1); for reaction (Insert) the RB primer of the vector was used (SPO119HF1 and pARTR1). See **Appendix 8.2** for primer sequences. The results of this PCR are shown in **Figure 3.10 B**, which illustrates that the wild type primer set amplifies a band of the predicted size of ~750bp with wild-type DNA, but that the LB vector primer does not amplify a band. This control shows that the primers sets specifically amplify the region to which they were designed. For most of the plants studied, a band was amplified in the (Insert) reaction, showing this to be an actual insertion site. Plants 2, 4 and 6 are

homozygous for the insert, and plants 3,5,7, and 8 are heterozygous for the insert, showing that this is the segregating insert of the 2.

After numerous runs of the TAIL PCR only these insertion sites were found. This included the use of new adapter primers AD3i, and AD4i, which contained inosine. This can bind to any base, so instead of having a mixture of different oligos, 1 can be made which has the potential to bind to numerous sequences. In most cases, sequencing revealed only the sequence of the pART vector. The fact that so few were found may be due to insertion sites being adjacent one another, which would explain why only vector sequence was amplified in many cases. In the absence of suitable restriction sites, this remains an appropriate method for future use in this regard.

3.7 Investigating the effect of reducing DSBs on crossover control

To investigate how reducing the total number of DSBs in a cell influences the crossover/non-crossover decision in *Arabidopsis*, final detailed analysis was carried out on a few selected lines. These included wild-type (Col-0) and the *spo11-1-4* null homozygote as controls, together with the *spo11-1-4* heterozygote and the *SPO11-1* RNAi lines 7A, 8A, 9H, 12R, 16C, which were shown in exhibit a range in expression of *SPO11-1* and chiasma frequency. The 4th generation (T_4) *SPO11-1* RNAi lines were used for analysis. This enabled investigation of whether crossover homeostasis is exhibited in *Arabidopsis*, and how the obligate crossover and crossover interference are affected by a reduction in the number of recombination initiating events (DSBs). By comparing the number of DSBs to the eventual number of crossovers per line, the ratio of crossovers to non-crossovers for each line can be calculated.

3.7.1 Relative quantification of expression by real-time PCR

To give a more accurate quantification of the expression levels of the *SPO11-1* gene, real-time PCR was employed. This involves the measurement of the transcript during the exponential phase of amplification, through quantification of a fluorescent dye reporter. In this case SYBR® green was used (Sensimix dt kit Quantace) in a relative quantification study. RNA was extracted from inflorescences from *SPO11-1* RNAi plants using the RNeasy extraction kit (Qiagen). This was DNase I treated (Qiagen), and subsequently reverse transcribed to cDNA using Superscript II (Invitrogen). Relative quantification was then performed using this DNA as a template, with 20ng used in each reaction. An endogenous control of *Actin-2* was included to take into account differences in cDNA concentration between samples, and the genes *SPO11-1* and *SPO11-2* were measured as target genes. Primer sets for each gene were designed using Primer Express software (Applied Biosystems), and primers subsequently validated to ensure amplification efficiency was consistent at a range of target concentrations (see section 2.13.27). For primer sequences, see **Appendix 8.2**. The comparative Ct method was used to analyse results using wild-type as the calibrator sample (expression set at 1).

The relative expression of *SPO11-2* was used as a meiotic gene control, to account for any changes in expression due to the amounts of sample at different stages of meiosis. The *SPO11-1* relative quantification data was normalised by assuming all samples expressed the same relative quantity of *SPO11-2*. The results of this are summarised in **Figure 3.11**, which shows the relative quantification of *SPO11-1*.

It can be seen that most of the *SPO11-1* RNAi lines show a reduction in gene expression, excluding 16C, which shows similar levels to wild-type. The other lines follow the same pattern of relative expression, as shown by reverse-transcription PCR on the T_3 plants (**Figure 3.5**). However, the relative expression is higher for the RNAi lines, and lower for the *spo11-1-4* heterozygote, which may reflect the increased accuracy of this method. The *spo11-1-4* homozygote (null) control shows almost no expression. This residual expression may be due to non-specific amplification when no template is present, or some template could be produced downstream of the T-DNA to which the primers are designed.

3.7.2 Quantification of DSBs

3.7.2.1 Immunolocalisation of γH2AX

To quantify the number of DSBs in each line, dual-immunolocalisation of γH2AX protein and ASY1 protein was completed. Labelling of ASY1 (axial element protein) permits recognition of the meiotic stage of each cell captured. **Figure 3.12** illustrates immunolocalisation of these proteins on zygotene stage nuclei of each line. The images illustrate that the number of DSBs varies between each line. A control of the *spo11-1-4* mutant (h) shows that γH2AX protein is not present in the absence of DSBs. From analysis of these images it appears that lines 7A, 16C, and the *spo11-1-4* heterozygote (images c,g,b respectively) exhibit wild-type levels of γH2AX localisation. The immunolocalisation demonstrates that the numbers of DSBs are reduced in the lines 8A, 9H, and 12R (images d-f respectively), with the most reduction observed for the line 9H. However, in many of the images of lines with reduced DSBs, large foci of γH2AX can be observed; for example in line 9H (**Figure 3.12 e**). It is possible that these could be the result of an aggregation of the antibody in cases where no protein is available for binding, or that the antibody is non-specifically bound to cytoplasm that has not been removed in slide preparation. It is unlikely to be a genuine signal, as these foci can occasionally be observed in the *spo11-1-4* null mutant, which does not form DSBs.

3.7.2.2 Quantification of γH2AX foci

It was originally thought that the total numbers of γH2AX foci could be quantified, and the mean number of foci for each line calculated for comparison. Preliminary studies showed clear γH2AX foci on lines with reduced DSBs (**Figure 3.6**). However, a new batch of the antibody was used for the final immunolocalisation study. The images in **Figure 3.12** show diffuse labelling of γH2AX foci, making them difficult to accurately count. This led to a problem of how to quantify the numbers of γH2AX foci.

Firstly, the total level of γH2AX (red) fluorescence was quantified in comparison to the ASY1 (green) fluorescence as a control. The ASY1 localisation is not affected by a reduction in DSB frequency, so levels of fluorescence should not be affected. Images were re-captured using manual exposure times. To prevent auto-normalisation of the images by the programme (Smart Capture 3), the save as 8-bit facility was disabled. The problem with this method was that the labelling of even wild-type cells varied from slide to slide. This would mean that manual exposure settings set up for one slide would result in over-exposure of the signal on a different slide of the same sample made at the same time. As it was not possible to include an internal control on every slide made, it was decided that this method of quantification was not suitable for this analysis.

To overcome the problem of quantification, the numbers of γH2AX foci were classified into ranges. Cells were classified by whether they displayed less than 50 foci, 50-100 foci, or greater than 100 γH2AX foci. It is known that in wild-type meiosis up to 140 foci of RAD51 and DMC1 (corresponding to sites of DSBs) have been observed (Sanchez-Moran et al, 2007). Therefore it would be expected that all wild-type nuclei would fall into the >100 foci category, and that cells with less foci would constitute a reduction in DSB frequency. The frequency of cells within each category for each line was assessed.

Figure 3.13 shows the relative frequency of cells within each range. It can be noted that the relative frequency of cells with >100 foci for the wild-type sample is 1, and the frequency of cells with <50 foci for the *spo11-1-4* mutant is also 1, giving good controls. It can be seen that a number of lines show wild-type levels of DSBs. These include the *spo11-1-4* heterozygote and the *SPO11-1* RNAi lines 7A and 16C. The line 16C has been shown to have wild-type

levels of gene expression; however the *spo11-1-4* heterozygote has about 70% of wild-type expression. This suggests that this level of expression is sufficient to produce enough SPO11-1 protein for wild-type numbers of DSBs to be produced.

By analysing the proportion of cells in each category, a comparison of the number of DSBs can be made. A number of lines show reduced levels of DSBs; these include the lines 8A, 9H, and 12R. For example for line 8A, 70% of cells show levels of 50-100 DSBs, and 15% show <50, and another 15% >100 foci. In contrast to this line 9H has a lower proportion of cells with 50-100 foci, and a greater proportion with <50 foci. This comparison shows that line 9H has a greater reduction in DSB formation than 8A. It can also be noted using this method, that 12R forms less DSBs than 8A, but more than 9H. These lines also exhibit a reduction in the levels of *SPO11-1* expression, confirming that this results in a reduction in DSB formation. However, the line 8A shows the lowest relative expression of *SPO11-1*, but higher numbers of DSBs than lines 9H and 12R. This may be due to differences in expression of *SPO11-1* between different plants of the same line, particularly in 8A as the insertion site and number have yet to be identified.

This technique allows relative quantification of DSBs in each line studied, but is not sufficient for absolute quantification of the total number of DSBs per cell. To enable the absolute quantification of DSBs to allow a comparison of the numbers of crossovers to non-crossovers it may be necessary to employ an alternative method.

3.7.3 Analysis of chiasma number and distribution

To study the effect of reducing DSBs on the number of chiasmata formed, and their distribution over each chromosome, meiotic chromosome spreads of metaphase I nuclei were analysed. At this stage chiasmata are visible. FISH using the 5s and 45s rDNA probes was applied to metaphase I chromosome spreads to allow identification of individual chromosomes. See **Figure 2.1** for probe localisation. The number of chiasmata on each chromosome was assessed by analysis of bivalent morphology as previously described (Sanchez-Moran et al, 2001).

3.7.3.1 Chiasma formation is reduced in lines with reduced DSBs

FISH of metaphase I chromosomes for each of the *SPO11-1* RNAi lines is illustrated in **Figure 3.14 A**. An example of a wild-type cell is illustrated in image (a), which shows 5 bivalents each with 2 chiasmata. Without formation of DSBs it is known that homologous chromosomes cannot synapse and recombine (Grelon et al, 2001). This prevents formation of chiasmata, which hold homologs together at metaphase I, and subsequently allow their correct segregation. In this case univalents can be observed, which correspond to unpaired homologues. This is exemplified in image (c) which shows 10 univalents in the *spo11-1-4* null mutant.

The *SPO11-1* RNAi lines exhibit a range in the number of chiasmata formed. The mean number of chiasmata per line is illustrated in **Figure 3.14 B**. The *SPO11-1* RNAi lines 7A and 16C, together with the *spo11-1-4* heterozygote, show wild-type formation of chiasmata, with 5 bivalents visible at metaphase I (images d,i, and b respectively). The mean number of chiasmata for each of these lines appears similar to wild-type. A paired *t*-test confirmed that there was no significant difference between the means. It had been previously observed that these lines also show wild-type levels of DSBs (**Figure 3.12 and 3.13**).

A number of the *SPO11-1* RNAi lines exhibit a reduction in the mean number of chiasmata, for example line 8A forms approximately 6 chiasmata per cell. **Figure 3.14 A,** images (e-f) show examples of 8A nuclei. In image (e) 4 bivalents can be observed with a total chiasma count of 4, with chromosome 1 forming 2 univalents (see arrows). This demonstrates that as DSB numbers are reduced the obligate crossover can be lost. Image (f) demonstrates that

pairing defects are evident in this line. This cell shows multiple chromosome associations (multivalent), seemingly involving all chromosomes. It is possible that some of these connections are non-homologous however, this is not clear. These structures resemble those formed by the ZYP1 mutant, which is defective for synapsis (Higgins et al, 2005). However, whether these connections involve chiasmata remains to be elucidated. Line 9H (image g) shows a more pronounced reduction in chiasma formation than 8A. Only 1 chiasma can be observed in the image, on chromosome 3. All other chromosomes are present as univalents, having lost their obligate chiasmata. A similar situation is exemplified by 12R (image h). This cell shows 2 bivalents with a total of 3 chiasmata, and 6 univalents. The reduction in chiasma frequency is confirmed by the mean chiasmata counts in **Figure 3.14 B**. These lines show a marked reduction in chiasmata formation. *t*-tests showed that that the mean number of chiasmata for lines 8A, 9H, and 12R were significantly different to wild-type. These lines also showed a reduction in the number of DSBs formed. These results show that as the number of DSBs decrease, this causes a proportional decrease in the number of chiasmata formed.

3.7.3.2 Distribution of chiasmata

To analyse how reducing the number of DSBs affects the distribution of chiasmata over individual chromosomes, the number of chiasmata per chromosome was quantified. It has been shown that as DSBs are lost there is a loss in the number of chiasmata formed. This led to the investigation of how these residual chiasmata are distributed. It was first thought that there could be a size specific effect of distribution over the chromosomes. It was thought shorter chromosomes might suffer a greater loss of chiasmata, as the probability of them receiving enough DSBs would be reduced. The distribution of chiasmata over each chromosome for each of the lines studied is shown in **Figure 3.15**. This shows the mean number of chiasmata per chromosome. Paired *t*-tests were carried out on each chromosome in comparison to wild-type to test whether the reduction in the mean numbers of chiasmata were significant. It can be observed that lines with wild-type levels of total chiasmata show similar distributions of chiasmata across chromosomes, with larger chromosomes having more chiasmata as would be expected. From this data, it can also be observed that shorter chromosomes do not lose more chiasmata than larger chromosomes. For example, **Figure 3.15 E** shows that the mean number of chiasmata on chromosome 4, which is the shortest of the 5 chromosomes, is not significantly different from chromosomes 5, one of the longest chromosomes. As the total number of chiasmata decrease, each chromosome appears to lose chiasmata evenly. The mean numbers of chiasmata on each chromosome do not appear to be significantly different from one another. However, in comparison to wild-type chromosome 4 tends to maintain a higher number of chiasmata, as the mean number of chiasmata is lower in wild-type for this short chromosome. An example of this is shown in line 8A, where the number of chiasmata on chromosome 4 is not significantly different from wild-type, whereas chromosomes 1, 2, and 5 show a significant reduction.

Previous studies have suggested that in situations where chiasmata are lost, longer chromosomes may lose their excess chiasmata, in favour of maintaining the obligate chiasma on each chromosome (Rees, 1957). To ascertain whether this was the case in *Arabidopsis*, the frequency distribution of chiasmata for each chromosome was assessed. This is shown in **Figure 3.16**, which includes the frequency distributions for wild-type (A), the *SPO11-1* RNAi line 8A, which has a slight reduction in the total number of chiasmata (B) and 9H, which exhibits a severe reduction in chiasma formation (C). In wild-type it can be noted that larger chromosomes tend to form more chiasmata than shorter chromosomes. From these data, it can also be seen that in the lines with reduced numbers of chiasmata, that chromosome 2 has a higher frequency of univalents than the longer chromosomes. Chromosome 4 however, has a lower frequency of univalents than the other chromosomes in 9H. In line 8A, chromosome 4 has a lower number of univalents than most chromosomes; however, it is similar to chromosome 5 which is the second longest chromosome. This suggests that there is not a tendency for longer chromosomes to lose excess chiasmata, in order to maintain the formation of an obligate chiasma on each chromosome.

By analysis of individual cells, it can be seen that some chromosomes form more than 1 chiasma, when others have lost their obligate chiasma. For example in **Figure 3.14** (e), which shows a metaphase I spread of line 8A; chromosome 5 has formed 2 chiasmata, while chromosome 1 has lost its obligate. This can also be observed in more severely knocked down lines. For example, **Figure 3.14** (h) shows a cell where most chromosomes have lost their obligate chiasma, but chromosome 4 has 2 chiasmata. In cases where this is observed, the chromosomes with more than 1 chiasma seem in exhibit interference, as bivalent morphology appears indistinguishable from wild-type. Further investigation will be needed to confirm whether this is the case. These observations are particularly interesting as chromosome 4 is the shortest, which corroborates the previous results that suggest the ability to form an obligate chiasma is independent of chromosome size in lines with reduced DSBs. These results also suggest that formation of the obligate chiasma is determined on a chromosome specific basis, which means each chromosome is controlled independently.

Statistical analysis was performed using the general linear model to analyse the relationship of chiasma frequency variation between lines and chromosomes. This analysis confirms that there is a significant difference in the frequency of chiasmata formed between lines. It also shows there is a significant difference in the frequency of chiasmata between chromosomes. This is likely to be due to the differences in chromosome size, as it was previously observed that larger chromosomes formed more chiasmata in wild-type. More importantly, it reveals a significant interaction. This indicates that the chiasma frequency of each chromosome varies between lines. This supports the observations previously discussed.

Source	df	Seq SS	Adj SS	Adj MS	F	*P*
Line	**6**	**503.478**	**503.478**	**83.913**	**307.89**	**<0.001**
Chromosome	**4**	**22.077**	**15.407**	**3.852**	**14.13**	**<0.001**
Interaction (lines x chromosomes)	**24**	**23.986**	**23.986**	**0.999**	**3.67**	**<0.001**
Error	**1185**	**322.966**	**322.966**	**0.273**		
Total	**1219**	**872.507**				

Table 3.1: General linear model analysis of variance for number of chiasmata, using adjusted SS for tests.

The chiasma distribution data indicates there may be a tendency to maintain chiasmata on chromosome 4. This raised the question of why this should be the case. Chromosome 4 bears a NOR (Nuclear Organising Region), and it was thought this may have an effect. The NOR regions bring the homologues into close alignment, so that in a situation where the numbers of DSBs are reduced, there could be a tendency to maintain chiasmata in these regions. To investigate whether the location of the NOR on the short arms of chromosomes 2 and 4 could affect the distribution of chiasmata; the number of chiasmata on each arm was quantified by analysing metaphase I chromosome spreads. **Figure 3.17** shows the relative frequency of chiasmata on the short and long arms of chromosomes 2 (a) and 4 (b). On chromosome 2 it can be seen that there is a higher proportion of chiasmata on the long arm than short arm in wild-type. A similar ratio of chiasmata between the long and short arms can be observed for the *spo11-1-4* heterozygote, 7A, and 12R. Lines 8A and 16C show a slight shift in the ratio, with an increase in the number of short arm chiasmata. This is however unlikely to be due to

reduced overall chiasmata formation, as 16C has wild-type levels of *SPO11-1* expression and DSB formation. The most striking effect can be seen in line 9H. Here it can be observed that the relative frequency of chiasmata on the short arm is greatly reduced, which suggests that the NOR has no effect.

On chromosome 4 a similar ratio of short arm to long arm chiasmata can be observed, with a higher proportion of chiasmata on the long arm in wild-type. The ratio appears to be similar in the *spo11-1-4* heterozygote and all *SPO11-1* RNAi lines excluding 9H. However, it can be seen that there are less chiasmata on the short arm in the wild-type than these lines. This could be due to sampling, as the *spo11-1-4* heterozygote, and 16C have a higher mean number of total chiasmata per cell. As for chromosome 2, the most pronounced effect could be seen in line 9H. However, unlike chromosome 2 the relative frequency of short arm chiasmata is increased, indicating there may be an effect from the NOR in this case. These data indicate that chromosomes 2 and 4 may act differently in response to a reduction in the number of DSBs.

3.8 Investigating how a reduction of DSBs affects pairing and synapsis of homologous chromosomes

To investigate how reducing the total number of DSBs in a cell affects pairing and synapsis of homologous chromosomes, studies were carried out on the same *SPO11-1* RNAi lines as used for the studies in section 3.7.

3.8.1 A reduction of DSBs does not affect pairing of telomeric and sub-telomeric regions

To determine whether DSBs are required for correct pairing and synapsis of homologous chromosomes, fluorescence *in situ* hybridisation (FISH) was used with probes to the telomeric repeat sequence and chromosome specific BACs. The *SPO11-1* RNAi lines with varying numbers of DSBs can be used to answer a number of questions, for example how many DSBs are sufficient for normal pairing of homologues?

Pairing of telomeric sequences was first studied, as in *Arabidopsis* these are the first regions of the chromosomes to become paired (Armstrong et al, 2001). FISH using the telomeric repeat probe was first applied to wild-type Col-0 and the *spo11-1-4* homozygote to investigate whether DSBs are necessary for telomere pairing. **Figure 3.18 A** shows examples of prophase I meiotic nuclei labelled with the telomeric repeat probe. Images (a-c) show that in wild-type, telomeres are paired from leptotene through to pachytene. It can also be observed that telomeres are paired in leptotene and zygotene in *spo11-1-4* as shown by the observation of approximately 10 foci; 20 foci would be expected if telomeres remained unpaired.

The mean number of foci that were observed per cell is shown in **Figure 3.18 B**. This data shows that no significant difference in the number of telomere foci can be observed between the two samples. In both wild-type and *spo11-1-4*, telomeres become progressively paired from early G_2-zygotene.

To verify whether this pairing was between homologous chromosomes, FISH with a chromosome 1 specific BAC (F19K16) to a distal sub-telomeric region was applied (for locus see **Figure 2.1**). The BAC showed a similar pattern of pairing in wild-type, the *spo11-1-4* heterozygote, and homozygote. **Figure 3.19 A** (a-i) shows examples of meiotic prophase I nuclei from each of these lines. It can be observed that foci become progressively paired from leptotene through to pachytene, with 1 focus of probe indicating the presence of paired chromosome 1 homologues. The signals were not always paired at zygotene, as they were for the telomeric probe. The mean number of F19K16 foci per cell is shown in **Figure 3.19 B**. This shows that there is no significant difference between the numbers of foci at each meiotic stage for each of the different lines. Therefore, the unpaired foci at zygotene may reflect slightly later pairing of sub-telomeric regions in a few cells.

As DSBs are thought to be important for alignment of homologues along their lengths prior to synapsis, it was decided to investigate pairing further by analysing pairing in more interstitial regions.

To examine whether DSBs are important for pairing and alignment of homologous chromosomes, FISH using a chromosome 1 specific BAC (F1N21) to an interstitial region was studied (for locus see **Figure 2.1**). A more proximal interstitial BAC was not available. To establish whether DSBs are necessary for alignment, and if so how many are sufficient, pairing in wild-type was compared to *spo11-1-4* and the *SPO11-1* RNAi line 9H, which has approximately half the number of DSBs as wild-type.

Figure 3.20 A (a-i) shows examples of FISH on meiotic spread nuclei with the BAC F1N21. It can be observed that foci become progressively paired from leptotene thorough to zygotene/pachytene. **Figure 3.20 B** shows the mean number of F1N21 foci per cell. At leptotene most cells show unpaired foci in all samples. This shows that more interstitial regions pair later than the telomeres. The numbers of paired foci at zygotene are also not significantly different for all of the lines, with most being paired. This may be due to the distal localisation of this BAC. Therefore, if telomeres are paired, interstitial regions that are closer to the distal end (telomere) may appear to be paired because of their relatively close organisation.

3.8.2 Synapsis is initiated but not completed in SPO11-1 lines with reduced DSBs

It is known that in *Arabidopsis*, initiation of recombination by programmed DSBs is necessary for synapsis and localisation of the synaptonemal complex (SC) protein ZYP1 to the chromatin (Higgins et al, 2005). This led to the question being asked, what happens to synapsis if DSBs are reduced? To investigate how reducing the number of DSBs influences synaptonemal complex formation (synapsis), immunolocalisation studies using an antibody to the SC protein ZYP1 on the *SPO11-1* RNAi lines were performed.

Dual-immunolocalisation of the ZYP1 protein together with ASY1 protein is shown in **Figure 3.21 A**. Images (a-f) show that synapsis is first initiated during late-leptotene to zygotene (a,d) in wild-type meiosis, as shown by the observation of ZYP1 foci. During zygotene foci begin to polymerise to form extended linear signals (e,f). These stretches of ZYP1 signal become progressively extended until pachytene, where homologous chromosomes are completely synapsed (c,f). In regions where ZYP1 becomes polymerised, the ASY1 signal becomes more diffuse, and can be seen to localise either side of ZYP1 (image f, boxed). In contrast to this, immunolocalisation of ZYP1 on the *spo11-1-4* mutant shows no localisation of the protein, showing that no synapsis is initiated in the absence of DSBs (g-l). This is in agreement with previous observations, which suggested DSBs are required for SC nucleation (Higgins et al, 2005).

To determine what the affect of reducing the numbers of DSBs has on synapsis, immunolocalisation was carried out on two of the *SPO11-1* RNAi lines. The lines 8A and 9H were chosen due to their different levels of DSB reduction **Figure 3.21B** illustrates dual-immunolocalisation of ZYP1 and ASY1 protein on these RNAi lines.

Images (a-f) show the localisation on the line 9H, which shows a severe reduction in DSB formation, and the number of chiasmata formed (Figures **3.13** and **3.14**). ZYP1 foci can be seen at early zygotene (**Figure 3.21 B** images a,d) in this line, as in wild-type. However, this shows that in contrast to wild-type these foci do not polymerise as normal. In wild-type, foci begin to polymerise in an asynchronous manner, with some initiation sites beginning to polymerise before others. In 9H these initiation sites appear to persist, which may point to a

delay in progression of synapsis in this line. These images also show that synapsis is initiated despite a reduction in numbers of DSBs. In mid to late-zygotene, short stretches of ZYP1 polymerisation can be observed (images b,e and c,f respectively). However, longer more continuous stretches of ZYP1 polymerisation fail to be observed, which indicates that despite some DSBs being formed in this line, the number of DSBs is insufficient for completion of synapsis.

To investigate whether synapsis can be completed with reduced DSBs, another less severely affected line was studied (8A). A greater number of DSBs was observed in this line, together with a smaller reduction in formation of chiasmata (**Figures 3.13** and **3.14**). **Figure 3.21B** images (g-l) show that ZYP1 foci can be observed at late leptotene/early zygotene, as in wild-type. These begin to polymerise with extended stretches of ZYP1 visible at mid-zygotene. At late-zygotene/pachytene, the ZYP1 localisation appears incomplete, indicating that synapsis fails to be completed in this line. This is illustrated in **Figure 3.21B** image (l) where stretches of clearly labelled ASY1 can be observed. Where ZYP1 polymerisation is complete, the ASY1 signal becomes more diffuse. Therefore, regions of clearly labelled ASY1 indicate regions where synapsis is not completed. In wild-type nuclei, 22 of 93 cells captured were shown to exhibit complete synapsis, in contrast to 8A, in which none of the 52 cells captured displayed complete synapsis.

The SC is thought to be nucleated from only a few DSB sites. To ascertain how the numbers of synapsis initiation sites were affected by the reduction in DSBs, the numbers of ZYP1 foci were quantified. As previously mentioned, ZYP1 foci without polymerisation were observed in line 9H, which showed the largest reduction in DSBs. This enabled foci to be quantified in this line. In wild-type it would not be feasible to count the number of ZYP1 foci, as they begin to polymerise asynchronously. To overcome this problem, the data was compared to the number of ZYP1 foci from the *dmc1* mutant (Armstrong, personal communication). This mutant is defective for DSB repair, and persistent ZYP1 foci can be observed without affecting their numbers. The mean number of foci for *dmc1* was 43 (n-3) per cell, in contrast to this 9H exhibited a reduction in the mean number of foci, with 23.6 (n-18) per cell. Only short stretches of ZYP1 polymerisation were observed for this line, which suggests that a

small reduction in the numbers of SC initiation sites has a considerable effect on SC formation.

These results demonstrate that synapsis can be initiated with only a small subset of DSBs, but for completion of ZYP1 polymerisation and synapsis, a much higher number of DSBs are required. The appearance of ZYP1 foci without polymerisation in 9H points to a delay in progression of synapsis.

3.8.3 Meiotic prophase I is delayed in SPO11-1 lines with reduced DSBs

To investigate whether defects in completion of pairing and synapsis led to a delay in progression of meiotic prophase I, a time-course using pulsed labelling of S-phase cells with bromodeoxyuridine (BrdU) was used. Stems from each line were given a pulse of BrdU for 2h and subsequently transferred to water. Influorescences were then fixed at intervals of 18, 24, and 36h for analysis. An anti-BrdU antibody was applied to meiotic chromosome spreads of each sample, and the number of labelled and non-labelled meiotic stages assessed (see Armstrong et al, 2003). **Figure 3.22** shows a summary of these results. For a more detailed break-down of results, see **Appendix 8.4.** For the purposes of this study, zygotene and pachytene stages were grouped, because true pachytene cells are not observed in the *spo11-1-4* homozygous mutant or the *SPO11-1* RNAi line 9H. The stages diplotene and diakinesis were also grouped.

At 18h after the BrdU pulse, labelled cells at leptotene and zygotene/pachytene were observed in the *spo11-1-4* mutant and 9H in addition to the wild-type. This observation demonstrates that there is no delay in progression through leptotene up to zygotene/pachytene in these lines. However, a higher percentage of cells are labelled in *spo11-1-4* and 9H, which indicates a possible delay subsequent to this. A similar pattern of labelling was observed at 24h. A further time point was carried out to examine whether lines were delayed in prophase I of meiosis. Previous studies have shown that mutations of SC components can result in a delayed progression through prophase I, for example ZYP1 in *Arabidopsis* (Higgins et al, 2005).

A time point of 36h post S-phase was chosen as completion of meiosis would be expected by this stage. Meiosis of wild-type Col-0 from the beginning of G_2-tetrad has previously been measured using a BrdU time course to be ~33h (Armstrong et al, 2003). From **Figure 3.22 C** it can be seen that wild-type meiosis has reached metaphase I by 36h. This is in contrast to what would be expected. However, meiotic progression can be influenced by environmental variables such as temperature, with progression slowing as temperature decreases. As the lines were treated at the same time as the wild-type, this still gives a good comparison as a control. It can also be observed that there are no BrdU labelled cells subsequent to zygotene/pachytene, for the RNAi lines and *spo11-1-4* at this time point, which indicates that these lines are delayed in prophase I. Further time points would be required to quantify the

length of this delay. The much larger percentage of labelled leptotene nuclei for lines 8A and 9H may represent of small delay at this stage, however as a higher percentage of zygotene nuclei are labelled in wild-type, this suggests these differences may be due to sampling variation.

These results illustrate that a delay in progression of meiotic prophase I is caused when the DSBs are reduced or abolished, and that this is likely to be due to defects in formation of the synaptonemal complex, and possibly pairing prior to this.

3.9 Discussion

SPO11-1 RNAi lines were constructed that exhibit incremental decreases in the numbers of DSBs formed. Preliminary analysis of these lines showed that the expression of *SPO11-1* was reduced to varying degrees between lines, and that this was linked to a reduction in the number of chiasmata formed and subsequently levels of fertility. These lines were used to investigate the effects of reducing DSBs on pairing of homologous chromosomes and crossover control.

3.9.1 The effect of reducing DSBs on crossover control

3.9.1.1 Arabidopsis exhibits a threshold number of DSBs below which chiasma frequency is reduced

In budding yeast, Martini et al, (2006) showed that in lines with varying reductions in DSBs, crossover numbers tended to be maintained at the expense of non-crossovers, which was termed crossover homeostasis (**Figure 1.3**). To investigate how reducing the total number of DSBs in a cell influences the crossover/non-crossover decision in *Arabidopsis*, the number of DSBs and chiasma frequency were measured in the *SPO11-1* RNAi lines with varying reductions in the numbers of DSBs. It was found that as the numbers of DSBs were reduced this resulted in a reduction in frequency of chiasmata formed. However, it cannot be concluded whether or not crossover homeostasis is present in *Arabidopsis*. This is due to problems in accurately quantifying the numbers of DSBs. From preliminary analysis, it was decided to use immunolocalisation of γH2AX as a method of quantifying DSBs, by directly counting the numbers of foci. This appeared to be the clearest technique, as foci were distinct. From the final analysis of lines, it was noted that the foci of γH2AX were diffuse, and foci could not be accurately distinguished. This difference is likely to have been due to the antibody used. It was the same as used in the preliminary analysis, but from a new batch. A further batch of antibody was tested, and this resulted in labelling of diffuse foci. From the relative quantification of DSBs, it can be noted that line 8A forms approximately 60% of wild-type DSB numbers (**Figure 3.13**). This line also exhibits a reduction chiasma formation, with a mean frequency of 6.48 (wild-type range 8-12). In yeast, crossover homeostasis was observed in lines with 80%, 30%, and 20% of wild-type DSBs. However, it was also observed that the mutants with 20-30% of wild-type DSBs exhibited a reduction in the numbers of 4-

spore viable tetrads, which is a sign of homologue non-disjunction (Martini et al, 2006). They proposed that a threshold exists between 80% and 30% of DSBs, below which there are insufficient numbers of DSBs to maintain the fidelity of recombination and chromosome segregation. This shows that crossover homeostasis is not 100% efficient. The threshold observed in *Arabidopsis* for maintaining wild-type levels of recombination appears to be within the same range as that observed in the yeast study. Therefore, it remains possible that crossover homeostasis could be a factor in *Arabidopsis*. An accurate method of DSB quantification will be needed to determine whether this is the case. This would allow the comparison of how the crossover to non-crossover ratio is affected. Martini et al, (2006) considered that crossover homeostasis may not be completely efficient due to the molecular mechanism being limited in some way, or by other influences for instance defects in pairing and synapsis. It has been previously shown that a reduction in the numbers of DSBs causes defects in synapsis (Tesse et al, 2003; Henderson and Keeney, 2004). This may also be the basis of the reduced chiasma frequency observed in *Arabidopsis*, as defects in synapsis were observed (see section 3.9.2 for further discussion).

In the yeast study, locus specific differences in the levels of crossover homeostasis were observed. In contrast to the *ARG4* locus, the *HIS4LEU2* locus showed little or no crossover homeostasis. The frequency of crossovers was measured in specific genetic intervals by segregation of markers and a method developed to measure the frequencies of crossover and non-crossover events at a single locus. In *Arabidopsis*, the frequency of crossovers was analysed globally by cytological analysis. Therefore, locus specific differences cannot be ascertained. Whether crossover homeostasis would be observed on a global basis in yeast is unclear, which makes future comparison challenging.

3.9.1.2 Chromosome size does not influence chiasma distribution in lines with reduced DSBs

The number of chiasmata formed on each chromosome was quantified to investigate whether reducing the numbers of DSBs would affect the distribution of residual chiasmata. In wild-type it was observed that larger chromosomes had a tendency to form more chiasmata, as would be expected (Rees, 1957). It was established that chromosome size did not influence chiasma distribution in the *SPO11-1* RNAi lines. It was hypothesised that the smaller

chromosomes may lose more chiasmata, as the probability of these chromosomes receiving enough DSBs could be reduced. An analysis of crossover distribution showed this not to be the case. This was particularly evident for chromosome 4 (shortest), which had a lower frequency of univalents than the other chromosomes in the intermediate line 8A.

Secondly, it was considered that there could be tendency for chromosomes to maintain the obligate crossover in the face of reduced DSBs. Rees, (1957) analysed the distribution of chiasmata in an asynaptic locust in which chiasma frequency was reduced, and found that larger chromosomes showed the greatest reduction in chiasma frequency. The longer chromosomes also had a significantly higher frequency of univalents, with the short chromosomes mostly forming an obligate chiasma as in normal individuals. It appeared as though excess chiasmata were lost from larger chromosomes in order to maintain the obligate on each chromosome in this case. They pointed to the short chromosomes having special properties in the ability to form the obligate chiasma. This does not appear to be true for the RNAi lines; for example in 8A chromosome 2 (short) had the highest frequency of univalents. However, chromosome 4 did appear to maintain a higher frequency of chiasmata relative to wild-type in the *SPO11-1* RNAi lines with reduced chiasmata, most evidently in 8A. Interchromosomal chiasma frequency compensation has also been described for *Hypochoeris*. In cases where chromosome specific univalence was observed, the frequency of chiasmata on unaffected chromosomes was markedly increased (Parker, 1975; cited by Tease and Jones, 1976). In *Crepis*, a desynaptic mutant was found to exhibit chromosome specific univalence, which varied between plants. It was thought that chromosomes were controlled independently, as interchromosomal effects were marginal, only being significant in 2 of 11 plants. It has been proposed that interchromosomal effects may be due to defects in control in mutants rather than a mechanism of chiasma control, as its extent varies widely between species studied (Hewitt and John, 1965; cited by Tease and Jones. 1976).

Particularly interesting in the *SPO11-1* lines was the observation that in many cases some chromosomes were found to form more than the obligate chiasma, whilst others formed univalents in the same cell. An example of this is shown for line 8A in **Figure 3.14** (e). In the cases where a chromosome forms more than 1 chiasma they appear in exhibit interference, as bivalent morphology appears wild-type. It can therefore be proposed that the control of

chiasma formation is separate for each chromosome in *Arabidopsis*, as was described in *Crepis*. This would fit with the stress relief model of crossover control, as 'stress' is a factor of individual chromosomes (Kleckner et al, 2004).

3.9.1.3 Chromosomes 2 and 4 behave differently with a reduction in DSB

Analysis of the distribution of chiasmata suggested that in lines with reduced DSBs, chromosome 4 tended to maintain more chiasmata than other chromosomes. It was thought that this may be due to the NOR of this chromosome. This could cause homologues to align closely via their association with the nucleolus, which may confer an advantage when DSBs are reduced. It is known that in somatic cells only the NOR bearing chromosomes 2 and 4 associate more frequently than expected at random (Pecinka et al, 2004). This led to the question of whether the NORs of chromosomes 2 and 4 affected the distribution of chiasmata in lines with a reduced number of DSBs. The distribution of chiasmata between the short and long arms of chromosomes 2 and 4 was compared for each line studied by analysis of FISH labelled metaphase I spreads (**Figure 3.17**). It was observed that only in line, 9H did the ratio between short and long arm chiasmata vary from the wild-type situation. For chromosome 2 the frequency of short arm chiasmata was reduced by half that of wild-type, with the long arm having an increased frequency. For this chromosome there did not appear to be a maintenance of chiasmata on the short arm, which therefore suggests that the NOR has no affect. In contrast to this, the frequency of short arm chiasmata on chromosome 4 was markedly increased in comparison to wild-type, with a corresponding decrease in long arm chiasmata. This implies that the NOR influences chiasma distribution in this case. This may explain the trend observed previously for chromosome 4 maintaining chiasmata. However, this raises an interesting question of why this trend is not observed in chromosome 2. This chromosome is a similar size to chromosome 4, in addition to this they are both acrocentric chromosomes containing a NOR on the short arm.

A difference in the behaviour of these chromosomes has also been observed in other meiotic mutants of *Arabidopsis*. Sanchez-Moran et al, (2001) found that the *asy1* mutant displayed a high frequency of univalents at metaphase I. However, some bivalent formation was retained. It was found that chromosome 2 had the highest frequency and that more short arm chiasmata were formed than on the long arm, which was in contrast to the wild-type control. Contrary to

this, chromosome 4 showed no such effect. Differences in the behaviour of these chromosomes have also been identified in multivalent formation of established autotetraploid lines (Santos et al, 2003). More recently, a histone hyperacetylation line was shown to result in changes in chiasma distribution on certain chromosomes (G. Perrella, personal communication, unpublished). Univalents were observed for chromosome 2, whilst the frequency of chromosome 4 ring bivalents was found to increase, with a specific increase of short arm chiasmata. These studies show a similar trend to that observed for the *SPO11-1* RNAi lines. Why chromosomes 2 and 4, which are structurally so similar, should behave differently remains unclear. These results suggest that in the case of the RNAi lines, it is not the NOR that confers an advantage for pairing and synapsis on chromosome 4, as this is not observed in chromosome 2. It is possible that these differences arise from a difference in chromatin conformation between the 2 chromosomes, particularly in view of the altered chiasma distribution of the hyperacetylation line. Sanchez-Moran et al, (2001) proposed that the short arms may exhibit different states of chromatin associated with their relative levels of rDNA transcription. Interestingly, mapping of crossovers on chromosome 4 has revealed several crossover 'hotspots' in the intergenic region adjacent to the NOR, resulting in a recombination rate 5 times greater than the average over the chromosome (Drouaud et al, 2006). It is possible that this could influence the capability of this region to form a crossover, or that the difference in chromatin conformation actually influences the capacity of this region to form DSBs. However, detailed mapping of crossovers has only been established for chromosome 4.

3.9.2 The effect of reducing DSBs on pairing and synapsis of homologous chromosomes

3.9.2.1 Pairing of homologous chromosomes

It is known that in *Arabidopsis*, pairing of homologous chromosomes begins with pairing of homologous telomeres at the G_2-leptotene transition while clustered around the nucleolus (Armstrong et al, 2001). To investigate whether DSBs were required for this stage of pairing, FISH was employed using a probe to the telomeric repeat sequence. The numbers of foci were quantified in the *spo11-1-4* homozygous mutant that does not form DSBs and compared to wild-type as a control. No significant difference between the mean numbers of telomere probe

foci was found between the mutant and wild-type (**Figure 3.19).** To confirm that telomeres were able to pair homologously, FISH was again used with a BAC specific to chromosome 1. The numbers of BAC foci were quantified in the mutant and wild-type control, and again no significant difference between the mean numbers of foci was observed (**Figure 3.20**). This demonstrated that telomeres were able to pair homologously in the absence of DSBs, indicating that telomere pairing is independent from DSB formation and recombination. In budding yeast, DSBs have been found to be dispensable for telomere clustering and bouquet formation. Mutants for *spo11* and *rad50S* were shown to form bouquets as in wild-type (Trelles-Sticken et al, 1999). These results are also consistent with the idea that pairing of homologous chromosomes in wild-type firstly involves early recognition, which has been shown to be independent of recombination, (Tesse et al, 2003) in this case telomere pairing around the nucleolus.

To investigate the effect of reducing DSBs on the close alignment of homologues in *Arabidopsis*, FISH using a BAC to a more interstitial region of chromosome 1 was employed (FIN21). The aim was to establish whether homologues are able to pair with a reduced number of DSBs, and if so, determine how many are sufficient for pairing by analysis of the *SPO11-1* RNAi knockdown lines. It is known that homologues are unable to pair in the complete absence of DSBs in *Arabidopsis*, as shown by a study of a *spo11-1* homozygous mutant (Grelon, et al 2001). The RNAi line 9H was studied, which has been shown to exhibit a severe reduction in chiasma formation. This was compared to wild-type and the *spo11-1-4* homozygote as controls. From the results, no significant difference between the mean numbers of BAC foci was observed between the lines studied. This shows that chromosome 1 pairs homologously in all the lines studied, and therefore suggests that homologues are able to pair in these lines. However, this also includes the *spo11-1-4* homozygous control that fails to form DSBs. Furthermore this is in contrast to studies in other organisms which suggest that DSBs mediate presynaptic alignment of homologues, possibly together with downstream protein complexes (including RAD51) forming inter-axis connections (Peoples et al, 2002; Pawlowski et al, 2003;). Tesse et al, (2003) showed that in *Sordaria ski8* and *spo11* mutants, the amount of co-alignment of homologues correlates with the number of endogenously or artificially induced DSBs. It is likely that the BAC (F1N21) used for this study is too distal for analysing pairing of interstitial regions. Telomeres were shown to pair in the absence of

DSBs, and therefore regions of the chromosomes that are sub-telomeric may appear paired by FISH analysis. This would explain why homologues appeared to be paired in the *spo11-1-4* homozygous null control. Further investigation will be required using a series of more interstitial BACs, for a more detailed analysis of how many DSBs are sufficient for pairing.

3.9.2.2 Synapsis is initiated but not completed in lines with reduced DSBs

Subsequent to their close alignment, homologues become connected by formation of the synaptonemal complex (SC). This process has been shown to require formation of DSBs. To investigate the relationship between the numbers of DSBs and SC nucleation in *Arabidopsis*, immunolocalisation studies were carried out on the *SPO11-1* RNAi knockdown lines with varying numbers of DSBs. Immunolocalisation of the transverse filament protein ZYP1 was used to visualise the extent of synapsis. Firstly, a control of the *spo11-1-4* homozygote was analysed and established that SC initiation fails in the absence of DSBs. This corroborates previous findings in *Arabidopsis,* (Higgins et al, 2005), budding yeast (Henderson and Keeney, 2004), and *Sordaria* (Tesse et al, 2003). The *SPO11-1* RNAi lines used for the study included 8A, which exhibits an intermediate reduction in chiasma formation, and 9H in which the chiasma frequency is severely reduced (see **Figure 3.14**). The results obtained showed that synapsis is initiated in lines with reduced DSBs, but that it does not reach completion. It was also found that with a higher number of DSBs, synapsis progresses further. In line 9H with lower numbers of DSBs, SC initiation sites were observed. These were shown to polymerise to form short stretches of SC. In a number of cases, synapsis initiation sites were observed without polymerisation (**Figure 3.21B**). In wild-type, synapsis initiates asynchronously, such that some synapsis initiation sites begin to polymerise before others (**Figure 3.21A**). It appears that in line 9H synapsis initiation sites persist before elongation. This suggests that synapsis may be delayed with a reduction in DSBs, as downstream repair mechanisms would not be affected. However, this remains to be confirmed. In line 8A synapsis appears to initiate and polymerise as in wild-type, however complete synapsis was never observed in this line.

These results show that for completion of synapsis, near wild-type levels of DSBs would be required. These observations are analogous to those in *Sordaria ski8* mutants with varying numbers of DSBs. They demonstrated that almost wild-type numbers of DSBs were required

for SC formation (Tesse et al, 2003). It was also noted that initiation of synapsis was not sufficient for complete polymerisation of the SC. In mutants with lower numbers of DSBs, only short segments of SC could be observed (Zickler et al, 2002; Tesse et al, 2003). This has also been shown to be the case in budding yeast, where short stretches of SC were observed in *spo11* mutants with partial reductions in the numbers of DSBs (Henderson and Keeney, 2004). These results correlate well with what has been observed in *Arabidopsis*, and leads to the question of why SC initiation at a subset of sites cannot permit elongation along the entire chromosome. Tesse et al, (2003) proposed that interference may control the extent to which the SC can polymerise, as it is thought that interference may precede formation of the SC. Fung et al, (2004) found that synapsis initiation sites were subject to interference.

The number of synapsis initiation sites was assessed to determine whether this was affected by the reduction in DSBs in *Arabidopsis*, as it is thought that the SC nucleates from only a small subset of DSBs. In budding yeast and *Sordaria,* it has been proposed that the SC nucleates from sites that are selected to form a crossover. Mutations in which the numbers of crossovers were reduced also exhibited fewer SC initiation sites (Zickler et al, 1992; Henderson and Keeney, 2004). The number of SC initiation sites was quantified in the 9H *SPO11-1* RNAi lines by counting the number of ZYP1 foci in those cells where foci had not begun to polymerise. This was then compared to the number of ZYP1 foci from the *dmc1* mutant of *Arabidopsis* (data from S.J. Armstrong, unpublished), which is blocked at the stage of DSB repair. This gives a count of the synapsis initiation sites from wild-type, as this stage is not affected by the mutation, but progression is delayed. The mean number of SC initiation sites in *Arabidopsis* from a limited number of cells (n-3) was 43, in comparison to the mean of line 9H at 23.6 (n-18) foci per cell. Line 9H exhibited the most severe reduction in chiasma formation with a mean frequency of only 1.25 per cell. Only short stretches of ZYP1 were observed in this line, with half the number of SC initiation sites. This shows that much higher numbers are needed for efficient synapsis. It will be interesting to assess how the numbers of SC initiation sites vary with the number of DSBs to more detail.

It can also be noted that the number of synapsis initiation sites far outweigh the number of chiasmata formed in *Arabidopsis*, even in line 9H with a severe reduction in the number of chiasmata. This is in contrast to those studies in budding yeast and *Sordaria* that suggest that

synapsis initiation sites correspond to sites of crossovers (reviewed by Henderson and Keeney, 2005). However, it has also been shown that plants with longer chromosomes have more synapsis initiation sites than crossovers for example in rye (Gillies, 1985). It is possible that organisms with larger or more complex genomes need a higher number of initiation sites for efficient SC formation. *Arabidopsis* has a low number of crossovers in comparison to yeast, which would mean if SC initiation only occurred at these points, synapsis may be inefficient.

By comparing the amount of synapsis against chiasma frequency, the level of synapsis necessary for maintenance of normal recombination can be established. From the data shown it appears that almost complete synapsis may be necessary to maintain wild-type levels of recombination. This is evident in the *SPO11-1* RNAi line 8A, which shows almost complete synapsis but does not achieve wild-type levels of recombination. The fact that synapsis is not completed in 8A strongly suggests that the non-homologous connections previously discussed are due to defective SC formation. This is supported by the observation of multivalents in *zyp1* null lines (Higgins et al, 2005). The reduced number of DSBs would be repaired, but without pairing and SC formation, this may permit non-homologous interactions. It has been proposed that the SC may be involved in resolving interlocks. Higgins et al, (2005) found that plants deficient for ZYP1 only exhibited a mild reduction in chiasma frequency, but a high rate of non-homologous connections. It can be proposed that in *Arabidopsis*, the SC functions in preventing non-homologous connections. Further work will be required to establish how this is achieved. It may function by removing non-homologous interactions before they are stabilised.

3.9.2.3 Prophase I is delayed in lines with reduced DSBs

To examine whether prophase I progression was delayed in lines with reduced DSBs where synapsis does not reach completion, a BrdU time course was applied to the *spo11-1-4* homozygote in addition to the RNAi lines 8A and 9H. Preliminary results showed that at 36h meiosis had progressed to zygotene/pachytene in the mutants, whilst the wild-type control had progressed to metaphase I. These results show that progression of prophase I is delayed in lines which have reduced or no DSBs. However, the length of delay has not been established and it will be interesting to determine whether there is a correlation between the number of

DSBs and length of delay. Higgins et al, (2004) proposed that the *msh4* mutant was delayed in prophase I due to a delay in synapsis. However, more recent studies of several *Arabidopsis* mutants suggest that a surveillance mechanism may operate during prophase I as has been suggested for budding yeast (Borner et al, 2004). For example, ZYP1 deficient lines exhibited a substantial delay of 20 hours (Higgins et al, 2005). In the lines with reduced DSBs the delay in prophase I is likely to be due to a delay in pairing and or synapsis, as the recombination machinery downstream of SPO11-1 would not be affected. Time course studies in conjunction with ZYP1 immunolocalisation would reveal if this were indeed the case. If synapsis was to occur with normal dynamics despite not reaching completion, this may point to the existence of a surveillance mechanism.

3.9.3 Conclusions and future perspectives

The results discussed above uncover an important aspect of crossover control in *Arabidopsis* not previously identified. That is that chromosomes are subject to an autonomous control of chiasma formation. Collectively, the results discussed are consistent with the notion that there is a threshold number of DSBs, which are required to maintain the fidelity of recombination. Analysis of the intermediate affected line 8A, suggests that this threshold lies in the range of 60-70% of DSBs. It can be proposed that chromosomes that have the threshold number of DSBs are able to synapse and form chiasmata, which apparently exhibit interference. In contrast, those that do not receive the threshold number of DSBs exhibit defects in synapsis due to defects in pairing and a reduction in the number of synapsis initiation sites. In most cases, this results in formation of univalents. However, in line 8A many cells exhibited non-homologous connections and even multivalent formation in some cases, pointing to a role for the SC in preventing non-homologous connections, and possibly in interlock resolution. A model for this is shown in **Figure 3.23**. Assuming that each chromosome is affected equally, it appears that this threshold may not be consistent for each chromosome. For example, the chiasma frequency for chromosome 4 in line 8A is not significantly different from wild-type. It seems that this difference is not due to size or chromosome morphology, as exemplified by the diverse behaviour of chromosomes 2 and 4, but chromatin organization may play a role.

Defects in SC formation were shown to cause a delay in the progression of meiotic prophase I. Investigation into the dynamics of ZYP1 polymerisation using a time course would give

further insight into the cause of this delay. For example if there were to be a relationship between the length of SC polymerisation and length of prophase I.

The main limitation of this study was the lack of a suitable method for accurately quantifying the numbers of DSBs. This would be required to study the crossover/non-crossover ratio, as currently there is no way of directly measuring the numbers of non-crossovers in *Arabidopsis*. Therefore no conclusion as to whether *Arabidopsis* exhibits crossover homeostasis could be reached. It will also be important to firmly establish whether interference is maintained in cases were chromosomes form more than 1 chiasma. In addition to this, the number of DSBs required for the completion of pairing and synapsis would be more accurately quantified. This would involve the study of more lines with an intermediate reduction in DSBs like 8A, which will give a more accurate measure of the threshold of DSBs needed. The complex interplay between pairing dynamics and recombination progression may make analysis of homeostasis challenging.

Chapter 4

A role for telomeres in pairing of homologous chromosomes

4.1 Introduction

One of the outstanding questions in meiosis is how homologous chromosomes recognise one another and pair, and how this process is regulated and controlled. Subsequently these early events permit downstream processes of synaptonemal complex formation, recombination, and chiasma formation. One event thought to be important for homologous recombination, is formation of the meiotic bouquet, which is a widely conserved feature of prophase 1. It is usually formed at the transition from leptotene to zygotene, and is defined as the clustering of telomeres on the inner nuclear envelope (Scherthan, 2001). The mechanism by which it is formed is not well understood, although recent advances have shown actin is important for telomere movement (Trelles-Sticken et al, 2005). The bouquet is proposed to bring homologues into a close association, thereby promoting the subsequent homology search (Cowan et al, 2001). It has been noted that the timing of telomere clustering varies between species. For further discussion, see Zickler and Kleckner, (1998). In *Arabidopsis,* this 'classical bouquet' has not been observed. Instead telomeres show persistent association with the nucleolus throughout meiotic interphase, where they become homologously paired at the G_2-leptotene transition (Armstrong et al, 2001). *Arabidopsis* therefore provides a unique situation in which to investigate a role for telomeres in pairing of homologues.

This chapter describes the investigation into a potential role for telomeres in controlling movement and pairing of homologous chromosomes. It describes the two approaches taken to disrupt the telomeres. Firstly, by introducing colchicine, a drug known to inhibit telomere movement, and secondly by analysing plants deficient for the telomerase subunit (TERT) with severely shortened telomeres.

4.2 Investigating a role for telomeres in homologous chromosome pairing using colchicine

A number of studies have used drugs that disrupt progression of meiosis to elucidate the mechanisms that control telomere movements and pairing during meiosis, particularly during bouquet formation. The most widely studied of these is colchicine. (See section 1.10). Colchicine is a microtubule depolymerising drug, which prevents formation of the meiotic

spindle; hence, chromosomes are not segregated correctly at anaphase 1. Colchicine has been shown to disrupt SC formation (Loidl, 1988; Tepperberg et al, 1997) and reduce the frequency of chiasmata (Driscoll et al, 1967; Bennett et al, 1979). More recently, direct evidence has shown colchicine blocks telomere clustering into the bouquet, but does not affect attachment of telomeres to the nuclear envelope. This has been shown to result in defects in pairing of homologous chromosomes. Cowan and Cande, (2002) showed that 100μM colchicine blocked bouquet formation, and this was not due to its effect on cytoplasmic microtubules. They proposed that the target of colchicine was involved in movement of telomeres, and that this may be a non-microtubule tubulin or related protein. This led to the question of whether colchicine would have a similar effect in *Arabidopsis*, which would give further insight into the role of telomeres during meiosis in this organism.

4.2.1 Evidence for uptake of colchicine via the transpiration stream

To test whether colchicine could be taken up via the transpiration stream, as has previously been demonstrated for BrdU, (Armstrong et al, 2003) later stages of meiosis were examined after a 36h treatment with 100μM or 10mM colchicine; a treatment of water as a control was also included. It is known that colchicine disrupts the meiotic spindle, which is required for correct chromosome segregation (Levan 1939; cited by Bennett and Smith, 1979). Therefore treatment would result in mis-segregation of chromosomes after metaphase I. **Figure 4.1** shows DAPI stained spread meiotic nuclei at tetrad stage from inflorescences subject to the above treatments. Image (a) shows an example from the untreated control, with 5 chromosomes per cell. Cells observed from treatments with 100μM showed no abnormalities at later stages. However, meiocytes treated with 10mM colchicine did exhibit mis-segregation at the tetrad stage, as shown in images (b-c), **Figure 4.1**. This is consistent with previous findings that demonstrated 100μM colchicine was sufficient to disrupt telomere pairing, but did not affect meiotic spindle formation in rye (Cowan and Cande, 2002).

4.2.2 Colchicine does not affect progression of meiotic prophase I

To investigate whether colchicine has an effect on the organisation and pairing of telomeres during prophase I of meiosis, a BrdU time course was carried out in order to analyse whether progression of meiotic prophase I was delayed as a result. A meiotic time course is used to allow identification of cells subject to the treatment and to provide a time frame for treatments by labelling of nuclear DNA in S-phase cells. Colchicine at a concentration of 100μM was used for the treatment, as this had previously been shown to be sufficient for disrupting telomere clustering (Cowan and Cande, 2002).

A meiotic time-course was carried out as described in section 2.3. Stems were transferred to 100μM colchicine or water as a control after the BrdU pulse to treat meiocytes during G2. Inflorescences were fixed at 6 hourly intervals subsequent to the labelling pulse, and BrdU detected using an anti-BrdU antibody on meiotic chromosome spread preparations. Preparations were analysed by fluorescence microscopy, with BrdU labelled cells indicating those that had undergone treatment. The numbers of BrdU labelled and unlabelled meiocytes of each meiotic stage, for each time point were recorded. By calculating the proportion of labelled cells at each time point and comparing the treated to the untreated control, any delay in progression can be deduced. The observations from a single time course are shown in **Table 4.1**, which shows the percentage of BrdU labelled meiocytes at each time point for the control and treated samples. A more detailed breakdown of the number of cells observed for each category is shown in **Appendix 8.6**.

From this data it can be noted that progression of meiotic prophase I was not prohibited by the treatment with 100μM colchicine. BrdU labelled pachytene meiocytes were observed at 18h subsequent to the treatment. If progression was prohibited, observation of BrdU labelled pachytene cells would not be expected, as meiosis would arrest prior to this stage, during the pairing of telomeres. The data also shows apparently similar percentages of labelled cells at each stage for treated and untreated control samples.

Sample Time (h)	Meiotic interphase		Leptotene		Zygotene/ pachytene		Diakinesis/ MI		MII		Tetrad	
	water	C100	water	C100	water	C100	water	C100	water	C100	water	C100
-2	**0**	**0**	**0**	**0**	**0**	**0**	**0**	**0**	**0**	**0**	**0**	**0**
0	**50**	**55**	**0**	**0**	**0**	**0**	**0**	**0**	**0**	**0**	**0**	**0**
6	**33**	**29**	**6**	**4**	**0**	**0**	**0**	**0**	**0**	**0**	**0**	**0**
12	**83**	**17**	**11**	**33**	**0**	**0**	**0**	**0**	**0**	**0**	**0**	**0**
18	**60**	**60**	**86**	**100**	**50**	**40**	**0**	**0**	**0**	**0**	**0**	**0**
24	**45**	**58**	**80**	**96**	**33**	**50**	**0**	**0**	**0**	**0**	**0**	**0**
30	**71**	**50**	**71**	**57**	**56**	**52**	**0**	**0**	**0**	**0**	**0**	**0**

Table 4.1: Percentage of BrdU labelled cells in controls and cells treated with 100µM colchicine. It can be observed that the percentage of cells labelled with BrdU in the treated versus untreated control appear to be similar. (MI) metaphase I. (MII) metaphase II. Colchicine treated (C100), control (water). Sample -2 taken prior to BrdU pulse as control.

4.2.3 Telomeres pair in the presence of colchicine

To determine whether colchicine would affect pairing of the telomeres during meiosis, fluorescence *in situ* hybridisation was carried out using a probe to the telomeric repeat sequence of *Arabidopsis*, in conjunction with a BrdU time course. For treatment of meiocytes during G2, stems were transferred to either 100 µM colchicine or water as an untreated control subsequent to the BrdU pulse, and inflorescences fixed after 14h. BrdU was detected using an anti-BrdU antibody, and the probe detected using DIG-rhodamine on meiotic chromosome spread preparations. BrdU labelling allows identification of cells that have been subject to the treatment from G2 stage onwards. **Figure 4.2** illustrates that telomere pairing is not inhibited by treatment with 100 µM during G2. Image (a) shows a BrdU labelled leptotene from an untreated control. In this cell 10 telomere probe foci can be observed, which demonstrates that telomeres are paired. In a situation where telomeres are not paired, a signal number close to 20 would be expected as a diploid nucleus contains 10 chromosomes. Image (b) shows a BrdU labelled leptotene cell with approximately 7 telomere probe foci showing telomeres are paired in the presence of colchicine. A signal number of 10 may not have been

observed due to an overlap or merging of the probe signals. To confirm this observation, the number of telomere probe foci was quantified in at least 5 cells per treatment and for each meiotic stage, BrdU labelled. The mean number of telomere probe foci per cell is shown in **Figure 4.2** (c), which shows there is no significant difference between the mean numbers of telomere probe foci between the treated and untreated samples. This data supports the previous observations.

Previous studies have suggested that different organisms exhibit different colchicine sensitive stages (for review see Zickler and Kleckner, 1998). As telomeres pair at the end of G2 to the beginning of leptotene, it was thought *Arabidopsis* might have an earlier colchicine sensitive stage. To test whether this was the case, stems were placed in either 100 μM colchicine or water as a control for 6h prior to the BrdU pulse. Stems were then transferred to water for a further 14h prior to fixation. Cells that are BrdU labelled at this point represent cells that were treated during G1 phase of the cell cycle. FISH with the telomere probe together with BrdU labelling was carried out as previously described. **Figure 4.3** illustrates that colchicine does not affect pairing of telomeres when introduced during G1. Images (a-b) show untreated and treated BrdU labelled leptotene stage cells respectively, with telomeres paired. To confirm this observation the number of telomere probe foci was quantified in at least 5 cells per treatment and of each meiotic stage BrdU labelled. The mean number of telomere probe foci per cell is shown in **Figure 4.3** (c), which shows there is no significant difference between the mean numbers of telomere probe foci between the treated and untreated samples in G2/early leptotene cells. For the late leptotene-zygotene stage nuclei the number of telomere probe foci was actually lower in the colchicine treated sample than the wild-type. These results together show that unlike other organisms, colchicine does not affect telomere pairing in *Arabidopsis*.

4.3 Investigating a role for telomeres in pairing of homologues in a telomere compromised mutant *tert*

The aim was to study the effect of shortening the telomeres on subsequent pairing, synapsis, and recombination of homologous chromosomes. Many previous studies have suggested that telomeres play an important role in pairing of homologous chromosomes. Studies in mice have shown that those deficient for telomerase show a reduction in fertility (Liu et al, 2004). The effects of shortening telomeres during meiosis were investigated in plants deficient for TERT (telomerase reverse transcriptase). This mutation leads to a gradual shortening of telomeres from one generation to the next, resulting in gradually more severe defects in growth and development (Fitzgerald et al, 1999).

4.3.1 Isolation and Characterisation of T-DNA insertion line tert G_8

Seeds from *Arabidopsis* homozygous *tert* generation 7 (line 69) plants were provided by D.E. Shippen (personal communication). Seeds were sown alongside a wild-type control, Col-0 for comparison. To confirm that plants contained a T-DNA insert in the *tert* gene (At5g16850), a PCR with gene specific primers was carried out on genomic DNA extracted from each plant (see **Figure 4.4 A**). For primer design, see **Appendix 8.2** and Fitzgerald et al, (1999). For DNA extractions, 1 young leaf from each plant was isolated, and DNA extracted using the Plant Extract-N-Amp kit (SIGMA). The products of the PCR are shown in **Figure 4.4 B**. This genotyping showed that all *tert* generation 8 (G_8) plants contained the insert, and could therefore be used for further analysis.

4.3.2 Phenotypic analysis of tert G_8

Previous reports have observed a wide variety of developmental defects in the later generations of the telomerase deficient *tert* mutant in *Arabidopsis* (Rhia et al, 2001). This was indeed the case for the *tert* G_8 mutant, as shown in **Figure 4.5 A**. A number of developmental defects were evident in the *tert* G_8 mutant. These included defects in both vegetative and reproductive development. **Figure 4.5 A** (b) shows an example of a *tert* G_8 plant. The severity of the phenotype differed between plants, with this an example of one of the less severely affected plants. Defects in vegetative development included leaves becoming curled and lobed; particularly rosette leaves. Some fasciation of the stems was also observed. Image (c) shows an example of a more severely affected plant. Here it can be observed that the rosette leaves do not form normally, and appear to form a clump.

Defects in the floral organs can also be seen, with sepals not forming normally, causing buds not to be enclosed. The reproductive organs also fail to develop normally, in both the more and less severely affected plants. Anthers often appear smaller than wild-type, and in some cases do not form at all. Due to this an Alexander stain of pollen from the *tert* G_8 and wild-type plants was performed. An example of Alexander stained pollen from *tert* G_8 is shown in image (e). The red staining indicates viable pollen, and the unstained pollen grains represent non-viable pollen. In wild-type, 3130 viable pollen grains and 82 non-viable pollen grains were observed, giving a ratio of 82:1 viable to non-viable pollen. In the *tert* G_8 mutant, just 469 viable pollen grains and 81 non-viable pollen grains were observed, giving a ratio of 6:1 viable to non-viable pollen. This shows that there is a large reduction in formation of viable pollen in the *tert* G_8 mutant. From **Figure 4.5 A** images (b-c) it becomes apparent that fertility is also greatly reduced, with silique length reduced to just 0.1-0.4 mm in the most severely affected plants, in comparison to approximately 1cm in wild-type plants. Seed counts were in agreement with these observations, with the *tert* G_8 plants showing a mean seed count of only 4% of wild-type. **Figure 4.5 B** shows the mean numbers of seeds per silique for each of these lines.

Due to the reduction in fertility observed, it was thought that a reduction in the length of telomeres could be having a meiotic effect. A detailed cytological analysis was carried out on *tert* G_8 plants, as G_9 plants mostly failed to germinate. Those that did germinate arrested in

vegetative development. An example is shown in **Figure 4.5 A** (d), which illustrates that leaf morphology is severely perturbed, and formation of a shoot merited is prevented as shown by no inflorescence bolt.

For the analysis of the *tert* G_8 line, 10 plants were selected for analysis. A larger number of plants were required due to the fact that fewer meiotic stages were observed by cytological analysis, in comparison to the wild-type control. These plants were all homozygous for the insertion and grown together with an appropriate control. **Figure 4.5 B** shows a low standard error for the mean number of seeds per silique for these plants, showing that the fertility of these plants was similar.

4.3.3 *tert* G_8 has severely shortened telomeres

Prior to investigating whether the *tert* mutant showed defects in meiotic progression, it was first established that the length of telomeres was reduced in the mutant. To do this, fluorescence *in situ* hybridisation was carried out on meiotic spread nuclei at pachytene stage (**Figure 4.6)**. A probe to the plant telomeric repeat sequence conjugated to a DIG label was used to probe the *tert* G_8 mutant (b) and a wild-type control (a). The wild-type cell shows labelling of approximately 9 telomere probe foci. A maximum signal number of 12 would be expected with paired telomeres at this stage. This includes the 2 interstitial sites, which are also recognised by the telomeric probe. The *tert* G_8 mutant shows no labelling of telomeric sequences, but does show labelling of the interstitial sequences, which would not be affected by this mutation. Labelling of these sites acts as a positive control. The results indicate that the telomeric repeat sequences are severely reduced in the mutant, such that they cannot be resolved by FISH.

4.3.4 Meiotic phenotype of *tert* G_8

To investigate whether the severe reduction in fertility was due to a defect in meiosis, meiotic chromosome spreads of pollen mother cells (PMCs) were prepared and stained with DAPI to visualise the chromatin by fluorescence microscopy. Examples of each meiotic stage from the *tert* G_8 mutant together with a wild-type control are shown in **Figure 4.7**.

Early prophase I nuclei from leptotene through to diakinesis were indistinguishable from wild-type. However, on closer inspection it appears that at pachytene synapsis may not be fully completed. The distal regions of 1 pair of homologues appear to be unpaired (see arrow image k). At metaphase I 5 bivalents can be observed suggesting that recombination is completed. Metaphase II nuclei appear similar to wild-type overall, however in some cases bridges can be observed between homologues. This observation suggests there may be repair of the telomeres as DSBs. The tetrads observed were all indistinguishable from wild-type, with 5 chromosomes observed per cell. However, the number of tetrads observed was lower than that of wild-type, so subtle defects resulting from bridges at metaphase II could have been overlooked.

4.3.5 Pairing of homologous chromosomes in the tert mutant

Analysis of meiotic spreads suggested that the sub-telomeric regions of homologues may not pair in the *tert* G_8 mutant. To investigate whether this was indeed the case, fluorescence *in situ* hybridisation of a BAC probe to the sub-telomeric region of chromosomes 1 (F19K16) was completed; see **Figure 2.1** for locus. **Figure 4.8** shows examples of FISH on both the mutant and a wild-type control. In a wild-type situation the sub-telomeric region of chromosome 1 becomes paired during leptotene, and remains paired through to pachytene; as shown in **Figure 4.8** images (a-c). From the images of the mutant, it was observed that the F19K16 BAC often remains unpaired (2 foci) throughout leptotene to pachytene, as shown in images (d-f) respectively. Image (g) shows a close up view of the distal regions of chromosome 1 homologues shown in image (f). Here it appears as though regions that are more proximal are synapsed, but that the distal ends of the homologues remain unpaired, and are splayed out (see arrows). A second example of this can be seen more clearly in image (h), where 1 pair of homologues can clearly be seen to be paired along their lengths apart from in the distal region where the ends are again splayed out (see arrow). However, this image also shows that the F19K16 locus is paired in this case. This may be due to synapsis of more proximal regions bringing the ends into a close alignment. To ensure that the F19K16 BAC did not recognise a duplicated second region FISH was performed on metaphase I chromosomes. Image (i) shows that the F19K16 BAC only recognises 1 site, which confirms that 2 foci indicate, unpaired homologous chromosomes.

To quantify these differences the numbers of F19K16 foci at each meiotic stage in both the mutant and wild-type were noted. The mean number of F19K16 foci observed at each stage is shown in **Figure 4.9**. In wild-type, the F19K16 foci become progressively more paired from leptotene up to pachytene, where foci were observed to be paired in all cells. From the data it appears that, the mutant exhibits more unpaired foci than in the wild-type. However, the F19K16 foci do become more paired as cells progress from leptotene through to pachytene. *t*-tests were carried out to test whether the differences observed between the mean values of foci between wild-type and the mutant for each meiotic stage were significant (see **Figure 4.9**). In each case, the mean number of F19K16 foci for the *tert* G_8 mutant was shown to be significantly higher than that of the wild-type control. This confirms that the sub-telomeric region of chromosome 1 frequently remains unpaired in the *tert* G_8 mutant. These results suggest that the telomeric repeat sequence is important for pairing of homologous telomeres and sub-telomeric regions.

4.3.6 Synapsis is completed in the tert G_8 mutant

An investigation was undertaken to establish whether pairing of the telomeres is required for normal synapsis. Previous studies in mice have shown that late generation telomerase mutants have defects in synaptonemal complex formation, as shown by immunolocalisation of the SC component SCP3 (Liu et al, 2004). To study the effects of reduced telomere length on synapsis in *Arabidopsis*, dual-immunolocalisation of ZYP1 protein (SC component) together with ASY1 protein was carried out on meiotic chromosome spreads. **Figure 4.10** shows immunolocalisation on *tert* G_8 nuclei alongside a wild-type control. Polymerisation of the ZYP1 protein in the *tert* mutant appears indistinguishable from that in wild-type. In wild-type meiosis, illustrated in images (a-f), ZYP1 foci first appear in early zygotene and begin to polymerise along the length of the homologues. This polymerisation continues progressively until pachytene, where homologues become completely synapsed. This also appears to be true of the *tert* mutant. However, at the pachytene stage in the *tert* mutant, synapsis does not appear to be complete. Image (l) in **Figure 4.10** illustrates that the ASY1 labelling is not diffuse along all of the chromatin. The ASY1 signal becomes diffuse in areas where ZYP1 polymerises. This indicates that these regions are synapsed. Regions that are not diffuse show areas that are not synapsed. Homologues may not fully synapse in the *tert* mutant due to the distal regions of the homologues that were shown to remain unpaired by FISH studies.

4.3.7 Telomere pairing is not required for recombination

To quantify the number of chiasmata, fluorescence *in situ* hybridisation of the 45s and 5s rDNA probes was carried out on meiotic chromosome spreads of metaphase I nuclei. **Figure 4.11** (a-b) shows examples of the distribution of chiasmata on wild-type and the *tert* G_8 mutant. Here it can be seen that the mutant is indistinguishable from wild-type. *tert* G_8 shows a slight reduction in the number of chiasmata, with a mean of 8.68 in comparison to wild-type with 9.15 per cell; as shown in **Figure 4.11** (c). This slight reduction may reflect changes in chiasmata distribution, however remains in the range of that expected in wild-type. Taken together these data show that telomere pairing is not required for the downstream events of synapsis, recombination, and chiasmata formation.

4.4 Discussion

4.4.1 Colchicine has no effect on telomere pairing or progression of meiotic prophase I in Arabidopsis

A number of studies have used drugs that disrupt progression of meiosis to elucidate the mechanisms that control telomere movement and pairing during meiosis. Of these drugs, colchicine has been one of the most widely studied. To investigate whether colchicine affected movement and pairing of homologous telomeres in *Arabidopsis*, a meiotic time course was performed in conjunction with colchicine treatment. Analysis showed progression of meiotic prophase I was not delayed (see **Table 4.1**). Secondly, colchicine had no effect on pairing of telomeres by observing no significant difference between the numbers of telomere probe signals in comparison to a wild-type control (see **Figure 4.2**).

Failure of colchicine to disrupt progression of meiotic prophase 1 or pairing of the telomeres in *Arabidopsis* is in contrast to what has been observed previously. Many studies have found that colchicine disrupts the association and synapsis of homologues (Loidl, 1988 and Tepperberg, 1997), and effects downstream events, for example chiasma formation, as demonstrated firstly in *Tradescantia* (Walker, 1938) and later in *Lilium* (Bennett et al, 1979). In rye it has been observed that colchicine prevents clustering of telomeres into the bouquet, and hence progression of meiotic prophase 1 (Cowan and Cande, 2002). Similar observations have also been observed in wheat-rye additions (Corredor and Naranjo, 2007). This lead to the question of why colchicine had no effect on pairing of telomeres in *Arabidopsis*.

One possibility is that the colchicine sensitive period in *Arabidopsis* could differ to other plant species. It has been proposed that in species where homologues pair prior to meiosis that the colchicine sensitive stage may be earlier (Zickler and Kleckner, 1998). For the majority of species that have been studied, the leptotene-zygotene transition of meiosis has been shown to be the stage most susceptible to colchicine treatment, with treatments after this having no effect on synapsis or chiasma formation (for a summary of colchicine sensitive stages, see **Figure 4.12**). This has been observed in a number of plant species, for example *Lilium* (Bennett et al, 1979), *Secale celeale* (Cowan and Cande, 2002), and in mammals (Tepperberg, 1997). This is now known to be a result of its effect on formation of the bouquet (Cowan and Cande, 2002). Whilst in wheat the colchicine sensitive stage has been shown to be earlier,

with colchicine only having an effect when applied in pre-meiotic interphase, (Discoll et al, 1967). This could be the case in *Arabidopsis* as it has been shown that homologues pair at the G_2-leptotene transition (Armstrong et al, 2001). This may indicate that treatment of colchicine during G_1 may have an effect on pairing. To test this theory FISH was used in conjunction with a BrdU pulse. To treat cells in G_1, influorescences were subjected to treatment with colchicine for 6h prior to the BrdU pulse. This enabled analysis of cells that had been treated in G_1, as these would be BrdU labelled. Buds were fixed at 14h subsequent to the BrdU pulse to examine meiocytes at leptotene, in order to determine whether telomeres were paired. As illustrated in **Figure 4.3,** no significant difference between the mean numbers of telomere probe foci compared to the untreated control could be observed. These results show that treatment with colchicine in G_1 has no effect on pairing of homologous chromosomes. These results together suggest that colchicine has no effect on meiosis in *Arabidopsis* unlike all other organisms that have been studied. One argument could be that the concentration of 100μM colchicine was not sufficient in this species. However, telomeres were found to pair in preliminary experiments using 10mM colchicine (which was shown to cause mis-segregation) at various stages.

One question that remains to be answered is what the target of colchicine is that causes failure of bouquet formation and homologue pairing. Cowan and Cande, (2002) noted that failure to form a bouquet was not due to its effect on cytoplasmic microtubules, as other microtubule depolymerising drugs had no effect on clustering. They observed that colchicine blocked the lateral movement of telomeres on the nuclear envelope, but not the association of telomeres with the nuclear envelope. The study showed that only colchicine and podophyllotoxin were able to inhibit telomere clustering, and these have previously been shown to bind the same site on β-tubulin (Morejohn, 1991, cited by Cowan and Cande, 2002). They proposed that the target could be a specific colchicine binding target with similarities to β-tubulin. In rats, the colchicine analog lumicolchicine that is unable to bind tubulin had no effect on chromosomes during meiotic prophase I (Solonen et al, 1982), which is consistent with this idea. Another possibility is that a specialised membrane associated tubulin or related protein could be the target. Hotta and Shepard, (1973) showed that the nuclear membrane of pollen mother cells in *Lilium* contained a protein that could bind colchicine. It is also possible that colchicine could target other membrane proteins. Studies have shown that colchicine can block the function of

many membrane ion channels, and more recently has been shown to be a competitive antagonist of the human $GABA_A$ receptor. Importantly this function was shown to be specific to colchicine, and not due to its role as a microtubule depolymerising agent (Weiner et al, 1998 and references therein). It is feasible that colchicine may act in a similar way in plants.

It is possible that the target of colchicine that has been described in other species and organisms is somehow different in *Arabidopsis*, and therefore is not affected. However targets like tubulin are highly conserved. The *Arabidopsis* β-tubulin protein is 97% identical to both wheat and rice in a BLASTp search, suggesting the colchicine binding sites to be correspondingly. Instead the difference may arise from the unique localisation of telomeres in *Arabidopsis*. It is known that telomere pairing occurs while they are localised around the nucleolus and is independent of subsequent nuclear membrane attachment. This may explain why colchicine does not disrupt telomere pairing and subsequent processes in *Arabidopsis*, as homologues have already begun to pair before moving to the nuclear envelope during leptotene. This may suggest that movement of telomeres on the nuclear membrane is not important for pairing in *Arabidopsis* however it remains unknown whether colchicine affects this.

4.4.2 Investigating the role of telomeres in homologous chromosome pairing by analysis of the tert mutant with severely shortened telomeres

Previous studies of the *tert* mutation in *Arabidopsis* have observed a number of developmental defects, including reduced fertility (Rhia et al, 2001). Studies in mice have revealed that female mice deficient for telomerase exhibit impaired synapsis and recombination due to shortened telomeres (Liu et al, 2004). The *tert* mutant was analysed in *Arabidopsis* to investigate the role of telomeres in pairing of homologous chromosomes. It was thought that defects in meiotic progression could be the cause of the reduced fertility that had been previously described. Questions that arose were whether telomeres are necessary for the localisation around the nucleolus, as they are for nuclear envelope attachment in other species, and whether their pairing is necessary for pairing of homologues along their length, and eventual synapsis and recombination. Analysis of the *tert* G_8 mutant has shown that severely shortened telomeres result in severe developmental defects, in addition to reduced fertility. It was found that telomeres remained unpaired until at least pachytene, but that this did not result in defects in synapsis and recombination.

4.4.2.1 Telomeres do not pair in the tert G_8 mutant

Plants from *tert* G_8 were used for analysis as these had been previously been shown in exhibit moderate to severe defects in development of reproductive organs (Rhia et al, 2001). Plants were similar in phenotype to those previously described, with defects in vegetative growth of leaves and stems in addition to a reduction in silique length, and number of seeds per silique (see **Figure 4.5 e**). It was first established that the telomeres were shortened in the *tert* G_8 mutant. To do this, FISH was carried out using a probe against the plant telomere repeat sequence on pachytene stage spread meiotic nuclei (see **Figure 4.6**). It was noted that the telomeric repeats were severely shortened in the *tert* G_8 mutant, as telomere probe signals were not visible at the telomeres. Liu et al, (2004) used FISH with a telomeric repeat probe to measure the length of telomeres in the 4^{th} generation of telomerase deficient mice. By measuring units of telomere fluorescence, they also found that telomere length was severely shortened in both male and female meiosis. The fact that no signal was observed in the *Arabidopsis* mutant, most likely reflects the shorter telomeric repeats in this organism.

To ascertain whether this had an effect on pairing of homologous telomeres and their localisation around the nucleolus, FISH was carried out using a sub-telomeric chromosome 1 specific BAC as a probe. The F19K16 BAC on chromosome 1 remained unpaired throughout early prophase I. Meiotic chromosome spreads revealed that in numerous cases the sub-telomeric ends were splayed apart from one another at pachytene, despite the rest of the chromosomes appearing paired (**Figure 4.8** images f-h). The mean number of F19K16 foci was shown to be significantly higher than in wild-type using a *t*-test, indicating that telomeres are unpaired. This was observed at leptotene through to pachytene (**Figure 4.9**). These results strongly suggest that the telomeric repeat sequence is required for pairing of homologous telomeres.

The telomeric repeat sequence has also been shown to be important for telomere pairing, through attachment to the nuclear envelope during bouquet formation. In mammals, ring chromosomes without telomeric repeats have been shown not to participate in telomere clustering and bouquet formation (Voet et al, 2003). Maize ring chromosomes that contain telomeric repeats have been shown to participate in telomere clustering during bouquet formation (Carlton and Cande, 2002). This lead to the question of whether the telomeric repeats in *Arabidopsis* are necessary for clustering of telomeric ends around the nucleolus. Chromosomes 2 and 4 contain a NOR on the short arm, and are therefore associated with the nucleolus. How the other chromosomes are associated remains to be elucidated. The nucleolus is not a membrane bound structure (Carmon-Fonseca et al, 2000) so the telomeres are unlikely to be attached to the periphery.

The localisation of telomeres was examined to ascertain whether it was altered in the *tert* mutant, but the results obtained were inconclusive. To study the localisation of telomeres during G_2 prior to meiosis, where telomeres cluster around the nucleolus in wild-type, FISH was carried out using a series of sub-telomeric BACs from different chromosomes. It was found that BAC signals were localised around the nucleolus in some cells, but not others in the *tert* mutant. This may be due to variation in the lengths of telomeres, with a critical length required for localisation to the nucleolus. However, the BAC signals were not always localised around the nucleolus of wild-type cells, which points to the fact that the cells that were examined may have been at different stages. To enable accurate investigation into the

localisation of telomeres at G_2, it would therefore be necessary to incorporate a BrdU pulse to both the *tert* mutant and a control of wild-type. FISH using these sub-telomeric BACs could then be carried out in conjunction with BrdU labelling to identify G_2 stage cells for an accurate comparison.

4.4.2.2 Homologous chromosomes synapse and recombine in the absence of telomere pairing

Sub-telomeric regions were unpaired in the *tert* mutant leading to the question of whether synapsis was able to proceed as in wild-type. To study whether synapsis was affected, immunolocalisation was performed using an antibody against the central element protein ZYP1. As shown in **Figure 4.10,** ZYP1 localisation was indistinguishable from that of wild-type; although complete synapsis was not observed. It was thought that this could be due to the unpaired ends observed in *tert* pachytene meiotic spreads (see **Figure 4.8**). The results illustrate that telomere pairing is not required for synapsis to occur, and therefore suggests that telomere pairing is not required for the downstream events of complete alignment and pairing of homologues, which are prerequisites of synapsis. Despite the observation that synapsis appeared to progress with wild-type dynamics, it was decided to analyse the frequency of chiasmata formation. As shown in **Figure 4.11,** the chiasma frequency was slightly reduced compared to wild-type, but remained in the range of that expected for wild-type meiosis. It was thought that this could be due to a change in chiasmata distribution, which may occur if the ends do not pair and synapse.

These observations are in contrast to previous findings in telomerase deficient mice. Liu et al, (2004) found that synapsis and recombination were impaired in late generation telomerase deficient female meiosis, in cells that reached pachytene. Mutants that result in defective bouquet formation also exhibit defects in pairing and synapsis of homologues. In maize, the *pam1* mutant blocks movement of telomeres on the nuclear envelope, resulting in incomplete and even non-homologous synapsis (Golubovskaya et al, 2002). In budding yeast, the mutant *ndj1Δ* is defective in telomere attachment to the membrane. It was observed that pairing, synapsis, and recombination were delayed as a result (Trelles-Sticken et al, 2000; Wu and Burgess, 2006). More recently, proteins have been found to link telomeres to the actin cytoskeleton via the nuclear envelope; termed SUN domain proteins. Ding et al, (2007)

demonstrated that both male and female mice deficient for the SUN-1 protein showed severe defects in pairing and synapsis as a result of telomeres not clustering on the membrane. MLH-1 foci (mark crossover sites) were found to be absent in the null mutant. They suggested that pairing, synapsis, and recombination can be initiated, but that completion of these processes is perturbed.

These results show that pairing and synapsis are not completely impeded, but become less efficient without telomere pairing and clustering, and shows that telomere pairing is not required for the homology search process. These results together with what was observed in the *Arabidopsis tert* mutant is in agreement with the notion that telomere clustering or bouquet formation in some species, is a mechanism that facilitates downstream pairing. Although synapsis and recombination appeared wild-type in the *tert* mutant, some chromosome ends remained unpaired. This suggests that telomere pairing is important for pairing of chromosome ends but not for complete pairing along the length of homologues. It will be interesting to investigate whether pairing of homologues is delayed in the *tert* mutant, which would implicate telomeres in a role of facilitating pairing.

In a number of organisms, DNA DSBs have been shown to be necessary for close juxtaposition of homologues, and have been suggested to be of importance for the homology search (reviewed by Zickler, 2006). This may be case in *Arabidopsis*, as it would explain why homologues were able to pair and synapse in the absence of telomere pairing. However, it is known that homologous telomeres pair whilst clustered around the nucleolus in *Arabidopsis*, prior to formation of DSBs. How this homology is specified remains to be elucidated.

4.4.2.3 What causes the reduced fertility of tert mutants?

As the levels of chiasma formation were in the range of that expected for wild-type meiosis, and tetrads were indistinguishable from wild-type, this suggested that unpaired telomeres were not the cause of the severely reduced fertility observed (see **Figure 4.5**). Therefore, this led to the question of what was the basis for this reduction in fertility. Meiotic chromosome spreads were prepared for the *tert* mutant alongside a wild-type control to study any defects caused by a reduction in telomere length. **Figure 4.7** shows representations of each meiotic stage. Generally, meiotic stages in the *tert* mutant appear the similar to wild-type; however, in

some instances metaphase II nuclei exhibit bridges. It has yet to be established whether these connections are homologous, although they do resemble those observed in mitotic anaphase I nuclei of *tert* deficient plants (Rhia et al, 2001). It is feasible that these represent telomeres that have undergone fusion events through the process of non-homologous end joining (NHEJ) or a similar pathway. A variety of end-joining pathways have been shown to occur during mitosis of *Arabidopsis* plants with severely shortened telomeres (Heacock et al, 2004). Further studies into fusion events of severely shortened telomeres have revealed that there is a strong correlation between the first observation of telomere fusions and the presence of at least 1 telomere that is less than or equal to 1 kb in length. Heacock et al, (2007) proposed this may represent a threshold length under which telomeres are unprotected and can undergo fusion events. *tert* G_8 mutants have been shown to contain telomeres in the range of over 1.5 kb to less than 1 kb in length (Rhia et al, 2001). Therefore, it is likely that some telomere lengths fall below this threshold in the *tert* G_8 mutants studied here, consequently resulting in the bridges observed. Despite the fact that the tetrad stage of the *tert* mutant appears similar to wild-type, breakage of the metaphase II bridges may result in incorrect segregation and therefore reduce fertility. It remains to be seen whether these bridges are present at anaphase, but this stage was not observed due to the low numbers of meiotic cells in the *tert* mutant.

While this may explain some reduction in fertility, it is unlikely to be the cause of the severely reduced fertility observed. An alternative explanation for such a severe reduction in fertility is that cells undergo programmed cell death (PCD). When analysing meiotic chromosome spread preparations, it was noted that less meiotic cells were observed from *tert* preparations than wild-type. Previous studies in mice found a reduction in the number of meiotic cells observed in late generation telomerase deficient males. They found that this was due to male germ cells undergoing apoptosis at the onset of meiosis (Hemann et al, 2001). This would explain the reduction in the number of meiocytes observed in the *Arabidopsis tert* mutant, and why fertility was reduced. However, contrary to this Rhia et al, (2001) found no evidence for PCD in the *tert* G8 and G9 mutants by looking for the presence of a classic PCD DNA fragmentation ladder. This may reflect the higher plasticity of plant development in dealing with telomere dysfunction. As the reduced numbers of meiotic cells could not be explained by PCD, this led to the consideration that more general defects in plant development maybe the cause of the severely reduced fertility. Defects in floral and reproductive organs were

observed in the *tert* G_8 plants (**Figure 4.4**). In most plants used in the study, anther development was perturbed, with anthers appearing much smaller than wild-type, or undeveloped. Alexander staining (**Figure 4.5 e**) showed that the number of viable pollen grains in the *tert* G_8 mutant was greatly reduced in comparison to wild-type. This is consistent with previous observations. Rhia et al, (2001) found that *tert* G_9 plants contained undeveloped anthers that contained few if any pollen grains. This evidence supports the notion that the reduction in fertility is due to defects in reproductive development rather than meiotic progression.

4.4.3 Conclusions and future perspectives

Telomeres clearly play an important role in the protection of chromosomes, although their precise role during meiosis remains unclear. Results so far point to a role for telomeres in facilitating pairing in a number of organisms, where bouquet formation brings homologues into a close alignment. Telomeres have been shown not to be required for pairing and synapsis of homologues (Moore and Shaw, 2009). In *Arabidopsis* telomeres become paired while localised around the nucleolus (Armstrong et al, 2001). It has been shown that introduction of colchicine at various points prior to the onset of meiosis has no effect on meiotic progression or telomere pairing. It has also been observed that shortening the telomeres prevents their pairing, but that this does not prevent pairing and synapsis of homologues, and the number of chiasmata formed are within the wild-type range. The results suggest that in *Arabidopsis*, telomere pairing is not required for pairing of homologues, but it remains unknown whether nucleolar clustering is important and whether it is the telomeric repeats that are necessary for this interaction (excluding NOR bearing chromosomes). However, it was observed that the sub-telomeric regions were unable to pair, so it is possible that this requires telomere repeats. Homologues were able to pair and synapse in the absence of telomere pairing, which suggests that the telomeres are not involved in homology recognition. However, it is known that homologous telomeres pair while around the nucleolus and prior to DSB formation, so it will be interesting to determine how this homology is specified.

It has been shown that colchicine specifically blocks movement of telomeres on the nuclear envelope, therefore this suggests that colchicine has no effect in *Arabidopsis* due to its unique

telomere localisation. It will be interesting to investigate the role of actin in the movement and pairing of homologues. Studies in yeast have shown that the actin depolymerising drug Latrunculin B prevents bouquet formation and more general chromosome movement, and more recently it has been proposed that telomere led movements on dynamic actin cables are important for resolving interlocks and non-specific connections (Trelles-Sticken, 2005; Koszul, 2008).

Chapter 5

Tracking the telomeres using POT1 telomere binding proteins

5.1 Introduction

To allow meiotic recombination and correct segregation of chromosomes during meiosis, homologous chromosomes must first recognise one another and pair. Telomeres have long been thought to be important in this process (see discussion section 1.9). It is unknown how telomere movements are controlled in *Arabidopsis* meiocytes. Armstrong et al, (2001) observed that telomeres show a dynamic organisation throughout prophase I using FISH with a telomere repeat probe. Currently, knowledge of telomere behaviour in *Arabidopsis* is limited to the study of fixed meiocytes. The development of a live imaging system would lead to major advances of our understanding of telomere and general chromosome movements during meiosis in this model organism. An improved method of labelling the telomeres would enable further study of the behaviour of chromosomes by this approach. It was thought that using a GFP tagged telomere binding protein would provide a clear method of labelling telomeres in live meiocytes. Studies in other organisms have used this approach to study telomere movements. Trelles-Sticken, et al (2005) used GFP labelled RAP1 to analyse the dynamics of yeast telomeres during meiosis in live cells. Telomere binding proteins have also been observed to play a direct role in the movement of telomeres. In budding yeast, the telomere binding protein Rap1 has been shown to bind a protein called Sad 1 (Tomita and Cooper, 2006). This is a SUN domain protein, which has been demonstrated to attach telomeres, via other proteins, to the nuclear membrane and actin cytoskeleton; already known to control telomere movements in yeast (Trelles-Sticken et al, 2005). A number of candidate telomere binding proteins have been found in *Arabidopsis* (for discussion see section 1.8). The potential single stranded telomere binding proteins POT1a and POT1b were chosen as the best candidates. Shakirov et al, (2005) investigated the effect of over-expressing truncations of the POT1 proteins in *Arabidopsis*. They determined that the POT1 proteins were involved in telomere length regulation and protection, and that they were functionally non-redundant.

This chapter describes the purification of recombinant proteins used to raise AtPOT1a and AtPOT1b specific antibodies, and the use of these in immunolocalisation and western blot analysis to investigate the localisation of telomeres during meiosis. The aim was to study the dynamics of telomeres in prophase I using these antibodies to label the telomeres. This would also confirm whether the proteins localised directly to telomeres, which had yet to be shown

in vivo, and thus confirm them as telomere binding proteins. It was thought that this could lead to the development of a GFP tagged protein that could be used in the future for live imaging analysis of telomere and general chromosome movement during meiosis.

5.2 Cloning POT1a and POT1b

Antibodies were raised against both POT1a and POT1b proteins. The regions used to design the primer sets were chosen based on sequence similarity. POT1a and POT1b share 49 % similarity, therefore the region with the least conserved sequence was chosen to ensure the antibodies would be specific to each protein. A ClustalW amino acid sequence alignment of the two proteins is shown in **Figure 5.1**. Sequences of recombinant proteins are highlighted as specified.

RNA was extracted from wild type Col-0 inflorescences and cDNA synthesised from this using reverse transcription with an oligo-dt primer. Primer sets were designed to amplify the specific regions of interest. The primers were designed with restriction sites incorporated at the ends to enable the inserts to be cloned into an expression vector in the correct orientation. For both recombinant proteins, *Nde1* and *Xho1* were used for the 5' and 3' ends respectively. The *NdeI* restriction site was chosen because it contains an ATG start codon. For cloning of POT1a, the primers POT1F1 and POT1R1 were used, and for POT1b, the primers POT2F1 and POT2R1 were used (See **Appendix 8.2** for primer sequences). Products from the PCR (**Figure 5.2 A**) were gel extracted and subsequently ligated into the pDRIVE vector (Qiagen), after which the presence of an insert was confirmed by boil preparation of bacterial DNA and digestion with the specific restriction enzymes. To ensure the inserts corresponded to the correct sequence and that they were in frame, DNA extractions (by wizard preparation) and sequence analysis were undertaken. Once it was confirmed that they corresponded to the correct sequence, the fragments of interest were sub-cloned into the pET21b expression vector (Novagen). This contains a hexahistidine tag downstream of the insert, which permits easier extraction and identification of the expressed protein. The nucleotide sequence obtained was translated using bcm sequence launcher (http://searchlauncher.bcm.tmc.edu) to ensure it translated the correct polypeptide.

5.3 Production of POT1a recombinant protein

5.3.1 Determining expression level and cellular localisation

Test inductions of the POT1a protein were performed together with crude protein extractions using BugBuster (Novagen) to determine the cellular localisation of the protein. Protein expression was induced in *E. coli* BL21 cell cultures containing the POT1-pET21b plasmid, and samples taken 2 and 4h post induction for analysis. A control of an uninduced culture was carried out in parallel. Proteins were separated into a soluble and insoluble fraction and were subsequently resolved by SDS-PAGE gel electrophoresis on a 15 % gel. Proteins were detected using coomassie blue (R250) staining. **Figure 4.2 B** shows that POT1a expression was not distinguishable by SDS-PAGE gel coomassie staining. A control of a meiotic protein called STAG3 (also in pET21b) was subject to the same growth and induction conditions, and analysed in conjunction. The expression of this protein is known to be high, and was found to

be highly expressed in the insoluble induced fraction (**Figure 4.2 B).** This demonstrates that POT1a was either not expressed, or expressed at a very low level. To ascertain whether the POT1a protein was being expressed, western blot analysis was performed, again including the STAG3 positive control. Both proteins were detected using a mouse anti-HIS antibody. A faint band was detected by the anti-HIS antibody in the POT1a sample that labels a protein of the predicted molecular weight of the recombinant protein; ~15 kDa. From **Figure 5.2C,** it can be seen that POT1a is expressed in the insoluble induced fraction only, at a low level.

Following confirmation that the POT1a fragment was being expressed, the growth and induction conditions were analysed to optimise the level of expression. Growth and induction temperatures were varied together with the time of induction from 16 ^{o}C-37 ^{o}C and 1-6 h respectively. Crude protein extractions were carried out for each of the conditions specified, and analysed by SDS-PAGE gel electrophoresis, which was visualised by coomassie staining. It was found that varying neither the temperature of growth and induction, nor the time the protein was induced, resulted in improved protein expression. The concentration of IPTG was also altered to 0.5 mM, or 10 mM, and shown to have no effect.

Following this, the expression level of the protein in different strains of *E. coli* was tested, as these have previously been shown to gives higher levels of protein expression in our laboratory. Competent cells were made from the *E. coli* strains SK1592, HB101, JM83, and JM101, and subsequently transformed with the pET21b construct containing the POT1a sequence for protein expression analysis. Crude protein extractions were made from all strains induced for protein expression, employing the same conditions used previously. From SDS-PAGE gels stained with coomassie, no protein expression of POT1a was detected in any of the strains tested. Due to the low expression of POT1a, it was decided purification of sufficient protein would prove too difficult and therefore this was therefore abandoned.

5.3.2 Cloning POT1aLONG into pET21b

Further regions of the POT1a protein were designed for recombinant protein expression and antibody production. Different length fragments were designed in different regions of the protein to test whether these would yield improved protein expression. Two recombinant proteins were designed, one in the same region as before to remain specific to the POT1a protein (POT1aSHORT), and one larger fragment, which was less specific to POT1a (POT1aLONG). Previous results from our laboratory have shown that larger proteins tend to be more highly expressed. Primer sets were designed for each of these fragments; again containing the *Nde1* and *Xho1* restriction sites for cloning into pET21b. For POT1aSHORT the primers POT1FB and POT1R1 were used, and for POT1aLONG, the primers POT1FA and POT1R1 were used (**Appendix 8.2**). The regions amplified for each are shown in **Figure 5.1**. Agarose gel analysis of the PCR products obtained for cloning is illustrated in **Figure 5.3A**. Lane one shows the POT1aSHORT fragment amplified using the POT1FB and

POT1R1 primers running at the predicted size of 280 bp. Lane 2 shows that of POT1aLONG, amplified with POT1FA and POT1RA primers running at the predicted size of 980 bp. Subsequent cloning into pET21b was performed as described in section 5.2. Cloning of the POT1aSHORT fragment into pET21b proved difficult for unknown reasons; it was therefore decided to proceed with POT1aLONG.

5.3.3 Testing POT1aLONG protein expression and cellular localisation

Test inductions of the POT1aLONG protein were performed together with crude protein extractions using BugBuster (Novagen). *E. coli* BL21 cell cultures containing the pET21b plasmid were induced with 1 mM IPTG, and expression permitted for 4 h before sampling. Proteins were separated into a soluble and insoluble fraction using the Bugbuster method and were subsequently resolved by SDS-PAGE gel electrophoresis on a 10 % gel, and visualised by coomassie staining. From **Figure 5.3B** it can be observed that the POT1aLONG-HIS recombinant protein is expressed in the insoluble induced fraction only, at a much higher level than the previously tested protein. Due to the high level of expression, large-scale protein purification of this recombinant protein was carried out.

5.3.4 Isolation of recombinant POT1aLONG-HIS

Large-scale extraction was performed under denaturing conditions given that POT1aLONG was shown to be expressed in the insoluble fraction. Purification of protein from the insoluble fraction requires the protein to be refolded. Large-scale expression of the protein was carried out, and proteins were extracted from isolated inclusion bodies as described in section 2.13.3.1. The proteins were subsequently dialysed to remove any denaturant (guanidine), and refolded before concentrating using PEG. The POT1aLONG protein precipitated during dialysis, which could have been due to the refolding being inefficient. To measure the concentration of the protein it was first re-denatured in 6M guanidine to remove some of the precipitate, and a Biorad assay then performed. The concentration of the POT1aLONG recombinant protein was estimated at 0.5 mg/ml from this. Following this, the purified protein was resolved by SDS-PAGE gel electrophoresis on a 10 % coomassie gel to assess the purity of the protein. **Figure 5.3C** shows 15 µl of recombinant protein run after addition of protein loading buffer, in parallel with a molecular weight marker (KDa). The purity was estimated

from this as approximately 90 %. The protein also migrates at the predicted molecular weight of POT1aLONG, 39KDa. A 2 ml aliquot of the recombinant protein was snap frozen in liquid N_2 and sent to BIOGENES (Germany) for inoculation of a rat and subsequent generation of antiserum.

5.4 Production of POT1b recombinant protein

5.4.1 Testing expression level of cellular localisation

As for the POT1a recombinant protein, an overnight culture of BL21 cells transformed with the POT1b pET21b construct was used to inoculate fresh LB media and grown to a suitable O.D. before inducing with 1mM IPTG. Induction was carried out for 4h before a sample was taken; a separate culture was not induced as a control. Crude protein extractions were performed using the BugBuster method, separating the lysate into a soluble and insoluble fraction, to assess the cellular localisation of the protein. These proteins were resolved by SDS-PAGE gel electrophoresis on a 15 % gel, and detected by coomassie blue. It can be observed in **Figure 5.4 A** that a protein migrates at the predicted molecular weight of 15 KDa in the insoluble fraction of the induced POT1b-HIS culture. This band however is very faint compared to the STAG3 control, also shown to run at its predicted molecular weight of ~50 KDa in the induced insoluble fraction. Due to the low intensity of this band an additional gel was run and electro-blotted to a nitrocellulose membrane for western blot analysis, to confirm whether POT1b-HIS was expressed. **Figure 5.4 B** shows a western blot using the mouse anti-HIS antibody. The antibody detects a band of the same size as that shown in **Figure 5.4 A,** in the insoluble induced fraction for POT1b, confirming that the POT1b-HIS protein is expressed in this fraction. Labelling of STAG3-HIS, is shown as a positive control. Due to the low level of protein expression for the recombinant POT1b-HIS it was decided to optimise the growth and induction conditions in an aim to improve the level of expression for large scale purification of the protein.

5.4.2 Optimising expression levels of POT1b-HIS

To improve the level of recombinant protein expression the growth and induction conditions were optimised. Cultures of BL21 *E.coli* cells transformed with the construct were grown overnight at 37 ^{o}C. Following this 50ml of LB broth was inoculated with 200 µl of overnight culture and grown to an $O.D_{600}$ of 0.6. The cultures were then transferred to growth chambers of varying temperatures; ranging from 22 ^{o}C to 37 ^{o}C and one was induced overnight at 16 ^{o}C. Cultures were induced with a final concentration of 1mM IPTG in all cases, and an uninduced control was included for each temperature. Culture samples of 1ml were taken at intervals subsequent to induction at 1, 2, 4, and 6h post induction for crude protein extractions. The extracts were subsequently resolved by SDS-PAGE. An example gel is shown in **Figure 5.4C**. The coomassie gel shows the extracts after 6h of induction at 30 ^{o}C, and 37 ^{o}C. The greatest expression of POT1b-HIS could be seen at 37 ^{o}C, with slightly less at 30 ^{o}C. No expression was observed at 16 ^{o}C, 22 ^{o}C, or 26 ^{o}C. This pattern of expression was seen at all time points (data not shown). From these observations, it can be noted that the conditions used previously were optimum for POT1b-HIS protein expression. Due to being unable to improve the expression recombinant POT1b-HIS was purified on a large scale using TALON resin, which allows concentration of protein from a large volume.

5.4.3 Isolation of recombinant POT1b-HIS protein using TALON resin

Due to the low level of recombinant protein expression, the POT1b-HIS protein was purified on a large scale using binding to a cobalt IMAC resin (TALON), which binds the polyhistidine tag. The resin has a reduced affinity to bacterial proteins when compared with nickel resins. This method is suitable for large-scale preparations, meaning protein can be concentrated from large culture volumes.

Small-scale test induction and purification was performed to optimise the buffer conditions and proportions of resin. Purification was undertaken in denaturing conditions, as the protein has been shown to be present in the insoluble fraction. Initially it was decided to use a pH gradient to elute the protein from the beads, as this technique is routinely used in our laboratory. Growth and induction conditions were the same as specified for the BugBuster test extractions. The pellet from 50 ml of culture was re-suspended in 4 ml of denaturing buffer

(pH 8) and incubated for 30 min before sonication. Debris was removed by centrifugation, and the sample incubated with 200 µl of TALON resin for 60 min with gentle agitation. Following this, the sample was centrifuged and the supernatant discarded. The beads were subsequently washed in the denaturing buffer before elution of the protein at pH 5.9. Below, **Figure 5.5A** shows an example of samples taken after each step of the process run on an SDS-PAGE gel, and blotted on a nitrocellulose membrane for western analysis. Lane 3 shows that not all the protein is bound to the beads, and lane 9 shows that much of the protein remains on the beads after elution. The POT1b-HIS protein is labelled by the arrow. Several other proteins of a higher molecular weight are also detected by the antibody. These are likely to be histidine rich bacterial proteins that have been pulled out using the beads.

The quantity of beads used, volumes of washes, and number of elutions were increased for a large-scale purification using the pH gradient. However, after purification of protein from 1 L of induced culture, the final concentration was only 0.2 mg/ml. To improve the efficiency of elution and remove more protein from the beads, imidazole was used for subsequent purification. Imidazole competitively binds to the resin at concentration of over 150 mM, resulting in elution of polyhistidine tagged proteins.

After large-scale expression, batch purification was performed using the TALON resin. Elutions were carried out using 150 mM and 250 mM imidazole as specified in section 2.14.3.4. The eluate was subsequently pooled for dialysis and concentrated using PEG solution. **Figure 5.5B** shows the final concentrated protein run by SDS-PAGE The final concentrated protein shows a high level of background proteins. The concentration of the protein was estimated using a BioRad assay at 0.5 mg/ml. A 2 ml sample was frozen and sent to Biogenes (Germany) for inoculation of rabbit. Inoculations were carried out on days 0, and boosts given on day 7 and 14 post inoculation. A pre-immune sample was taken prior to inoculation, and a test bleed delivered which was tested before final bleeding.

5.5 Isolation and characterisation of *pot1a* and *pot1b* mutants

To provide controls for testing the respective antisera, the NASC database was screened for T-DNA insertions for each of the POT1 proteins. The SAIL lines SAIL_1273, and SAIL_38_GO1 were studied for POT1a and POT1b, and designated *pot1a-3* and *pot1b-2* respectively. For the insertion sites, see **Figure 5.6 A-B**. A single mutant for POT1b (*pot1b-1*) and a double knockout mutant for both proteins was provided by D.E. Shippen (personal communication), which corresponds to the insert sites *pot1a-1* and *pot1b-1*. No plants were found to contain the *pot1b-2* insert therefore *pot1b-1* was used for analysis. The growth and development of the plants was indistinguishable from wild-type, so plants were genotyped prior to use as a control (**Figure 5.6C**). The primers used for genotyping and their sequences are shown in **Appendix 8.2**.

5.6 Testing the POT1b rabbit antibody

5.6.1 Testing against recombinant POT1b-HIS protein

To test the whether the antiserum specifically detected the POT1b-HIS recombinant protein, western blot analysis was carried out. To test whether the antiserum raised by inoculation of a rabbit with the POT1b-HIS antigen was specific, a control of STAG3-HIS was run alongside the POT1b-HIS protein. Approximately 5 μg of POT1b-HIS protein was run in replicate by SDS-PAGE gel electrophoresis. This was then electroblotted to a nitrocellulose membrane for probing. The blot was subdivided and to test the specificity of the POT1b antiserum a variety of antisera were used. Pre-immune serum (1:1000) was compared against the mouse anti-HIS antibody (1:5000) and the POT1b antiserum (1:1000). The rabbit antibodies were detected using an anti-rabbit secondary conjugated to horseradish peroxidase, and the mouse anti-HIS detected using an anti-mouse secondary conjugated to horseradish peroxidase (both 1:10000). All antibodies were diluted in milk block (1 % PBS, 5 % Milk) ECL was used to visualise the blots in all cases.

Figure 5.7A shows the results of these blots. The corresponding SDS-PAGE gel stained with coomassie is shown in **Figure 5.7A** (a), which illustrates POT1b-HIS (see arrow), and STAG3-HIS recombinant proteins loaded in lanes 1 and 2 respectively. The antiserum raised against the POT1b-HIS antigen can be observed to specifically bind the recombinant protein. Bands of an equal size to the recombinant protein are detected in lane 1 but not in lane 2 with the POT1b antisera (see **Figure 5.7A c**). The anti-HIS antibody (**Figure 5.7A b**) specifically labels POT1b-HIS and STAG3-HIS, showing the control to be present. **Figure 5.7A** (d) shows that no bands are detected with the pre-immune serum (taken prior to immunisation). These results taken together demonstrate that the antiserum specifically recognises the recombinant protein to which it was raised.

From the blot in image (c), it can be noted that the antiserum to POT1b is not clean. The anti-HIS antibody (**Figure 5.7A b**) also detects a number of background proteins of a larger molecular weight. These background proteins are also detected by the POT1b antiserum. These are likely to be histidine rich proteins that were pulled out using the TALON beads, and included in the total protein used for immunisation of the rabbit. To attempt to produce a cleaner antibody, affinity purification of the POT1b antiserum was carried out. Approximately

0.5 mg of recombinant POT1b-HIS, was resolved by SDS-PAGE and electroblotted to PVDF membrane. This was stained with coomassie, and the band corresponding to POT1b cut into strips. These were subsequently incubated with the test bleed antiserum, to allow only antisera to POT1b to bind. These were later eluted into a small volume and used in western analysis as before. **Figure 5.7A** (e) shows the blot of POT1b-HIS with the primary antibody of the affinity-purified antiserum. A band corresponding to the size of POT1b-HIS was detected, which is less intense than observed prior to purification. This shows all background non-specific binding is removed, but also shows the titre of the antibody is greatly reduced. This was repeated, but the titre of the antibody was again reduced, therefore the original antiserum was used for further analysis.

5.6.2 Specificity of POT1b

To analyse whether the antiserum raised against the POT1b-HIS recombinant protein specifically recognised the POT1b recombinant protein, and not POT1a, a western blot was carried out on both recombinant proteins. The POT1a-HISLONG, and POT1b-HIS recombinant proteins were resolved by SDS-PAGE gel electrophoresis in parallel with a molecular weight marker, and subsequently electro-blotted to a nitrocellulose membrane for detection. A primary antibody of POT1b antiserum, together with a secondary of anti-rabbit conjugated to alkaline phosphatase was used to detect the proteins. **Figure 5.7B** shows the result of this western blot. Lane 2 (POT1b) shows a band migrating at the predicted size for the recombinant protein at ~15 KDa, as expected. In lane 1 (POT1a) shows no labelling of the protein, which demonstrates that the antiserum is specific for POT1b.

5.6.3 Testing against native POT1b from inflorescence cell lysates

To test whether the POT1b antiserum specifically recognises the native POT1b protein, western blot analysis on total inflorescence protein extracts was performed. A negative control of pre-immune antiserum and a positive control of an antibody to the protein SMC3 were included. SMC3 forms part of the cohesin complex in both mitosis and meiosis (Lam et al, 2005), and should therefore be present in all of the tissues extracted as for POT1. Total protein was extracted from *Arabidopsis* inflorescences using PEB, boiled with 5x protein loading buffer, and 45 µl resolved by SDS-PAGE gel electrophoresis on a 10 % gel. Western blot analysis from several attempts failed to detect bands for POT1b or the control of SMC3, showing that the proteins were not at a high enough concentration to be detected. It was therefore repeated with *Brassica oleracea* inflorescence protein lysates, which yield a higher concentration of protein. No signal was observed for the pre-immune serum and the POT1b antiserum on protein extracts, as shown in **Figure 5.8 (a-b)** respectively. A band of 50 KDa would be observed in blot (b) if the antiserum bound POT1b native protein. The blot in image (c) shows a band of 120 KDa which corresponds to the native SMC3 protein. This may indicate that the antiserum does not recognise native POT1b, or that the levels of this protein in the sample are too low to be detected by the antiserum. Therefore, to establish whether the antiserum recognised native POT1b, a second approach of immunolocalisation was undertaken.

5.6.4 Immunolocalisation of POT1b on spread meiotic nuclei

To establish whether the POT1b antiserum recognised the native POT1b protein, and localised to the telomeres, immunolocalisation using the spreading technique (see section 2.7) was carried out on *Arabidopsis* spread meiocytes. Slides were incubated with pre-immune serum, or the POT1b antiserum as a primary antibody (both diluted 1:200 with EM block). **Figure 5.9** (a-b) shows that no POT1b signal is visible at the telomeres (see arrow on image a). Approximately 10 foci would be observed if the POT1b antiserum was to localise to telomeres. A number of diffuse foci of POT1b were seen to localise to the axial elements. However, in image (a) more foci are observed than that expected if POT1b were to localise to the telomeres. This suggests the signal observed is background labelling, and that the POT1b antiserum may not recognise the native protein, or that the amount of protein is not sufficient to be detected by immunofluorescence.

Following this immunolocalisation was carried out on *Brassica* meiocytes, as these are larger than *Arabidopsis* it was thought they would give clearer signals with the POT1b antiserum. Slides were incubated with the pre-immune serum as a control, or the POT1b antiserum. **Figure 5.9** images (c-f) show dual-immunolocalisation of POT1b antiserum together with an antibody to ASY1 on *Brassica* leptotene meiocytes. ASY1 labels axial elements allowing staging of the cell. Image (c) illustrates no labelling with the pre-immune serum, with only background labelling observed. Images (d-f) show meiocytes labelled with the POT1b antiserum. In contrast to the control, it can be observed that the nucleolus is labelled by the POT1b antiserum. However, this may not be specific, as many antibodies that have been produced in our laboratory have been observed to concentrate in the nucleolus. Some foci were observed, however none of the foci were observed close to the telomeres (see arrows image e), and was therefore concluded to be background labelling. Image (f) shows that the POT1b antiserum non-specifically localises to sites of the axial elements.

These results support what was previously observed in *Arabidopsis* meiocytes. A recent study demonstrated that POT1a interacts with telomerase. POT1a was shown to interact with the telomeres in a cell cycle dependent manner. This interaction was found to be enriched during S-phase (Surovtseva et al, 2007). It is therefore possible that the protein is not localised at the telomeres at this point of meiosis. This led to the analysis of cells at an earlier stage.

5.6.5 Immunolocalisation of POT1b on somatic s-phase cells

To determine the stage of the meiotic cell cycle, inflorescences were pulsed with BrdU for 2h to label cells in S-phase. Slides were made immediately after this pulse for immunolocalisation. Slides were incubated with anti-BrdU before incubation with the POT1b antiserum, and secondary antibodies subsequently applied together prior to washing. Cells labelled with BrdU would therefore be in S-phase/G_2.

Foci of POT1b were observed to be localised around the nucleolus in wild-type somatic cells (**Figure 5.10** a-b and e), as would be expected for a telomere binding protein. However, the number of foci observed in each case was low, with approximately 10 signals. This would be expected with paired telomeres, but they are not paired at this stage. To ascertain whether the foci observed were genuine, the immunolocalisation was repeated on the *pot1b-2* homozygous mutant. The double homozygous mutant was also studied to eliminate the possibility that the antiserum recognised POT1a native protein. As shown in images (c-d), foci of the POT1b antiserum are localised around the nucleolus as in wild-type. This can be more clearly observed in images (e-f) where the localisation of the POT1b foci are similar in the double mutant and wild-type, which shows this labelling to be non-specific background. These observations suggest that the POT1b antiserum does not recognise the native protein, or that there is not enough present at the telomeres to be detected.

5.7 POT1a rat antibody

5.7.1 Testing against recombinant POT1a-HISLONG protein

To assess whether the antiserum raised against the POT1a-HISLONG recombinant protein was able to detect the recombinant protein, and that it specifically recognised POT1a, western blot analysis was carried out. Approximately 5 μg of POT1a-HISLONG (1), and POT1b-HIS (2) proteins were run on a 12 % SDS-PAGE gel, and electro-blotted to a nitrocellulose membrane for detection. The results of this western analysis are shown in **Figure 5.11A**, which illustrates that (a) the pre-immune serum primary antibody (taken prior to inoculation) shows no signal for either POT1a or POT1b. (b) The test bleed 1 antiserum recognises a band that migrates at the molecular weight predicted for the POT1a-HISLONG recombinant protein (39KDa) in lane 1 (shown by arrow), and shows no signal corresponding to the POT1b-HIS protein in lane 2. A low amount of background labelling of *E. coli* proteins can be observed. For the test bleed 2 antiserum (c), a band of equal size to the POT1a recombinant protein is also observed in lane 1 of this blot. These results indicate that the antisera recognise the recombinant protein to which they were raised. The fact that no signal was observed with the pre-immune serum and that the POT1a antisera did not recognise the POT1b-HIS recombinant protein, demonstrates that the antisera to specifically recognise the POT1aLONG-HIS recombinant protein. A dilution series of the recombinant protein was performed to measure the titre of the antibody. **Figure 5.11B** shows a western blot of these serial dilutions with the POT1a test bleed 1 antiserum. It can be seen that the antiserum can detect protein diluted 1/50, which equates to approximately 80 ng of protein run on the gel.

5.7.2 Immunolocalisation of POT1a antiserum on somatic cells

To investigate whether the POT1a antiserum was able to specifically recognise the native protein, and that it localised to telomeres, immunolocalisation was carried out on spread nuclei as for POT1b. It was decided to analyse S-phase cells due to a previous study that POT1a interaction with the telomeres is enriched at this stage (Surovsteva et al, 2007). As for POT1b, inflorescences were given a BrdU pulse prior to slide production so that cells labelled with BrdU would be in S-phase/G_2. The POT1a antiserum was tested alongside a peptide antibody for POT1a (provided by D.E. Shippen, personal communication). Labelling of the POT1a peptide antibody and antiserum were both shown to localise around the nucleolus in wild-type, where a number of foci could be observed (**Figure 5.12** a-c). The foci observed were not as diffuse as for the POT1b antiserum. To establish whether these signals were genuine, immunolocalisation was carried out on the *pot1a-3* and double mutants. As shown in images (d-h), foci of the POT1a antiserum can be seen to localise around the nucleolus, which shows that the localisation of the antiserum labelling is similar in both the wild-type and mutants. This indicates that the signal is not genuine, and does not represent labelling of POT1a protein.

These results mirror those observed for the POT1b antiserum. It is possible that neither antiserum raised is able to recognise the native protein. However, the fact that neither were found to localise to their respective native protein suggests that the level of protein is not sufficient to be visualised by immunolocalisation. This would also fit with the observation that the antiserum cannot detect a protein from *Brassica* protein extracts.

5.8 Discussion

5.8.1 Purification of recombinant proteins

The telomere binding proteins POT1a and POT1b were selected for recombinant protein purification in order to raise antibodies against both proteins. The regions of the protein selected were those that were least similar, in order to raise specific antibodies to each protein (**Figure 5.1**). The level of protein expression for POT1a-HIS and POT1b-HIS was shown to be low (**Figure 5.2** and **Figure 5.4** respectively). The low level of protein expression may have been due to the protein having a toxic effect on the *E.coli* cells. This would therefore select for those with low protein expression. To determine whether this was the case, growth curves were obtained from induced and un-induced cultures by measuring the $O.D_{600}$ at several time points. To establish whether production of the POT1 recombinant proteins was having a negative effect on growth, the growth rate was compared to a control of a highly expressed protein (STAG3-HIS). The growth of the bacterial cultures induced for POT1a-HIS and POT1b-HIS was shown to be lower than that of a STAG3-HIS induced control. In contrast the growth patterns were shown to be similar in the non-induced cultures for the POT1 and STAG3 recombinant proteins (see **Appendix 8.7**). It can therefore be proposed that the POT1a-HIS and POT1b-HIS proteins were toxic to bacterial cells.

5.8.2 Testing antibodies by western blotting

To determine whether the antiserum raised against the POT1a and POT1b recombinant proteins was able to recognise its respective protein, western blot analysis was first carried out. Western analysis of both antisera showed that they were able to detect the recombinant protein. For the POT1b antiserum, a 15KDa band was observed and for the POT1a antiserum a 39KDa band was observed, which corresponds to the respective predicted molecular weights of each recombinant protein (See **Figure 5.7** and **Figure 5.11**). To ascertain whether the native protein could be detected by the antiserum, total protein was extracted using PEB buffer from whole inflorescences from wild-type *Arabidopsis* Col-0 and *Brassica* plants. Extracted proteins were resolved by SDS-PAGE electrophoresis, and subsequently transferred to a nitrocellulose membrane for western blot analysis. From *Arabidopsis* protein extracts no bands could be detected for the control protein SMC3, which forms part of mitotic and meiotic cohesin complexes (Lam et al, 2005). It was thought that this was likely to be due to

the concentration of protein being too low for detection. This can be a problem when studying *Arabidopsis*, so *Brassica* protein extracts were then analysed. **Figure 5.8** illustrates that the POT1b antiserum does not detect a band corresponding to the POT1b protein. The control of SMC3 shows a band migrating at the predicted molecular weight of the protein. It is possible that the concentration of POT1b protein in the protein extracts was too low to be detected, despite being able to detect SMC3. However, Surovsteva et al, (2007) were able to immunoprecipitate the native POT1a protein from suspension culture extracts using peptide antibodies, and found that the level of protein does not vary during the mitotic cell cycle. This may imply that the titre of the POT1b antiserum may not be sufficient to detect the level of protein present. Alternatively, the reason for this difference could be due to the tissue studied, or method of protein extraction employed.

5.8.3 Testing antibodies by immunolocalisation

Another approach used to determine whether the antiserum recognised the native protein was immunolocalisation. This was also carried out to study whether POT1 signals could be detected at the telomeres, which would confirm these proteins as genuine telomere binding proteins. POT1b antiserum was studied first. *Arabidopsis* spread meiotic chromosomes were labelled with ASY1 to allow identification of the meiotic stage, together with the POT1b antiserum. Diffuse foci of POT1b antiserum were observed on zygotene stage nuclei. However, many of the foci appeared not to localise to the chromatin, suggesting that this was background labelling. In addition to this, no foci were observed at the telomeres, which would be expected if POT1b protein were to bind to the telomeres (**Figure 5.9**). This was repeated on *Brassica* meiotic nuclei, as these are larger, it was thought they would give clearer signals with the POT1b antiserum. Again, no localisation of POT1b foci at the telomeres could be observed. Some foci were visible, but these seemed to associate non-specifically with the axial elements. Labelling of the nucleolus was observed with the antiserum, but not pre-immune serum. This could be due to protein concentrating in the nucleolus, but may be non-specific. These results support the previous observations in *Arabidopsis*, that only background labelling is seen.

Subsequent to these findings, POT1a was demonstrated to physically associate with telomerase to regulate telomere length (Surovsteva et al, 2007). This study also noted that

POT1a association with the telomeres *in vivo* varied throughout the cell cycle, with interaction significantly increased during S-phase by using chromatin-immunoprecipitation. It is possible that POT1b plays a similar role, and therefore may have a similar pattern of interaction. This may provide an alternative explanation for the results seen in meiocytes, as POT1 proteins may not associate with telomeres at this point. It was therefore decided to analyse the localisation of both POT1 antisera on S-phase cells. To stage the cells a BrdU pulse was applied to influorescences for 2 h, and immunolocalisation using the POT1b, or POT1a antiserum subsequently carried out. As BrdU is incorporated into cells during S-phase, any BrdU labelled cells after 2h should be in S-phase or early G2 (Armstrong et al, 2003). **Figure 5.10** and **Figure 5.12** illustrate labelling of POT1b and POT1a antiserum on somatic S-phase/G2 cells respectively. For both antisera, labelling of foci can be observed to localise around the nucleolus in wild-type cells. Immunolocalisation was also carried out on the respective POT1 mutants. For both POT1b and POT1a, the localisation of foci around the nucleolus was similar in the mutants as in the wild-type. This indicates that this labelling is non-specific background and that the antisera may not be able to recognise the native proteins. This may be due to the correct epitope not being available. The epitope is the antigenic determinant, and is the specific region of the antigen that is recognised by the antibody (Griffiths et al, 2000). The recombinant protein was refolded prior to immunisation, however the conformation of this refolded protein may not be the same as the native protein, due to problems with refolding, or because the recombinant proteins used were not full-length proteins. This may mean that the epitope that the antiserum recognises may not be available in the native conformation, due to differences in folding of the recombinant and native proteins, leading to differences in the tertiary structure of the molecules. However, immunolocalisation was also carried out using a peptide antibody to POT1a, which has previously been shown to interact with native POT1a *in vivo*, through chromatin-immunoprecipitation (Surovtseva et al, 2007). This antibody also revealed the same pattern of localisation as the antisera produced in this investigation. This suggests that at least in this case, there would not have been a problem with the antibody recognising the epitope. This implies that there may not be enough molecules of POT1a or POT1b protein present to detect by immunofluorescence, or that the titre of the antibody is not high enough to detect the amount of protein present. A recent study has shown that POT1a and POT1b fail to bind single stranded telomeric DNA *in vitro* or *in vivo,* and proposed that POT1 proteins in the *Brassicaceae* species studied are not the major

single-stranded telomeric DNA binding proteins, unlike in other organisms (Shakirov et al, 2009). This would explain why the POT1a and POT1b antiserum did not localise to the telomeres in the immunolocalisation. The precise role of POT1 proteins in plants is yet to be elucidated.

5.7.4 Conclusions and future perspectives

This chapter describes the development of POT1a and POT1b recombinant proteins for production of antibodies, in order to find a suitable protein for labelling the telomeres. The aim was to use this for subsequent live imaging analysis of telomere movements and homologous chromosome pairing. The results described above show that the antisera produced did not detect the native POT1 proteins by western blot or immunolocalisation. These results support those of more recent studies that have shown POT1a interacts with telomerase and its interaction with the telomeres is cell cycle dependent (Surovtseva et al, 2007). In addition to this, Shakirov et al, (2009) showed that neither POT1a nor POT1b proteins interact with single-stranded telomeric DNA in *Arabidopsis*, and proposed that plant POT1 proteins have diverged in function. This is likely to be the reason that the antisera produced could not be shown to detect their respective native proteins. It can be concluded that the POT1 proteins are not suitable for the investigation of telomere movements in *Arabidopsis*. Potential telomere binding proteins that could be studied include the single-stranded binding protein STN1, which is critical for chromosome end protection, and has been shown to co-localise with telomeres in *Arabidopsis* (Song et al, 2008). The protein complexes that protect telomeres appear to be complex, and remain poorly understood. Once the full complement of proteins at plant telomeres has been elucidated, this will provide further candidates for investigation. The development of live imaging for *Arabidopsis* meiocytes will be of immense importance for the further study of not only homologous chromosome pairing, but all aspects of meiotic prophase I.

Chapter 6
General Discussion

6.1 Introduction

Meiosis is central to the lifecycles of all sexually reproducing organisms. The mechanisms that control pairing of homologous chromosomes and recombination remain poorly understood. The aim of the research presented was to gain further insight into the mechanisms that control pairing and crossover formation in *Arabidopsis*. The main findings of this research and future perspectives are presented in this discussion.

6.2 Pairing and synapsis of homologous chromosomes in *Arabidopsis*

An important aspect of meiosis that remains poorly understood is how homologous chromosomes recognise one another, and how pairing and synapsis are controlled. The clustering of telomeres during bouquet formation has long been thought to facilitate these processes (Bass et al, 2000). Recombination has also been shown to be necessary for pairing and synapsis of homologues in a number of organisms. Mutants deficient for the SPO11 protein that do not produce DSBs show no pairing or synapsis (Keeney et al, 1997). To investigate how pairing of homologous chromosomes in *Arabidopsis* is controlled, two approaches were taken. The first was to investigate whether telomeres play a role in promoting pairing and downstream events in *Arabidopsis*, which has a unique localisation of telomeres (Armstrong et al, 2001). The second was to study the effects of reducing DSBs on pairing and synapsis, as it is known that these processes are DSB dependent (Grelon et al, 2001). A summary of the results is shown in **Figure 6.1**.

6.2.1 Telomere pairing is dispensable for pairing and synapsis in Arabidopsis

To study whether telomeres play an important role during meiosis, the drug colchicine was introduced to meiocytes via the transpiration stream. Colchicine is a microtubule depolymerising drug, which has been widely used in the study of meiotic progression (Zickler and Kleckner, 1998). It has recently been shown to prevent movement of telomeres on the NE, thereby preventing bouquet formation (Cowan and Cande, 2002). The results described in chapter 4 show that colchicine did not affect progression of meiosis or pairing of telomeres in *Arabidopsis*. This is in contrast to other organisms that have been studied (Zickler and Kleckner, 1998). Cowan and Cande, (2002) showed that the effect of colchicine was not due to depolymerisation of microtubules, as other drugs did not block telomere clustering. It was

proposed that colchicine may bind a non-microtubule form of tubulin; however, the target of colchicine remains unknown. It is possible that this target of colchicine differs in *Arabidopsis*, therefore preventing its binding. However, tubulin proteins are highly conserved between species. It was therefore thought that this difference may arise from the unique localisation of telomeres in this organism.

To further investigate the role of telomeres in pairing and synapsis, a mutant for the telomerase reverse transcriptase subunit (TERT) was analysed. Previous studies had shown successive generations of the *Arabidopsis tert* mutant exhibit shortening of the telomeric repeat sequence, leading to developmental defects (Rhia et al, 2001). In female mice, telomere shortening was shown to cause defects in synapsis and recombination (Liu et al, 2004). Analysis of meiosis in the *Arabidopsis tert* mutant revealed that telomeres failed to pair, whilst interstitial regions appeared paired (**Figure 4.8**). This was confirmed by analysis of a chromosome 1 specific BAC. The mean number of BAC probe foci was shown to be significantly higher in the mutant than wild-type, indicating that telomeres were unpaired (**Figure 4.9**). Failure of telomere pairing did not result in failure of synapsis, as indicated by immunolocalisation of the SC protein ZYP1. This also suggests that telomere pairing is not required for pairing of homologous chromosomes, as this is a prerequisite of synapsis. However, it appears that the telomeric repeats may be required for telomere pairing. Wild-type levels of chiasmata were also observed in the *tert* mutant. It is therefore likely that the severely reduced fertility observed was due to developmental defects of the reproductive organs rather than meiotic progression.

The results presented here show that unlike a number of organisms, in which telomere clustering is thought to facilitate pairing and synapsis of homologues, *Arabidopsis* telomere pairing is dispensable for pairing and synapsis. Mutants defective in bouquet formation have been shown exhibit defects in synapsis in *pam1* of maize (Golubovskaya et al, 2002), and delay in progression of synapsis and recombination, in *ndj1Δ* of budding yeast (Trelles-Sticken et al, 2000). However, observations in *Sordaria* have challenged this view. Storlazzi et al, (2003) observed that co-alignment of homologues is completed prior to formation of the bouquet. Therefore, the bouquet could have an alternative role during meiosis, or the role of the bouquet may show organism specific differences. The bouquet may facilitate synapsis in

Sordaria, as this was found to be concomitant with the transient formation of a bouquet (Storlazzi et al, 2003). Alternatively, the bouquet stage may act as a surveillance mechanism that monitors the progression of recombination. In *Sordaria,* the *spo11* mutant was shown to be delayed in exit from the bouquet (Storlazzi et al, 2003). In support of this, Liebe et al, (2006) demonstrated that mice deficient for SPO11 or ATM showed a marked delay in exit from the bouquet stage.

The dynamic movements of chromosomes during prophase I have been shown to require telomere attachment to the nuclear membrane in budding yeast (Koszul et al, 2008). This links chromosomes to cytoskeletal actin cables, necessary for movements during zygotene/pachytene. It has been proposed that these movements may function in resolving interlocks, and removing non-specific connections, thereby promoting recombination (Koszul et al, 2008; Wanat et al, 2008). The *pam1* mutant in maize, which is defective for telomere movement on the NE and bouquet formation, showed an increased frequency of interlocks at pachytene (Golubovskaya et al, 2002).

In *Arabidopsis*, telomere clustering appears to have evolved a unique localisation that allows rapid cycling. Telomere pairing has been shown to be dispensable for pairing and synapsis, however, it is possible that nucleolus clustering is sufficient for facilitating these processes. It is unclear how this localisation is mediated for chromosomes without an NOR. Subsequent to this clustering, telomeres move to the nuclear envelope. It is therefore possible that actin mediated movements on the NE may be important in *Arabidopsis*.

6.2.3 The effects of reducing DSBs on pairing and synapsis

Subsequent to the pairing of telomeres in *Arabidopsis*, recombination is initiated by formation of programmed DSBs by the protein SPO11. In the absence of DSBs, homologues fail to pair and synapse (Grelon et al, 2001). To ascertain how reducing the number of DSBs affects pairing and synapsis, *SPO11-1* RNAi lines with varying reductions in DSBs were analysed; as described in chapter 3. The aim was to investigate how the dynamics of pairing and synapsis were altered by reducing DSBs, and to establish how many are required to maintain ‘normal’ pairing and synapsis. It was found that telomere pairing and the subsequent close

juxtaposition of homologues are discrete events, as telomeres were able to pair homologously in the absence of DSBs. This shows that telomere pairing is independent of recombination in *Arabidopsis*, which is consistent with observations made in budding yeast (Trelles-Sticken et al, 1999). Due to the limitations of accurately measuring DSBs, it was not possible to ascertain the level of DSBs necessary for accurate pairing.

Immunolocalisation of the SC transverse filament protein ZYP1, revealed that synapsis could be initiated but not completed with reduced DSBs. Importantly, this was observed in the intermediate line 8A (**Figure 3.21**), which formed approximately 60-70% of wild-type DSB levels. This shows that almost wild-type numbers of DSBs are required for completion of synapsis. These results are analogous to observations in *Sordaria* and budding yeast (Tesse et al, 2003; Henderson and Keeney, 2004). The failure of complete SC formation was associated with a reduction in the number of synapsis initiation sites. In budding yeast, synapsis initiation sites are thought to correspond to sites of crossovers (Henderson and Keeney, 2004). The number of synapsis initiation sites in *Arabidopsis* far outweighed the number crossovers even in the most affected line. This is consistent with other plant species studied (Gillies 1985). This may be due to the lengths of chromosomes in plants, which are much longer than those in budding yeast. Organisms with more complex and larger genomes may require more synapsis initiation sites for efficient SC formation. For example, *Arabidopsis* contains many duplicated regions, which could make accurate synapsis of homologues more challenging. In the *SPO11-1* RNAi line 8A, which showed incomplete synapsis, non-homologous connections and even multivalent formation were observed at metaphase I. This demonstrates that complete synapsis may be required to maintain wild-type levels of recombination. The phenotype observed reflects that of the *zyp1* deficient RNAi line (Higgins et al, 2005). Therefore, the non-homologous connections observed in the *SPO11-1* RNAi line are likely to be due to defective SC formation. From these observations, it can be proposed that the SC functions in preventing non-homologous connections in *Arabidopsis*, although how this is achieved remains to be elucidated. These results are summarised in **Figure 6.1**.

6.3 Control of crossover formation in *Arabidopsis*

Crossover formation during meiosis requires a complex interplay between a number of processes, to control the number and placement of crossovers by selection from numerous initiating events (DSBs). How crossover formation is controlled remains poorly understood. It appears that a subset of sites is selected to give rise to crossovers, whilst others are directed to the non-crossover pathway (Bishop and Zickler, 2004). A previous study in budding yeast analysed mutants for the protein SPO11, with varying reductions in DSBs, and showed that crossovers tended to be maintained at the expense of non-crossovers, which they termed crossover homeostasis (Martini, et al 2006). To give further insight into the mechanisms of crossover control in *Arabidopsis*, the *SPO11-1* RNAi lines with varying numbers of DSBs were studied. The aim was to determine if the phenomenon of crossover homeostasis was present, and to give further insight into the basis of crossover formation in this organism.

It was found that as the number of DSBs was reduced, the frequency of chiasmata formed was also reduced (**Figure 3.14**). To analyse how these residual chiasmata were distributed, the chiasma frequency of each chromosome was scored. It was found that shorter chromosomes did not lose more chiasmata than larger chromosomes, as may be expected. There was also not a tendency for chromosomes to maintain the obligate chiasma in the face of reduced DSBs. Rees, (1957) showed that this was the case in an asynaptic locust, which appeared to lose excess chiasmata from longer chromosomes in order to maintain the obligate. Interestingly, from the chiasma distribution data, chromosome 4 appeared to maintain more chiasmata than other chromosomes (**Figure 3.15, 3.16**). It was therefore hypothesised that the NORs of chromosomes 2 and 4 may give these regions an advantage, as they are associated with each other at the nucleolus. Analysis of chiasma distribution on the short and long arms of these chromosomes revealed chromosome specific differences. Chromosome 2 showed a relative increase in long arm chiasmata, whereas chromosome 4 showed a relative increase in short arm chiasmata, in the severely affected line 9H (**Figure 3.17**). This suggests that chromosome structure does not affect chiasma distribution, as these are very similar, with an NOR on the short arm. A difference in the chiasma distribution of these chromosomes has been observed in other meiotic mutants (Sanchez-Moran et al, 2001). Recently, analysis of a hyperacetylation line in *Arabidopsis* has been shown to cause changes in chiasma distribution, with a specific increase in chromosome 4 short arm chiasmata (G. Perrella, personal

communication). Drouaud et al, (2006) showed that this region of chromosome 4 contained a number of crossover hotspots. It is possible that the differences in distribution between these chromosomes arise from a difference in chromatin structure.

Analysis of chiasma distribution across individual meiocytes revealed an interesting aspect of crossover control. It appears that in *Arabidopsis*, chromosomes are subject to an autonomous control of chiasma formation. This means that formation of the obligate chiasma is determined for each chromosome individually. This has previously been observed in *Crepis* (Tease and Jones, 1976). It was observed that some chromosomes were able to form more than 1 chiasma, whilst others were present as univalents, having lost their obligate. In cases where greater than 1 chiasma was observed, these appeared to exhibit interference.

6.4 Integrating the control of pairing and synapsis with recombination

Pairing of the telomeres has been shown to be dispensable for the downstream processes of the close juxtaposition and synapsis of homologues together with recombination in *Arabidopsis*. However, the results presented show that the processes of pairing and synapsis are intimately integrated with recombination to ensure accurate segregation of homologues at the first meiotic division. Importantly there appears to be a threshold number of DSBs, which are required to maintain the fidelity of pairing and recombination. Chromosomes that receive this threshold number are able to pair and synapse fully, to ensure formation of the obligate chiasma. In cases where more than 1 chiasma is observed, they appear to exhibit interference. In contrast, chromosomes that do not receive this threshold of DSBs show a reduction in the number of SC initiation sites together with incomplete synapsis. This frequently results in failure of the obligate chiasma, and univalent formation. However, non-homologous connections were also observed at metaphase I in the threshold line 8A; see **Figure 3.23** for model. The results also suggested that this threshold number of DSBs may vary between different chromosomes (e.g. chromosome 4), and that chromatin organisation may be an important factor.

6.5 Future perspectives

Investigation into the control of pairing showed that telomeres were not required for downstream processes, but the telomeric regions of chromosomes remained unpaired in the *tert* mutant with shortened telomeres. This suggests that the telomeric repeats may be important for telomere pairing. However, this does not explain how homology is specified, as telomeres are known to pair homologously prior to subsequent pairing of homologues (Armstrong et al, 2001). It will be interesting to determine how this homology is specified.

Despite the fact that telomeres are dispensable for downstream processes, is will be of interest to determine whether general chromosome movements during prophase I play an important role in maintaining recombination. Dynamic chromosome movements have been observed in budding yeast from zygotene through to pachytene (Scherthan et al, 2007), and disruption has been shown to affect recombination (Koszul et al, 2008). It is likely that actin may play a role in these movements, as in budding yeast (Trelles-sticken et al, 2005). An attempt was made to disrupt actin using the depolymerising drugs LatB and Cytochalasin D in this study, however, a method of introducing these drugs to meiocytes was not found.

Development of live imaging of meiocytes in *Arabidopsis* will bring great advances in studying these movements and meiotic progression in general. Although a suitable telomere binding protein for labelling the telomeres was not found in this study, advances in this area of research will provide new candidates. It may also be useful to study meiotic proteins by live imaging. For example, the axial element protein ASY1 may be suitable for production of a GFP-fusion protein for analysis of chromatin movements, as has been shown for ZYP1-GFP of budding yeast (Scherthan et al, 2007). It will be interesting to determine whether the control of movement is conserved in *Arabidopsis*; for example, whether telomeres attach to the inner nuclear membrane via SUN domain proteins. Two potential candidates have been found with 80% identity at the protein level. Single knockouts showed no phenotype, which may point to a redundant function.

For the *SPO11-1* RNAi lines, it will be important to develop a more accurate method of quantifying DSBs, in order to establish whether crossover homeostasis is observed. To establish the threshold level of DSBs required for accurate pairing and recombination, further

intermediate lines like 8A will be analysed. Further detailed analysis of SC formation in these lines will be necessary in determining how the SC functions in preventing non-homologous connections. To ascertain whether chiasmata exhibit interference the distribution of MLH1 foci (crossover sites) could be analysed. To genetically measure interference in defined genetic intervals, as in yeast, it may be possible to utilise tetrad analysis of coloured transgenic markers developed by Berchowitz and Copenhaver, (2008).

6.6 Final words

Meiosis consists of a complex interplay between the mechanisms of pairing, synapsis and recombination. How these processes are controlled remains to be fully elucidated in any organism. *Arabidopsis* has emerged as an excellent model for studying meiosis, through the combination of cytological and molecular techniques. The results presented show that the *Arabidopsis* may have evolved a different telomere localisation to allow rapid cycling. As the results suggest, that telomere pairing is dispensable for meiotic progression in this species. The control of pairing and synapsis appears to be conserved between eukaryotes dependent on DSBs. Differences in control between different organisms are apparent. Future research will be important for elucidating these differences and mechanisms of control. This remains an important and exciting area of research.

2000; Armstrong et al., 2001; Armstrong and Jones, 2003; Bass et al., 2000; Baudat and de Massy, 2007; Bennett, 1979; Berchowitz and Copenhaver, 2008; Bishop and Zickler, 2004; Blat et al., 2002; Bleuyard et al., 2004; Bleuyard et al., 2004; Blitzblau et al., 2007; Borde et al., 2009; Borner et al., 2008; Borner et al., 2004; Bundock and Hooykaas, 2002; Carlton and Cande, 2002; Caryl et al., 2003; Chen et al., 2001; Chen et al., 2008; Chicheportiche et al., 2007; Chikashige et al., 1994; Chikashige et al., 2006; Conrad et al., 2008; Cooper et al., 1998; Copenhaver et al., 2002; Corredor and Naranjo, 2007; Couteau et al., 1999; Cowan and Cande, 2002; Cowan et al., 2001; de Lange, 2005; De Muyt et al., 2007; Dernburg et al., 1998; Ding et al., 2004; Ding et al., 2007; Dover and Riley, 1977; Driscoll, 1967; Driscoll and Darvey, 1970; Drouaud et al., 2006; Fitzgerald et al., 1999; Franklin et al., 1999; Franklin et al., 2006; Fung et al., 2004; Gallego et al., 2001; Gerton et al., 2000; Gerton and Hawley, 2005; Golubovskaya et al., 2002; Grandin et al., 1997; Grelon et al., 2001; Hamant et al., 2006; Harper et al., 2004; Hartung and Puchta, 2000; Hartung et al., 2007; Heacock et al., 2004; Heacock et al., 2007; Hemann et al., 2001; Henderson and Keeney, 2004; Higgins et al., 2004; Higgins et al., 2008; Higgins et al., 2005; Higgins et al., 2008; Hockemeyer et al., 2006; Hotta, 1973; Hwang et al., 2001; Hwang et al., 2005; Jackson et al., 2006; Jin et al., 2002; Jones, 1984; Jones et al., 2003; Jones and Franklin, 2006; Joshi et al., 2009; Karamysheva et al., 2004; Kauppi et al., 2004; Keeney, 2001; Keeney et al., 1997; Kleckner, 2006; Kleckner et al., 2003; Kleckner et al., 2004; Koszul et al., 2008; Kuchar and Fajkus, 2004; Kugou et al., 2009; Li et al., 2004; Liu et al., 2004; Liu and Chen, 2007; Loidl, 1988; Loidl, 1990; Mahadevaiah et al., 2001; Martinez-Perez and Colaiacovo, 2009; Martini et al., 2006; McKim and Hayashi-Hagihara, 1998; McKnight and Shippen, 2004; Mercier et al., 2005; Moens et al., 2002; Pecinka et al., 2004; Penkner et al., 2007; Peoples et al., 2002; Puizina et al., 2004; Rees, 1957; Riha et al., 2001; Riha and Shippen, 2003; Roberts et al., 2009; Roeder, 1997; Rossignol et al., 2007; Salonen et al., 1982; Sanchez-Moran et al., 2002; Sanchez-Moran et al., 2007; Sanchez Moran et al., 2001; Santos et al., 2003; Scherthan, 2001; Scherthan, 2006; Scherthan, 2007; Scherthan et al., 2000; Scherthan et al., 2007; Schmitt et al., 2007; Shakirov et al., 2009; Shakirov et al., 2005; Siaud et al., 2004; Snowden et al., 2004; Song et al., 2008; Stacey et al., 2006; Stahl et al., 2004; Stern and Hotta, 1973; Stewart and Weinberg, 2000; Storlazzi et al., 2003; Storlazzi et al., 2008; Surovtseva et al., 2007; Tamura et al., 2002; Tani and Murata, 2005; Tepperberg et al., 1997; Tepperberg et al., 1999; Terasawa et al., 2007; Tesse et al., 2003; Thomas, 1977; Tomita and Cooper, 2006; Trelles-Sticken et al., 2005; Trelles-Sticken et al., 2000; Trelles-Sticken et al., 1999; Vignard et al., 2007; Voet et al., 2003; Walker, 1938; Wanat et al., 2008; Waterworth et al., 2007; Weiner et al., 1998; Wu and Burgess, 2006; Zickler, 2006; Zickler and Kleckner, 1998; Zickler and Kleckner, 1999; Zickler et al., 1992Alberts, 1983; Argueso et al., 2004; Armstrong, 2003; Armstrong et al., 2002; Bass, 2003; Bennett and Smith, 1979; Carmo-Fonseca et al., 2000; de los Santos et al., 2003; Gallego, 2000; Gerlach and Bedbrook, 1979; Gillies, 1985; Greider and Blackburn, 1985; Griffiths, 2000; Ishiguro, 2007; Kuchar, 2006; Lam et al., 2005; Moore and Shaw, 2009; Paques, 1999; Pawlowski et al., 2003; Phillips and Dernburg, 2006; Siroky, 2003; Smith et al., 1996; Tease, 1976

7
Reference list

Reference list

The Arabidopsis initiative. (2000). Analysis of the genome sequence of the flowering plant Arabidopsis thaliana. *Nature* **408**(6814): 796-815.

Alberts, B., Bray, D., Lewis, J., Raff, M., Roberts, K., Watson, J.D. (1983). Molecular biology of the cell. New york, Garland**:** 1146

Argueso, J. L., J. Wanat, Z. Gemici and E. Alani (2004). Competing crossover pathways act during meiosis in Saccharomyces cerevisiae. *Genetics* **168**(4): 1805-16.

Armstrong, S. J., A. P. Caryl, G. H. Jones and F. C. Franklin (2002). Asy1, a protein required for meiotic chromosome synapsis, localizes to axis-associated chromatin in Arabidopsis and Brassica. *J Cell Sci* **115**(Pt 18): 3645-55.

Armstrong, S. J., F. C. Franklin and G. H. Jones (2001). Nucleolus-associated telomere clustering and pairing precede meiotic chromosome synapsis in Arabidopsis thaliana. *J Cell Sci* **114**(Pt 23): 4207-17.

Armstrong, S. J., Franklin, F.C.H, Jones, GH. (2003). A meiotic time-course for *Arabidopsis thaliana*. *Sexual Plant Reproduction* **16**: 141-149.

Armstrong, S. J. and G. H. Jones (2003). Meiotic cytology and chromosome behaviour in wild-type Arabidopsis thaliana. *J Exp Bot* **54**(380): 1-10.

Bass, H. W. (2003). Telomere dynamics unique to meiotic prophase: formation and significance of the bouquet. *Cell Mol Life Sci* **60**(11): 2319-24.

Bass, H. W., O. Riera-Lizarazu, E. V. Ananiev, S. J. Bordoli, H. W. Rines, R. L. Phillips, J. W. Sedat, D. A. Agard and W. Z. Cande (2000). Evidence for the coincident initiation of homolog pairing and synapsis during the telomere-clustering (bouquet) stage of meiotic prophase. *J Cell Sci* **113 (Pt 6)**: 1033-42.

Baudat, F. and B. de Massy (2007). Regulating double-stranded DNA break repair towards crossover or non-crossover during mammalian meiosis. *Chromosome Res* **15**(5): 565-77.

Bennett, M. D. and J. B. Smith (1979). The effect of colchicine on fibrillar material in wheat meiocytes. *J Cell Sci* **38**: 33-47.

Bennett, M. D., Toledo, L.A., Stern, H. (1979). The effect of colchicine on meiosis in Lillium speciosum cv "Rosemede". *Chromosoma* **72**: 175-189.

Berchowitz, L. E. and G. P. Copenhaver (2008). Division of labor among meiotic genes. *Nat Genet* **40**(3): 266-7.

Bishop, D. K. and D. Zickler (2004). Early decision; meiotic crossover interference prior to stable strand exchange and synapsis. *Cell* **117**(1): 9-15.

Bleuyard, J. Y., M. E. Gallego and C. I. White (2004). The atspo11-1 mutation rescues atxrcc3 meiotic chromosome fragmentation. *Plant Mol Biol* **56**(2): 217-24.

Bleuyard, J. Y., M. E. Gallego and C. I. White (2004). Meiotic defects in the Arabidopsis rad50 mutant point to conservation of the MRX complex function in early stages of meiotic recombination. *Chromosoma* **113**(4): 197-203.

Blitzblau, H. G., G. W. Bell, J. Rodriguez, S. P. Bell and A. Hochwagen (2007). Mapping of meiotic single-stranded DNA reveals double-stranded-break hotspots near centromeres and telomeres. *Curr Biol* **17**(23): 2003-12.

Borde, V., N. Robine, W. Lin, S. Bonfils, V. Geli and A. Nicolas (2009). Histone H3 lysine 4 trimethylation marks meiotic recombination initiation sites. *Embo J* **28**(2): 99-111.

Borner, G. V., A. Barot and N. Kleckner (2008). Yeast Pch2 promotes domainal axis organization, timely recombination progression, and arrest of defective recombinosomes during meiosis. *Proc Natl Acad Sci U S A* **105**(9): 3327-32.

Borner, G. V., N. Kleckner and N. Hunter (2004). Crossover/noncrossover differentiation, synaptonemal complex formation, and regulatory surveillance at the leptotene/zygotene transition of meiosis. *Cell* **117**(1): 29-45.

Bundock, P. and P. Hooykaas (2002). Severe developmental defects, hypersensitivity to DNA-damaging agents, and lengthened telomeres in Arabidopsis MRE11 mutants. *Plant Cell* **14**(10): 2451-62.

Carlton, P. M. and W. Z. Cande (2002). Telomeres act autonomously in maize to organize the meiotic bouquet from a semipolarized chromosome orientation. *J Cell Biol* **157**(2): 231-42.

Carmo-Fonseca, M., L. Mendes-Soares and I. Campos (2000). To be or not to be in the nucleolus. *Nat Cell Biol* **2**(6): E107-12.

Caryl, A. P., G. H. Jones and F. C. Franklin (2003). Dissecting plant meiosis using Arabidopsis thaliana mutants. *J Exp Bot* **54**(380): 25-38.

Chen, C. M., C. T. Wang and C. H. Ho (2001). A plant gene encoding a Myb-like protein that binds telomeric GGTTAG repeats in vitro. *J Biol Chem* **276**(19): 16511-9.

Chen, S. Y., T. Tsubouchi, B. Rockmill, J. S. Sandler, D. R. Richards, G. Vader, A. Hochwagen, G. S. Roeder and J. C. Fung (2008). Global analysis of the meiotic crossover landscape. *Dev Cell* **15**(3): 401-15.

Chicheportiche, A., J. Bernardino-Sgherri, B. de Massy and B. Dutrillaux (2007). Characterization of Spo11-dependent and independent phospho-H2AX foci during meiotic prophase I in the male mouse. *J Cell Sci* **120**(Pt 10): 1733-42.

Chikashige, Y., D. Q. Ding, H. Funabiki, T. Haraguchi, S. Mashiko, M. Yanagida and Y. Hiraoka (1994). Telomere-led premeiotic chromosome movement in fission yeast. *Science* **264**(5156): 270-3.

Chikashige, Y., C. Tsutsumi, M. Yamane, K. Okamasa, T. Haraguchi and Y. Hiraoka (2006). Meiotic proteins bqt1 and bqt2 tether telomeres to form the bouquet arrangement of chromosomes. *Cell* **125**(1): 59-69.

Conrad, M. N., C. Y. Lee, G. Chao, M. Shinohara, H. Kosaka, A. Shinohara, J. A. Conchello and M. E. Dresser (2008). Rapid telomere movement in meiotic prophase is promoted by NDJ1, MPS3, and CSM4 and is modulated by recombination. *Cell* **133**(7): 1175-87.

Cooper, J. P., Y. Watanabe and P. Nurse (1998). Fission yeast Taz1 protein is required for meiotic telomere clustering and recombination. *Nature* **392**(6678): 828-31.

Copenhaver, G. P., E. A. Housworth and F. W. Stahl (2002). Crossover interference in Arabidopsis. *Genetics* **160**(4): 1631-9.

Corredor, E. and T. Naranjo (2007). Effect of colchicine and telocentric chromosome conformation on centromere and telomere dynamics at meiotic prophase I in wheat-rye additions. *Chromosome Res* **15**(2): 231-45.

Couteau, F., F. Belzile, C. Horlow, O. Grandjean, D. Vezon and M. P. Doutriaux (1999). Random chromosome segregation without meiotic arrest in both male and female meiocytes of a dmc1 mutant of Arabidopsis. *Plant Cell* **11**(9): 1623-34.

Cowan, C. R. and W. Z. Cande (2002). Meiotic telomere clustering is inhibited by colchicine but does not require cytoplasmic microtubules. *J Cell Sci* **115**(Pt 19): 3747-56.

Cowan, C. R., P. M. Carlton and W. Z. Cande (2001). The polar arrangement of telomeres in interphase and meiosis. Rabl organization and the bouquet. *Plant Physiol* **125**(2): 532-8.

de Lange, T. (2005). Shelterin: the protein complex that shapes and safeguards human telomeres. *Genes Dev* **19**(18): 2100-10.

de los Santos, T., N. Hunter, C. Lee, B. Larkin, J. Loidl and N. M. Hollingsworth (2003). The Mus81/Mms4 endonuclease acts independently of double-Holliday junction resolution to promote a distinct subset of crossovers during meiosis in budding yeast. *Genetics* **164**(1): 81-94.

De Muyt, A., D. Vezon, G. Gendrot, J. L. Gallois, R. Stevens and M. Grelon (2007). AtPRD1 is required for meiotic double strand break formation in Arabidopsis thaliana. *Embo J* **26**(18): 4126-37.

Dernburg, A. F., K. McDonald, G. Moulder, R. Barstead, M. Dresser and A. M. Villeneuve (1998). Meiotic recombination in C. elegans initiates by a conserved mechanism and is dispensable for homologous chromosome synapsis. *Cell* **94**(3): 387-98.

Ding, D. Q., A. Yamamoto, T. Haraguchi and Y. Hiraoka (2004). Dynamics of homologous chromosome pairing during meiotic prophase in fission yeast. *Dev Cell* **6**(3): 329-41.

Ding, X., R. Xu, J. Yu, T. Xu, Y. Zhuang and M. Han (2007). SUN1 is required for telomere attachment to nuclear envelope and gametogenesis in mice. *Dev Cell* **12**(6): 863-72.

Dover, G. A. and R. Riley (1977). Inferences from genetical evidence on the course of meiotic chromosome pairing in plants. *Philos Trans R Soc Lond B Biol Sci* **277**(955): 313-26.

Driscoll, C. J. and N. L. Darvey (1970). Chromosome pairing: effect of colchicine on an isochromosome. *Science* **169**(942): 290-1.

Driscoll, C. J., Darvey, N.L, and Barber, H.N (1967). Effect of colchicine on meiosis of hexaploid wheat. *Nature* **216**(18): 687-688.

Drouaud, J., C. Camilleri, P. Y. Bourguignon, A. Canaguier, A. Berard, D. Vezon, S. Giancola, D. Brunel, V. Colot, B. Prum, H. Quesneville and C. Mezard (2006). Variation in crossing-over rates across chromosome 4 of Arabidopsis thaliana reveals the presence of meiotic recombination "hot spots". *Genome Res* **16**(1): 106-14.

Fitzgerald, M. S., K. Riha, F. Gao, S. Ren, T. D. McKnight and D. E. Shippen (1999). Disruption of the telomerase catalytic subunit gene from Arabidopsis inactivates telomerase and leads to a slow loss of telomeric DNA. *Proc Natl Acad Sci U S A* **96**(26): 14813-8.

Franklin, A. E., J. McElver, I. Sunjevaric, R. Rothstein, B. Bowen and W. Z. Cande (1999). Three-dimensional microscopy of the Rad51 recombination protein during meiotic prophase. *Plant Cell* **11**(5): 809-24.

Franklin, F. C., J. D. Higgins, E. Sanchez-Moran, S. J. Armstrong, K. E. Osman, N. Jackson and G. H. Jones (2006). Control of meiotic recombination in Arabidopsis: role of the MutL and MutS homologues. *Biochem Soc Trans* **34**(Pt 4): 542-4.

Fung, J. C., B. Rockmill, M. Odell and G. S. Roeder (2004). Imposition of crossover interference through the nonrandom distribution of synapsis initiation complexes. *Cell* **116**(6): 795-802.

Gallego, M. E., White, C.I. (2000). RAD50 function is essential for telomere maintenance in *Arabidopsis*. *Proceedings of the National Academy of Sciences* **98**: 1711-1716.

Gerlach, W. L. and J. R. Bedbrook (1979). Cloning and characterization of ribosomal RNA genes from wheat and barley. *Nucleic Acids Res* **7**(7): 1869-85.

Gerton, J. L., J. DeRisi, R. Shroff, M. Lichten, P. O. Brown and T. D. Petes (2000). Inaugural article: global mapping of meiotic recombination hotspots and coldspots in the yeast Saccharomyces cerevisiae. *Proc Natl Acad Sci U S A* **97**(21): 11383-90.

Gerton, J. L. and R. S. Hawley (2005). Homologous chromosome interactions in meiosis: diversity amidst conservation. *Nat Rev Genet* **6**(6): 477-87.

Gillies, C. B. (1985). An electron microscopic study of synaptonemal complex formation at zygotene in rye. *Chromosoma* **92**: 165-175.

Golubovskaya, I. N., L. C. Harper, W. P. Pawlowski, D. Schichnes and W. Z. Cande (2002). The pam1 gene is required for meiotic bouquet formation and efficient homologous synapsis in maize (Zea mays L.). *Genetics* **162**(4): 1979-93.

Grandin, N., S. I. Reed and M. Charbonneau (1997). Stn1, a new Saccharomyces cerevisiae protein, is implicated in telomere size regulation in association with Cdc13. *Genes Dev* **11**(4): 512-27.

Greider, C. W. and E. H. Blackburn (1985). Identification of a specific telomere terminal transferase activity in Tetrahymena extracts. *Cell* **43**(2 Pt 1): 405-13.

Grelon, M., D. Vezon, G. Gendrot and G. Pelletier (2001). AtSPO11-1 is necessary for efficient meiotic recombination in plants. *Embo J* **20**(3): 589-600.

Griffiths, A. J. F., Miller, JH., Suzuki, D.T., Lewontin, R.C., Gelbart, W.M. (2000). An introduction to genetic analysis. New York, W.H.Freeman company**:** 860

Hamant, O., H. Ma and W. Z. Cande (2006). Genetics of meiotic prophase I in plants. *Annu Rev Plant Biol* **57**: 267-302.

Harper, L., I. Golubovskaya and W. Z. Cande (2004). A bouquet of chromosomes. *J Cell Sci* **117**(Pt 18): 4025-32.

Hartung, F. and H. Puchta (2000). Molecular characterisation of two paralogous SPO11 homologues in Arabidopsis thaliana. *Nucleic Acids Res* **28**(7): 1548-54.

Hartung, F., R. Wurz-Wildersinn, J. Fuchs, I. Schubert, S. Suer and H. Puchta (2007). The catalytically active tyrosine residues of both SPO11-1 and SPO11-2 are required for meiotic double-strand break induction in Arabidopsis. *Plant Cell* **19**(10): 3090-9.

Heacock, M., E. Spangler, K. Riha, J. Puizina and D. E. Shippen (2004). Molecular analysis of telomere fusions in Arabidopsis: multiple pathways for chromosome end-joining. *Embo J* **23**(11): 2304-13.

Heacock, M. L., R. A. Idol, J. D. Friesner, A. B. Britt and D. E. Shippen (2007). Telomere dynamics and fusion of critically shortened telomeres in plants lacking DNA ligase IV. *Nucleic Acids Res* **35**(19): 6490-500.

Hemann, M. T., K. L. Rudolph, M. A. Strong, R. A. DePinho, L. Chin and C. W. Greider (2001). Telomere dysfunction triggers developmentally regulated germ cell apoptosis. *Mol Biol Cell* **12**(7): 2023-30.

Henderson, K. A. and S. Keeney (2004). Tying synaptonemal complex initiation to the formation and programmed repair of DNA double-strand breaks. *Proc Natl Acad Sci U S A* **101**(13): 4519-24.

Higgins, J. D., S. J. Armstrong, F. C. Franklin and G. H. Jones (2004). The Arabidopsis MutS homolog AtMSH4 functions at an early step in recombination: evidence for two classes of recombination in Arabidopsis. *Genes Dev* **18**(20): 2557-70.

Higgins, J. D., E. F. Buckling, F. C. Franklin and G. H. Jones (2008b). Expression and functional analysis of AtMUS81 in Arabidopsis meiosis reveals a role in the second pathway of crossing-over. *Plant J* **54**(1): 152-62.

Higgins, J. D., E. Sanchez-Moran, S. J. Armstrong, G. H. Jones and F. C. Franklin (2005). The Arabidopsis synaptonemal complex protein ZYP1 is required for chromosome synapsis and normal fidelity of crossing over. *Genes Dev* **19**(20): 2488-500.

Higgins, J. D., J. Vignard, R. Mercier, A. G. Pugh, F. C. Franklin and G. H. Jones (2008a). AtMSH5 partners AtMSH4 in the class I meiotic crossover pathway in Arabidopsis thaliana, but is not required for synapsis. *Plant J* **55**(1): 28-39.

Hockemeyer, D., J. P. Daniels, H. Takai and T. de Lange (2006). Recent expansion of the telomeric complex in rodents: Two distinct POT1 proteins protect mouse telomeres. *Cell* **126**(1): 63-77.

Hotta, Y., Shepard, J. (1973). Biochemical aspects of colchicine action in meiotic cells. *Molecular General Genetics* **122**: 243-260.

Hwang, M. G., I. K. Chung, B. G. Kang and M. H. Cho (2001). Sequence-specific binding property of Arabidopsis thaliana telomeric DNA binding protein 1 (AtTBP1). *FEBS Lett* **503**(1): 35-40.

Hwang, M. G., K. Kim, W. K. Lee and M. H. Cho (2005). AtTBP2 and AtTRP2 in Arabidopsis encode proteins that bind plant telomeric DNA and induce DNA bending in vitro. *Mol Genet Genomics* **273**(1): 66-75.

Ishiguro, K., Watanabe, Y. (2007). Chromosome cohesion in mitosis and meiosis. *Journal of Cell Science* **120**: 367-368.

Jackson, N., E. Sanchez-Moran, E. Buckling, S. J. Armstrong, G. H. Jones and F. C. Franklin (2006). Reduced meiotic crossovers and delayed prophase I progression in AtMLH3-deficient Arabidopsis. *Embo J* **25**(6): 1315-23.

Jones, G. H. (1984). The control of chiasma distribution. *Symp Soc Exp Biol* **38**: 293-320.

Jones, G. H., S. J. Armstrong, A. P. Caryl and F. C. Franklin (2003). Meiotic chromosome synapsis and recombination in Arabidopsis thaliana; an integration of cytological and molecular approaches. *Chromosome Res* **11**(3): 205-15.

Jones, G. H. and F. C. Franklin (2006). Meiotic crossing-over: obligation and interference. *Cell* **126**(2): 246-8.

Joshi, N., A. Barot, C. Jamison and G. V. Borner (2009). Pch2 links chromosome axis remodeling at future crossover sites and crossover distribution during yeast meiosis. *PLoS Genet* **5**(7): e1000557.

Karamysheva, Z. N., Y. V. Surovtseva, L. Vespa, E. V. Shakirov and D. E. Shippen (2004). A C-terminal Myb extension domain defines a novel family of double-strand telomeric DNA-binding proteins in Arabidopsis. *J Biol Chem* **279**(46): 47799-807.

Kauppi, L., A. J. Jeffreys and S. Keeney (2004). Where the crossovers are: recombination distributions in mammals. *Nat Rev Genet* **5**(6): 413-24.

Keeney, S. (2001). Mechanism and control of meiotic recombination initiation. *Curr Top Dev Biol* **52**: 1-53.

Keeney, S., C. N. Giroux and N. Kleckner (1997). Meiosis-specific DNA double-strand breaks are catalyzed by Spo11, a member of a widely conserved protein family. *Cell* **88**(3): 375-84.

Kleckner, N. (2006). Chiasma formation: chromatin/axis interplay and the role(s) of the synaptonemal complex. *Chromosoma* **115**(3): 175-94.

Kleckner, N., D. Zickler, G. H. Jones, J. Dekker, R. Padmore, J. Henle and J. Hutchinson (2004). A mechanical basis for chromosome function. *Proc Natl Acad Sci U S A* **101**(34): 12592-7.

Koszul, R., K. P. Kim, M. Prentiss, N. Kleckner and S. Kameoka (2008). Meiotic chromosomes move by linkage to dynamic actin cables with transduction of force through the nuclear envelope. *Cell* **133**(7): 1188-201.

Kuchar, M. (2006). Plant telomere-binding proteins. *Biologia Plantarum* **50**: 1-7.

Kuchar, M. and J. Fajkus (2004). Interactions of putative telomere-binding proteins in Arabidopsis thaliana: identification of functional TRF2 homolog in plants. *FEBS Lett* **578**(3): 311-5.

Kugou, K., T. Fukuda, S. Yamada, M. Ito, H. Sasanuma, S. Mori, Y. Katou, T. Itoh, K. Matsumoto, T. Shibata, K. Shirahige and K. Ohta (2009). Rec8 guides canonical Spo11 distribution along yeast meiotic chromosomes. *Mol Biol Cell* **20**(13): 3064-76.

Lam, W. S., X. Yang and C. A. Makaroff (2005). Characterization of Arabidopsis thaliana SMC1 and SMC3: evidence that AtSMC3 may function beyond chromosome cohesion. *J Cell Sci* **118**(Pt 14): 3037-48.

Li, W., C. Chen, U. Markmann-Mulisch, L. Timofejeva, E. Schmelzer, H. Ma and B. Reiss (2004). The Arabidopsis AtRAD51 gene is dispensable for vegetative development but required for meiosis. *Proc Natl Acad Sci U S A* **101**(29): 10596-601.

Liu, L., S. Franco, B. Spyropoulos, P. B. Moens, M. A. Blasco and D. L. Keefe (2004). Irregular telomeres impair meiotic synapsis and recombination in mice. *Proc Natl Acad Sci U S A* **101**(17): 6496-501.

Liu, Y. G. and Y. Chen (2007). High-efficiency thermal asymmetric interlaced PCR for amplification of unknown flanking sequences. *Biotechniques* **43**(5): 649-50, 652, 654 passim.

Loidl, J. (1988). The effect of colchicine on synaptonemal complex formation in Allium ursinum. *Exp Cell Res* **178**(1): 93-7.

Loidl, J. (1990). The initiation of meiotic chromosome pairing: the cytological view. *Genome* **33**(6): 759-78.

Mahadevaiah, S. K., J. M. Turner, F. Baudat, E. P. Rogakou, P. de Boer, J. Blanco-Rodriguez, M. Jasin, S. Keeney, W. M. Bonner and P. S. Burgoyne (2001). Recombinational DNA double-strand breaks in mice precede synapsis. *Nat Genet* **27**(3): 271-6.

Martinez-Perez, E. and M. P. Colaiacovo (2009). Distribution of meiotic recombination events: talking to your neighbors. *Curr Opin Genet Dev* **19**(2): 105-12.

Martini, E., R. L. Diaz, N. Hunter and S. Keeney (2006). Crossover homeostasis in yeast meiosis. *Cell* **126**(2): 285-95.

McKim, K. S. and A. Hayashi-Hagihara (1998). mei-W68 in Drosophila melanogaster encodes a Spo11 homolog: evidence that the mechanism for initiating meiotic recombination is conserved. *Genes Dev* **12**(18): 2932-42.

McKnight, T. D. and D. E. Shippen (2004). Plant telomere biology. *Plant Cell* **16**(4): 794-803.

Mercier, R., S. Jolivet, D. Vezon, E. Huppe, L. Chelysheva, M. Giovanni, F. Nogue, M. P. Doutriaux, C. Horlow, M. Grelon and C. Mezard (2005). Two meiotic crossover classes cohabit in Arabidopsis: one is dependent on MER3,whereas the other one is not. *Curr Biol* **15**(8): 692-701.

Moens, P. B., N. K. Kolas, M. Tarsounas, E. Marcon, P. E. Cohen and B. Spyropoulos (2002). The time course and chromosomal localization of recombination-related proteins at meiosis in the mouse are compatible with models that can resolve the early DNA-DNA interactions without reciprocal recombination. *J Cell Sci* **115**(Pt 8): 1611-22.

Moore, G. and P. Shaw (2009). Improving the chances of finding the right partner. *Curr Opin Genet Dev* **19**(2): 99-104.

Paques, F., Haber, J.E (1999). Multiple pathways of recombination induced by double-strand breaks in Saccharomyces cerevisiae. *Microbiology and Molecular Biology Reviews* **63**: 349-404.

Pawlowski, W. P., I. N. Golubovskaya and W. Z. Cande (2003). Altered nuclear distribution of recombination protein RAD51 in maize mutants suggests the involvement of RAD51 in meiotic homology recognition. *Plant Cell* **15**(8): 1807-16.

Pecinka, A., V. Schubert, A. Meister, G. Kreth, M. Klatte, M. A. Lysak, J. Fuchs and I. Schubert (2004). Chromosome territory arrangement and homologous pairing in nuclei of Arabidopsis thaliana are predominantly random except for NOR-bearing chromosomes. *Chromosoma* **113**(5): 258-69.

Penkner, A., L. Tang, M. Novatchkova, M. Ladurner, A. Fridkin, Y. Gruenbaum, D. Schweizer, J. Loidl and V. Jantsch (2007). The nuclear envelope protein Matefin/SUN-1 is required for homologous pairing in C. elegans meiosis. *Dev Cell* **12**(6): 873-85.

Peoples, T. L., E. Dean, O. Gonzalez, L. Lambourne and S. M. Burgess (2002). Close, stable homolog juxtaposition during meiosis in budding yeast is dependent on meiotic recombination, occurs independently of synapsis, and is distinct from DSB-independent pairing contacts. *Genes Dev* **16**(13): 1682-95.

Phillips, C. M. and A. F. Dernburg (2006). A family of zinc-finger proteins is required for chromosome-specific pairing and synapsis during meiosis in C. elegans. *Dev Cell* **11**(6): 817-29.

Puizina, J., J. Siroky, P. Mokros, D. Schweizer and K. Riha (2004). Mre11 deficiency in Arabidopsis is associated with chromosomal instability in somatic cells and Spo11-dependent genome fragmentation during meiosis. *Plant Cell* **16**(8): 1968-78.

Rees, H. (1957). Distribution of chiasmata in an asynaptic locust. *Nature* **180**(4585): 559.

Riha, K., T. D. McKnight, L. R. Griffing and D. E. Shippen (2001). Living with genome instability: plant responses to telomere dysfunction. *Science* **291**(5509): 1797-800.

Riha, K. and D. E. Shippen (2003). Telomere structure, function and maintenance in Arabidopsis. *Chromosome Res* **11**(3): 263-75.

Roberts, N. Y., K. Osman and S. J. Armstrong (2009). Telomere distribution and dynamics in somatic and meiotic nuclei of Arabidopsis thaliana. *Cytogenet Genome Res* **124**(3-4): 193-201.

Roeder, G. S. (1997). Meiotic chromosomes: it takes two to tango. *Genes Dev* **11**(20): 2600-21.

Rossignol, P., S. Collier, M. Bush, P. Shaw and J. H. Doonan (2007). Arabidopsis POT1A interacts with TERT-V(I8), an N-terminal splicing variant of telomerase. *J Cell Sci* **120**(Pt 20): 3678-87.

Salonen, K., J. Paranko and M. Parvinen (1982). A colcemid-sensitive mechanism involved in regulation of chromosome movements during meiotic pairing. *Chromosoma* **85**(5): 611-8.

Sanchez-Moran, E., S. J. Armstrong, J. L. Santos, F. C. Franklin and G. H. Jones (2002). Variation in chiasma frequency among eight accessions of Arabidopsis thaliana. *Genetics* **162**(3): 1415-22.

Sanchez-Moran, E., J. L. Santos, G. H. Jones and F. C. Franklin (2007). ASY1 mediates AtDMC1-dependent interhomolog recombination during meiosis in Arabidopsis. *Genes Dev* **21**(17): 2220-33.

Sanchez Moran, E., S. J. Armstrong, J. L. Santos, F. C. Franklin and G. H. Jones (2001). Chiasma formation in Arabidopsis thaliana accession Wassileskija and in two meiotic mutants. *Chromosome Res* **9**(2): 121-8.

Santos, J. L., D. Alfaro, E. Sanchez-Moran, S. J. Armstrong, F. C. Franklin and G. H. Jones (2003). Partial diploidization of meiosis in autotetraploid Arabidopsis thaliana. *Genetics* **165**(3): 1533-40.

Scherthan, H. (2001). A bouquet makes ends meet. *Nat Rev Mol Cell Biol* **2**(8): 621-7.

Scherthan, H. (2006). Factors directing telomere dynamics in synaptic meiosis. *Biochem Soc Trans* **34**(Pt 4): 550-3.

Scherthan, H. (2007). Telomere attachment and clustering during meiosis. *Cell Mol Life Sci* **64**(2): 117-24.

Scherthan, H., H. Wang, C. Adelfalk, E. J. White, C. Cowan, W. Z. Cande and D. B. Kaback (2007). Chromosome mobility during meiotic prophase in Saccharomyces cerevisiae. *Proc Natl Acad Sci U S A* **104**(43): 16934-9.

Schmitt, J., R. Benavente, D. Hodzic, C. Hoog, C. L. Stewart and M. Alsheimer (2007). Transmembrane protein Sun2 is involved in tethering mammalian meiotic telomeres to the nuclear envelope. *Proc Natl Acad Sci U S A* **104**(18): 7426-31.

Shakirov, E. V., T. D. McKnight and D. E. Shippen (2009). POT1-independent single-strand telomeric DNA binding activities in Brassicaceae. *Plant J* **58**(6): 1004-15.

Shakirov, E. V., Y. V. Surovtseva, N. Osbun and D. E. Shippen (2005). The Arabidopsis Pot1 and Pot2 proteins function in telomere length homeostasis and chromosome end protection. *Mol Cell Biol* **25**(17): 7725-33.

Siaud, N., E. Dray, I. Gy, E. Gerard, N. Takvorian and M. P. Doutriaux (2004). Brca2 is involved in meiosis in Arabidopsis thaliana as suggested by its interaction with Dmc1. *Embo J* **23**(6): 1392-401.

Siroky, J., Zluvova, J., Rhia, K, Shippen, D.E., Vyskot, B. (2003). Rearrangement of ribosomal DNA clusters in late generation telomerase-deficient *Arabidopsis*. *Chromosoma* **112**: 116-123.

Smith, R. F., B. A. Wiese, M. K. Wojzynski, D. B. Davison and K. C. Worley (1996). BCM Search Launcher--an integrated interface to molecular biology data base search and analysis services available on the World Wide Web. *Genome Res* **6**(5): 454-62.

Snowden, T., S. Acharya, C. Butz, M. Berardini and R. Fishel (2004). hMSH4-hMSH5 recognizes Holliday Junctions and forms a meiosis-specific sliding clamp that embraces homologous chromosomes. *Mol Cell* **15**(3): 437-51.

Song, X., K. Leehy, R. T. Warrington, J. C. Lamb, Y. V. Surovtseva and D. E. Shippen (2008). STN1 protects chromosome ends in Arabidopsis thaliana. *Proc Natl Acad Sci U S A* **105**(50): 19815-20.

Stacey, N. J., T. Kuromori, Y. Azumi, G. Roberts, C. Breuer, T. Wada, A. Maxwell, K. Roberts and K. Sugimoto-Shirasu (2006). Arabidopsis SPO11-2 functions with SPO11-1 in meiotic recombination. *Plant J* **48**(2): 206-16.

Stahl, F. W., H. M. Foss, L. S. Young, R. H. Borts, M. F. Abdullah and G. P. Copenhaver (2004). Does crossover interference count in Saccharomyces cerevisiae? *Genetics* **168**(1): 35-48.

Stewart, S. A. and R. A. Weinberg (2000). Telomerase and human tumorigenesis. *Semin Cancer Biol* **10**(6): 399-406.

Storlazzi, A., S. Tesse, S. Gargano, F. James, N. Kleckner and D. Zickler (2003). Meiotic double-strand breaks at the interface of chromosome movement, chromosome remodeling, and reductional division. *Genes Dev* **17**(21): 2675-87.

Storlazzi, A., S. Tesse, G. Ruprich-Robert, S. Gargano, S. Poggeler, N. Kleckner and D. Zickler (2008). Coupling meiotic chromosome axis integrity to recombination. *Genes Dev* **22**(6): 796-809.

Surovtseva, Y. V., E. V. Shakirov, L. Vespa, N. Osbun, X. Song and D. E. Shippen (2007). Arabidopsis POT1 associates with the telomerase RNP and is required for telomere maintenance. *Embo J* **26**(15): 3653-61.

Tamura, K., Y. Adachi, K. Chiba, K. Oguchi and H. Takahashi (2002). Identification of Ku70 and Ku80 homologues in Arabidopsis thaliana: evidence for a role in the repair of DNA double-strand breaks. *Plant J* **29**(6): 771-81.

Tani, A. and M. Murata (2005). Alternative splicing of Pot1 (Protection of telomere)-like genes in Arabidopsis thaliana. *Genes Genet Syst* **80**(1): 41-8.

Tease, C., Jones, G.H. (1976). Chromosome-specific control of chiasma formation in *Crepis capillaris*. *Chromosoma* **57**: 33-49.

Tepperberg, J. H., M. J. Moses and J. Nath (1997). Colchicine effects on meiosis in the male mouse. I. Meiotic prophase: synaptic arrest, univalents, loss of damaged spermatocytes and a possible checkpoint at pachytene. *Chromosoma* **106**(3): 183-92.

Tesse, S., A. Storlazzi, N. Kleckner, S. Gargano and D. Zickler (2003). Localization and roles of Ski8p protein in Sordaria meiosis and delineation of three mechanistically distinct steps of meiotic homolog juxtaposition. *Proc Natl Acad Sci U S A* **100**(22): 12865-70.

Thomas, J. B., Kaltsikes, P.J. (1977). The effect of colchicine on chromosome pairing. *Canadian Journal of Genetics and Cytology* **19**: 231-249.

Tomita, K. and J. P. Cooper (2006). The meiotic chromosomal bouquet: SUN collects flowers. *Cell* **125**(1): 19-21.

Trelles-Sticken, E., C. Adelfalk, J. Loidl and H. Scherthan (2005). Meiotic telomere clustering requires actin for its formation and cohesin for its resolution. *J Cell Biol* **170**(2): 213-23.

Trelles-Sticken, E., M. E. Dresser and H. Scherthan (2000). Meiotic telomere protein Ndj1p is required for meiosis-specific telomere distribution, bouquet formation and efficient homologue pairing. *J Cell Biol* **151**(1): 95-106.

Trelles-Sticken, E., J. Loidl and H. Scherthan (1999). Bouquet formation in budding yeast: initiation of recombination is not required for meiotic telomere clustering. *J Cell Sci* **112 (Pt 5)**: 651-8.

Vignard, J., T. Siwiec, L. Chelysheva, N. Vrielynck, F. Gonord, S. J. Armstrong, P. Schlogelhofer and R. Mercier (2007). The interplay of RecA-related proteins and the MND1-HOP2 complex during meiosis in Arabidopsis thaliana. *PLoS Genet* **3**(10): 1894-906.

Voet, T., B. Liebe, C. Labaere, P. Marynen and H. Scherthan (2003). Telomere-independent homologue pairing and checkpoint escape of accessory ring chromosomes in male mouse meiosis. *J Cell Biol* **162**(5): 795-807.

Walker, R. I. (1938). The effect of colchicine on icrospore mother cells and microspores of Tradescantia paludosa. *American Journal of Botany* **29**: 280-285.

Wanat, J. J., K. P. Kim, R. Koszul, S. Zanders, B. Weiner, N. Kleckner and E. Alani (2008). Csm4, in collaboration with Ndj1, mediates telomere-led chromosome dynamics and recombination during yeast meiosis. *PLoS Genet* **4**(9): e1000188.

Waterworth, W. M., C. Altun, S. J. Armstrong, N. Roberts, P. J. Dean, K. Young, C. F. Weil, C. M. Bray and C. E. West (2007). NBS1 is involved in DNA repair and plays a synergistic role with ATM in mediating meiotic homologous recombination in plants. *Plant J* **52**(1): 41-52.

Weiner, J. L., A. V. Buhler, V. J. Whatley, R. A. Harris and T. V. Dunwiddie (1998). Colchicine is a competitive antagonist at human recombinant gamma-aminobutyric acidA receptors. *J Pharmacol Exp Ther* **284**(1): 95-102.

Wu, H. Y. and S. M. Burgess (2006). Ndj1, a telomere-associated protein, promotes meiotic recombination in budding yeast. *Mol Cell Biol* **26**(10): 3683-94.

Zickler, D. (2006). From early homologue recognition to synaptonemal complex formation. *Chromosoma* **115**(3): 158-74.

Zickler, D. and N. Kleckner (1998). The leptotene-zygotene transition of meiosis. *Annu Rev Genet* **32**: 619-97.

Zickler, D. and N. Kleckner (1999). Meiotic chromosomes: integrating structure and function. *Annu Rev Genet* **33**: 603-754.

Zickler, D., P. J. Moreau, A. D. Huynh and A. M. Slezec (1992). Correlation between pairing initiation sites, recombination nodules and meiotic recombination in Sordaria macrospora. *Genetics* **132**(1): 135-48.

8
Appendix

List of Contents

8.1 General buffers and solutions

Cytology

1x PBS

Phosphate saline buffer 1 tablet per 100ml pH 7

HYBRIDISATION MIX

Detran suphate	1g
Deionised formamide	5ml
20xSSC	1ml
to 7ml with water, pH	

CITRATE BUFFER

Citric acid	0.1M
Sodium citrate	0.1M

diluted 1:10 with sterile distilled water pH5.4

20 x SSC

3M NaCl
300mM trisodium citrate

Made to pH 7 using HCL

ALEXANDER STAIN

Ethanol 95%	10 ml
Malachite green (1% in 95% Ethanol)	1 ml
Fuchsin acid (1% in water)	5 ml
Orange G (1% in water)	0.5 ml
Phenol	5g
Chloral hydrate	5 g
Glacial acetic acid	2 ml
Glycerol	25 ml
Distilled water	50 ml

DNA and RNA manipulations

DNA LOADING BUFFER

Bromophenol blue	50 µl
1 Kb ladder (Invitrogen)	12 µl
SDW	138 µl

5x TBE

Tris	0.445 M
Boric acid	0.445 M
EDTA	0.01 M

TFBI

Potassium acetate	30 mM
Rubidium chloride	100mM
Calcium chloride	10 mM
Manganese chloride	50 mM
Glycerol	15 % (v/v)

pH 5.8

TFBII

MOPS	10mM
Calcium chloride	75 mM
Rubidium chloride	10 mM
Glycerol	15 % (v/v)

pH 6.5

DNA EXTRACTION BUFFER

KCL	0.25M
EDTA	10mM
Tris-HCL	100mM

pH9.5

DILUTION BUFFER

3x BSA in water (Bovine serum albumin)

LB medium

1-1bacto-tryptone	10g
1-1 bacto-yeast extract	5g
NaCl	10g

LB agar

1-1bacto-tryptone	10g
1-1 bacto-yeast extract	5g
NaCl	10g
Bacto-agar	15g

Media was prepared in SDW and sterilised by autoclaving at 15psi at 121 ^{o}C for 20min.

Sequence manipulation programmes

Higgins DG, Thompson JD, Gibson TJ. (1996). Using CLUSTAL for multiple sequence alignments.*Methods of Enzymology*. **266**:383-402.

Smith RF, Wiese BA, Wojzynski MK, Davison DB, Worley KC. (1996). BCM Search Launcher--an integrated interface to molecular biology data base search and analysis services available on the World Wide Web.*Genome Research*. **6**:454-62.

Protein manipulations

5X PROTEIN LOADING BUFFER (PLB)

Tris-HCL (pH 6.8)	12.5% (v/v)
SDS	2% (w/v)
Glycerol	10% (v/v)
B-Mercatoethanol	5% (v/v)
Bromophenol blue	0.001% (w/v)

RESERVOIR BUFFER 1X

Tris	25 mM
Glycine	192 mM
SDS	0.1 % (w/v)

pH 8.3

WESTERN TRANSFER BUFFER

Methanol	20 % (v/v)
Sodium hydrogen carbonate	0.01 M
Sodium carbonate	3.0mM

MILK BLOCK

PBS	1x
Milk powder	5 % (w/v)

COOMASSIE BLUE

Coomassie Blue R-2500	1 %
SDW	45 % (v/v)
Methanol	45 % (v/v)
Glacial acetic acid	10%

DESTAIN

Methanol	30 % (v/v)
Glacial acetic acid	10 % (v/v)

GEL DRYING BUFFER

Glycerol	2 %
Methanol	20 %
SDW	78 %

LYSIS BUFFER

Tris HCL	50 mM
NaCl	100mM
EDTA	1 mM

pH 8

DENATURING BUFFER

NaH_2PO_4	100mM
Tris HCL	10 mM
Urea pH 8	8 M

ELUTION BUFFER

Tris HCL	50 mM
NaCl	300 mM
Urea	8 M

Varying concentrations of Imidazol, pH 8

REFOLDING BUFFER

Tris	0.1 M
EDTA	2 mM
L-arginine hydrochloride	0.5 M
Cystamine dihydrochloride	10mM
Glycerol	5 %

to a final pH 8

Protein extraction buffer

HEPES pH 7.6	20mM
NaCl	420mM
$MgCl_2$	1.2mM
EDTA	0.2mM
Glycerol	25%
Protease inhibitor	1 Tablet

Made up to 10ml with SDW, aliquoted and stored at $^{-}20^{o}C$

8.2 Primer Sequences

Name of primer	Primer sequence 5'- 3'	Tm (^{0}C)	PCR technique
T7 promoter	TAATACGACTCACTATAGGG		Sequencing
M13 forward	TGACCGGCAGCAA AATG		Sequencing
M13 reverse	AACAGCTATGACCATG		Sequencing
Oligo dt 24	TTTTTTTTTTTTTTTTTTTTTTTT	42.2	Reverse transcription
WISCLB	AACGTCCGCAATGTGTTAAGTTGT	62.2	Genotyping
SAILLB	TTCATAACCAATCTCGATACAC	54.7	Genotyping
TERTP6	GGACATATCCATCAAGG	60.1	Genotyping
TERTP7	GGAAGCTGTATTGCACG	52.8	Genotyping
AtPOT1F1	G**CATATG**GCTAAGAGAAGTGAAGAAGACAAGG	66.9	Cloning
AtPOT1R1	G**CTCGAG**ACAATTGTCATCTGTCTCTGTTAATC	68.3	Cloning
AtPOT2F1	G**CATATG**GTTAAGTCAGAAAGGCTTCC	63.4	Cloning
AtPOT2R1	G**CTCGAG**ATCGTCATGGGCAACCCCTG	71	Cloning
AtPOT1FA	G**CATATG**GCGAAGAAGAGAGAGAGTCCCAAGC	70.8	Cloning
AtPOT1FB	G**CATATG**CTGCTCAGCTTTCCAACCGTTGGAACG	71.9	Cloning
JL202	CATTTTATAATAACGCTGCGGACATCTAC	62.4	Genotyping *pot1a-1*
P1DBD-XBAI	CTATCTTGATCTCTCTCAAGAAGGA	59.7	Genotyping *pot1a-1*
P1NEW	ATGGCGAAGAAGAGAGAGAGTCCCAAGCTCATC	70.7	Genotyping *pot1a-1*
P2GT1F	AAACCCCAACGATCAGAGAC	57.3	Genotyping *pot1b-1*
P2GT3R	AGACGAAGAGGTTGTTTCATTGCA	59.4	Genotyping *pot1b-1*
DS3-1	ACCCGACCGGATCGTATCGGT	63.7	Genotyping *pot1b-1*
POT1ASAILF1	TTCCAACCGTTGGAACGATC	57.3	Genotyping
POT1ASAILR1	TAGGAGAGGATGCAGCACTCGA	62.1	Genotyping
POT1BSAILF1	TCTCTGATGGACATCCTGACC	59.8	Genotyping
POT1BSAILR1	CAGCCAAGTGTGACGTTGACT	59.8	Genotyping
SPO11EXPF1	GGAAGCTGTAGATTGTTCGG	57.3	RT-PCR
SPO11EXPR1	GTTCCCTGTTCTTGTAGAGG	57.3	RT-PCR/Genotyping
SPO11F4	GAGGATATCCAGATGTCTC	54.5	Genotyping

SPO11-1QF1	TGCCACAATGGAGGTTGGA	56.7	Real-time
SPO11-1QR1	TTCACGACGAATCTTAGAAGGAATATATA	59.6	Real-time
SPO11-2QF3	CCTGATCTGCCAATTCTTGTTCT	58.9	Real-time
SPO11-2QR3	TCACATTGCAAGCGTATCTGTATG	59.3	Real-time
ACT2QF1	CCAGTGGTCGTACAACCGGT	61.4	Real-time
ACT2QR1	ACGGAGGATGGCATGAGGA	58.8	Real-time
AD1	(AGCT)TCGA(GC)T(AT)T(GC)G(AT)GTT	43.7	TAIL
AD2	(AGCT)GTCGA(GC)(AT)GA(AGCT)A(AT)GAA	46.6	TAIL
AD3i	GTG I AG I A I CA I AGA	39.6	TAIL
AD4i	I AA I T I AG I TAA	34.2	TAIL
pARTRBF1	AGCTATGCATCCAACGCGTTG	59.8	IPCR
pARTRBF2	CACAGGAAACAGCTATGACC	57.3	IPCR
pARTRBR1	AAACCTGTCGTGCCAGCT	58.8	IPCR/ TAIL
pARTRBR2	TAATTGCGTTGCGCTCACTG	57.3	IPCR/ TAIL
pARTRBR3	GGTGCCTAATGAGTGAGCTAACTCAC	64.8	IPCR/TAIL
1`SPO1116CF2	TCCCCATTGCAACACAACACC	59.8	Genotyping
SPO1116CR2	TGACTCCGCAATGCTTCTTG	57.3	Genotyping
SPO119HF1	GCCAAGACCAACTCAAATCG	57.3	Genotyping
SPO119HR1	ACAGATTGTAGTCACGCTGG	57.3	Genotyping

Table 8.1: Primer sequences and uses. Locations of restriction sites shown in red bold.

8.3: Real-time PCR primer validation

A

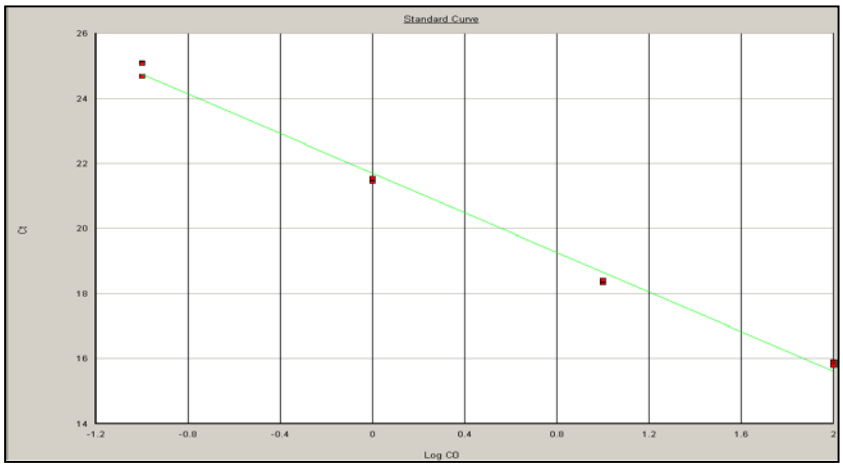

B

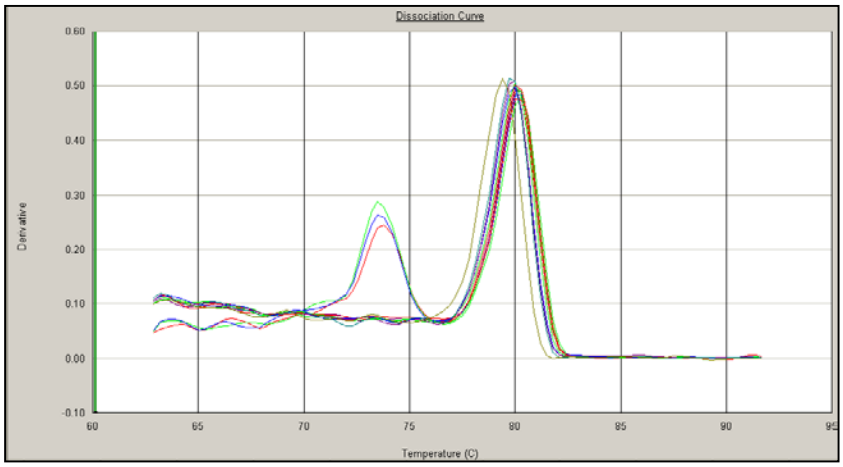

Figure 8.1: Actin 2

(A) Standard curve showing data points from 10-fold serial dilutions of cDNA. slope -3.04, r^2:0.994.

(B) Dissociation curve. Peaks indicate the number of products formed by the primer pair. The large peak indicates specific amplification of the gene, and the small peak, non-specific amplification, which was only observed when using 100ng cDNA.

A

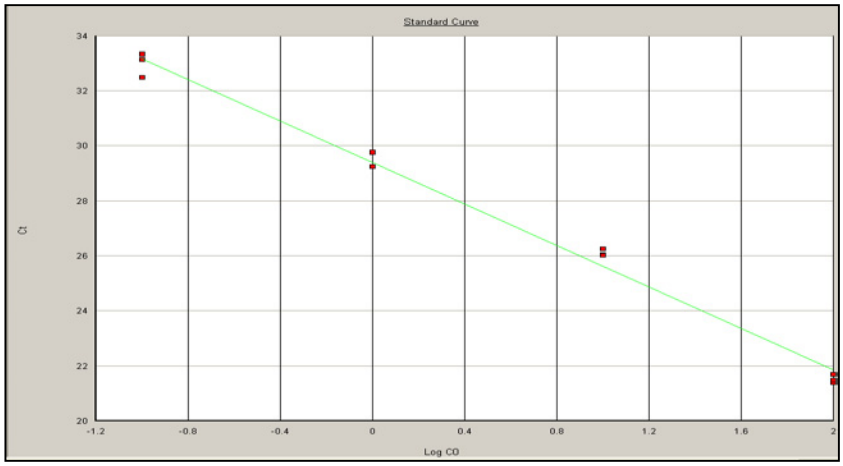

B

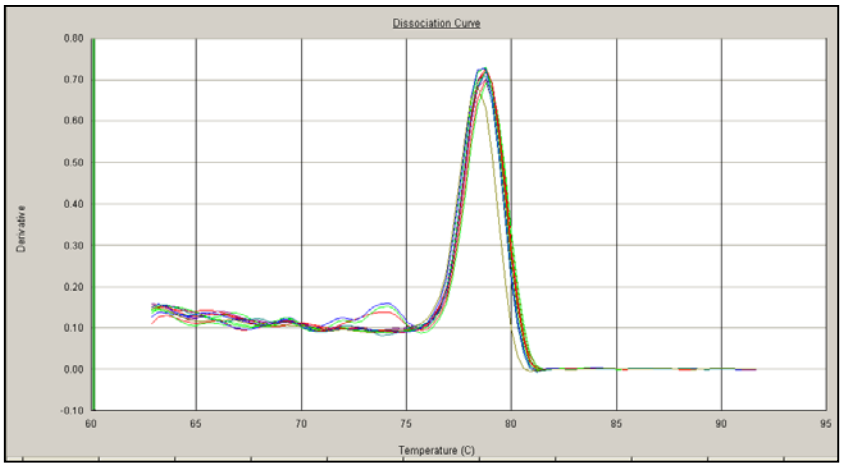

Figure 8.2: SPO11-1

(A) Standard curve showing data points from 10-fold serial dilutions of cDNA. slope -3.77 r^2:0.991.

(B) Dissociation curve. Shows the number of products formed by the primer pair. The large peak shows specific amplification of the gene. A very low amount of non-specific product was formed using 100ng of template cDNA.

A

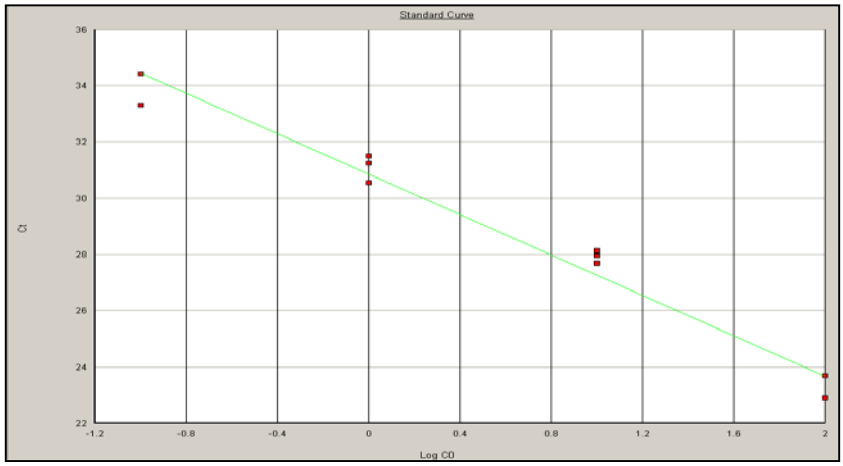

B

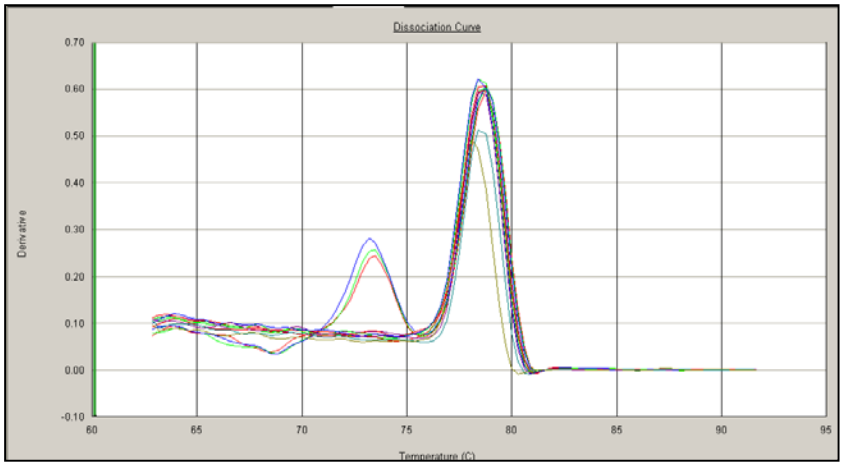

Figure 8.3: SPO11-2 (Q3)

(A) Standard curve showing data points from 10-fold serial dilutions of cDNA. slope -3.58, r_2:0.972, which is slightly below the threshold recommended. This is most likely to be due to inaccurate pipetting.

(B) Dissociation curve. The large peak shows specific amplification and the small peak non-specific amplification, which was observed when using 100ng cDNA. 20ng of cDNA was used in the final assays, for which no non-specific amplification was observed.

8.4 SPO11 RNAi BrdU time course

	18H			24H			36H			
	WT	**9H**	**HOM**	**WT**	**9H**	**HOM**	**WT**	**8A**	**9H**	**HOM**
L	5\6	51\91	37\39	26\57	7\17	46\57	1\8	11\13	54\63	2\13
Z/P	7\26	36\158	71\88	24\143	5\63	33\92	10\15	33\58	45\97	27\101
Dip/Dia	0\25	0\61	0\56	0\37	0\20	0\19	3\13	0\30	0\73	0\51
MI	0\2	0\17	0\3	0\3	0\8	0\1	2\5	0\11	0\8	0\1
MII	0\3	0\18	0\12	0\6	0\22	0\1	0\6	0\6	0\22	0\11
T	0\11	0\34	0\7	0\19	0\20	0\2	0\12	0\37	0\12	0\10

Table 8.2: *SPO11* RNAi BrdU time course

Detailed observations from a single time course. Time points that inflorescences are shown above. The data shows the number of BrdU labelled cells versus the total number of cells observed. (WT) wild-type. (9H) RNAi line 9H. (8A) RNAi line 8A. (HOM) *spo11-1-4* null homozygote. Meiotic stages (L) leptoene, (Z/P) zygotene/pachytene, (Dip/Dia) diplotene/diakinesis, (MI) metaphase I. (MII) metaphase II. (T) tetrad.

8.5 IPCR SEQUENCING

NCCCCCACACGTGTGGTCTAGAGCTAGCCTAGGCTCGAGAAGCTTGTCGACGAAT
TCAGATTAAACCTGTCGTGCCAGCTGCATTAATGAATCGGCCAACGCGCGGGGAG
AGGCGGTTTGCGTATTGGGGCTGAGTGGCTCCTTCAACGTTGCGGTTCTGTCAGTT
CCAAACGTAAAACGGCTTGTCCCGCGTCATCGGCGGGGGTCATAACGTGACTCCC
TTAATTCTAAGCTGTCAATTATATGAGTTCTGAGATCAGGTTGGAATGAGAAAAGAG
ATGGGTTCTCCNGGATGAAATTGAAAAGGGAGATGCCTTTCCAGGATTTGATATCT
GGGTCTGATAAAATACGGCGAAGAGTGGAGAGATTGAGATCGGAGAGTGGTGTTT
CCGGTGAAGCAAGAGTNNGGTTTATAGAGGAAGAATTGAGGAG

Figure 8.4: Sequencing of fragment from *SacI* digested line 16C DNA amplified by iPCR.Yellow region denotes the pDRIVE vector into which the fragment was cloned. The red region the pART vector, and the green region is the primer pARTRBR1. The blue region shows the gene into which the construct has inserted. At2g28050, a gene of unknown function. Further primers were designed either side of this sequence for genotyping.

8.6 Colchicine BrdU time course

A

	Meiotic interphase	Leptotene	Zygotene /Pachytene	Diakinesis/ MI	MII	tetrad
-2						
0	25/50	0/15	0/25	0/7	0/2	0/15
6	8/24	1/16	0/34	0/5	0/1	0/10
12	5/6	2/18	0/10	0/8	0/13	0/11
18	6/10	6/7	10/20	0/8	0/10	0/12
24	5/11	4/5	5/15	0/8	0/11	0/12
30	17/24	5/7	5/9	0/10	0/5	0/12

B

	meiotic interphase	leptotene	zygotene /pachytene	diakinesis/ MI	MII	tetrad
-2						
0	12/22	0/12	0/17	0/20	0/6	0/10
6	6/21	1/25	0/5	0/10	0/10	0/15
12	1/6	5/15	0/16	0/11	0/2	0/15
18	15/25	25/25	10/25	0/1	0/5	0/24
24	15/26	27/28	17/34	0/5	0/4	0/13
30	8/16	4/7	11/21	0/1	0/1	0/20

Table 8.3: The number of BrdU labelled cells for different meiotic stages at each time-point together with the total numbers of cells observed. Time point 0h is the end of the 2h BrdU labelling pulse. The control samples were collected and fixed at the start of the 2h pulse. This table shows the data for one time course of the Col-0 accession of *Arabidopsis*. (A) Inflorescences treated with distilled water (control). (B) Inflorescences treated with 100µM colchicine.

8.7 Growth curves of E.coli cells expressing POT1a and POT1b pET21b constructs

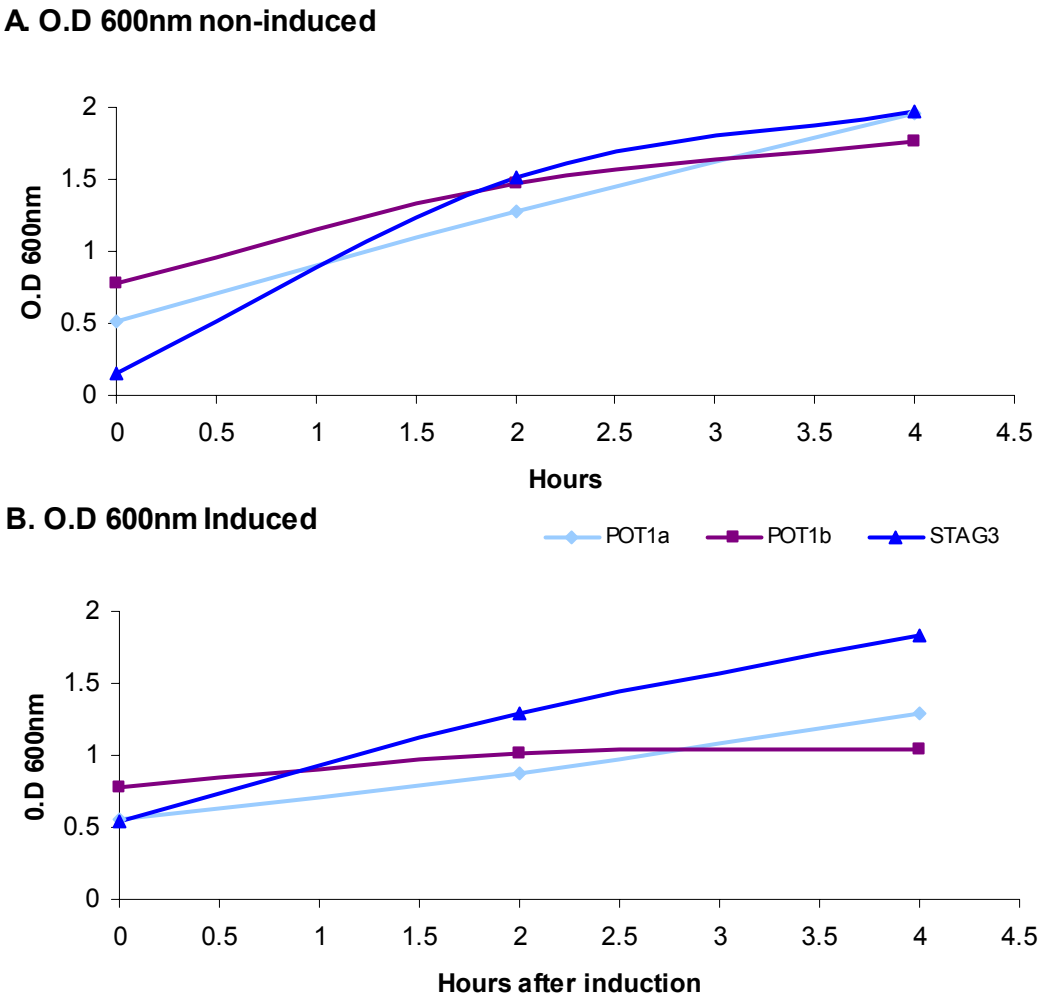

Figure 8.5: Growth curves of BL21 *E.coli* cultures transformed with POT1a, POT1b, or the STAG3 control pET21b constructs. Spectrophotometer readings at O.D.600nm for non-induced (A) cultures, and those induced for protein expression with IPTG (B). In the induced cultures, growth is affected by the POT1 constructs relative to the STAG3 control protein.

8.8 List of presentations

Poster presentations

Roberts, N.Y., and Armstrong, S.J. (2006). Progression of meiosis in *Arabidopsis thaliana*. European meiosis meeting: Meiosis and the causes and consequences of recombination. University of Warwick (UK).

Roberts, N.Y., and Armstrong, S.J. (2007). A Role for the Bouquet in *Arabidopsis*? European meiosis meeting. Kanagawa, Japan.

Roberts, N.Y. J.D. Higgins, F.C.H. Franklin, and S.J. Armstrong (2008). Investigating Crossover Control in *Arabidopsis* Meiosis Using *SPO11* RNA Interference. Bioscience Graduate Research School Symposium, University of Birmingham, (UK).

Talks

Roberts, N.Y., and Armstrong, S.J. (2006). Dynamics of Homologous Chromosome Pairing in *Arabidopsis* Meiosis: A Central Role for the Telomere? Seminar during visit, to Telomere and genome stability laboratory. Gregor Mendel Institute Vienna (Austria).

Roberts, N.Y. J.D. Higgins, F.C.H. Franklin, and S.J. Armstrong (2009). Investigating crossover control in *Arabidopsis* meiosis using *SPO11-1* RNA interference. Bioscience Graduate Research School Symposium, University of Birmingham, (UK).

Publications

Review article:
Roberts, N.Y., Osman, K., and Armstrong, S.J. (2009). Telomere Distribution and Dynamics in Somatic and Meiotic Nuclei of *Arabidopsis thaliana*. *Cytogenetic and Genome Research.* 124:193–201

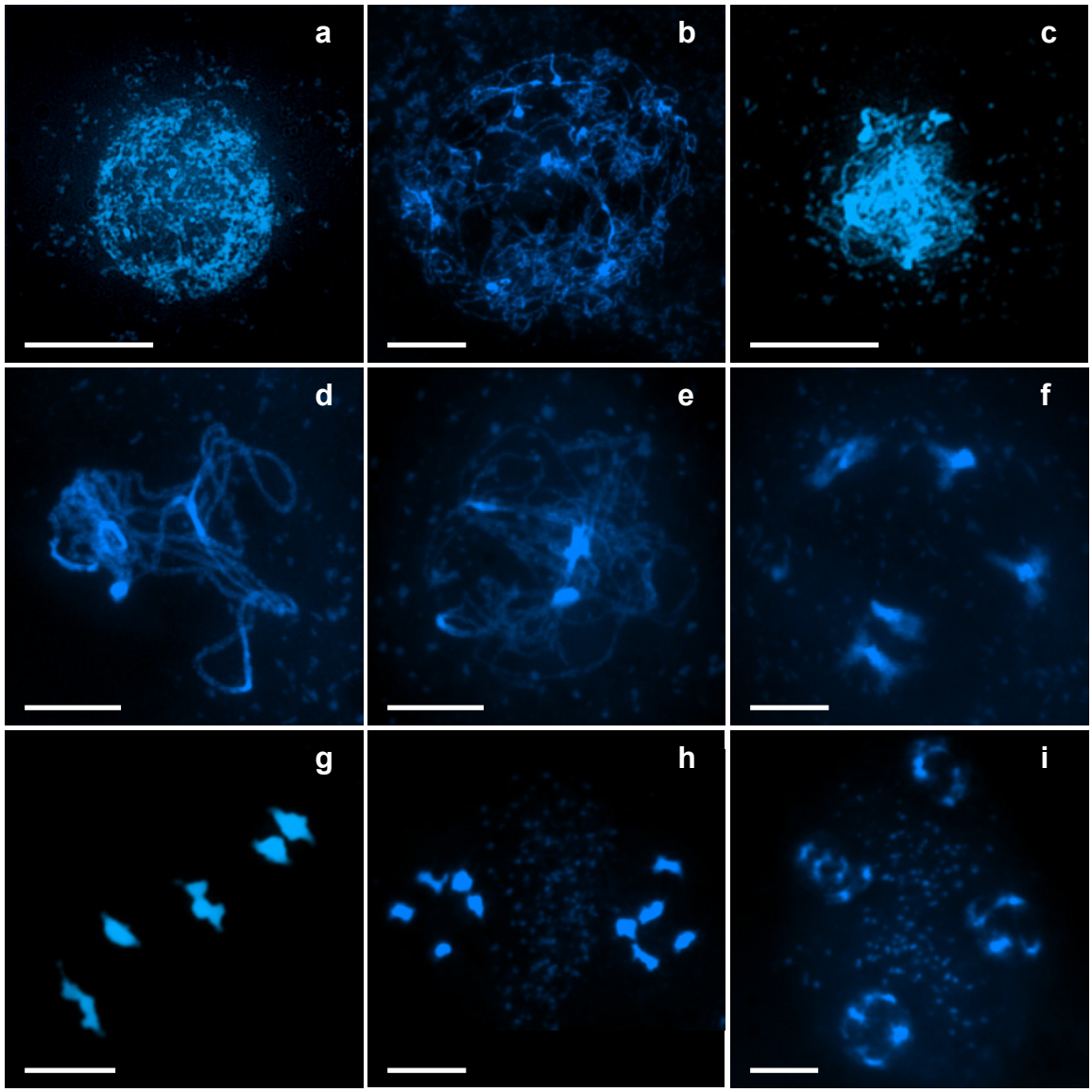

Figure 1.1: Meiotic atlas of *Arabidopsis* meiosis Col-0.
(a) Preleptotene: undifferentiated nuclear structure. (b) Leptotene: chromatin begins to condense, with chromosomes becoming visible as fine threads (c) Zygotene: synapsis in progress, both synapsed and unsynapsed regions visible. Asymmetric distribution of organelles. (d) Pachytene: fully synapsed chromosomes held together by a proteinaceous structure called the synaptonemal complex, with organelles evenly distributed. (e) Diplotene: chromosome pairs progressively becoming desynapsed (excluding chiasmata), organelles dispersed (f) Diakinesis: condensed bivalent structures seen. (g) Metaphase I: five completely condensed bivalents visible, lined up on spindle equator. Homologues are held together by chiasmata. (h) Metaphase II: Two daughter nuclei each containing five chromosomes, (as a result of anaphase1), separated by a band of organelles (organelles are excluded from the spindle during anaphase1). (i) Tetrad: Sister chromatids become separated at Anaphase II to yield four haploid microspores.

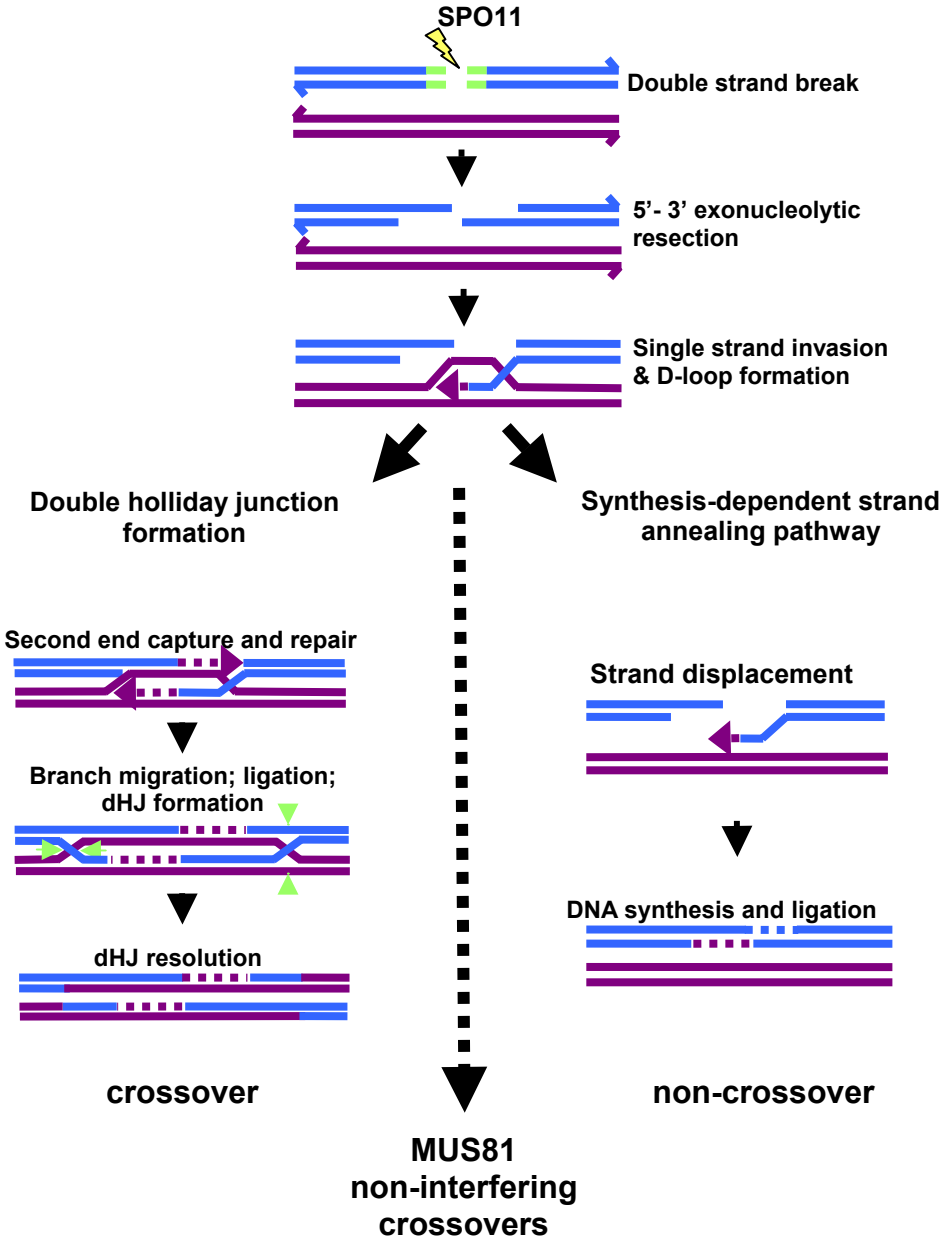

Figure 1.2: Early crossover decision model

Homologous chromosomes are indicated by different colours, with one chromatid shown for simplicity. H2AX phosphorylation shown green. Holliday junction (dHJ). At the stage of single strand invasion, DSBs are selected to be repaired as a crossover or non-crossover.

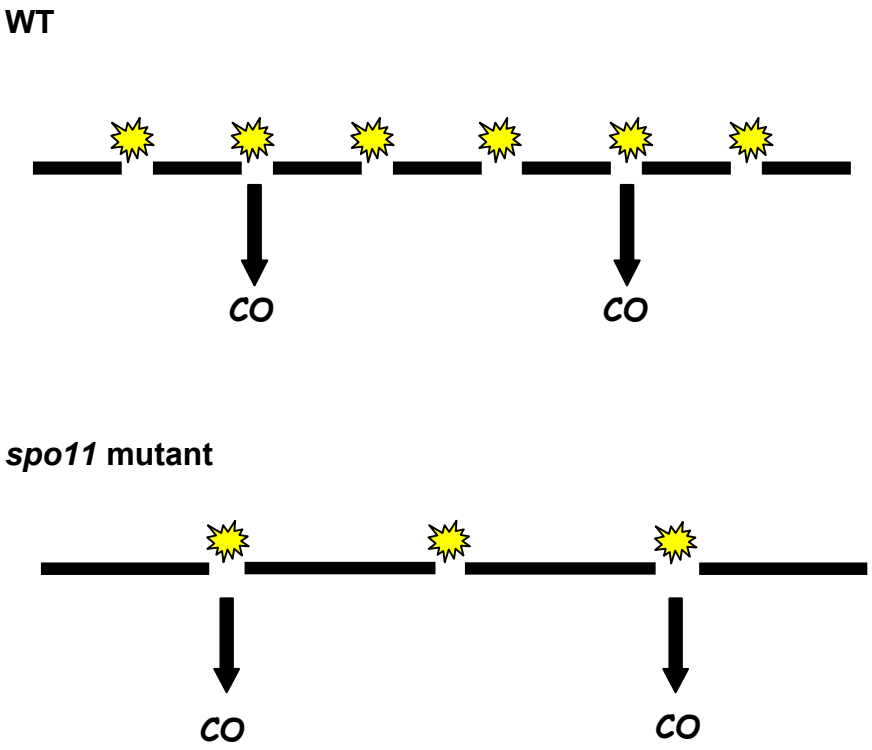

Figure 1.3: Crossover Homeostasis. In yeast, the crossover number is maintained when the number of crossover initiating events (DSBs) is reduced. SPO11 induced DSBs, shown by stars. Crossover (CO).

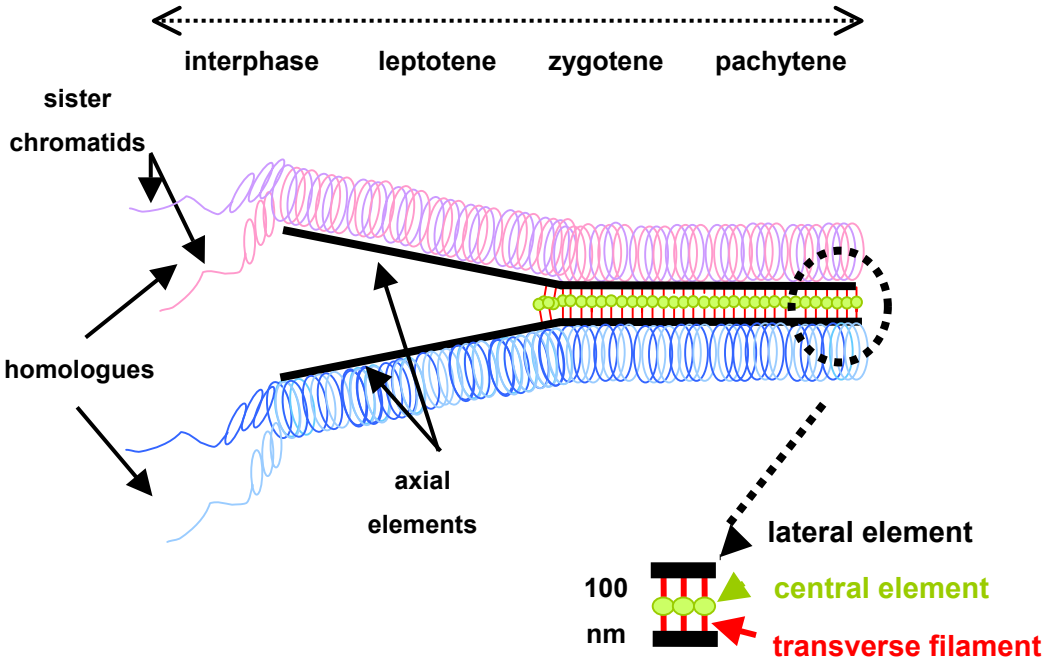

Figure 1.4: Formation of the synaptonemal complex
Homologous chromosomes become associated with axial elements at early leptotene. In *Arabidopsis,* this is the ASY1 protein. During leptotene, homologues become aligned at a distance of 400nm. At late leptotene/early zygotene, synapsis is initiated. In *Arabidopsis* ZYP1 foci can be observed at this point (transverse filament protein), and begins to polymerise until pachytene, where homologues can be seen to be connected along their lengths at a distance of 100nm by the SC. Modified from Alberts et al, (1983).

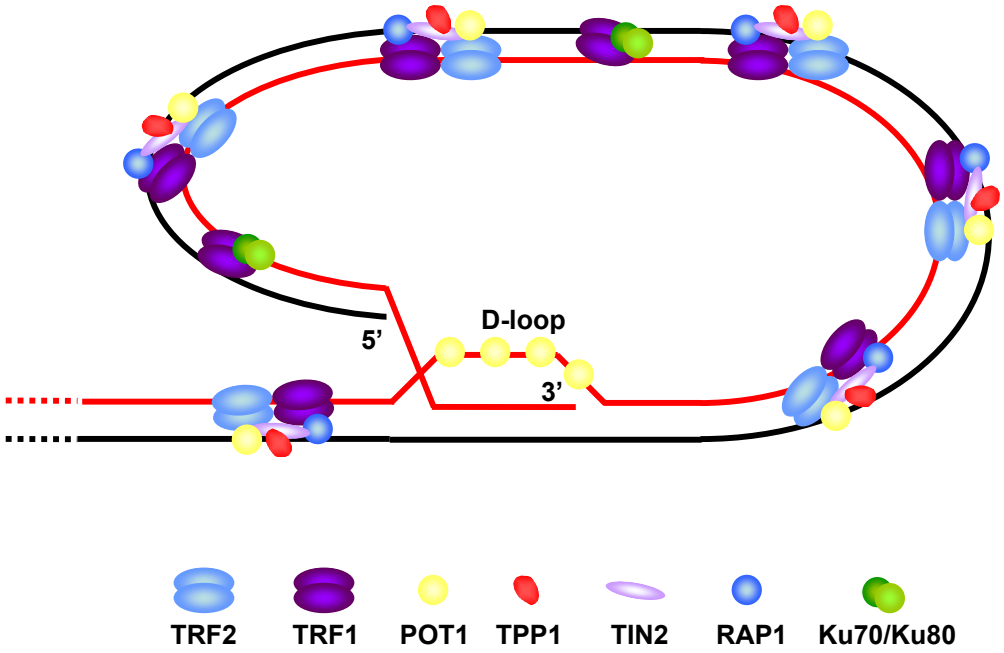

Figure 1.5: Mammalian telomere structure and associated proteins. The diagram shows the telomere in the protected conformation (T-loop). This is formed by invasion of the 3’ G-rich overhang into the adjacent duplex telomeric region, creating a D-loop. This is ss-DNA associated with POT1. Most of the telomeric DNA is bound by the shelterin complex of telomeric proteins.

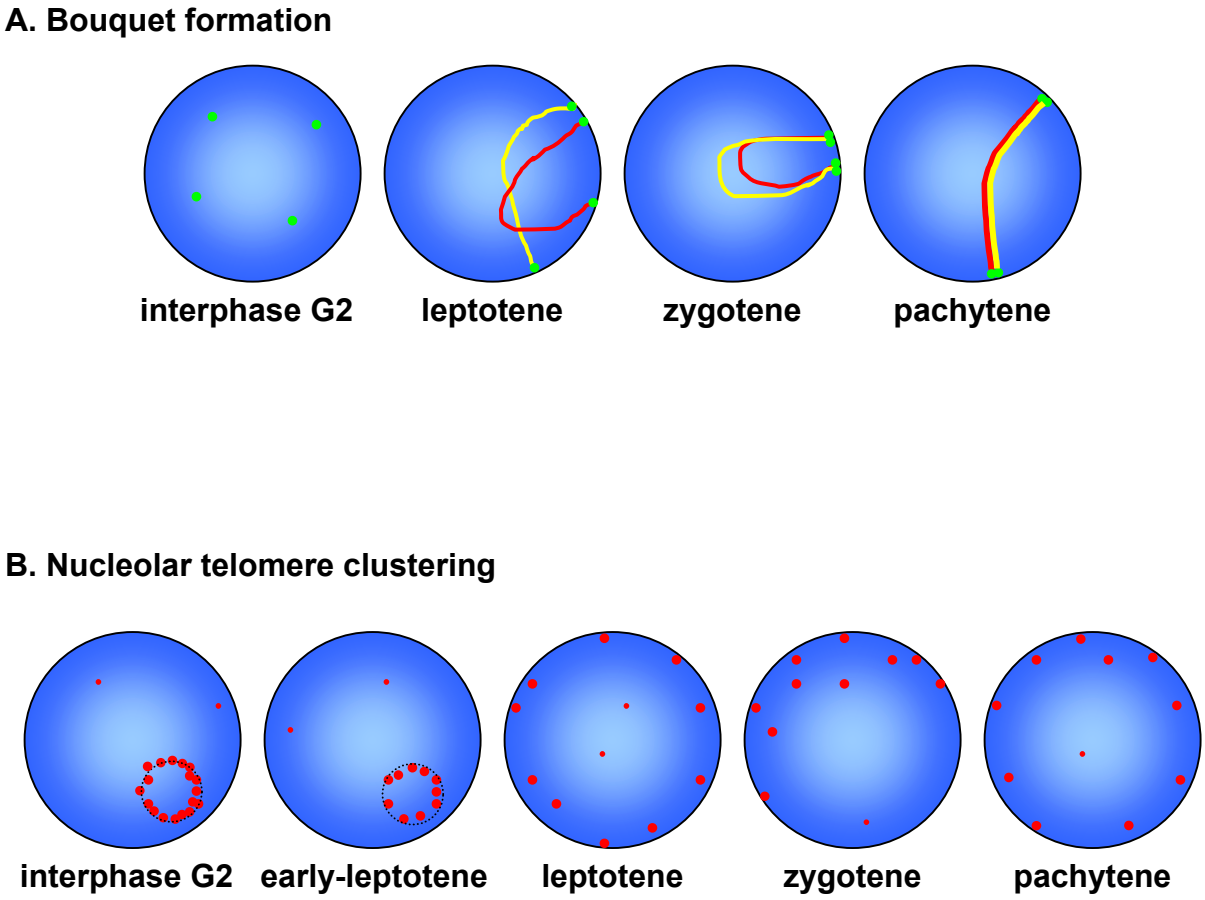

Figure 1.6: Telomere clustering during meiosis

(A) Bouquet formation. One pair of homologues shown for simplicity. At leptotene, telomeres (green) become associated with the nuclear envelope At the leptotene-zygotene transition telomeres move along the membrane and become clustered in the bouquet. At pachytene homologues are synapsed, and telomeres disperse.

(B) Nucleolar clustering. Diagram to represent results of FISH analysis shows localisation of telomeres during each stage of meiotic prophase 1 in *Arabidopsis*. Telomeres cluster around the nucleolus from interphase to the beginning of leptotene. At this point telomeres become homologously paired, prior to the close juxtaposition of homologues. Telomeres become dispersed during leptotene.

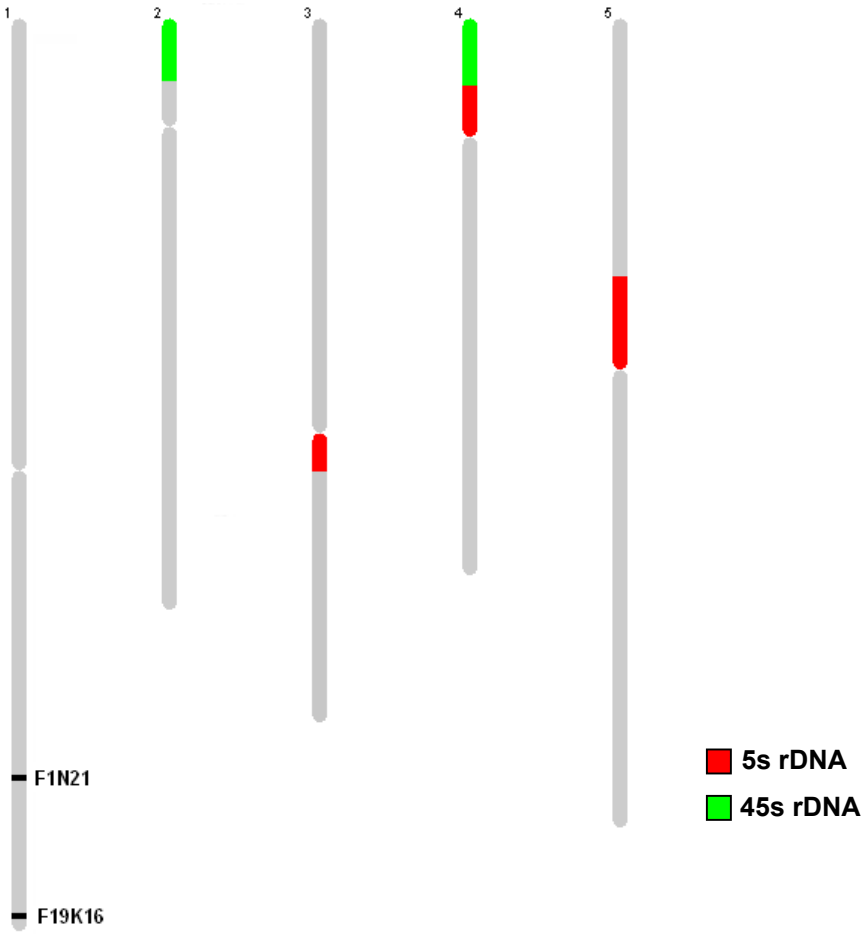

Figure 2.1: Schematic diagram showing a haploid set of *Arabidopsis* chromosomes with positions of probes labelled. Chromosome number labelled above. Black bars indicate locations of BAC probes; green and red bars, 45s and 5s rDNA respectively.

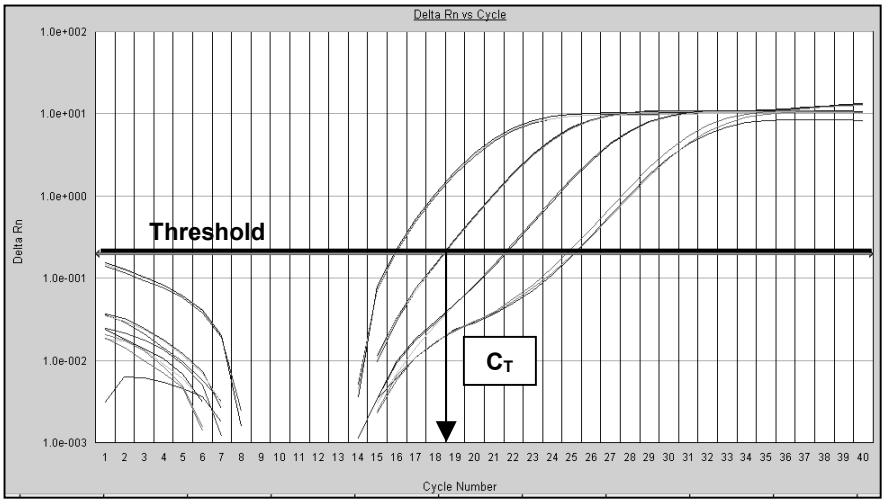

Figure 2.2: Amplification plot showing the threshold. Where the curve crosses the threshold the C_T value is determined (see arrow).

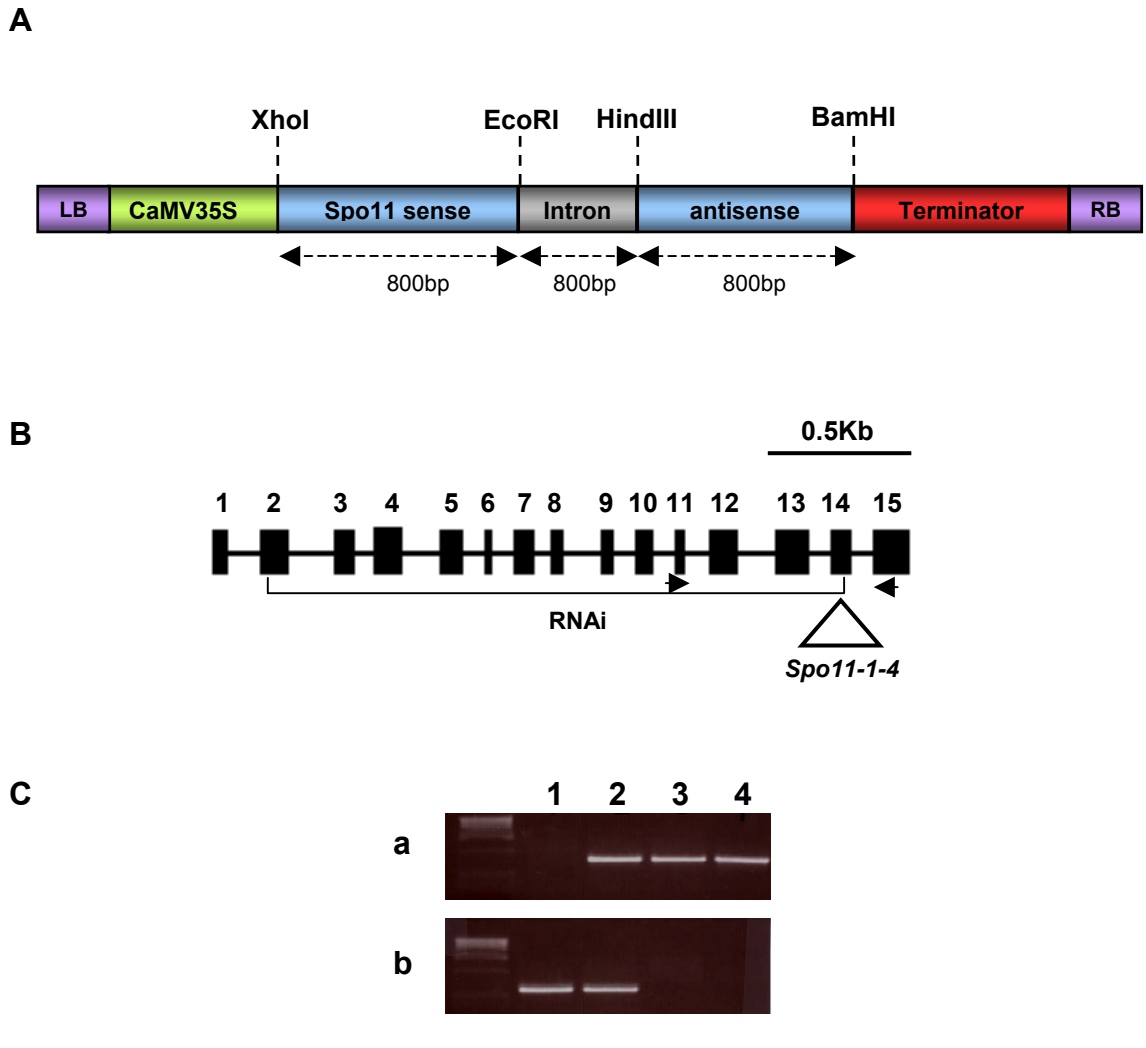

Figure 3.1: (A) *SPO11-1* RNAi construct in pART27. A schematic diagram of the construct is shown. Restriction sites between each section are indicated, together with the sizes of each section. The construct is transcribed with the CaMV35S promoter, which is constitutively expressed. (B) Map of the At3g13170 locus, showing the exon/intron organisation. (Exons shown in bold). The localisation of *spo11-1-4* is indicated by the triangle in exon 14. Locations of the primers used to genotype the plants are shown by the arrows. The RNAi construct spans exons 2-14. (C) Agarose gel analysis of PCR products from genotyping. Lanes 1-4 indicate plants 1-4 respectively. (a) Denotes DNA amplified with WT primers (SPO11EXPR1, SPO11F4). (b) Bands show DNA amplified with insert primer set (SPO11EXPR1, WISCLB). Plant 2 is heterozygous for the insert and plant 1 is homozygous for the insert.

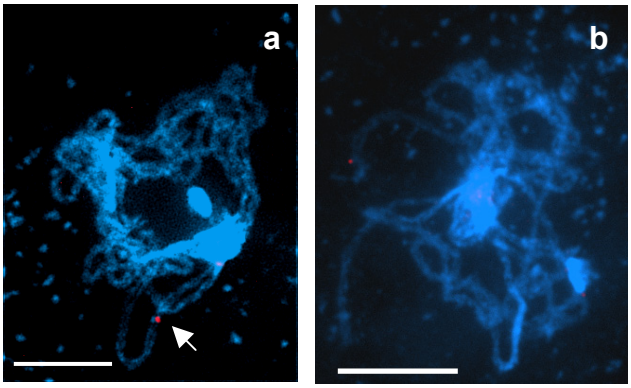

Figure 3.2: Meiotic chromosome spreads of pachytene nuclei, showing number of insertion sites of the construct. Fluorescence *in situ* hybridisation (FISH) with a probe designed against the construct; detected by a secondary fluorescent probe of DIG Rhodamine (labelled red). (a) *SPO11-1* RNAi line 16C, shows 1 heterozygous insert present. (b) Wild-type Col-0 control showing no insert present. Counterstained with DAPI (blue) to visualise chromatin. Bars 10µm.

Figure 3.3: ***Arabidopsis*** **plants showing reduced silique lengths in the T_2** ***SPO11-1*** **RNAi lines. (a) Whole plant images; far left shows** ***SPO11-1-4*** **null plant; far right wild type Col-0; plants between show** ***SPO11-1*** **RNAi plants with a range of silique lengths. Bar 3cm. A close up view of silique lengths. (e.g. of silique shown by the red bars) (b)** ***spo11-1-4*** **null (c) Wild type (Col-0). Bar 1cm.**

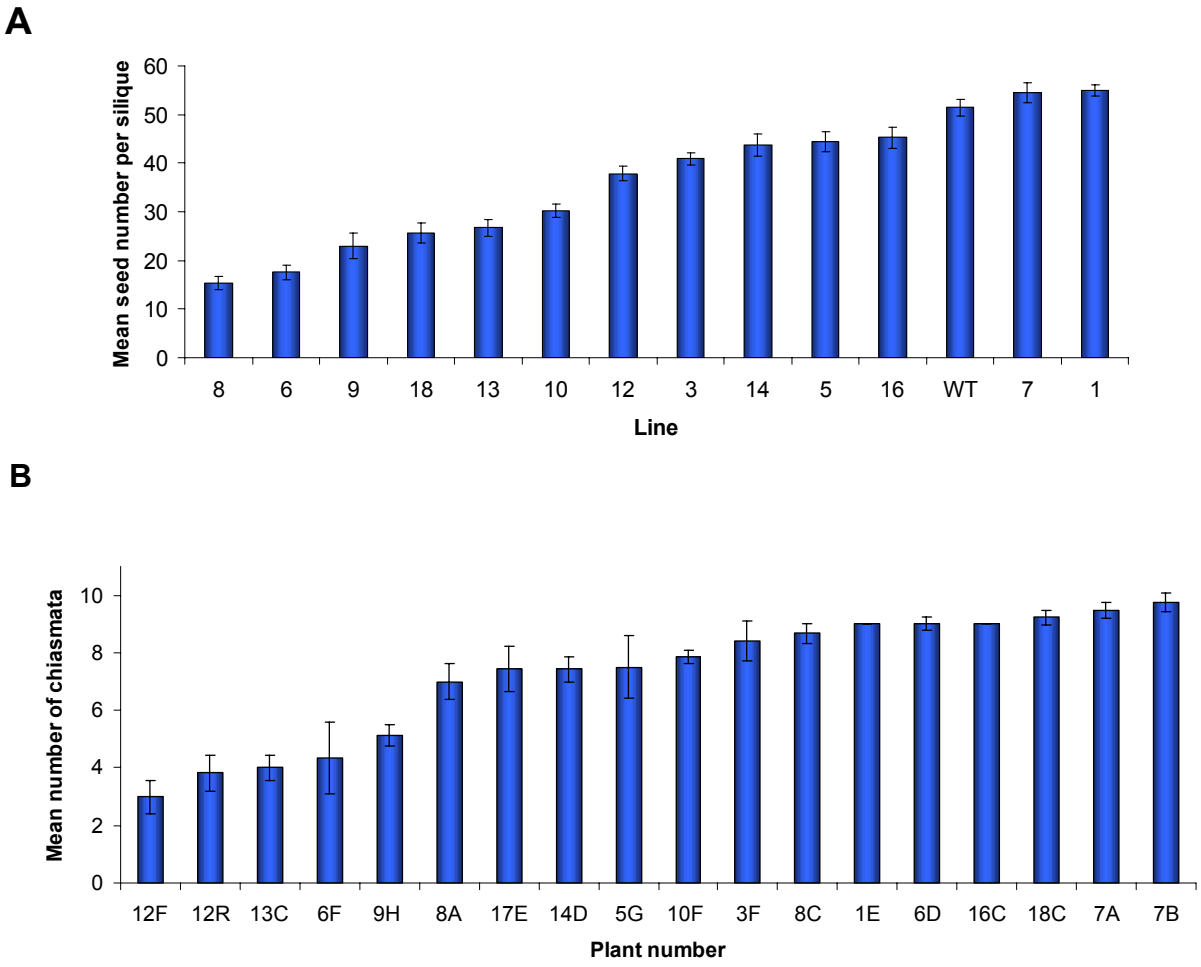

Figure 3.4: Preliminary analysis of *SPO11-1* RNAi lines

(A) Mean number of seeds per silique for each line studied. This data supports the differences observed in silique length from the images. Standard error bars shown. (B) Mean number of chiasmata at metaphase I for individual plants. *SPO11-1* RNAi lines show a range in the mean number of chiasmata, varying from wild-type levels (9-12 chiasmata) to approximately 30% of wild-type. (WT) wild-type. Standard error bars shown.

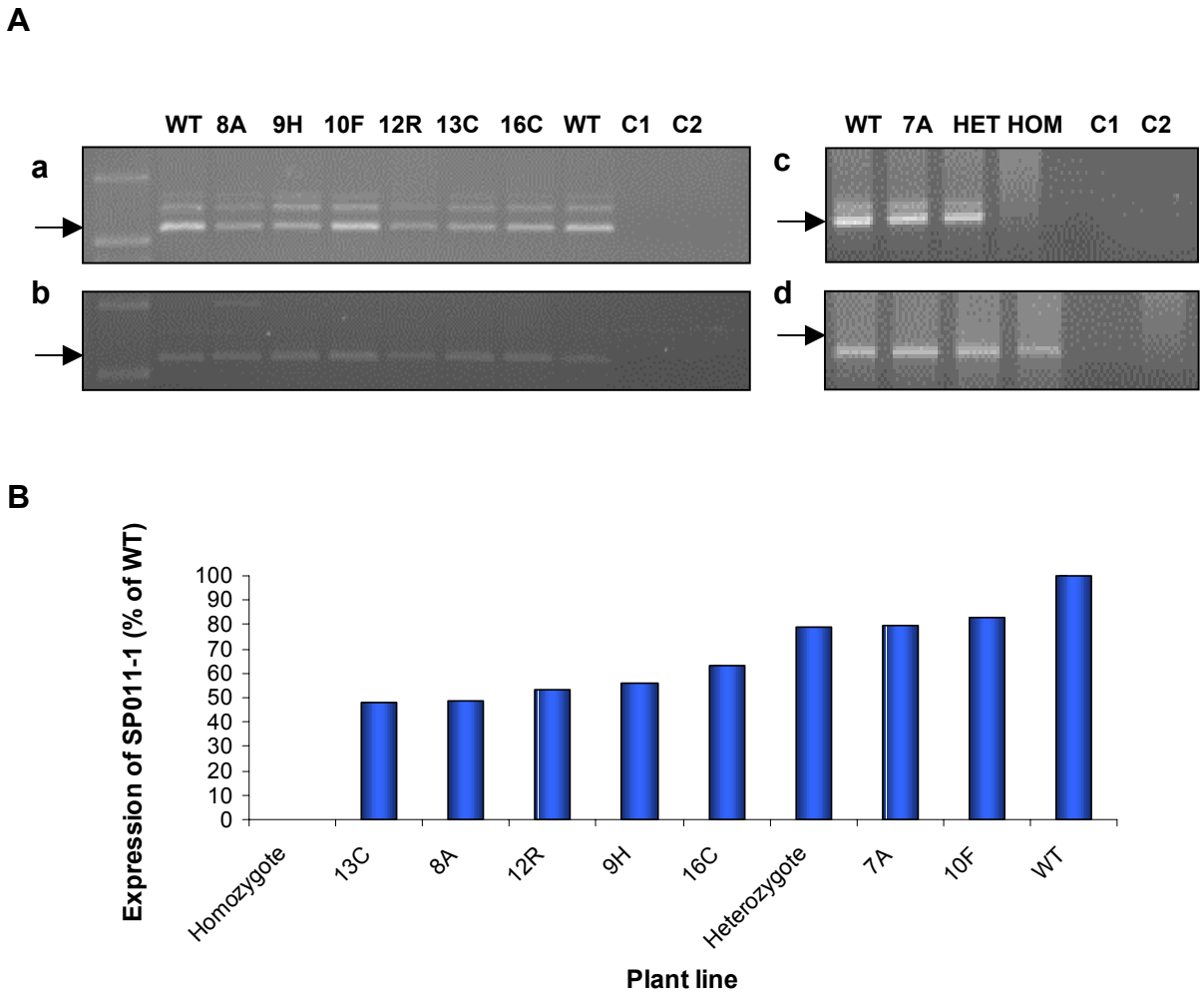

Figure 3.5: Analysis of *SPO11-1* expression levels by reverse transcription PCR. (A) Agarose gel analysis of PCR products. (b and d) Show the control gene expression of *SPO11-2*, with equal amounts of expression in all samples (amplified with *SPO11-2* specific primers). (a and c) Illustrate the different levels of *SPO11-1* expression, by amplification with *SPO11-1* specific primers. All gene specific bands run at the predicted size of ~600bp (see arrows). A second band is amplified by the *SPO11-1* gene specific primers (shown at ~800bp), which has been shown to be a splice variant. (WT) wild type Col-0. (C1) control 1 primers and water. (C2) control 2 WT cDNA with no primers. (HET) heterozygous *spo11-1-4*. (HOM) homozygous *spo11-1-4*. (B) Summary of *SPO11-1* expression levels as a percentage of wild-type. Each line is labelled on the x axis (1 plant selected for expression analysis). Values measured as the peak band intensity for each sample, normalised using the control *SPO11-2* values.

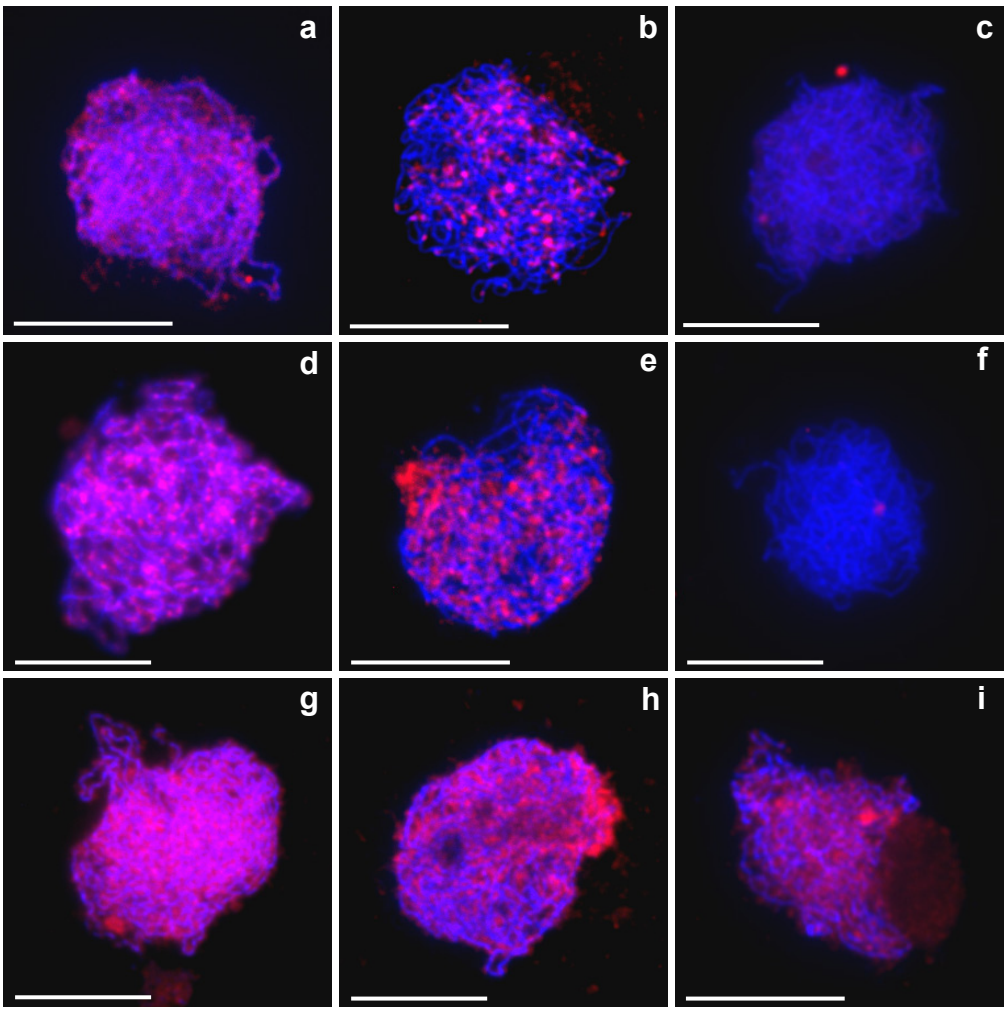

Figure 3.6: Quantifying DSBs by immunolocalisation. Meiotic chromosome spreads of zygotene nuclei. (a-c) Dual immunolocalisation of γH2AX (labelled red) and ASY1 protein (blue), on (a) wild-type Col-0, (b) *SPO11-1* RNAi line 8A, and (c) *spo11-1-4* null. (d-f) Dual immunolocalisation of RAD51 protein (red) and ASY1 protein (blue) on, (d) wild-type Col-0, (e) SPO11-1 RNAi line 12R, and (f) *spo11-1-4* null. (g-i) Dual immunolocalisation of DMC1 protein (red) and ASY1 protein (blue) on, (g) wild-type Col-0, (h) SPO11-1 RNAi line 8A, (i) *spo11-1-4* null. Bar 10µm.

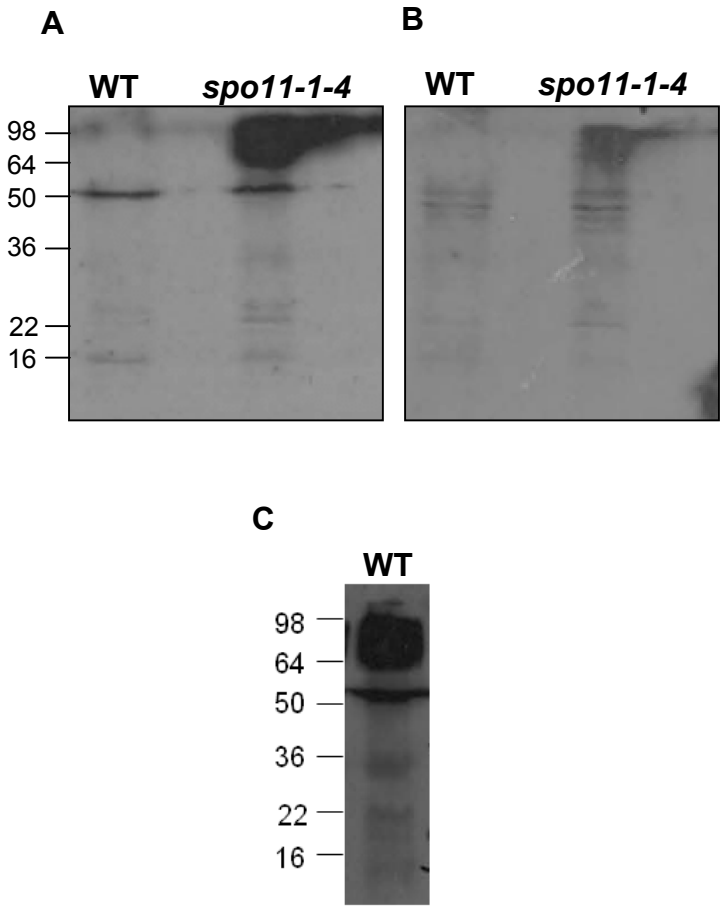

Figure 3.7: Quantifying DSBs using western blotting on bud protein extracts. (A) Blot labelled with anti- γH2AX (rabbit) primary antibody (1:1000 milk block), and anti-rabbit HRP secondary antibody (1:10000 milk block). (B) Blot labelled with anti-SPO11-1 (rabbit) primary antibody (1:50 milk block) and detected with anti-rabbit HRP secondary antibody (1:10000 milk block). (C) Protein extract from cisplatin treated plants. Blot labelled with anti- γH2AX (rabbit) primary antibody (1:1000 milk block), and anti-rabbit HRP secondary antibody (1:10000 milk block). Samples loaded labelled above each lane, with 40µl of protein extracts loaded in each lane. Proteins were run together with a molecular weight marker (KDa).

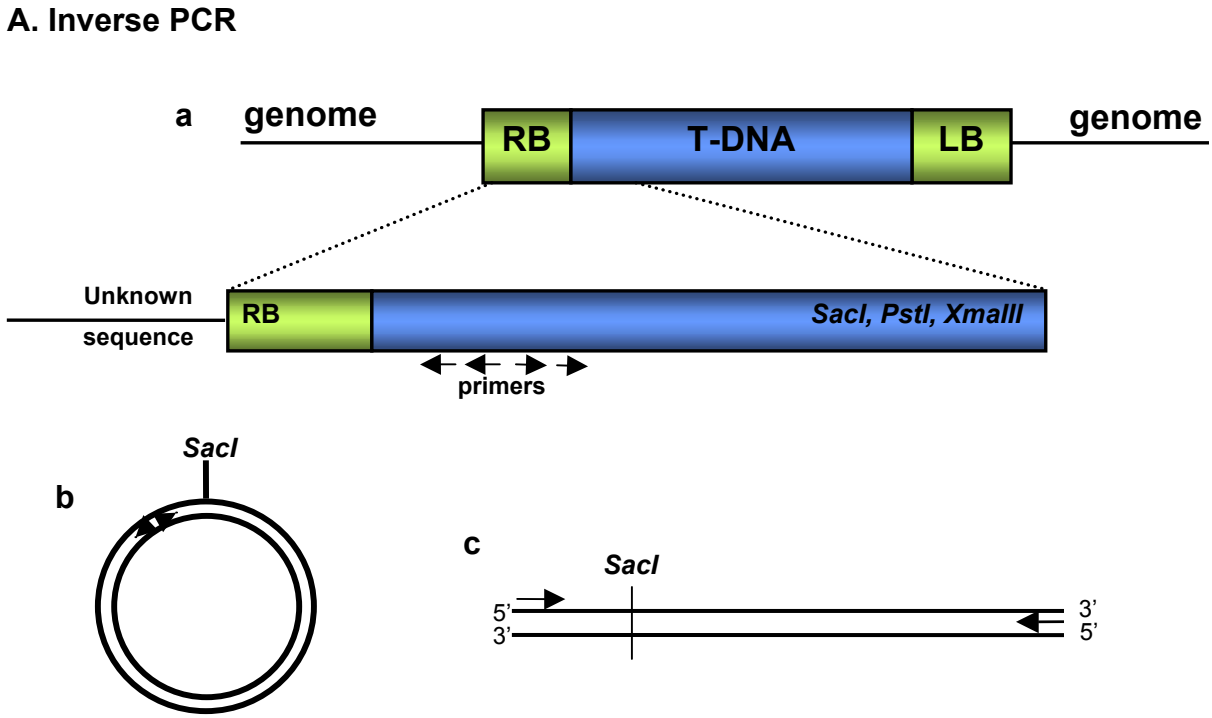

Figure 3.8: Locating sites of T-DNA insertions. (A) Inverse PCR; primers are designed in a region of known sequence. Extracted gDNA is digested with restriction enzymes present adjacent to the primers (a). The fragments are permitted to self ligate to form circularised DNA (b) on which PCR is performed with nested primers (c). (B) TAIL PCR; PCR is performed on extracted genomic DNA using primers designed in a region of known sequence in the T-DNA insert, and degenerate adapter primers, which bind to unknown sequences. Nested primers are then used to produce a specific product.

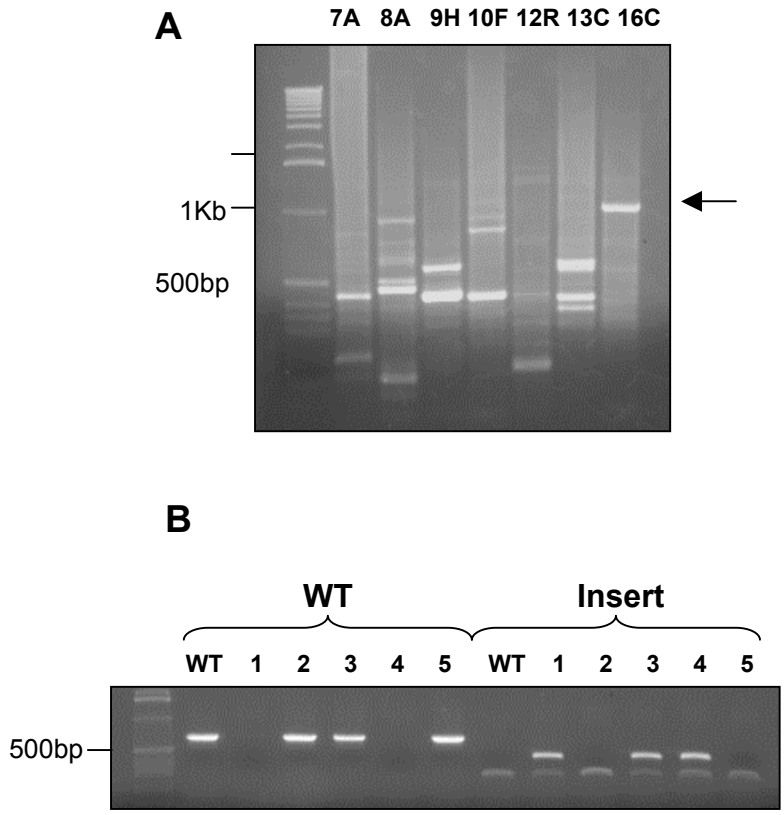

Figure 3.9: Inverse PCR. (A) Products from inverse PCR with gDNA from the *SPO11-1* RNAi lines, digested with *SacI.* (B) Genotyping of line 16C. Agarose gel analysis of PCR products amplified with (WT) wild-type primers spanning the insertion site and (Insert) the RB vector primer together with the reverse WT primer to show the presence of an insert. Products were run alongside the 1Kb DNA ladder.

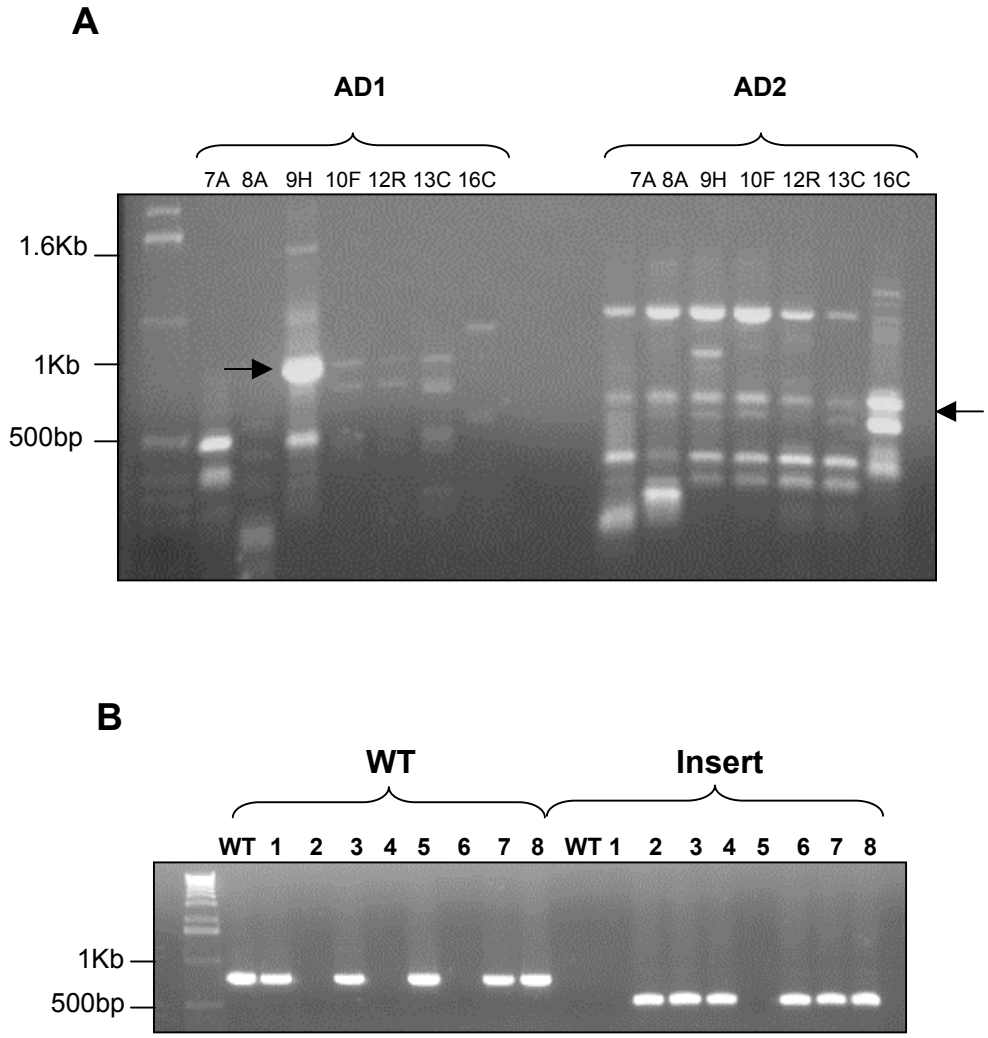

Figure 3.10: TAIL PCR. (A) Products from the TAIL PCR using gDNA from the *SPO11-1* RNAi lines. (AD1) Adapter primer 1. (AD2) Adapter primer 2. The plant line the reaction was carried out on is indicated above each lane. Bands that were cut out for gel extraction are indicated by arrows. (B) Genotyping of line 9H. (WT) Reaction with wild type primers spanning the insertion site. (Insert) Reaction with RB construct primer shows presence of an insert. Numbers correspond to plant number or wild type (WT). Products were run alongside the 1Kb DNA ladder.

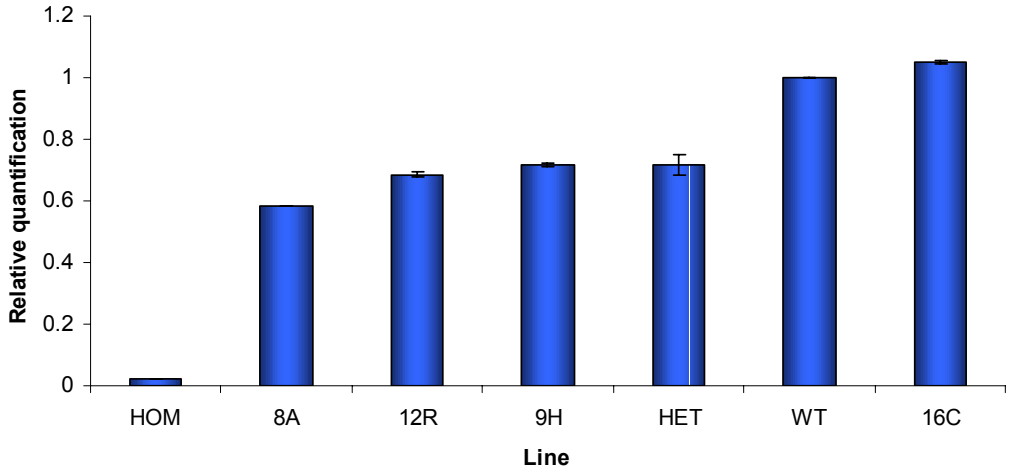

Figure 3.11: Relative quantification of *SPO11-1* using real-time PCR. Mean values from two independent relative quantification studies performed on RNA extracted from plants grown at different times. Standard error bars shown.

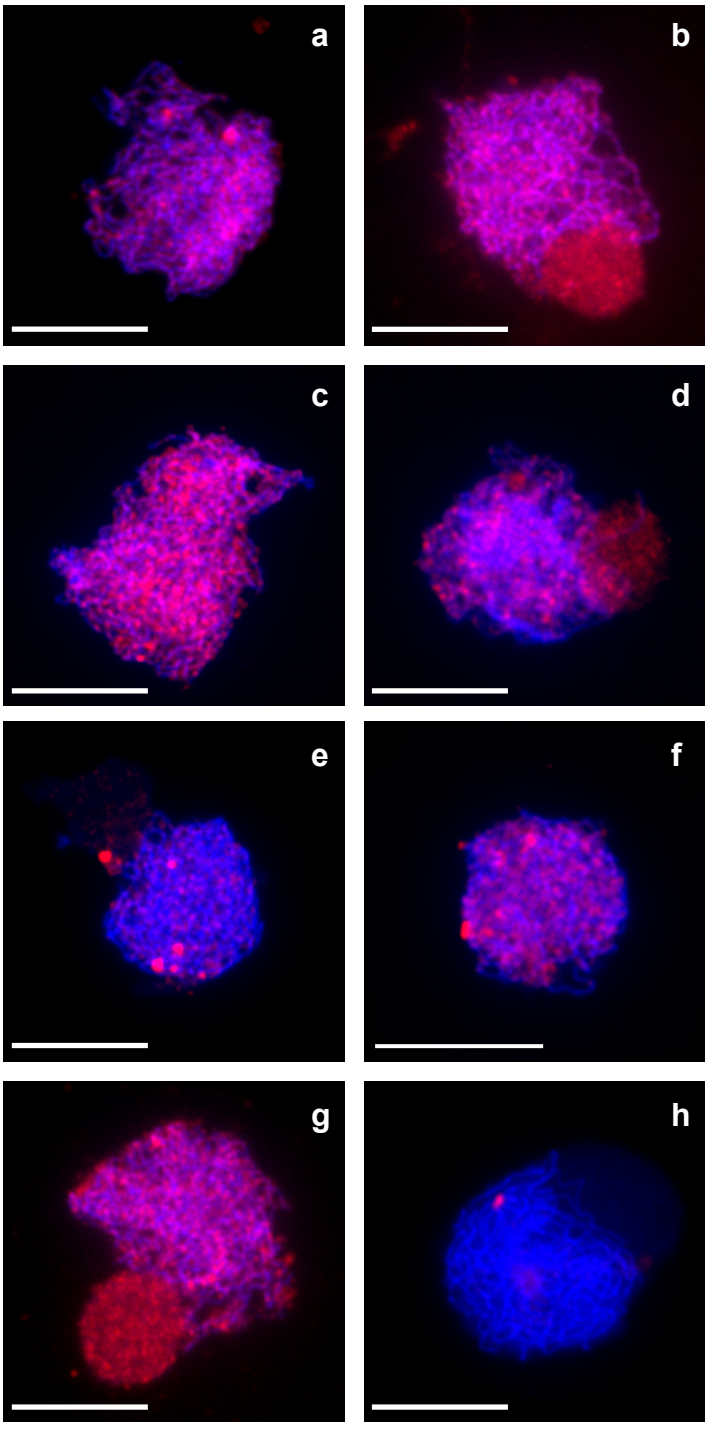

Figure 3.12: Quantifying DSBs by immunolocalisation. Dual immunolocalisation of γH2AX (shown red) and ASY1 protein (shown blue) on meiotic chromosome spreads of zygotene nuclei. (a) wild-type Col-0. (b) *spo11-1-4* heterozygote. (c) SPO11-1 RNAi 7A (d) 8A. (e) 9H. (f) 12R. (g) 16C. (h) *spo11-1-4* homozygote. Bars 10µm.

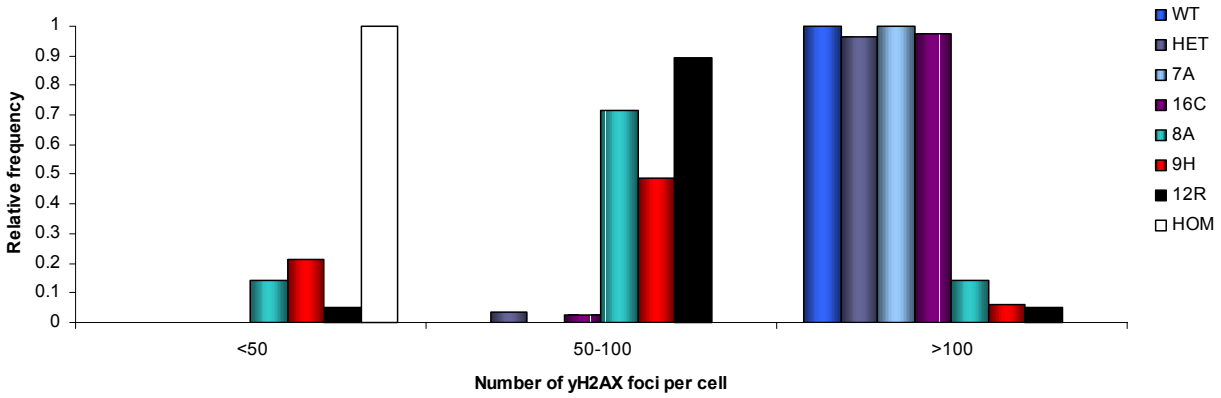

Figure 3.13: Number of γH2AX foci per cell. The relative frequency of cells with either <50, 50-100, or >100 γH2AX foci is shown. Lines (WT) wild-type Col-0, (HET) *spo11-1-4* heterozygote, (HOM) *spo11-1-4* homozygote, (7A, 8A, 9H, 12R, 16C) SPO11-1 RNAi lines.

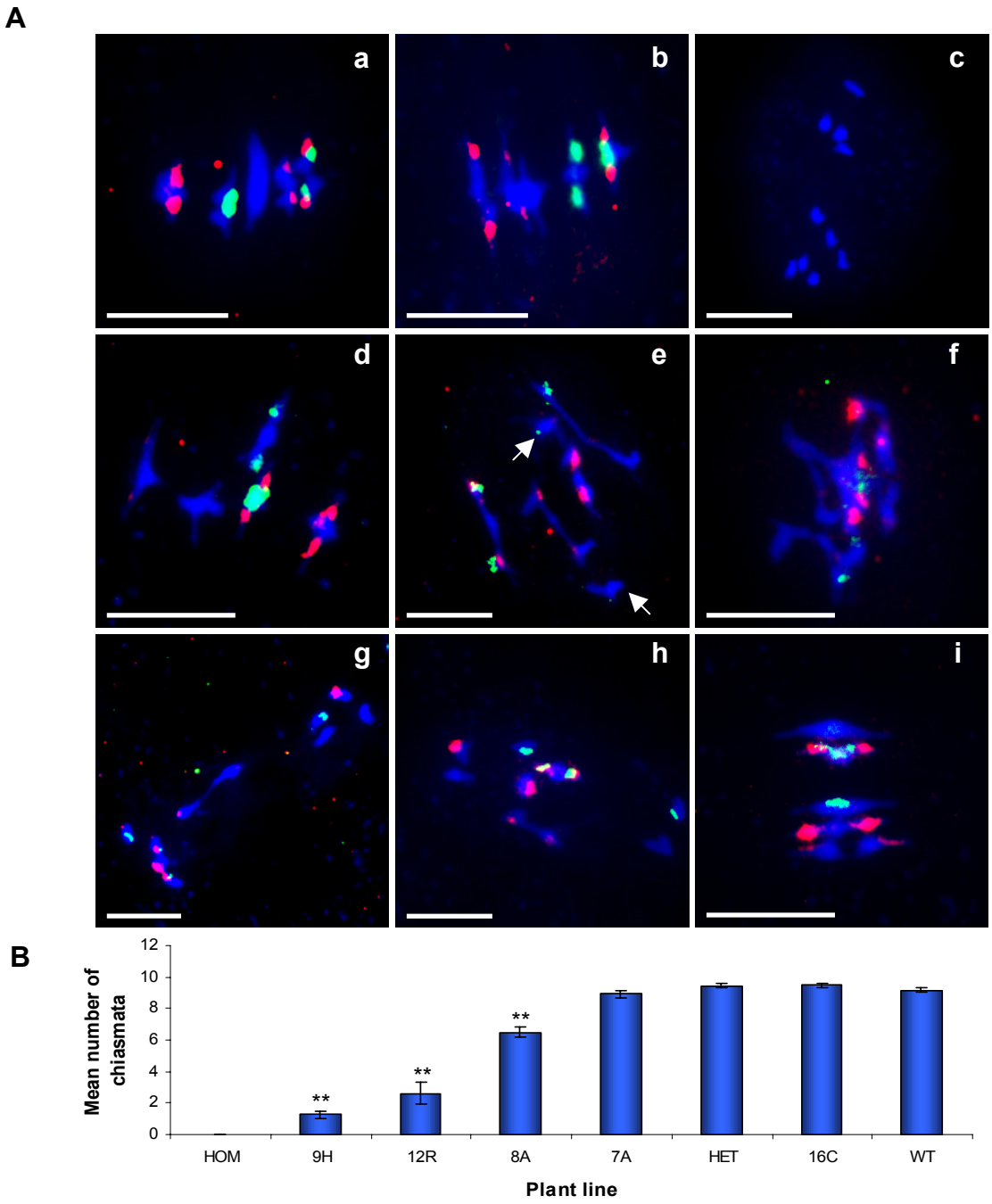

Figure 3.14: Frequency of chiasmata for the *SPO11-1* RNAi lines. (a-i) Fluorescence *in situ* hybridisation of metaphase I nuclei with probes to 45s (green) and 5s (red) rDNA, labelled with DIG-FITC, and BIOTIN-Cy3 respectively. (a) Wild-type Col-0. (b) *spo11-1-4* heterozygote. (c) *spo11-1-4* homozygote. (d) 7A. (e) 8A. (f) 8A showing multivalent formation. (g) 9H. (h) 12R. (i) 16C. Bars 10µm. Chromosomes are counterstained with DAPI (blue). (B) Mean number of chiasmata for each plant line. 8A $t_{(64)}$ = 28.18, 12R $t_{(47)}$ =7.01, 9H $t_{(19)}$ =8.89.(WT) wild-type Col-0, (HET) *spo11-1-4* heterozygote (HOM) *spo11-1-4* homozygote. Significance in paired *t*-test ** (p= <0.01). Standard error bars shown.

A. Wild-type

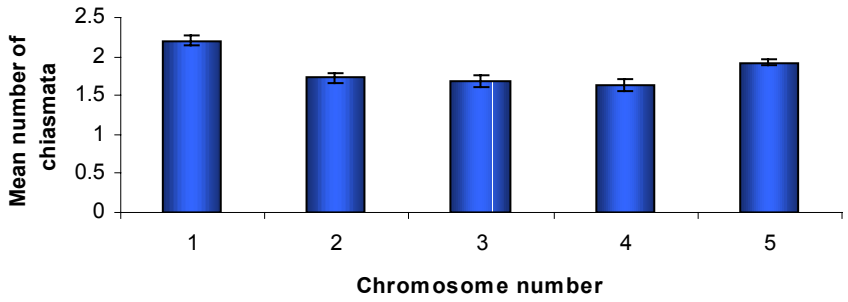

B. *spo11-1-4* Heterozygote

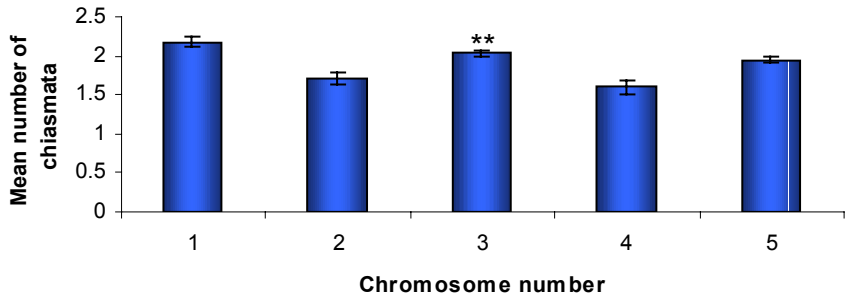

C. 16C

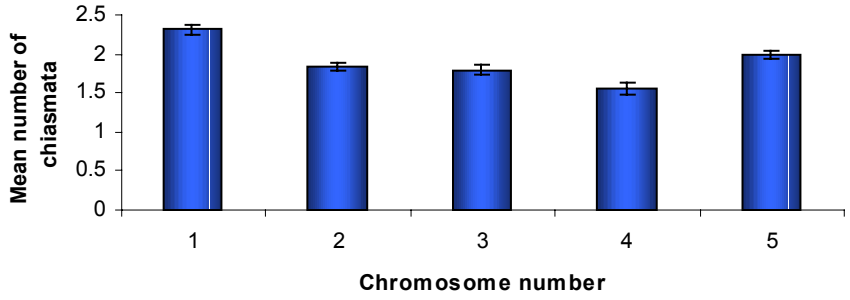

D. 7A

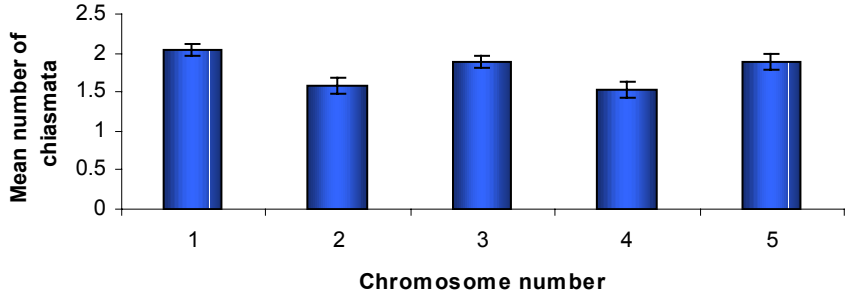

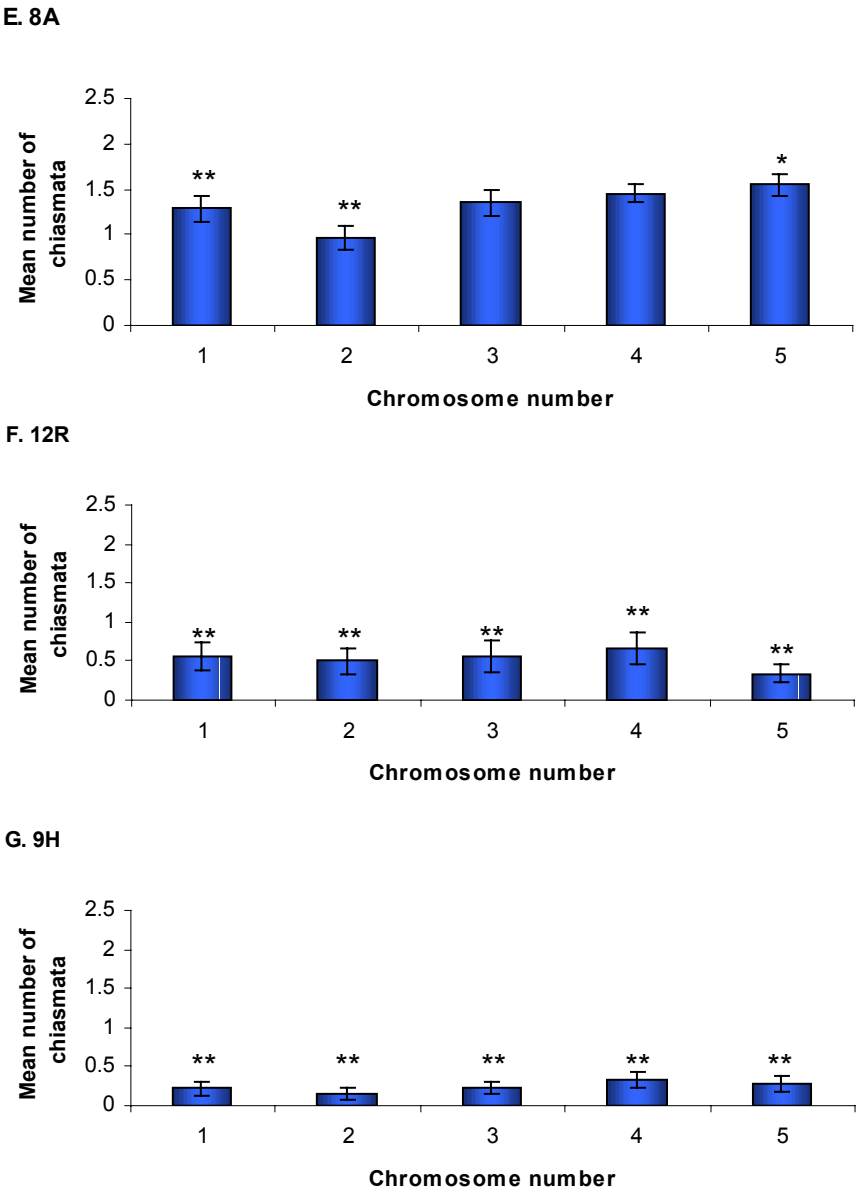

Figure 3.15: Mean number of chiasmata for individual chromosomes of each line. Standard error bars shown. (A) wild-type, (B) *spo11-1-4* heterozygote, (C) 16C, (D) 7A, (E) 8A, (F) 12R, (G) 9H. Paired *t*-test significance p <0.01 (**), p <0.05 (*).

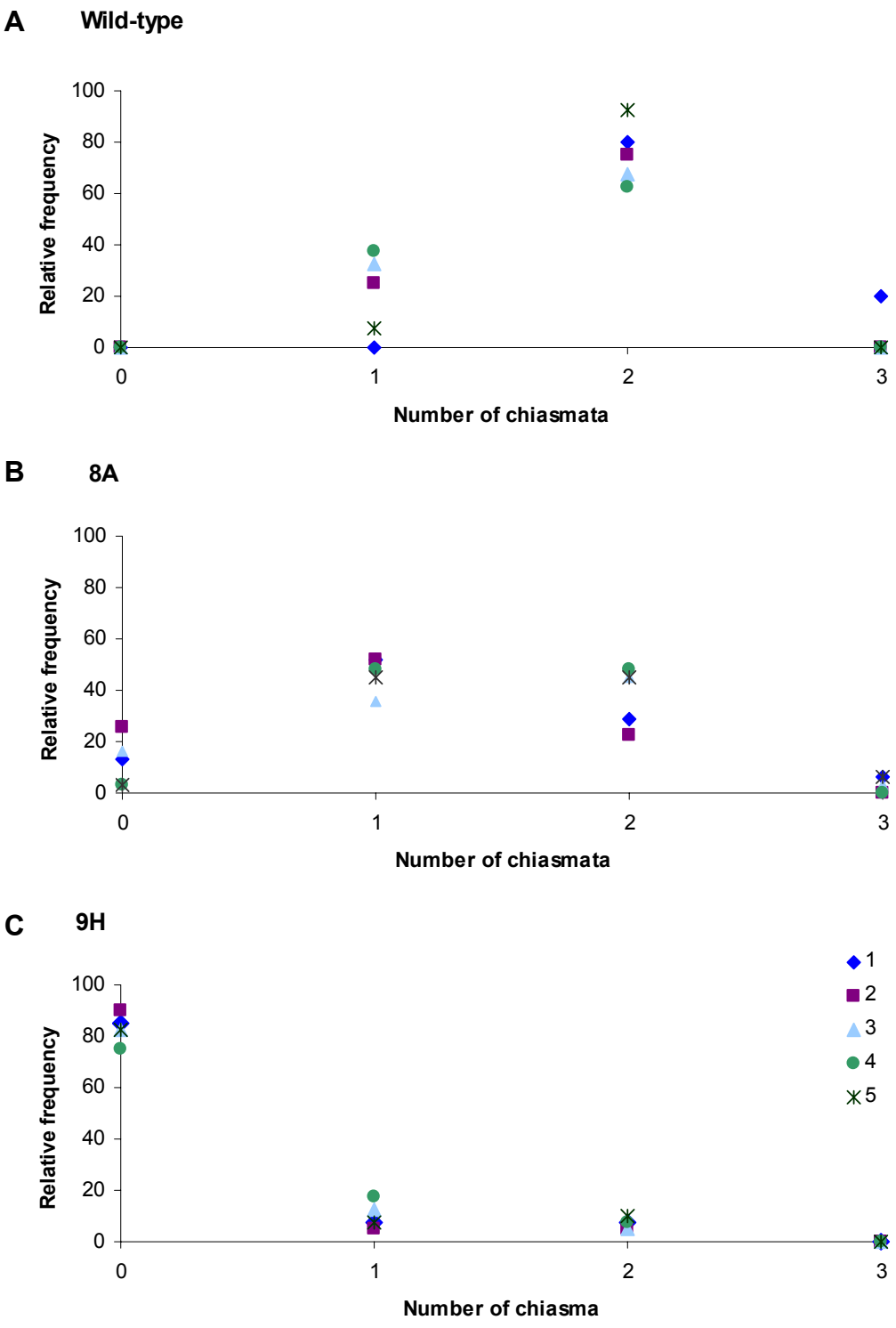

Figure 3.16: Frequency distribution of chiasmata for each individual chromosome. For wild-type (A), and *SPO11-1* RNAi lines 8A (B), and 9H (C). Individual chromosomes are labelled as indicated in the legends to the right.

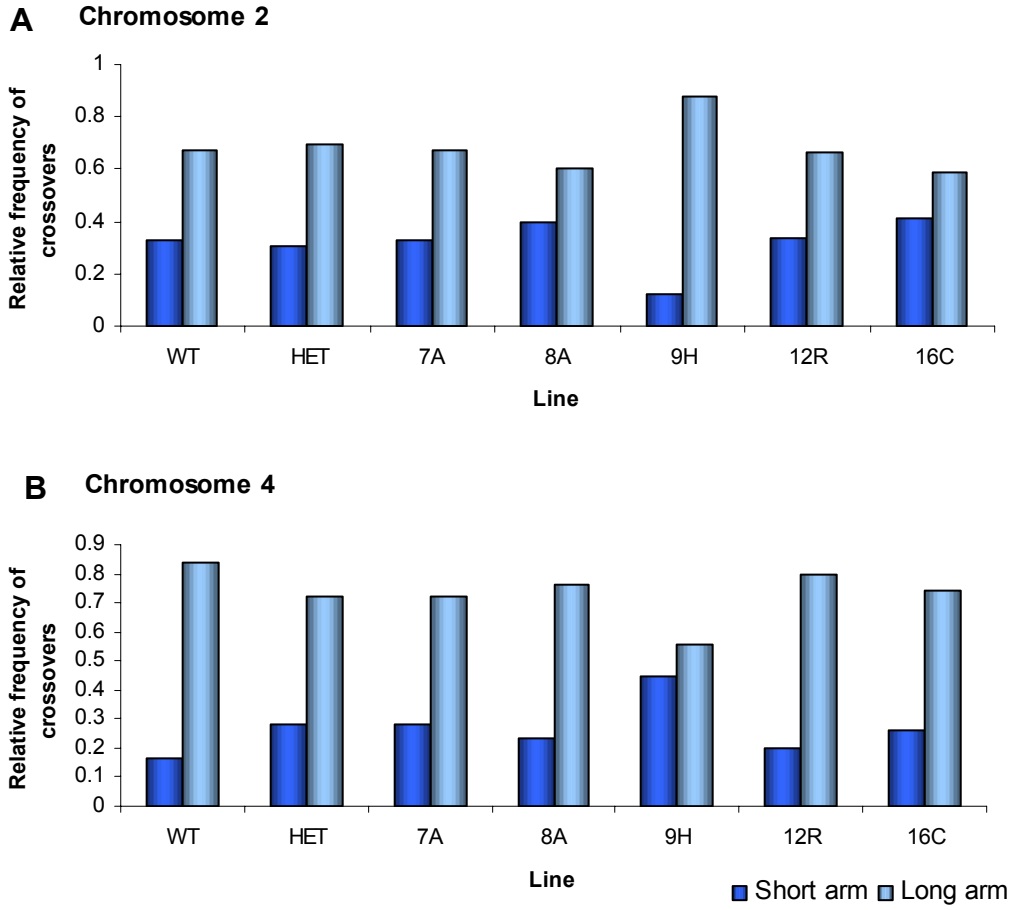

Figure 3.17: Relative frequency of chiasmata on the short and long arms of chromosomes 2 (A) and 4 (B).

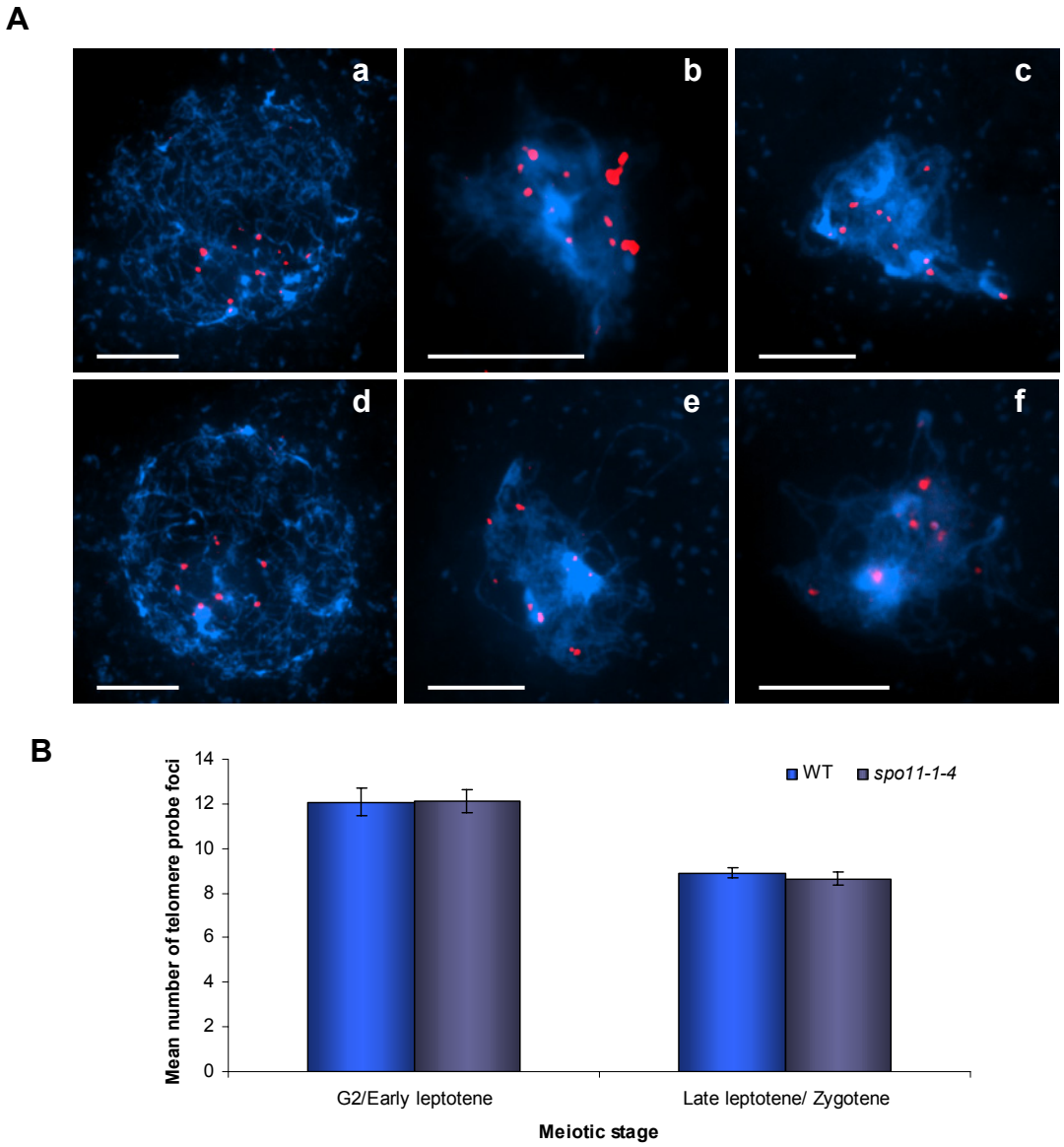

Figure 3.18: Pairing of telomeres in the T-DNA insertion line *spo11-1-4*.

(a-f) Fluorescence *in situ* hybridisation of meiotic prophase I nuclei of wild-type (a-c), and *spo11-1-4* (d-f), with a probe that labels the telomeric repeat sequence. (a,d) leptotene. (b,e and f) zygotene. (c) pachytene. In all of the images, approximately 10 foci of the probe can be seen, which indicates that telomeres are paired in both wild-type and *spo11-1-4*. Bars 10µm. (g) Mean numbers of telomere foci per cell. No significant difference can be seen between the wild-type and *spo11-1-4*. Standard error bars shown.

A

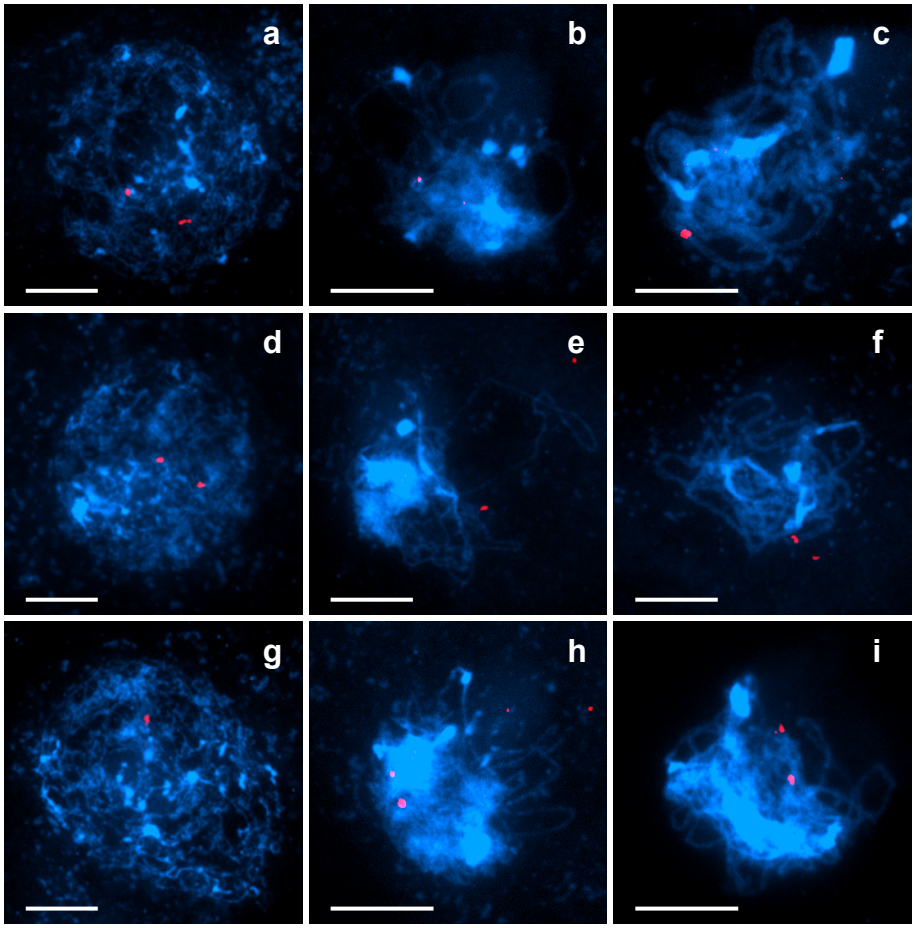

B

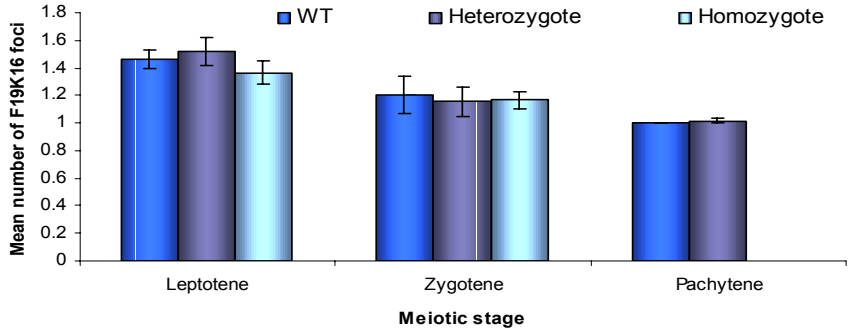

Figure 3.19: Pairing of homologous telomeres in the T-DNA insertion line *spo11-1-4*.
(A) Fluorescence *in situ* hybridisation of BAC F19K16 (labelled DIG-rhodamine, red) to chromosome 1 on meiotic prophase I nuclei of wild-type (a-c), *spo11-1-4* heterozygote (d-f), and *spo11-1-4* homozygote (g-i). (a,d,g) leptotene. (b,e,h,i) zygotene. (c,f) pachytene. 1 focus represents paired telomeres, and 2 foci represent unpaired telomeres. Counterstained with DAPI. Bars 10µm. (B) Mean number of F19K16 foci per cell. No significant difference can be seen between the lines, showing that telomere pairing is homologous in the *spo11-1-4* line.

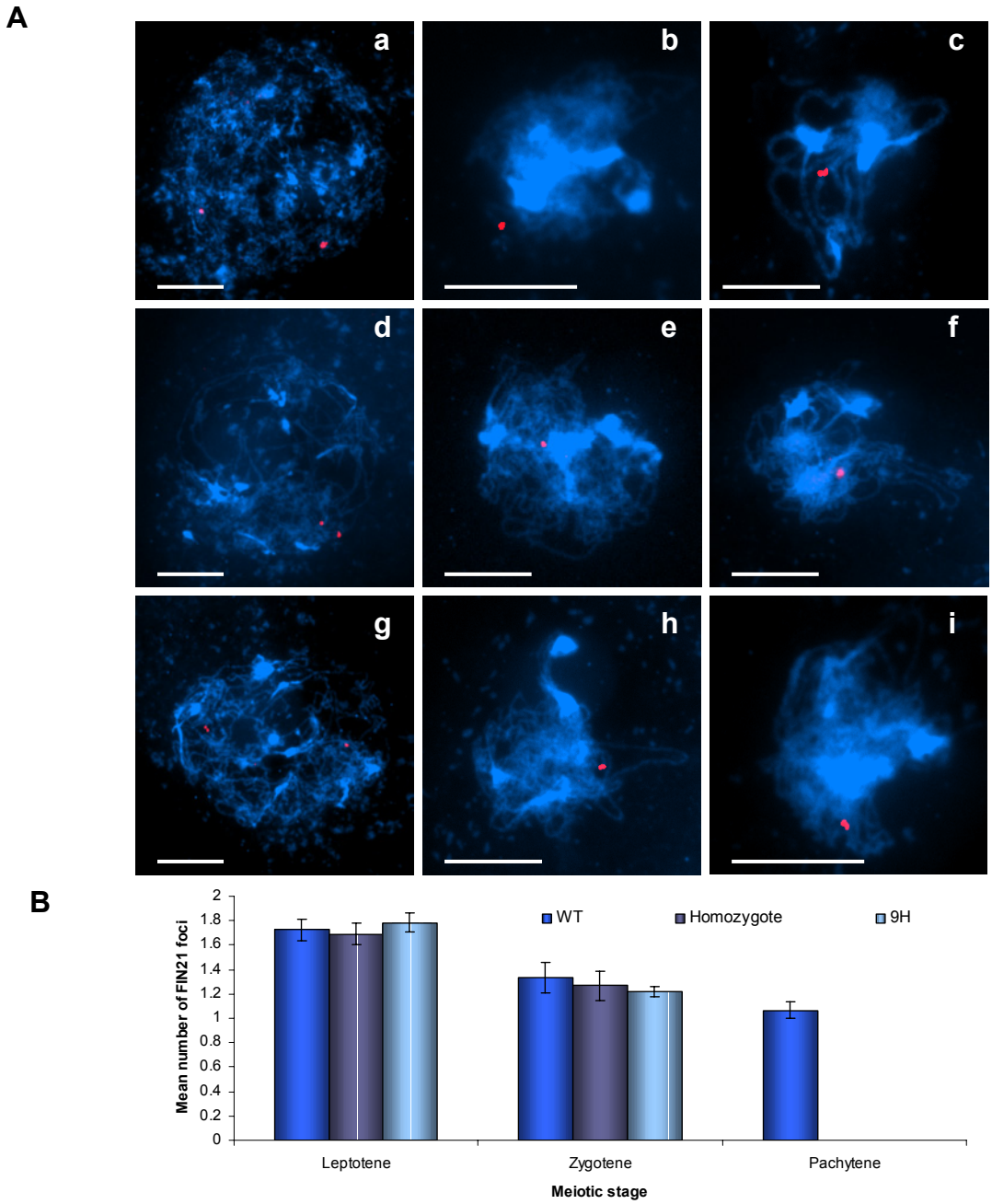

Figure 3.20: Pairing of sub-telomeric regions of *spo11-1-4* and SPO11-1 RNAi line 9H. (A) Fluorescence *in situ* hybridisation of BAC F1N21 (labelled DIG-rhodamine, red) to chromosome 1 on meiotic prophase I nuclei of, (a-c) wild-type, (d-f) *SPO11-1* RNAi 9H, (g-i) *spo11-1-4* homozygote. (a,d,g) leptotene. (b,e,f,h,i) zygotene. (c) pachytene. 1 focus represents paired BACs, and 2 foci represent unpaired BACs. Counterstained with DAPI. Bars 10µm. (B) Mean number of FIN21 foci per cell. No significant difference in the mean number of foci can be observed between lines, showing that sub-telomeric regions are paired in *spo11-1-4* and 9H.

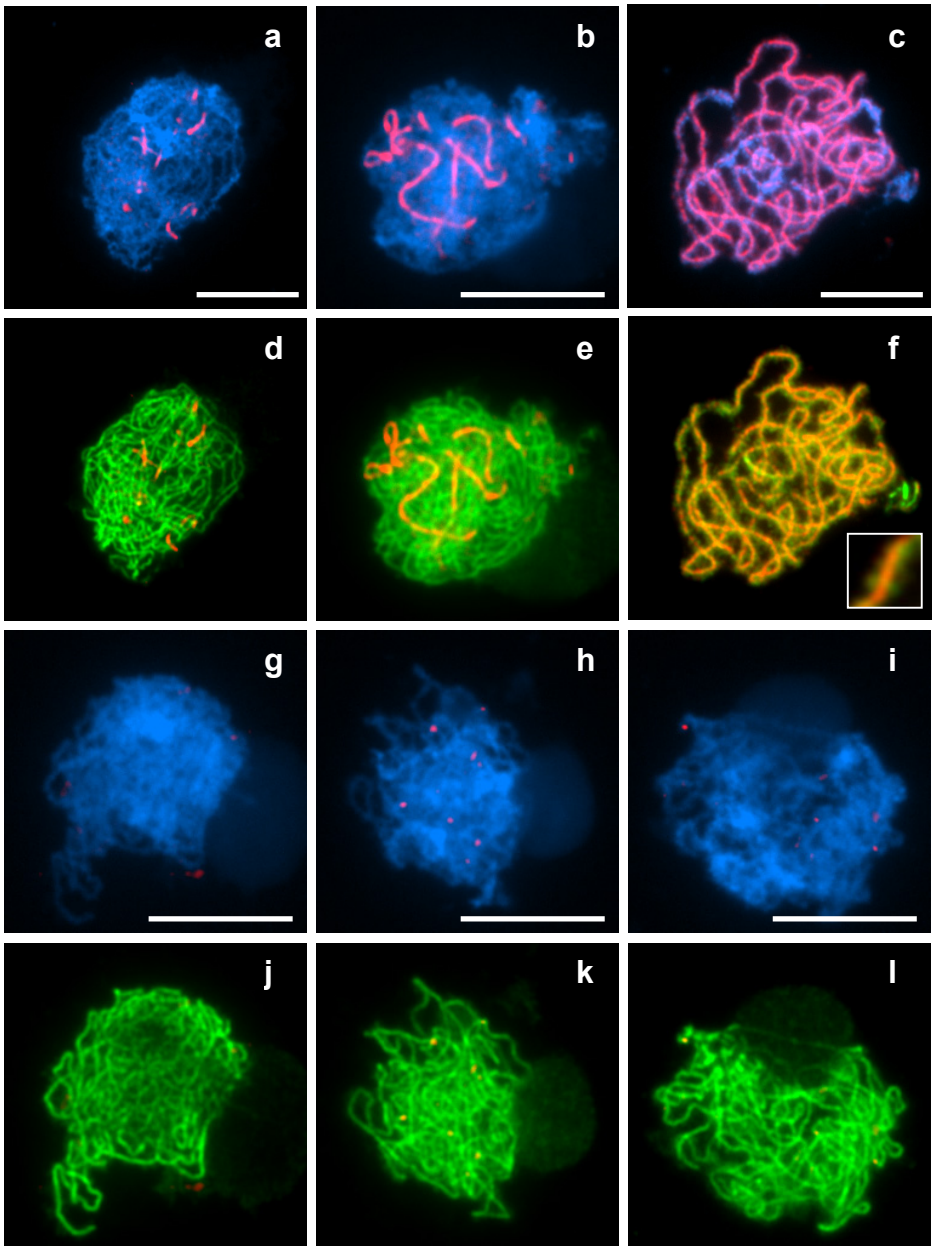

Figure 3.21A: Dual immunolocalisation of ZYP1 protein (red) and ASY1 protein (green) on *SPO11-1* lines. (a-f) wild-type. (a,d) early zygotene, (b,e) mid-zygotene (c,f) pachytene, showing progressive synapsis of ZYP1. (g-l) *spo11-1-4* mid-late zygotene nuclei showing no localisation of ZYP1, but ASY1 appears as in wild-type. Chromosomes counterstained with DAPI (blue). Bars 10µm.

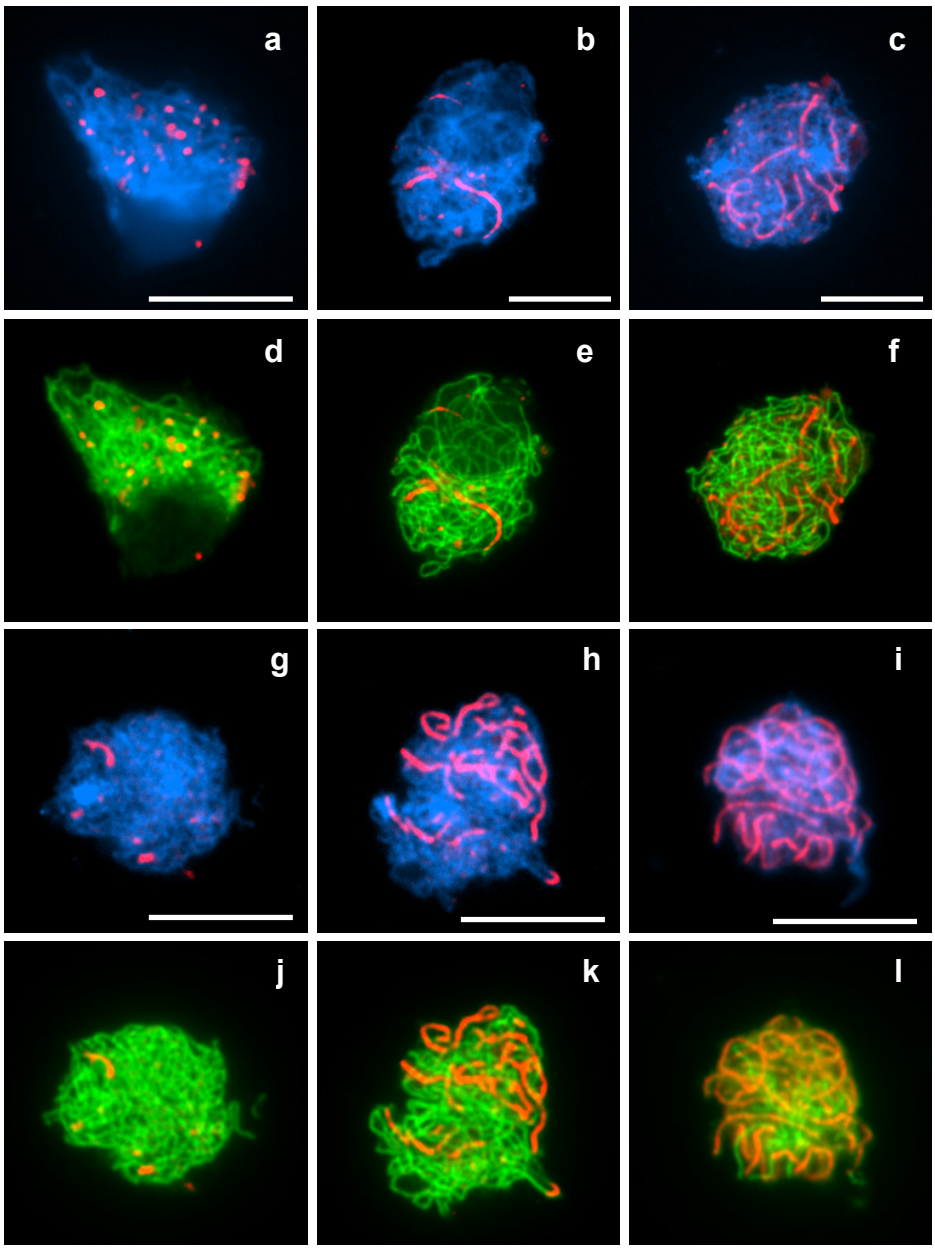

Figure 3.21B: Dual immunolocalisation of ZYP1 protein (red) and ASY1 protein (green) on meiotic prophase I spread nuclei of the *SPO11-1* lines. (a-f) *SPO11-1* RNAi line 9H. (a,d) early zygotene. (b,e) mid-zygotene. (c,f) late-zygotene/pachytene (g-l) *SPO11-1* RNAi line 8A. (g,j) early zygotene. (h,k) mid-zygotene. (i,l) late-zygotene. Polymerisation of ZYPI protein does not appear to be completed in the RNAi lines. Chromosomes counterstained with DAPI (blue). Bars 10µm.

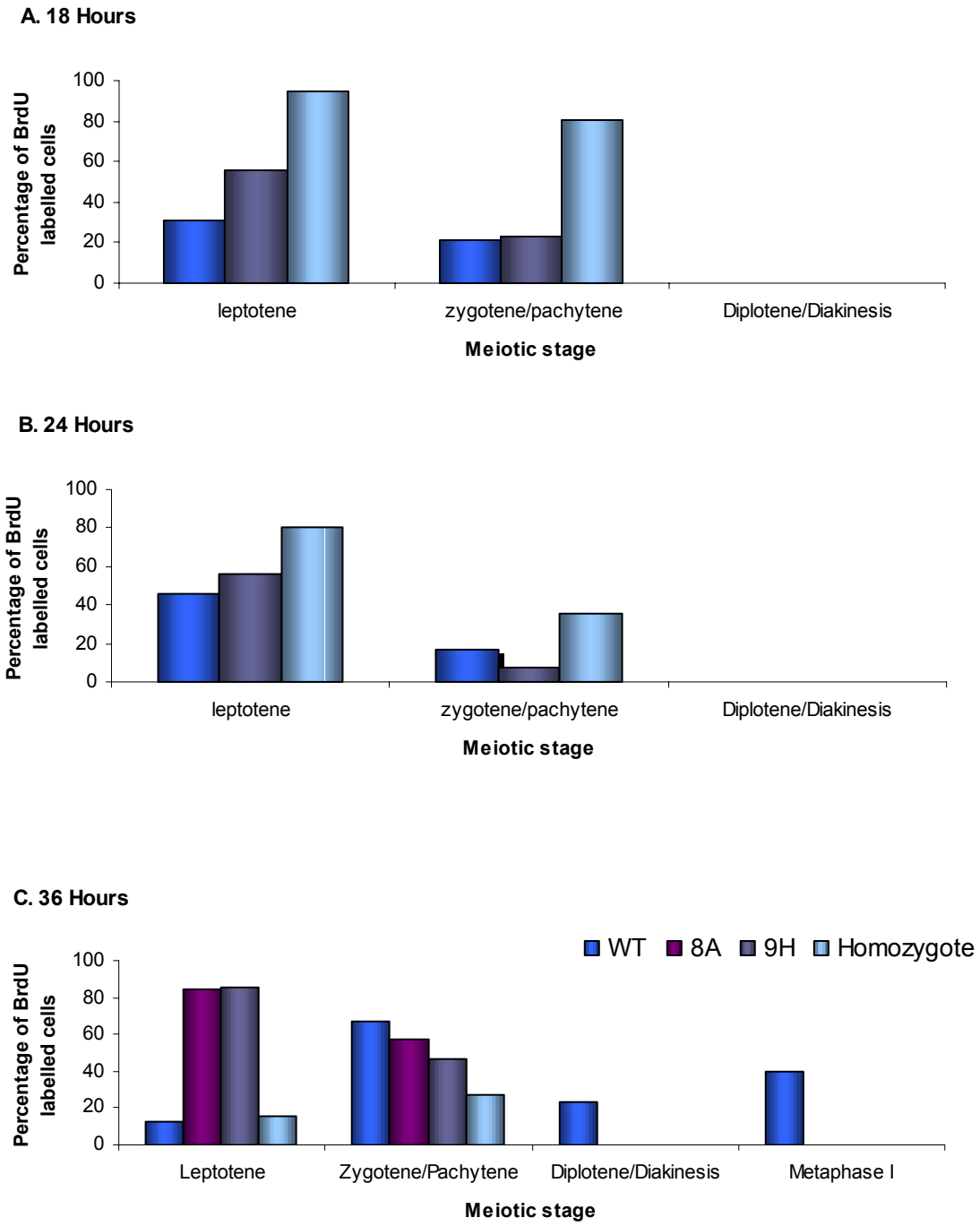

Figure 3.22: BrdU time course data shown as percentage of BrdU labelled cells of each meiotic stage. A-C show data for time points 18, 24, and 36 hours respectively for the lines, wild-type Col-0 (WT), *SPO11-1* RNAi lines (8A, 9H), and *spo11-1-4* (Homozygote). Line 8A was only included for the 36h time point.

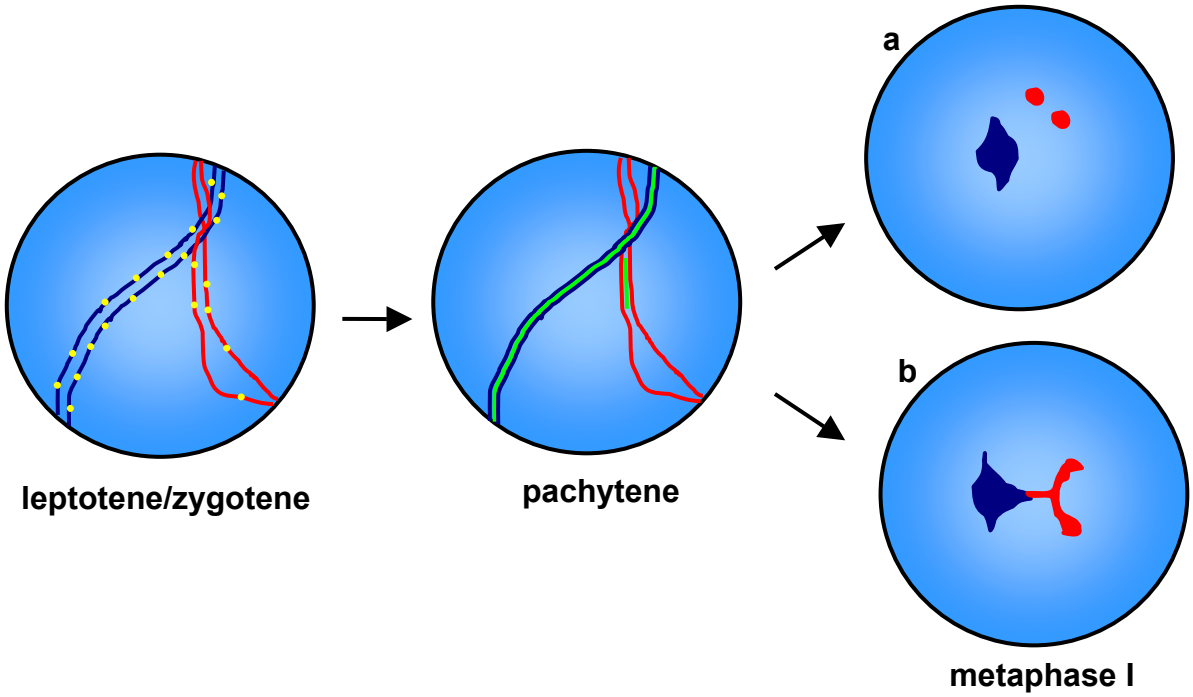

Figure 3.23: Pairing and synapsis of homologous chromosomes with reduced DSBs.

Shows a chromosome that has sufficient DSBs to pair and synapse (blue), may form 1 or more chiasmata at metaphase I, and a chromosome that has a number of DSBs below the threshold needed to pair and synapse (red), which may result in univalent formation (a) or non-homologous connections (b) and multivalent formation in extreme cases. DSBs shown in yellow, and SC in green. 2 homologous chromosomes pairs are shown for simplicity.

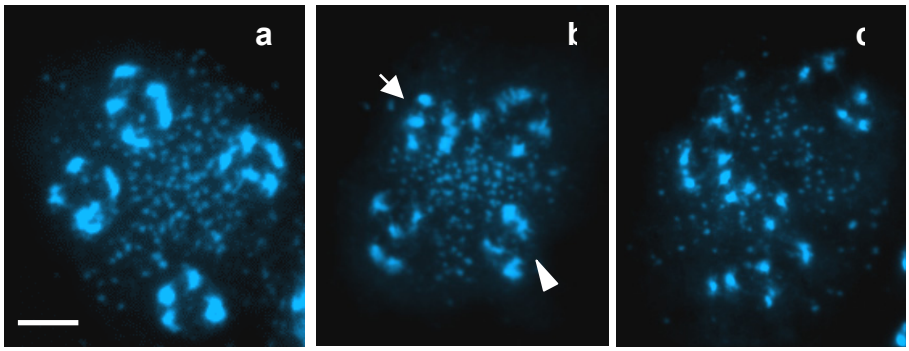

Figure 4.1: Evidence for uptake of colchicine. (a) Untreated tetrad (control) shows normal conformation of 5 chromosomes per cell. (b-c) Tetrads treated with 10mM colchicine show mis-segregation. For example (b) arrows show cells with 6 (arrow) or 4 (triangle) chromosomes. (c) Cell conformation altered, cells are not divided. Chromatin labelled DAPI (blue). Bar 10 µM.

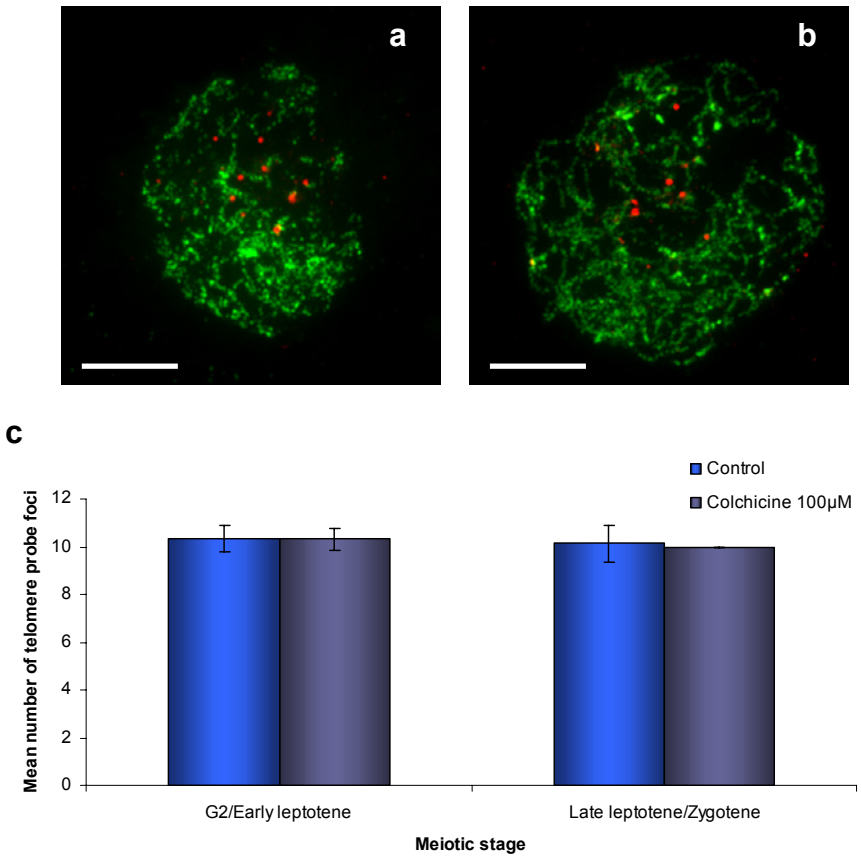

Figure 4.2: Telomere pairing in G2 stage colchicine treated meiocytes.

Fluorescence *in situ* hybridisation the telomere probe and BrdU labelling. (a) Untreated control, showing BrdU (shown green) labelled leptotene at 14h post BrdU pulse. Approximately 10 telomere probe foci (shown red) are visible, indicating telomeres are paired. (b) Treatment with 100 µM colchicine; showing a BrdU labelled leptotene at 14h post BrdU pulse with approximately 7 telomere probe foci visible indicating telomeres are paired. (c) Mean number of telomere probe foci observed per BrdU labelled cell. Standard error bars shown. Results show that there is no significant difference between the control and treated sample means.

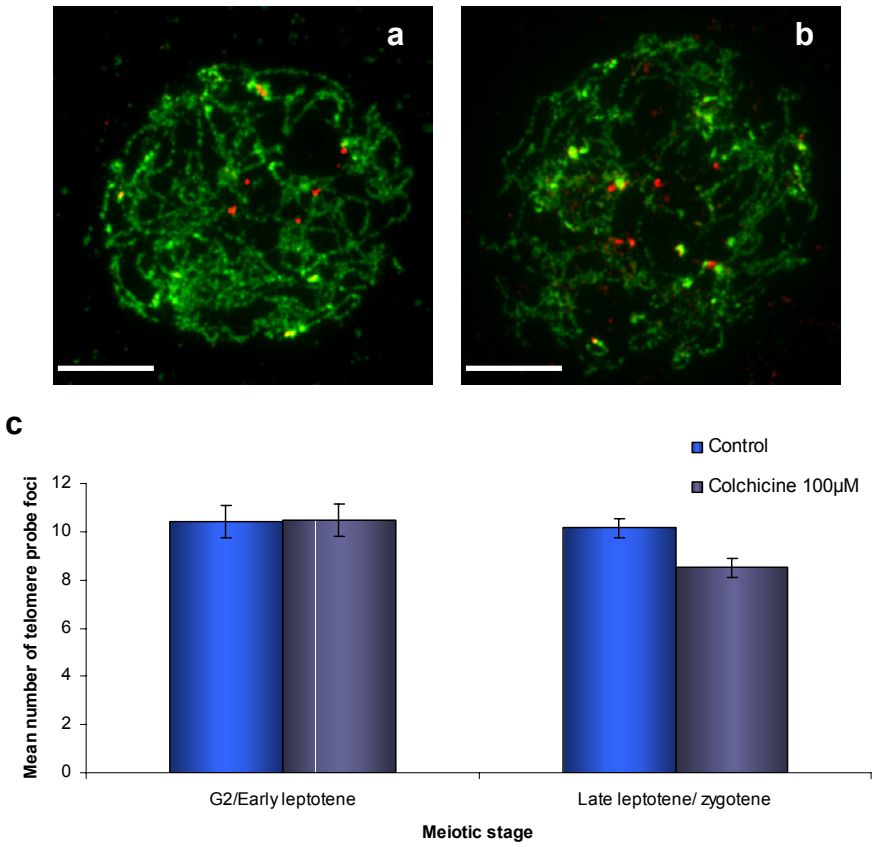

Figure 4.3: Telomere pairing in G1 stage treated meiocytes.

Fluorescence *in situ* hybridisation the telomere probe and BrdU labelling. (a) Untreated control, showing BrdU (shown green) labelled leptotene at 14h post BrdU pulse. Approximately 7 telomere probe foci (shown red) are visible, indicating telomeres are paired. (b) Treatment with 100 µM colchicine; showing a BrdU labelled leptotene at 14h post BrdU pulse with approximately 6 telomere probe foci visible indicating telomeres are paired. (c) Mean number of telomere probe foci observed per BrdU labelled cell. Standard error bars shown. Results show that there is no significant difference between the control and treated sample means.

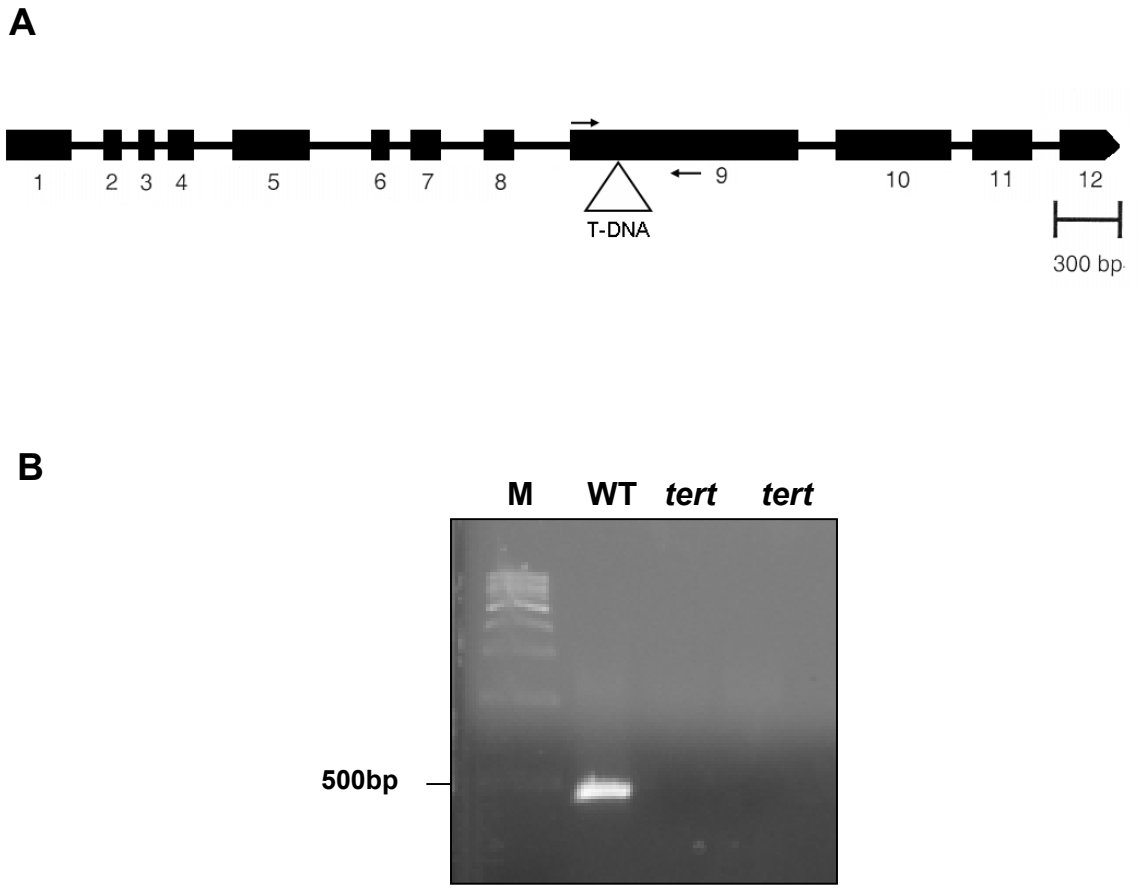

Figure 4.4: (A) Map of the At5g16850 locus showing intron/ exon organisation. (Exons shown in bold). The location of the T-DNA insertion line in exon 9 is indicated by a triangle. The arrows represent the locations of gene specific primers used for genotyping of plants. These primers were previously used by Fitzgerald et al, (1999). (B) Agarose gel analysis of PCR products from PCR with gene specific primers. DNA was run alongside a 1Kb DNA ladder (M). Lane (WT) shows PCR products from DNA extracted from a wild-type control plant. A band that runs close to the expected size (457bp) can be observed, showing that no T-DNA insert is present. The lanes (*tert*) contain the PCR products from DNA extracted from tert G_8 mutants. No bands are amplified by the primers, showing these plants contain a T-DNA insert in this location.

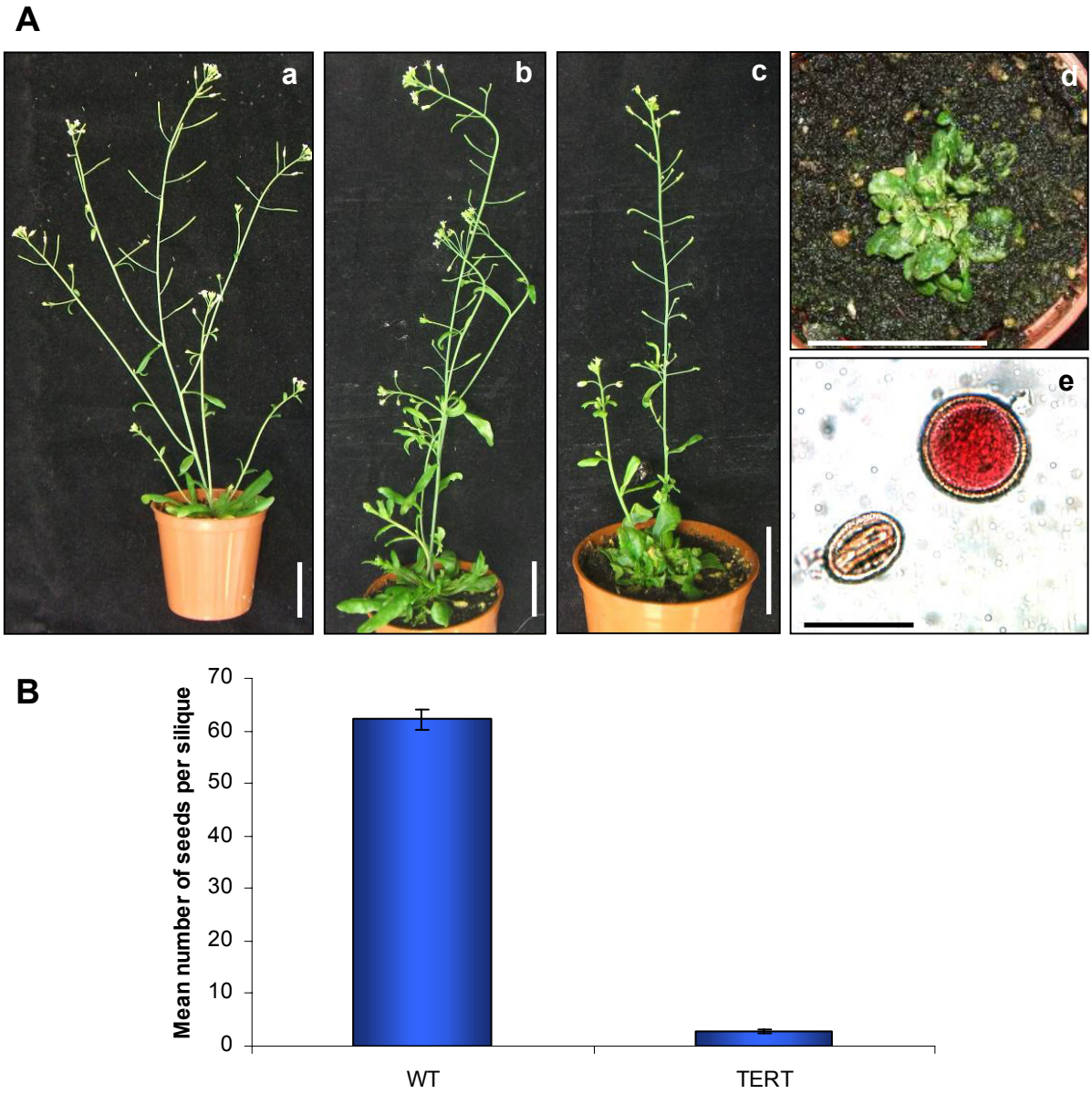

Figure 4.5: (A) Phenotype of the telomerase deficient *tert* line 69 plants. (a) Wild-type Col-0 control, showing normal vegetative growth. (b-c) *tert* G_8 plant showing perturbed vegetative and reproductive development. (d) *tert* G_9 plant showing severe vegetative abnormalities, and no shoot formation. Bars 3cm. (e) Alexander staining of pollen from *tert* G_8 showing an example of viable pollen (red), and non-viable pollen (green). Bars 10µM. (B) Fertility of *tert* G_8 plants is severely reduced in comparison to wild-type (WT). Mean number of seeds per silique shown together with error bars.

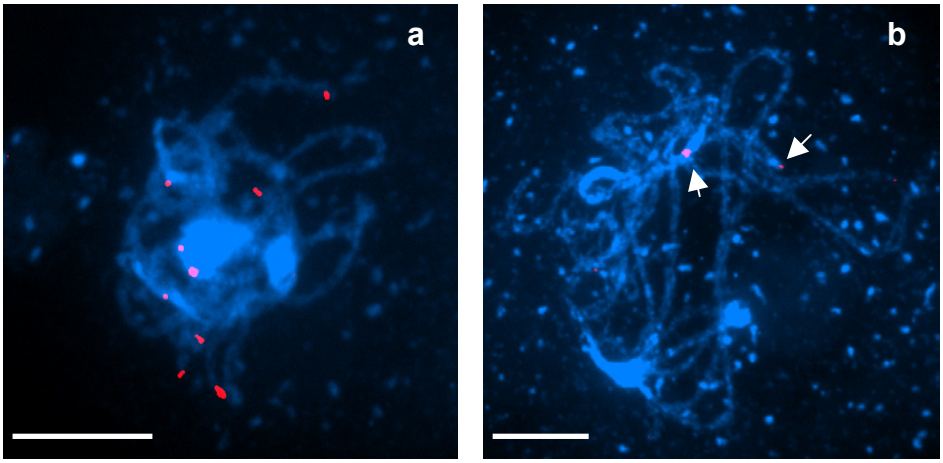

Figure 4.6: Fluorescence *in situ* hybridization of the telomere probe on wild-type (a) and the *tert* G_8 mutant (b). The probe was detected with a secondary antibody, DIG-rhodamine (shown red). (a) Approximately 9 foci observed. (b) Approximately 2 foci can be observed (see arrows). These signals represent the interstitial telomeric sequence recognised by the probe, which acts as a positive control. Bars 10µM.

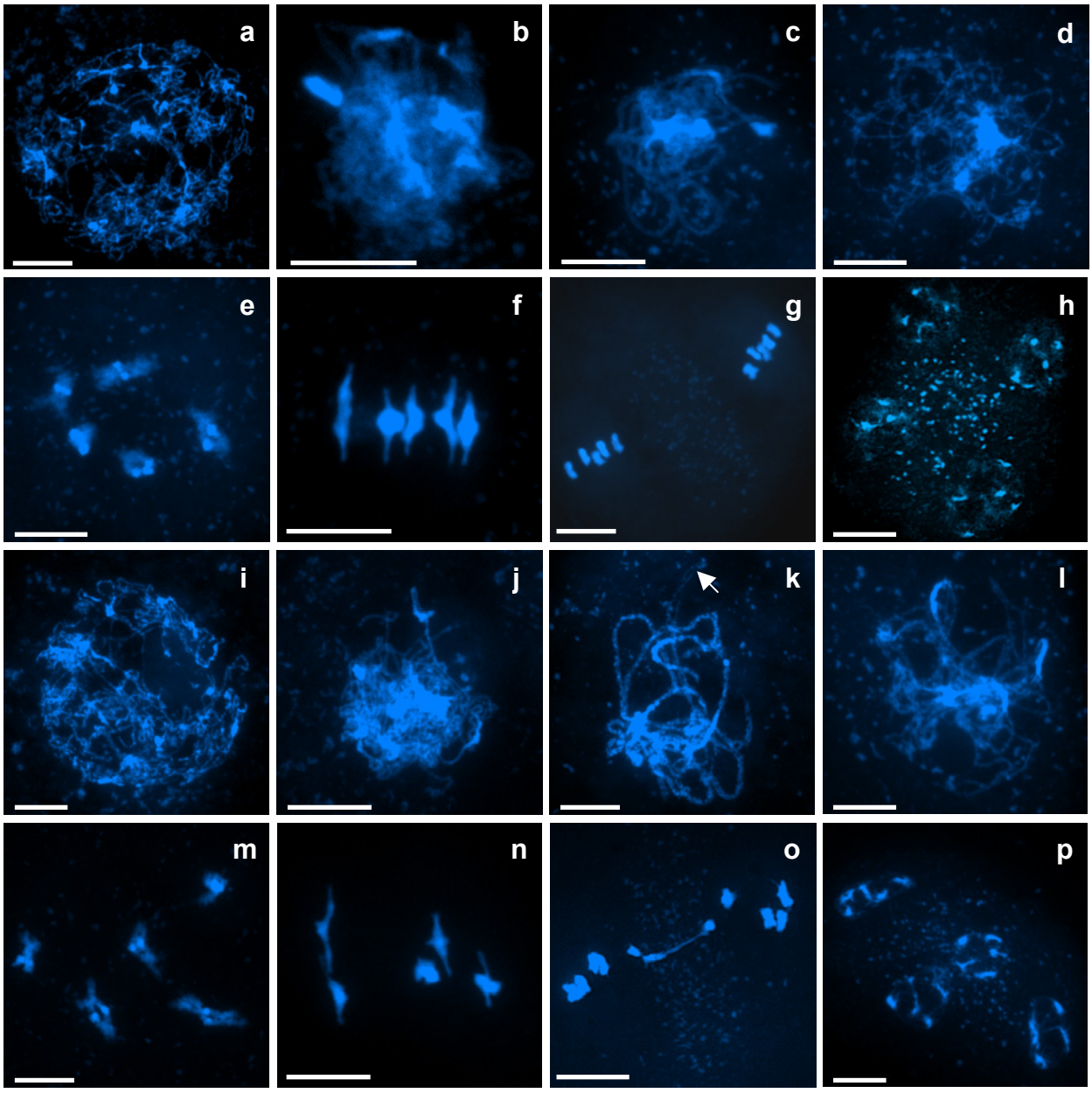

Figure 4.7: Meiotic phenotype of the *tert* G_8 mutant (i-p) in comparison to wild-type Col-0 (a-h). (a,i) Leptotene. (b,j) Zygotene. (c,k) Pachytene. (d,l) Diplotene. (e,m) Diakinesis. (f,n) Metaphase I. (g,o) Metaphase II. (h,p) Tetrad. Leptotene through to Diakinesis are similar in appearance in wild-type and the *tert* G_8 mutant. Apart from pachytene where the ends of the chromosomes appear to be unpaired in the *tert* G_8 mutant (see arrow image k). At metaphase I 5 bivalents are observed in *tert* G_8. Metaphase II resembles wild-type on the whole. But occasionally bridges are observed in *tert* G_8 (see arrow image o). Tetrads appear similar to wild-type. Chromatin stained DAPI (blue). Bars 10µM.

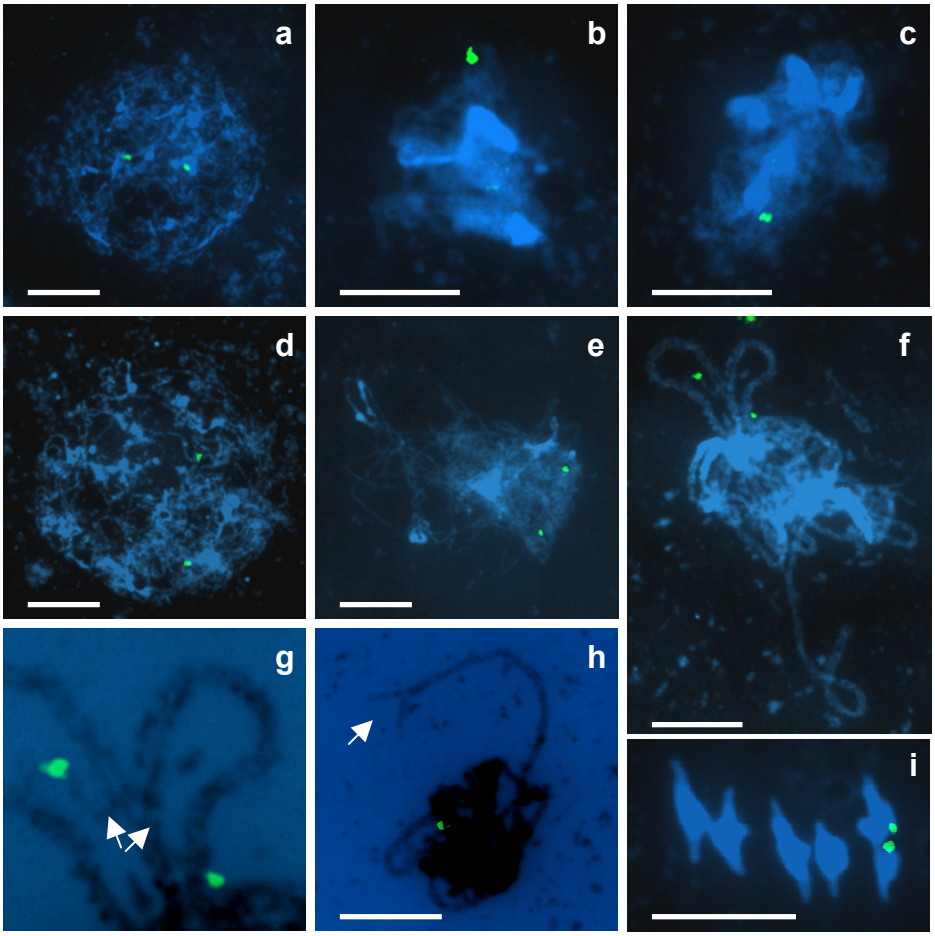

Figure 4.8: Pairing of sub-telomeric regions in the *tert* G_8 mutant. Fluorescence in situ hybridisation of BAC F19K16 to chromosome 1, labelled DIG-FITC (green), counterstained DAPI (blue). Wild-type Col-0 stages (a-c) show that the sub-telomeric region of chromosome 1 becomes paired (stages leptotene, zygotene, and pachytene respectively). *tert* G_8 meiotic stages (d-i). (d) Leptotene showing 2 unpaired foci. (e) Zygotene showing 2 unpaired foci. (f) Pachytene showing 2 unpaired foci. (g) Close-up of image f showing the homologues of chromosome 1 spread at the ends (see arrows). (h) Pachytene (DAPI inverted, black) showing 1 paired focus of F19K16. Also shows another end of unpaired chromosomes (see arrow). Metaphase I *tert* G_8 (i). Bars 10µM.

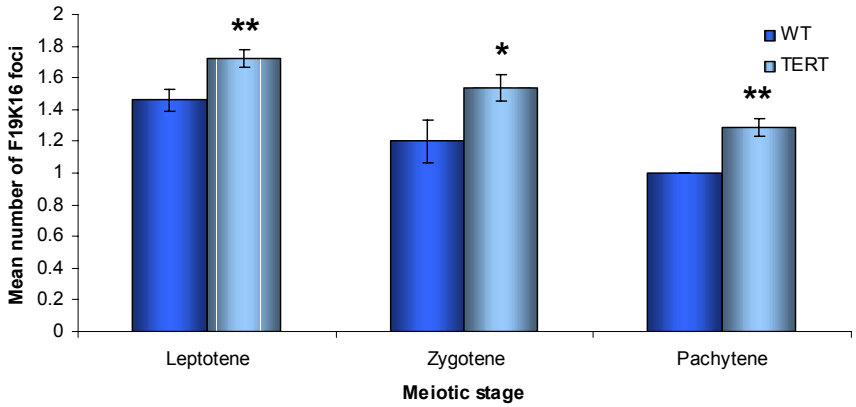

Figure 4.9: Mean number of F19K16 foci per cell, for wild-type (WT), and the *tert* G_8 mutant at each meiotic stage. Error bars shown. *t*-test: leptotene $t_{(103)} = 2.86$, p= < 0.01. Zygotene $t_{(16)} = 2.17$, p= <0.05. Pachytene $t_{(71)} = 3.33$, p= <0.01. Levels of significance are shown as (*) 95% confidence, or (**) 99% confidence. The mean numbers of F19K16 foci are significantly higher in the *tert* mutant at each meiotic stage.

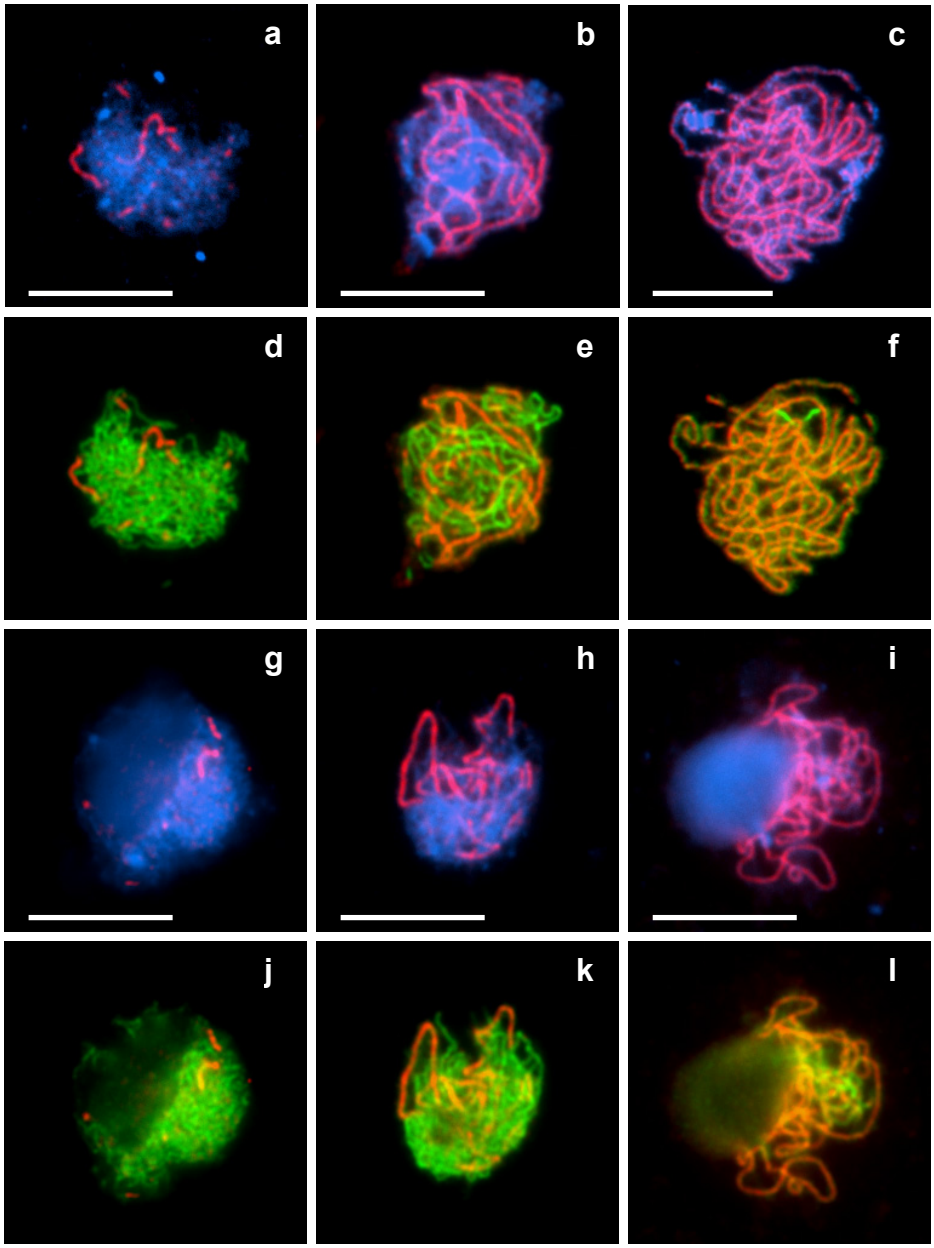

Figure 4.10: Dual-immunolocalisation of ZYP1 protein (red) and ASY1 protein (green), on the *tert* G_8 mutant and a wild-type control. (a-f) Wild-type Col-0 at early zygotene, mid-zygotene, and pachytene respectively. (g-l) *tert* G_8 at early zygotene, mid-zygotene, and pachytene respectively. ZYP1 polymerisation appears similar to wild-type in the *tert* G_8 mutant. Bars 10µM.

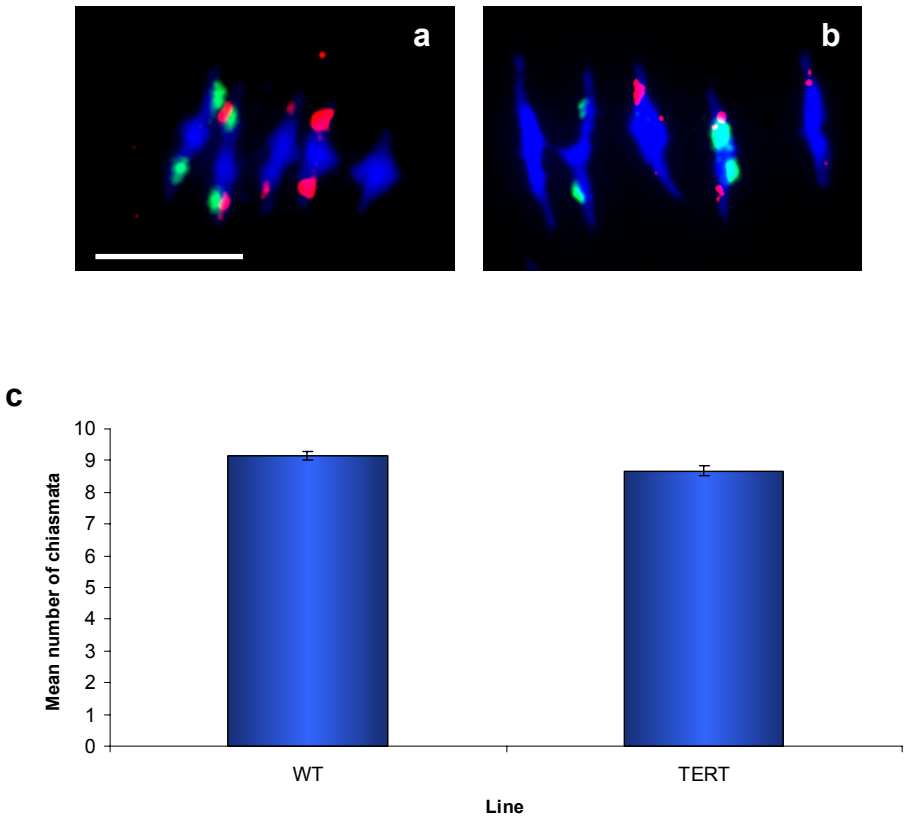

Figure 4.11: The chiasma frequency for the *tert* G_8 mutant is slightly reduced in comparison to wild-type. (a-b) Fluorescence in situ hybridisation of rDNA probes 45s and 5s, allow identification of chromosomes. (a) Wild-type Col-0. (b) *tert* G_8. Both show 8 chiasmata. Bars 10µM. (c) Mean number of chiasmata in the wild-type (WT) and *tert* G_8. Error bars shown.

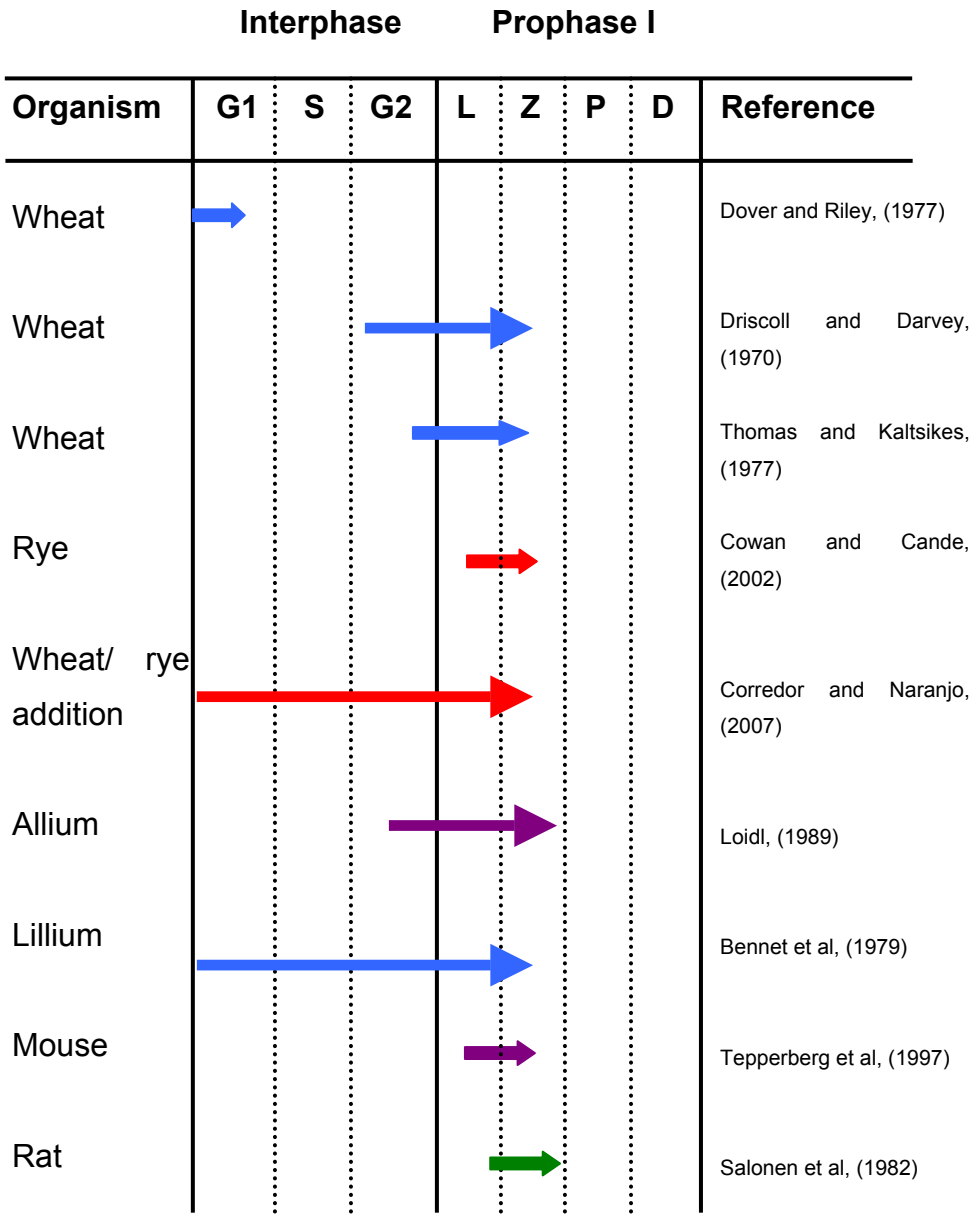

Figure 4.12: Summary of the stages of colchicine sensitivity.

The arrows show the timing of colchicine sensitivity for a number of organisms. The bar colours denote the method used to infer this timing. Blue corresponds to a reduction in chiasma frequency at diakinesis/metaphase I. Purple corresponds to defects in SC formation. Green indicates disruption of chromosome movements at zygotene by colcemid. Red indicates failure of bouquet formation. (S) S-phase. (L) Leptotene. (Z) Zygotene. (P) Pachytene. (D) Diakinesis. Adapted from Loidl, (1990).

Figure 5.1: ClustalW (EBI) sequence alignment of full length AtPOT1a and AtPOT1b amino acid sequences. (*) denotes identical amino acids, (:) denotes similar amino acids. Highlighted regions indicate sequences selected for recombinant protein design. Yellow shows the POT1a-HIS recombinant protein, and blue shows that of POT1b-HIS. The red markers designate the start and end of a second recombinant protein to POT1a, POT1aLONG-HIS, and a third in green markers, POT1aSHORT-HIS.

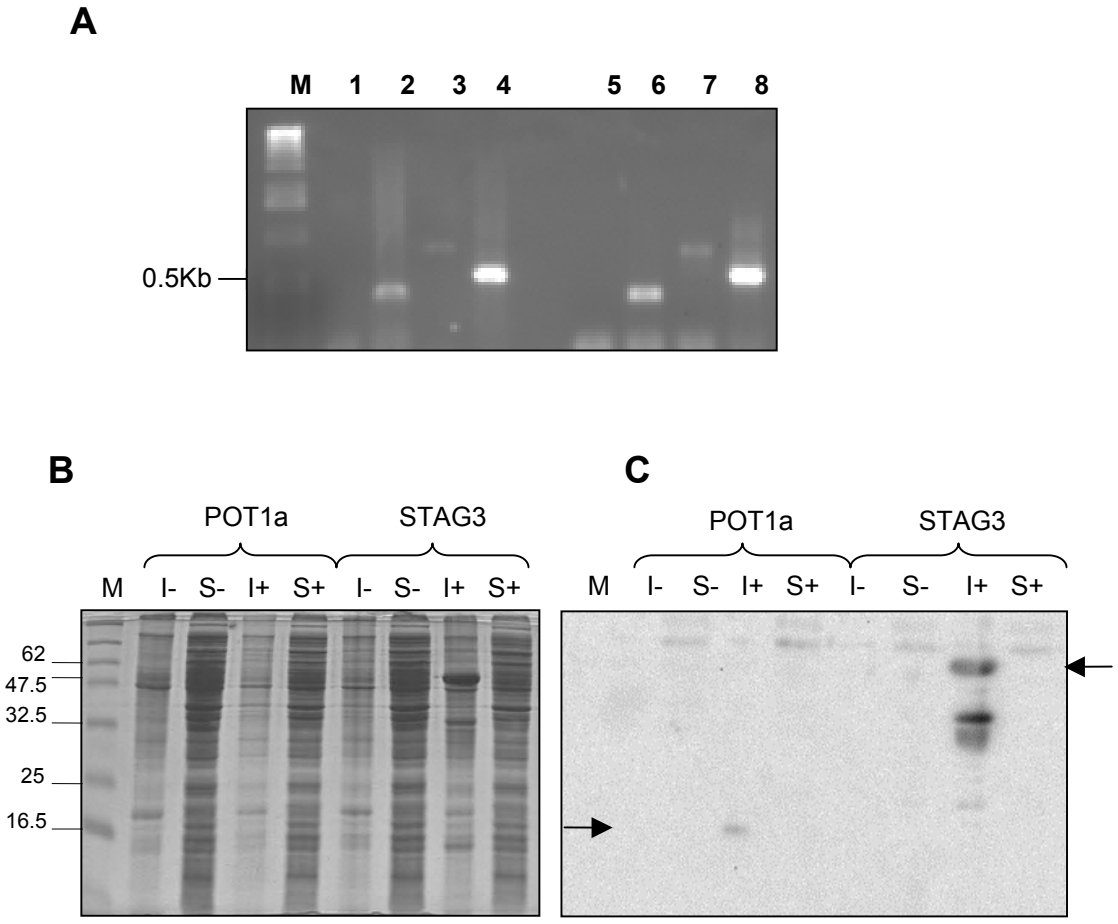

Figure 5.2: Cloning and expression of POT1aHIS-SHORT recombinant protein

(A) Agarose gel (1 %) analysis of PCR products using the primer sets specific for POT1a and POT1b, or GAPD as a control. Lanes 1. POT1a gDNA 2. POT1a cDNA 5. POT1b gDNA 6. POT1b cDNA. 3 and 7 GAPD gDNA 4 and 8. GAPD cDNA. Both fragments run at the predicted molecular weight of 400bp.

(B) SDS-PAGE analysis of crude extracts using BugBuster. (I) insoluble, (S) soluble, (+) induced, (-) non-induced. A band of the predicted molecular weight of STAG3-HIS is observed in the induced insoluble lane for this sample (~50 KDa). No detectable labelling of induced POT1a-HIS is observed (15 KDa).

(C) Western blot analysis of POT1a crude protein extracts. The blot was probed with a mouse anti-HIS primary antibody (1:2000), and a horseradish peroxidase conjugated anti-mouse secondary antibody (1:10000); visualised by ECL. The blot shows that POT1a is expressed only in the insoluble induced fraction at a low level, as indicated by the arrow. STAG3 is shown to be present in the induced insoluble fraction with a much higher level of expression.

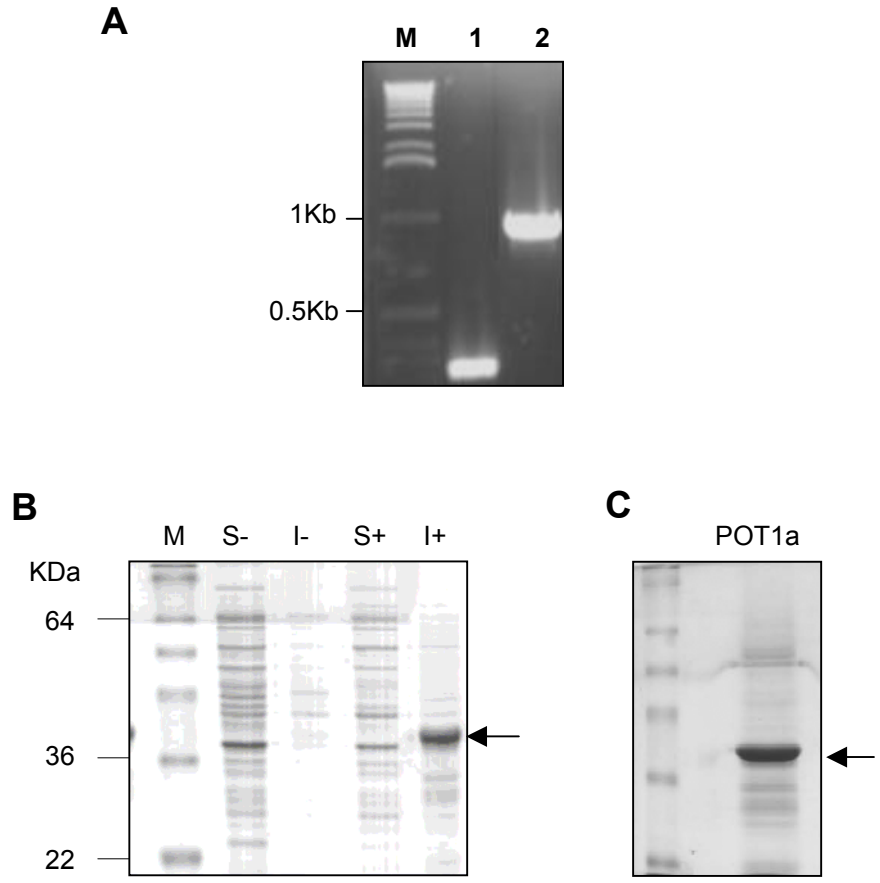

Figure 5.3: Cloning and expression of POT1aHIS-LONG recombinant protein

(A) Agarose gel analysis of POT1a PCR fragments, run in parallel with a molecular size marker. (1Kb ladder, Invitrogen). Fragments were amplified with specific primer sets; 1. POT1aSHORT. 2. POT1aLONG.

(B) SDS PAGE coomassie gel resolution of crude protein extracts using BugBuster. (I) insoluble, (S) soluble, (+) Induced, (-) non-induced. A protein is observed in the induced insoluble fraction, which runs at the predicted molecular weight of POT1aLONG, ~39 KDa.

(C) Resolution of purified POT1aLONG on a 10% SDS-PAGE gel stained with coomassie. The protein is indicated by the arrow. 15 µl of 0.5 mg/ml protein was loaded. Some *E. coli* proteins remain so purity was estimated at 90 %.

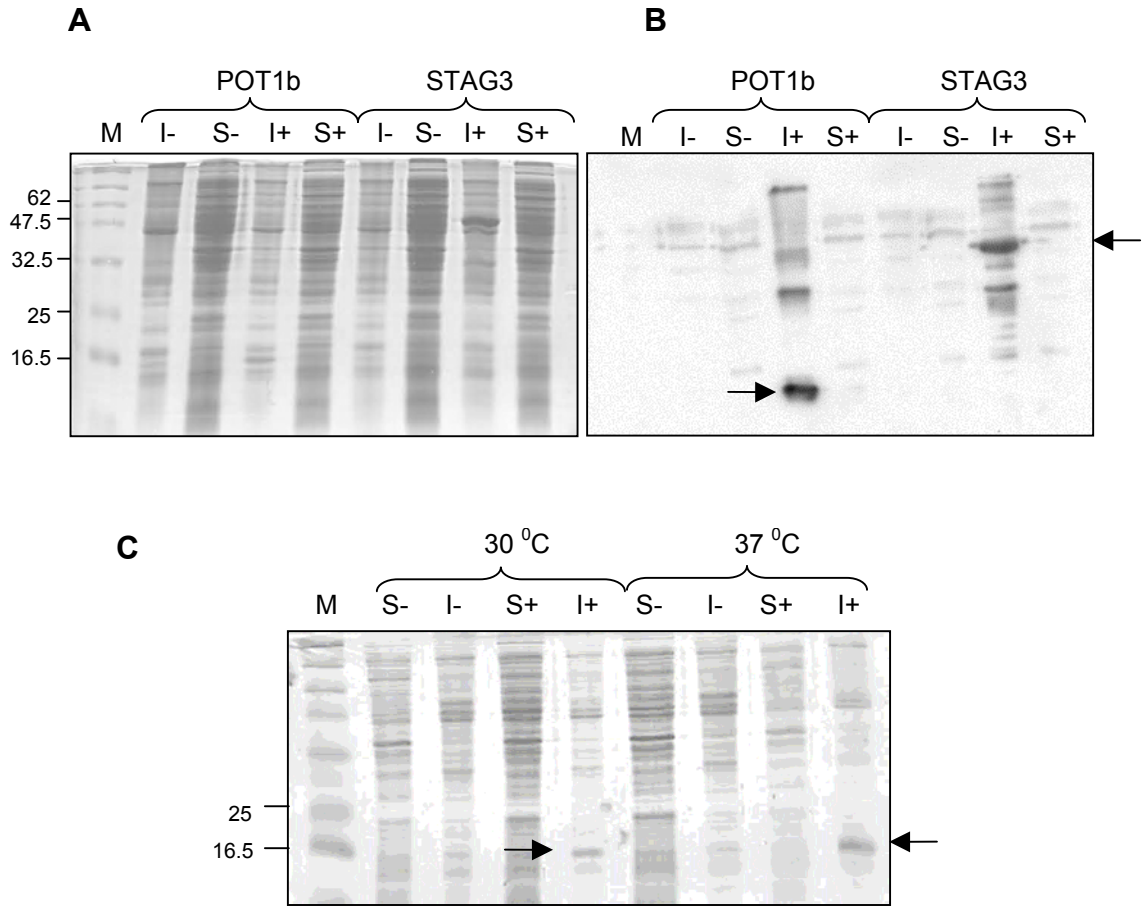

Figure 5.4: Expression of POT1b-HIS recombinant protein

(A) Resolution of crude protein extracts from cells containing the pET21b POT1b construct, induced with 1mM IPTG or an uninduced control. Samples were run together with a molecular weight marker (KDa). Coomassie stained 10 % SDS PAGE gel showing POT1b migrating at 15KDa in the induced insoluble fraction, and STAG3 migrating at ~50 KDa in the insoluble induced fraction. (I) insoluble, (S) soluble, (+) Induced, (-) non-induced.

(B) Western blot corresponding to the coomassie gel labelled with mouse anti-His antibody (1:2000) and a secondary antibody of anti-mouse conjugated to horseradish peroxidase (1:10000). Again the POT1b and STAG3 samples are labelled in the same fractions as the coomassie gel.

(C) SDS-PAGE gel electrophoresis of crude protein extracts using BugBuster at 30 ^{o}C induction, and 37 ^{o}C induction. The coomassie staining shows a band at the predicted molecular weight of 15 KDa in the induced insoluble fraction in both cases. Higher expression of POT1b-HIS is observed at the higher temperature.

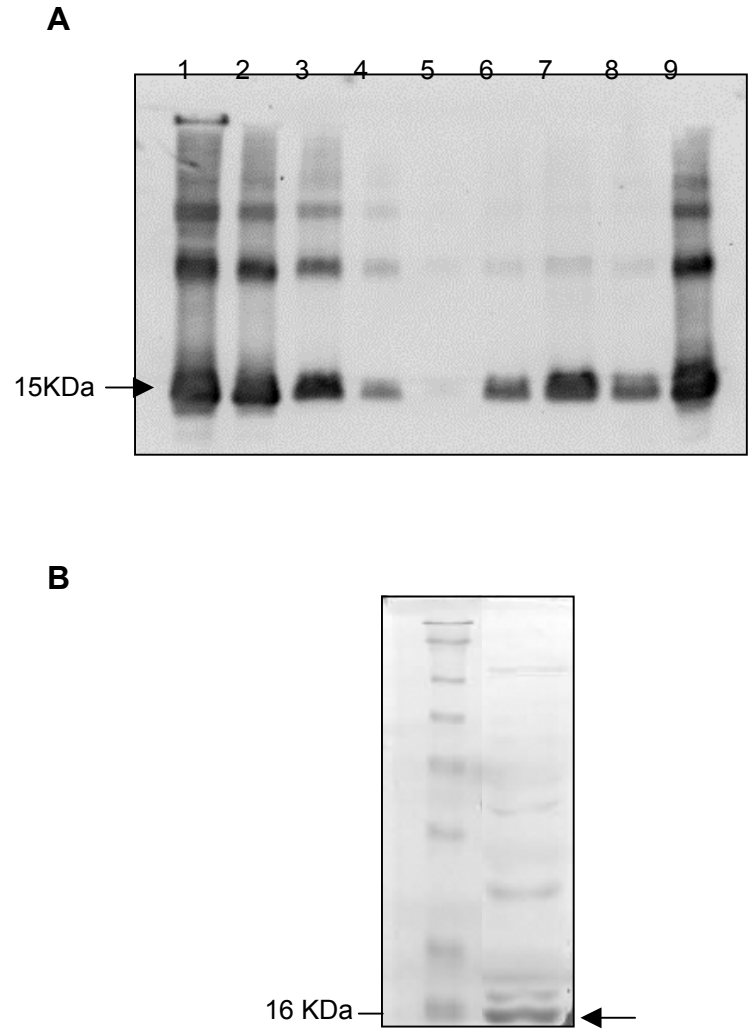

Figure 5.5: Isolation of recombinant POT1b-HIS protein

(A) Western blot showing sample fractions from each step of the batch purification. Lanes 1. Supernatant after binding. 2. Beads after binding. 3-5. Washes. 6-8. Elutions. 9. Beads after elution. The blot was labelled with mouse anti-His primary antibody (1:2000) and anti-mouse conjugated to horseradish peroxidase secondary (1:10000). The blot was visualised by ECL. POT1b-HIS indicated by arrow, migrating at 15KDa. Some background proteins also eluted.

(B) SDS-PAGE coomassie gel (15 %) of the final concentrated recombinant POT1b-HIS protein (15µl loaded). Run alongside a molecular weight marker (KDa). Protein concentration measured at 0.4 mg/ml using Biorad.

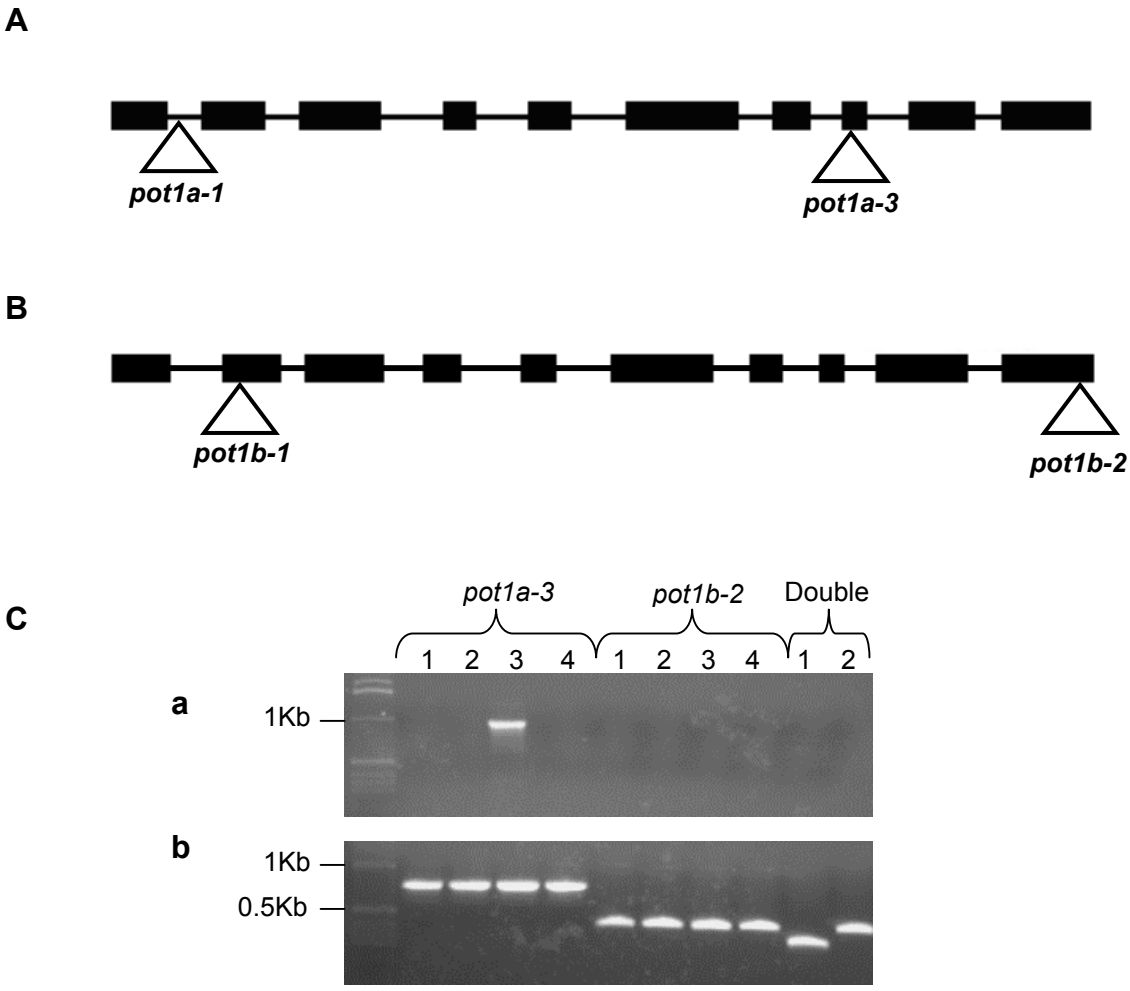

Figure 5.6: Isolation of POT1a and POT1b mutants

(A) Map of the At2g05210 locus showing intron/exon organisation (exons shown in bold). The localisation of insertion sites are indicated by triangles. For the single mutant the *pot1a-3* (SAIL_1273, NASC) was analysed. The *pot1a-1* insert formed part of the double knockout provided by D.E. Shippen (Personal communication)
(B) Map of the At5g06310 locus. The localisation of the T-DNA insertion sites are indicated by triangles. For the single mutant the *pot1b-2* (SAIL_38_GO1, NASC) was analysed. The *pot1b-1* insert formed part of the double knockout.

(C) Agarose gel analysis of genotyping PCR products. Numbers denote individual plants genotyped for either *pot1a-3* or *pot1b-2* lines. gDNA was amplified using gene specific primers spanning the insert site (a), or a gene specific primer together with a left border primer to detect the presence of an insert (b). For the double knockout one plant was analysed. Lane 1 denotes PCR with POT1a specific primers and 2 with POT1b specific primers.

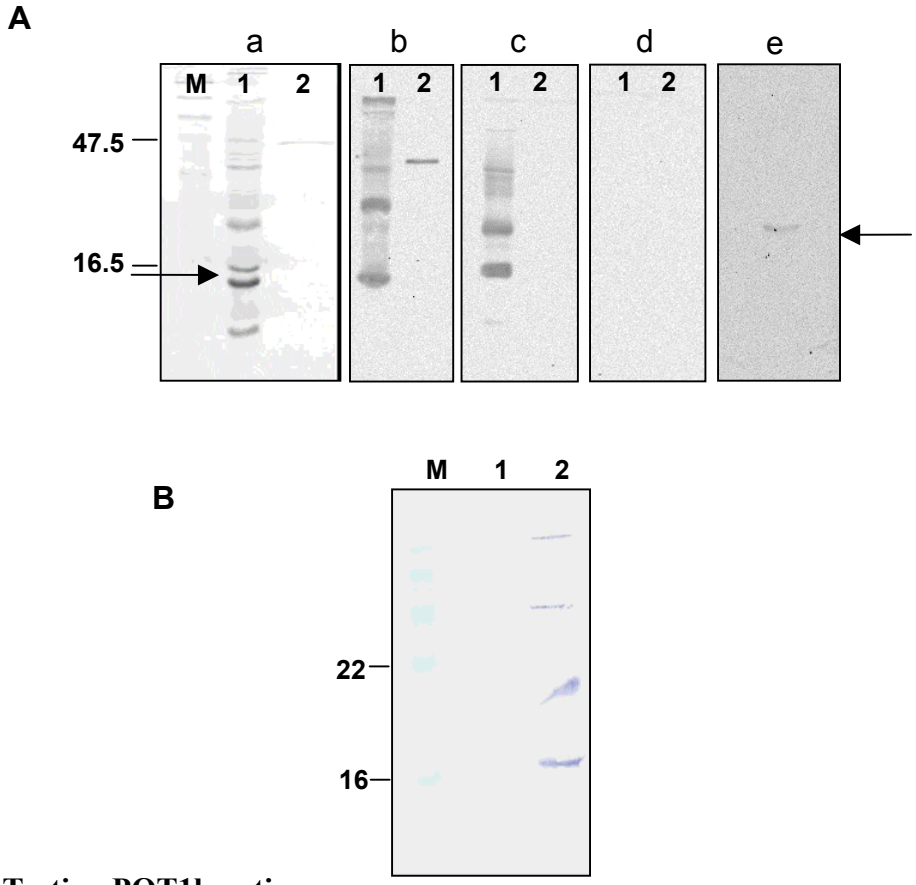

Figure 5.7: Testing POT1b antiserum

(A) Recombinant proteins were run alongside a molecular weight marker in KDa. Lane 1. POT1b-HIS recombinant protein. Lane 2. STAG3-HIS recombinant protein. 15µl of protein loaded in all lanes. (a) Coomassie stained 15 % SDS-PAGE gel showing a band migrating at the predicted molecular weight for POT1b-HIS (arrow) and a band in lane 2 corresponding to STAG3-HIS. (b) Western blot using mouse anti-HIS antibody Lane 2 shows a clean band of STAG3 and lane 1 shows a HIS labelled protein migrating at the predicted molecular weight of POT1b-HIS recombinant. (c) POT1b test bleed antiserum. A protein is labelled with the antibody that migrates at the predicted molecular weight of POT1b-HIS recombinant protein, but does not label STAG3-HIS, showing the antibody specifically recognises POT1b-HIS recombinant protein. (d) Pre-immune serum control (taken prior to inoculation). (e) Affinity purified antibody. Recombinant POT1b-HIS was run against a molecular weight marker in KDa. A band migrating at the predicted molecular weight of the POT1b-HIS recombinant protein can be observed, with no background visible. However the titre of the antibody appears severely reduced, as observed by the faint band.

(B) Specificity of POT1b antiserum for POT1b-HIS recombinant protein. Recombinant proteins (1. POT1a-HISLONG recombinant protein. 2. POT1b-HIS recombinant protein) were resolved in parallel with a molecular weight marker (M), and detected using POT1b test bleed antiserum primary antibody (1:1000), and a secondary antibody of anti-rabbit conjugated to alkaline phosphatase(1:5000).

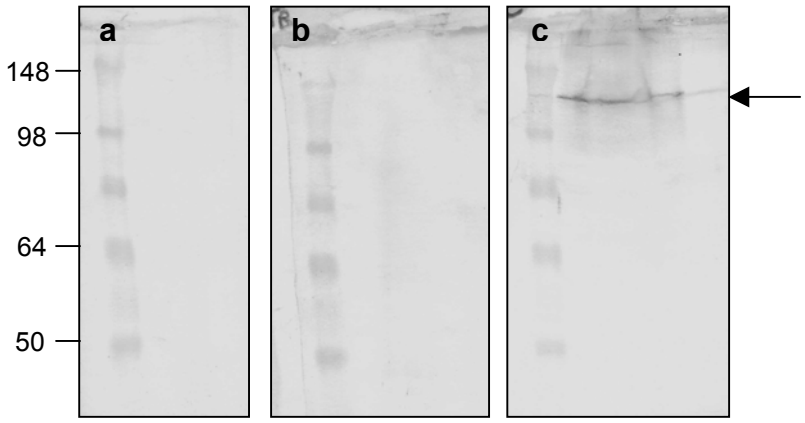

Figure 5.8: Western blot of *Brassica oleracea* inflorescence protein lysates. Total protein cell lysates extracted using PEB were resolved on a 10% SDS-PAGE gel in parallel with a molecular weight marker in KDa, and transferred to a nitrocellulose membrane for western analysis. (a) Primary antibody of pre-immune serum, taken prior to immunisation. (b) Primary antibody, POT1b antiserum. (c) Positive control of SMC3 primary antibody. (All 1:1000). These were detected using a secondary of anti-rabbit for the POT1b antiserum, and anti-rat for the SMC3 antiserum, conjugated to alkaline phosphatase (1:5000). For the POT1b antiserum, no bands could be detected. The control of SMC3 showed a band of the predicted size at 120 KDa.

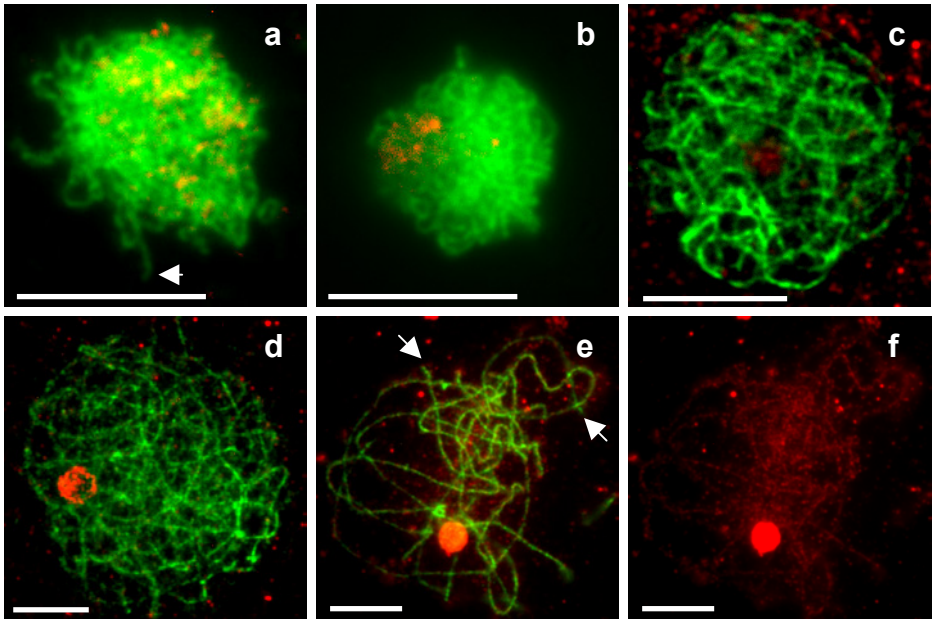

Figure 5.9: Dual-immunolocalisation of POT1b test bleed antiserum (1:200) and ASY1 (1:200) on *A. thaliana* and *B.oleracea* spread meiotic chromosomes.

ASY1 (Rat) labelled with secondary antibody of anti RAT-FITC (green) designates axial elements. POT1b antiserum (Rabbit) labelled with secondary antibody of anti-Rabbit Texas Red. Images (a-b) all show zygotene stage meiocytes of *Arabidopsis* with diffuse labelling of POT1b. Images (c-f) show Brassica meiocytes at leptotene. (c) Control of POT1b pre-immune serum, shows no labelling. (d-f) POT1b antiserum. Images (d-f) show labelling of nucleolus only. Some foci are observed, but these appear to be non-specific background labelling, as shown in (f). Bars 10 µM.

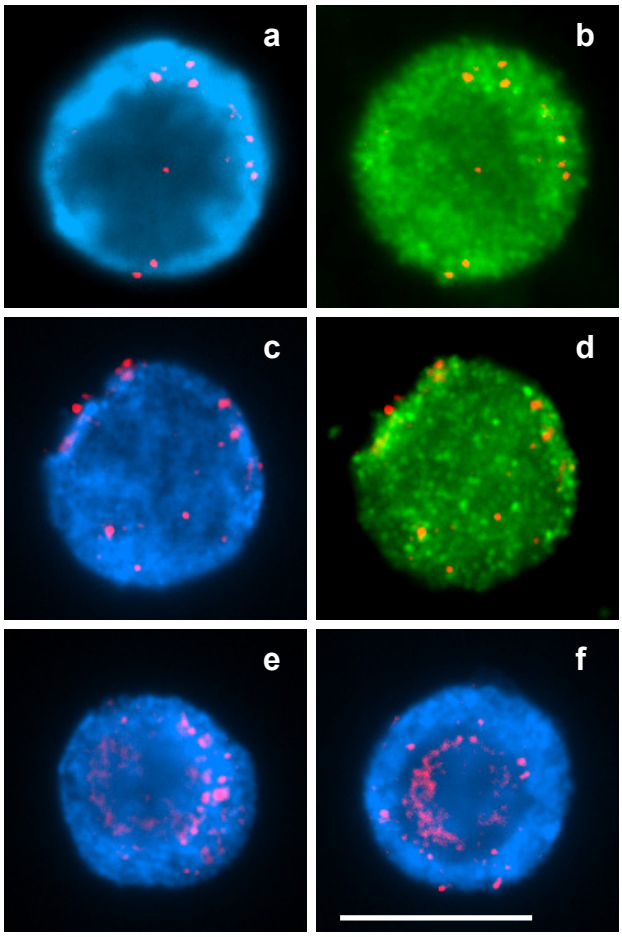

Figure 5.10: Immunolocalisation of POT1b antiserum on somatic cells from floral tissue.

Images show POT1b test bleed antiserum (1:50) (labelled rabbit texas red), with chromatin labelled DAPI (blue), or anti-BrdU (green). (a-b) Wild-type. (c-d) *pot1b-2* mutant. (e) Wild-type. (f) Double knockout (*pot1a-1, pot1b-1*). Bar 10µM.

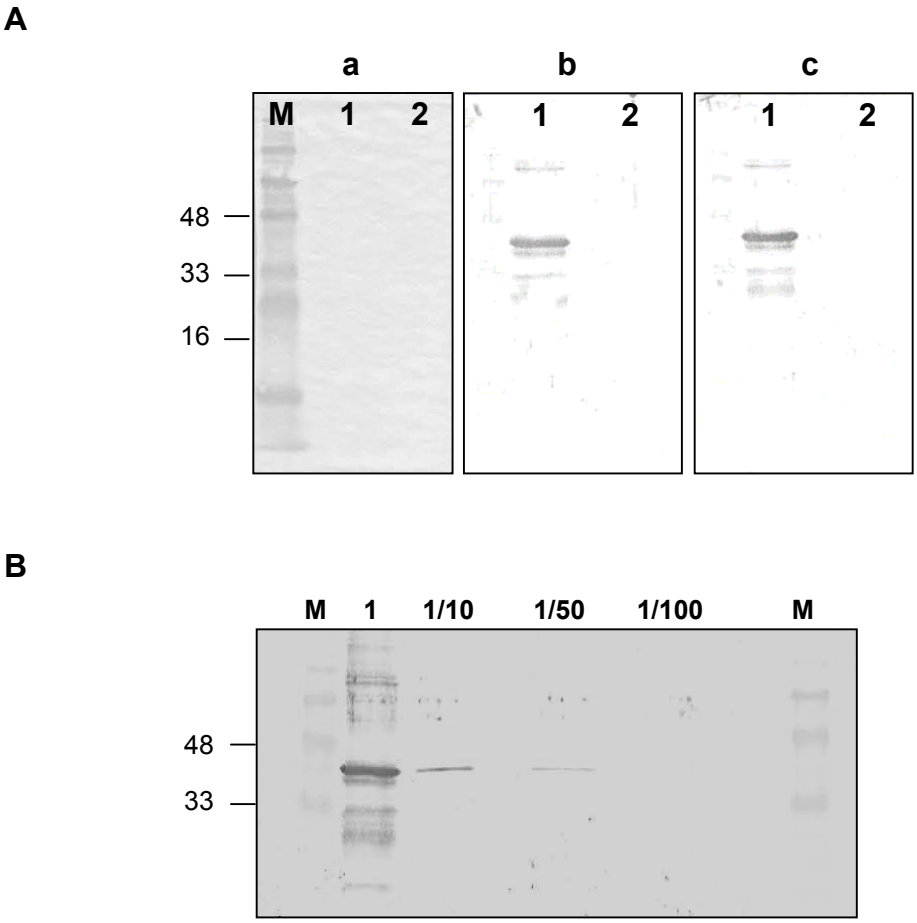

Figure 5.11: Testing POT1a anti-serum using western blotting

(A) Western blots of POT1a antiserum on POT1a-HISLONG (1) and POT1b-HIS (2) recombinant proteins; run alongside a molecular weight marker (KDa). Primary antibodies diluted in milk block: (a) Pre-immune serum control (1:1000), (b) Test bleed 1 antiserum (1:1000), (c) Test bleed 2 antiserum. All blots subject to a secondary antibody of anti-rat conjugated to alkaline phosphatase (1:5000).

(B) Dilution series of POT1a recombinant protein, detected by the POT1a primary antibody. Dilution of the protein shown above each lane, with 15 µl of each loaded. A band at the predicted size of 39KDa can be observed in all lanes but the 1/100 dilution. This shows that the antibody can detect 80 ng of protein. Prior to incubation with the primary antibody, the blots were blocked with *E.coli* proteins to reduce the background labelling.

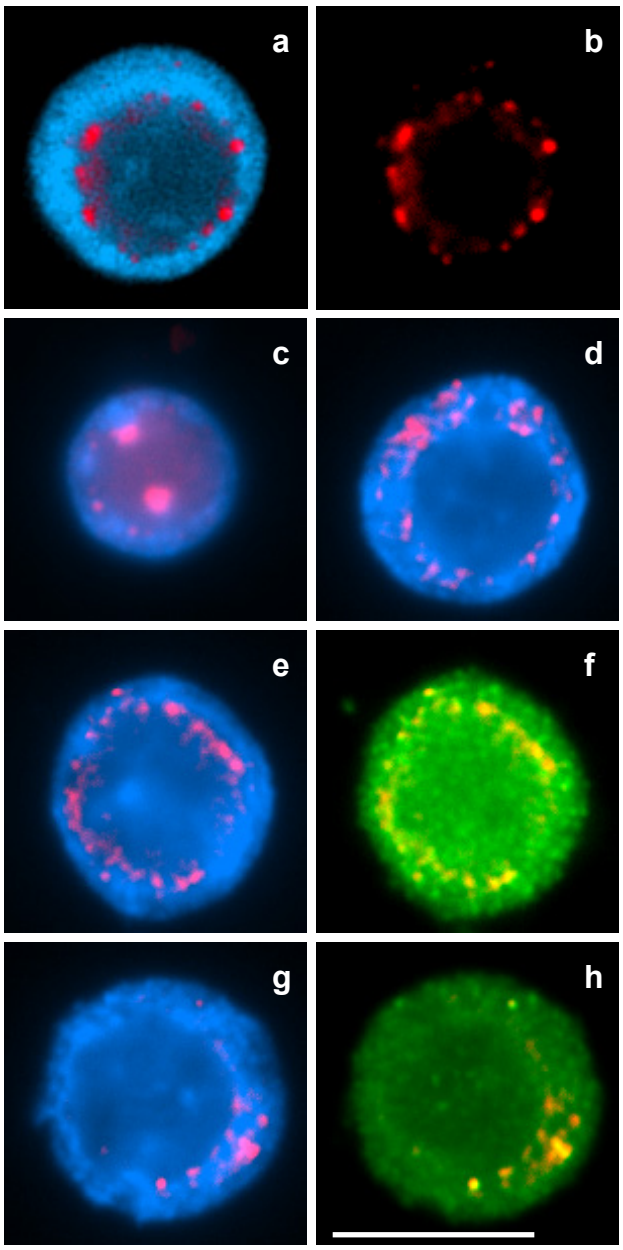

Figure 5.12: Immunolocalisation of POT1a on somatic cells from floral tissue

Images show POT1a test bleed antiserum (1:50) (labelled rabbit texas red), with chromatin labelled DAPI (blue), or anti-BrdU (green). (a-b) POT1a peptide antibody on wild-type (c) POT1a antiserum on wild-type (d) Double knockout (*pot1a-1, pot1b-1*) (e-f) *pot1a-3* mutant (g-h) Double knockout (*pot1a-1, pot1b-1*). Bar 10 µM.

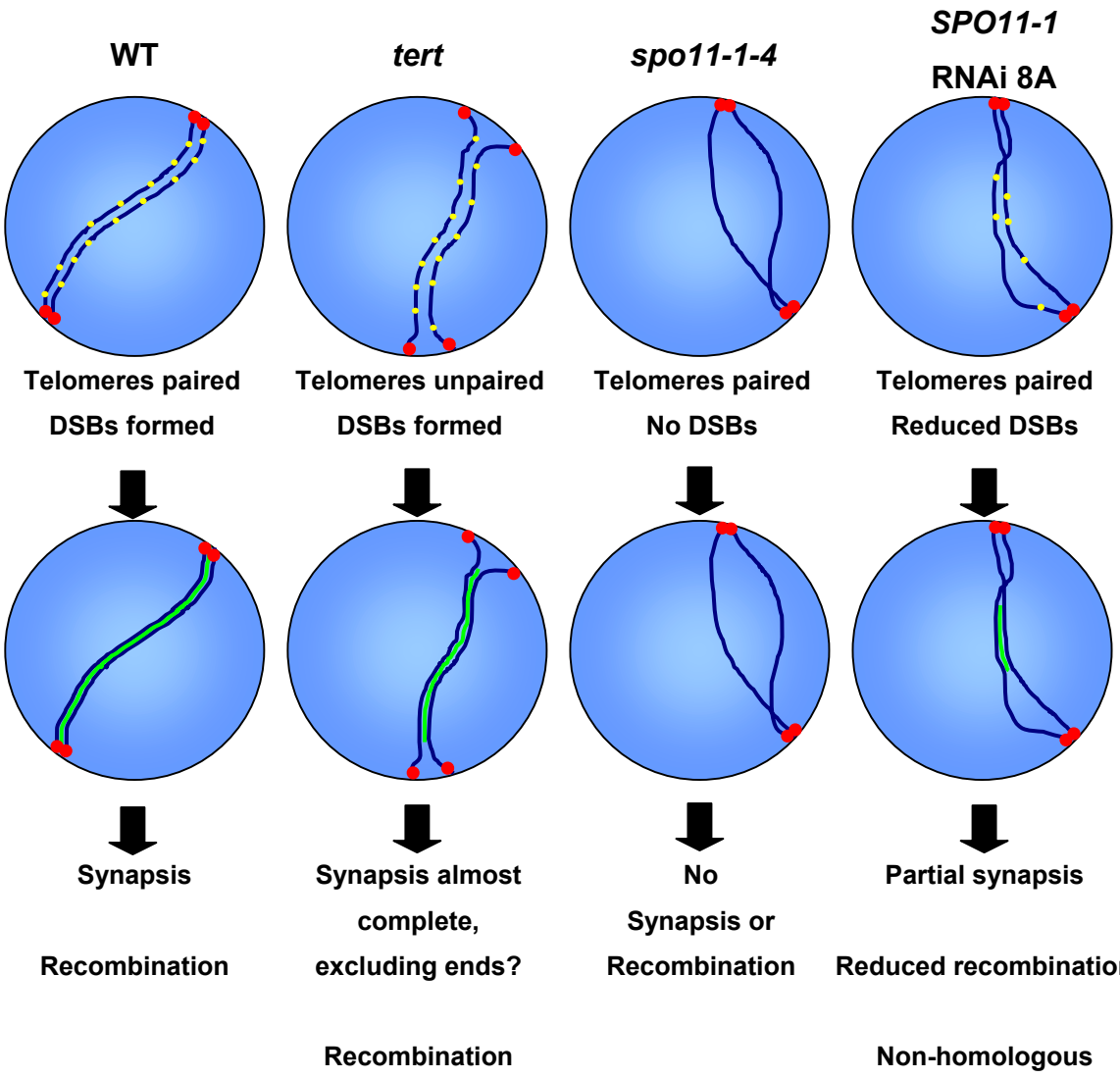

Figure 6.1: Summary of telomere pairing and synapsis of homologues in *Arabidopsis* wild-type and mutants studied. DSBs shown in yellow, telomeres in red, and SC in green.